Dynamique de l'érosion fluviatile consécutive à une chute du niveau de base. L'exemple de la Crise de Salinité Messinienne

Nicolas Loget

N° d'ORDRE de la thèse 3194

THESE

Présentée

DEVANT L'UNIVERSITE DE RENNES I

Pour obtenir

le grade de **DOCTEUR DE L'UNIVERSITE DE RENNES 1**
Mention Sciences de la Terre

PAR
Nicolas LOGET

Equipe d'accueil : Géosciences Rennes UMR 6118 CNRS
Ecole doctorale : Sciences de la Matière
Composante universitaire : U.F.R. Structure et Propriétés de la Matière

DYNAMIQUE DE L'EROSION FLUVIATILE CONSECUTIVE A UNE CHUTE DU NIVEAU DE BASE. L'EXEMPLE DE LA CRISE DE SALINITE MESSINIENNE

Soutenue le 7 Juillet 2005 devant la Commission d'Examen

COMPOSITION DU JURY

Jacques DEVERCHERE : Université de Bretagne Occidentale - Rapporteur

Peter VAN DER BEEK : Université Joseph Fourier - Rapporteur

Jean BRAUN : Université de Rennes I - Examinateur

Wout KRIJGSMAN : University of Utrecht - Examinateur

Jean VAN DEN DRIESSCHE : Université de Rennes I - Directeur de thèse

Philippe DAVY : Université de Rennes I - Co-directeur de thèse

REMERCIEMENTS

Je remercie tout d'abord les membres du jury d'avoir accepter d'examiner et d'évaluer ce travail : Jacques Deverchère (Université de Bretagne Occidentale), Peter van der Beek (Université Joseph Fourier), Jean Braun (Université de Rennes 1) et Wout Krijgsman (Universiteit Utrecht).

Ce travail a vu le jour grâce à la confrontation des idées des géomorphologues rennais que sont Jean Van Den Driessche et Philippe Davy. Merci Philippe de m'avoir accueilli dans l'univers des processus d'érosion et de la modélisation numérique. Merci à toi Jean d'être aller dénicher le plus bel exemple de chute du niveau de base, pas de chance il était en Méditerranée… Merci aussi de m'avoir initier au plaisir du terrain et des objets « grandeur nature » dans ton eldorado pyrénéen.

Merci aussi à tous les instigateurs de l'équipe rennaise de « géomorpho »: Alain, Stéphane et Dimitri ainsi qu'à mes acolytes directs : Julien et Jérôme ; ou reculés : Castor.
Je salue également tous mes condisciples présents ou passés du labo : Blez, Flo, Ben, Katia, Charly, Stéphanie, Pavel, Christelle, Rico, Miriam, Romain, Céline, Tanguy, Marie, Sylvie, Laure, Nolwenn, Jeroen, la délégation chilienne et j'en oublie ; ainsi qu'une mention spéciale à mes « collocs » de bureau d'hier et d'aujourd'hui: Steph et Oliv.

Enfin, je remercie ma famille pour leurs encouragements quotidiens tout au long de ces années, en particulier à mes deux soutiens de la rue de St Malo sans qui l'aventure aurait été bien difficile…

A Delphine et Marius

Résumé

Les variations du niveau de base entraînent une perturbation de la dynamique érosive d'un système continental. Une chute du niveau de base se traduit par la propagation d'une incision fluviatile vers l'amont entraînant un rajeunissement du paysage. Cette étude a pour but de montrer comment cette érosion affecte l'évolution d'un paysage, suivant les paramètres du système morphologique préexistant. Elle s'appuie sur un exemple préservé de chute du niveau de base de grande ampleur pendant la Crise de Salinité Messinienne en Méditerranée il y a 5.5 Ma. L'étude morphologique des incisions messiniennes couplée à une modélisation numérique montre qu'il existe une dichotomie entre la vitesse de croissance d'un réseau et ses effets sur l'évolution à long terme d'un paysage en présence d'une pente régionale préexistante. L'absence de pente régionale peut conduire à une modification drastique comme la capture de l'Atlantique au niveau de Gibraltar qui a entraîné la fin de la Crise Messinienne.

Abstract

Base-level variations involve a perturbation of the erosional dynamics of a continental system. A base-level drop results in the upstream propagation of an incision that rejuvenates the landscape. This work aims to show how this erosional stage will affect the evolution of a landscape, depending on the parameters of the preexisting morphological system. It is based on an example of preserved base-level drop of large amplitude, which occurred during the Mediterranean Messinian Salinity Crisis, 5.5 Ma ago. Morphological analysis combined with a numerical modeling show that there is a divergence between the network growth and its effects on the long-term evolution of a landscape due to the occurrence of a regional slope line. The absence of a regional slope line can result in a major change such as the capture of the Atlantic waters in the Gibraltar Strait area, inducing the end of the Messinian Salinity Crisis.

TABLE DES MATIÈRES

1. Introduction 1

2. Dynamique de l'érosion messinienne :
Propagation des incisions messiniennes en contexte morphologique « stable » 21

2.1. Le bassin versant du Rhône 27
Article 1: *Propagation of large length scale fluvial incision: Insight from the Messinian sea-level drop modelling* 29

2.2. Contrôle de l'aire drainée sur l'incision fluviatile : l'exemple de la Crise de Salinité Messinienne 63
Article 2: *Drainage area control on fluvial incision : the case of the Messinian Salinity Crisis (Mediterranean*) 65

2.3. Annexes à la partie 2 83

3. Dynamique de l'érosion messinienne :
Conséquences sur les zones morphologiquement « instables » 109

3.1. Propagation de l'incision messinienne dans le détroit de Gibraltar 115

3.1.1. Comment s'est terminé la Crise de Salinité Messinienne ? 115
Article 3: *How did the Messinian Salinity Crisis End ?* 117

3.1.2. Sur l'origine du détroit de Gibraltar 125
Article 4 : *On the Origin of the Strait of Gibraltar* 127

3.2. Propagation de l'incision messinienne dans le bassin de l'Ebre 163
Article 5 : *Does the Ebro river connect to the Mediterranean before the Messinian Salinity Crisis ?* 165

3.3. Annexes à la partie 3 187

4. Conclusion 195

Références 199

1. INTRODUCTION

Les paysages à la surface du globe sont façonnés par le réseau hydrographique au cours du temps. Ce dernier soustrait de la matière là où existent des excédents de masse (comme dans les zones orogéniques) pour la redéposer là où réside un déficit (mer, lac), ou encore lorsque il n'a plus l'énergie nécessaire pour transporter les produits d'érosion (c.a.d. lorsque la pente du réseau est nulle ou que le flux d'eau est nul). La dynamique érosive (E) est fonction de deux paramètres fondamentaux, que sont la pente (S) et le flux d'eau (Q) approchée par l'aire drainée amont (A). Dans la majorité des études récentes, cette loi physique s'exprime sous la forme (e.g. Howard and Kerby, 1983 ; Howard et al., 1994 ; Whipple and Tucker, 1999):

$$E = f\,(A^m * S^n)$$

m et n représentant des constantes positives. En schématisant, la pente est contrôlée par la tectonique, tandis que le flux d'eau est contrôlé par le climat, l'aire drainée étant contrôlée à la fois par les processus tectoniques, qui vont imposer la taille et la morphologie des bassins versants, et le climat qui contrôle la quantité d'eau circulant dans le bassin versant.

Un paradoxe existe en géomorphologie entre l'âge d'un paysage et celui de son réseau hydrographique. Un paysage jeune est un paysage présentant des vallées fortement incisées, un paysage vieux est un paysage présentant des collines et des vallées émoussées. L'âge d'un réseau est déterminé par la date à laquelle des rivières permanentes se sont installées (e.g. Potter, 1978). Si les réseaux hydrographiques sont responsables en grande partie du façonnement des paysages, les formes de ces derniers peuvent être héritées d'une évolution à long terme indépendante des réseaux hydrographiques actuels. C'est le cas par exemple des pénéplaines ré incisées. Aussi l'âge jeune ou vieux est une notion ambiguë : les paysages observables sont par définition actuels, et un paysage « vieux » fait référence à l'existence d'une « morphologie héritée », aujourd'hui en phase de rajeunissement plus ou moins intense par un réseau hydrographique. Dans le cas d'un paysage dit « jeune », les formes du paysage apparaissent directement liées aux réseaux hydrographiques actuels. Les paysages du nord-ouest et du sud-est de la France illustrent ce paradoxe : le nord-ouest de la France présente des paysages « vieux » et un réseau de drainage jeune (~1 Ma) tandis que le sud-est de la France présente des paysages « jeunes » et un réseau de drainage relativement plus vieux (plusieurs

Ma). En fait l'âge d'un réseau reflète celui de l'acquisition de l'orientation des pentes régionales, tandis que l'âge d'un paysage réfère à l'évolution de la rugosité de la topographie, c'est-à-dire à celle des pentes locales (ou encore des versants).

La marque d'une incision fluviatile, consécutive à une chute du niveau de base ou un soulèvement tectonique, permet d'intégrer cette information à la fois spatiale et temporelle quant à l'évolution d'un réseau hydrographique au cours du temps. Au-delà de la position qu'occupait jadis une rivière, elle peut en effet renseigner sur les paramètres qui ont contrôlé le développement d'un réseau, à savoir la pente et l'aire drainée. Deux cas de figures sont envisageables : (1) soit l'incision ne se superpose pas au réseau préexistant, elle correspond alors à la formation d'un nouveau réseau de drainage et témoigne d'un changement de pente régionale (cas d'une pénéplaine ré incisée), (2) soit elle réemprunte le réseau de drainage préexistant.

Le premier cas peut sembler au premier abord le plus propice à l'étude de la dynamique fluviatile puisque le développement du réseau se fait à partir d'une « remise à zéro » de la topographie, mais les processus d'érosion fluviatile étant par essence « destructeurs », la préservation des marqueurs (comme par exemples les terrasses) de cette dynamique reste aléatoire. Se placer dans le second cas revient à étudier la dynamique d'un système à travers sa réponse à une perturbation de son état d'équilibre. Il a par exemple été montré expérimentalement que la vitesse de ré-incision d'une rivière consécutivement à une chute de son niveau de base était contrôlée par l'aire drainée amont (Parker, 1977).

C'est donc dans ce second cas que nous nous sommes placés pour aborder la dynamique de l'érosion fluviatile. Nous avons choisi comme fil directeur de ce travail un exemple de chute de niveau de base « dramatique » qui s'est produit en Méditerranée il y a environ 5.5 Ma. Cet événement est connu sous le nom de « Crise de salinité messinienne » (Hsü et al., 1973a) du fait de l'important dépôt d'évaporites contemporain de cette chute. A cette époque, la Méditerranée, isolée de l'océan Atlantique, s'apparentait peu ou prou à un désert dont le niveau de base était situé 1500 m en contrebas du niveau actuel (Hsü et al., 1973b ; Hsü, 1983), tant et si bien que les réseaux hydrographiques, dont l'exutoire se trouvait sur le rivage méditerranéen, ont du s'adapter à ce brusque changement de conditions aux limites en incisant profondément le domaine continental depuis l'aval vers l'amont. Les incisions messiniennes ont fortement marqué le paysage en affectant à la fois une large gamme, quant à la dimension de bassins versants (entre 10^3 km² et 3.10^6 km²), et dans des

régions où les pentes régionales soit sont restées stables depuis le Miocène (vallée du Rhône, vallée du Nil) soit ont changé depuis cette même époque (Bétiques, Apennins).

Croissance des réseaux hydrographiques

La mise en place d'un réseau de drainage s'établit dès lors qu'une pente s'installe et qu'un flux d'eau circule sur celle-ci. Plusieurs modèles conceptuels de croissance de réseau ont été proposés (Glock, 1931 ; Horton, 1945 ; Schumm, 1956, Howard, 1971) (Figure 1) et modélisés (Parker, 1977 ; Schumm et al., 1987 ; Hasbargen and Paola, 2000 ; Pelletier, 2003). Cependant, ces modèles ne rendent pas compte de la vitesse de mise en place d'un réseau qui reste toujours énigmatique. Comme discuté précédemment, une manière de s'intéresser à la croissance d'un réseau est d'étudier le « rajeunissement » d'un relief qui, par définition, voit se surimposer un nouveau réseau sur le réseau préexistant en empruntant le même bassin de drainage. Seule la condition au limite va être modifiée, à savoir, le niveau de base[1] du bassin versant. Le rajeunissement est provoqué par la chute de ce niveau de base, imputable à une chute du niveau de la mer ou à son antagoniste à savoir un uplift tectonique. Dans le paysage, l'empreinte de ce nouveau réseau est facilement identifiable, elle se traduit par une incision marquée des rivières au sein d'une ancienne surface (surface d'érosion, terrasses marines, terrasses fluviatiles) (Figure 2).

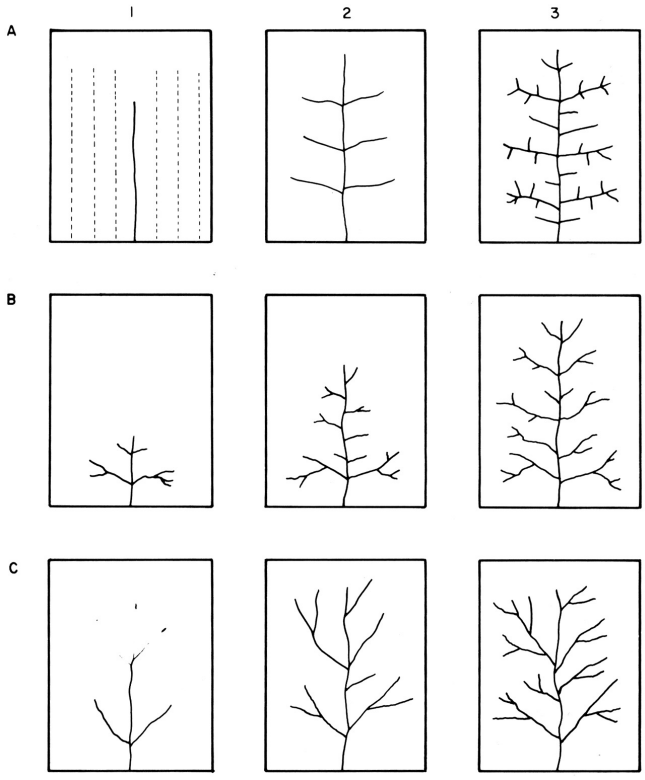

Figure 1 *: Modèles de croissance des réseaux hydrographiques (d'après Schumm et al., 1987)*
a : modèle de Horton (1945)
b :modèle « headward growth» (Schumm, 1956 ; Howard, 1971)
c : modèle d'expansion (Glock, 1931)

[1]Etant donné le paradigme résidant autour de ce terme, nous utilisons dans ce travail la notion de niveau de base sous sa forme la plus simple, telle que développée par Powell (1875), comme le niveau au dessous duquel le substratum ne s'érode plus. Ce niveau peut être le lit d'une rivière, un lac, un piedmont, le niveau de base ultime étant la mer.

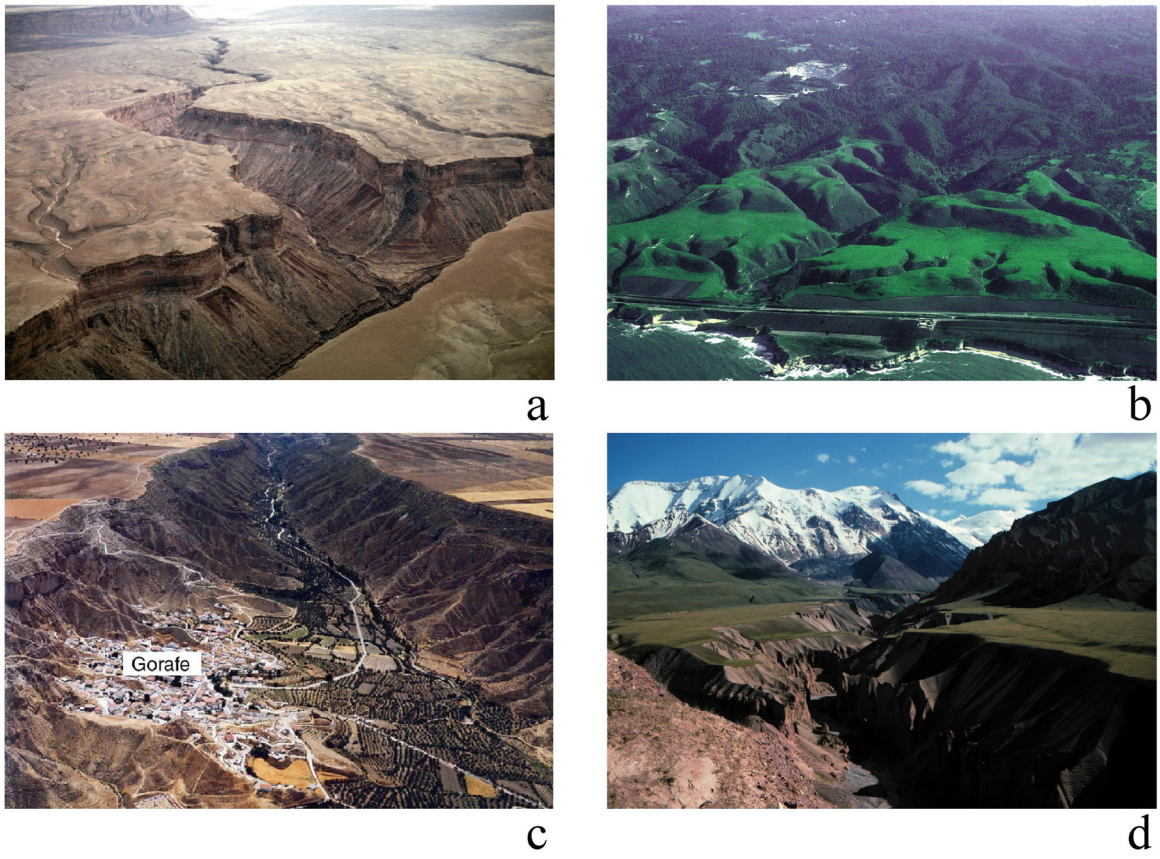

Figure 2 *: Exemples de rivières en incision (rajeunissement du relief) consécutif à une chute du niveau de base.*
a- Colorado River-Marble canyon, USA (photo : http://www.geology.wisc.edu/~maher/air/air00.htm)
b- Terrasses marines de Santa Cruz, USA (Rosenbloom et al., 1994) ; c- Vallée de l'Arroyo de Gor, Espagne (Azanon et al., 2005) ; d- Vallée du Minjar, Kyrgyzstan (Arrowsmith and Strecker, 1999)

L'érosion régressive des rivières est le processus le plus rapide développé par un système continental en réponse à une chute du niveau de base (e.g. Schumm et al., 1987 ; 1993). Plus la vitesse de chute du niveau de base est rapide, plus le paysage s'en trouvera rajeuni. La Figure 3 montre l'effet d'un changement de la vitesse d'uplift sur l'évolution d'un paysage.

A quantité égale de matière soulevée durant une période de temps donnée, le paysage ne présentera pas les mêmes stades d'évolution. Ceci traduit simplement la capacité du système continental à « absorber » un changement de conditions aux limites via la réponse érosive du système versant/rivière. Le système continental possède intrinsèquement un temps de réponse « τ ». Le rapport entre le temps pendant lequel le taux d'uplift perdure et le temps de réponse ($t_T/\ \tau$) va contrôler la morphologie du paysage (Figure 4). Si $t_T/\ \tau >> 1$, le forçage tectonique est beaucoup trop lent par rapport au temps de réponse et donc le paysage, même si son altitude moyenne ou son taux de dénudation varie, va conserver la même morphologie. Le taux de dénudation et le taux d'uplift vont évoluer étroitement de la même façon, l'érosion

contrebalançant au cours du temps l'uplift tectonique. A chaque instant, l'évolution de la morphologie est alors en contexte d'équilibre dynamique (e.g. Hack, 1960). Lorsque $t_T/\tau \sim 1$, l'érosion va dans les grandes lignes suivre l'évolution de l'uplift tectonique. Cependant, le taux d'érosion n'atteindra jamais l'amplitude atteinte par le taux d'uplift, de même qu'il présentera toujours un retard par rapport à ce dernier. Le paysage présentera donc des phases de croissance et de décroissance, comme l'a envisagé Penck (1924). A l'inverse, si $t_T/\tau << 1$, ou en considérant le cas limite d'un forçage instantané, le temps de réponse du système va permettre d'observer toutes les phases d'évolution d'un relief au sens de Davis (1899), à savoir « la jeunesse », « la maturité » et « la pénéplénation » du relief.

La présence d'un relief fortement incisé indique, en l'absence de fort contraste lithologique, la quasi-simultanéité d'une importante, et quasi instantanée, chute du niveau de base à l'échelle des temps géologiques. Ceci a par exemple permis à Baulig (1928) de proposer bien avant de disposer des données issues du Leg 13 en Méditerranéen (Ryan et al., 1973) que : "… tout s'est passé comme ci, conformément au schéma de Davis le mouvement relatif de la terre et de la mer avait été instantané… ", de sorte que ce dernier exclue : " l'idée que le rajeunissement fluvial peut se faire progressivement et à une allure assez lente pour que la dégradation des versants marche du même pas et maintienne constamment les formes dans un état de maturité … ".

La recherche et l'analyse de ces objets naturels, notamment depuis l'avènement des modèles numériques de terrain, renseignent sur l'état de déséquilibre des réseaux (e.g. Young and Mc Dougall, 1993 ; Seidl et al., 1994 ; Weissel and Seidl, 1998 ; Pazzaglia et al., 1998 ; Stock and Montgomery, 1999). Le degré de croissance d'un réseau de drainage pourra être apprécié par la position des têtes d'incision, des ruptures de pente dans le profil (knickpoints), ou de l'extension maximale des terrasses dans le réseau hydrographique. Les processus de migration opèrent à des vitesses qui sont extrêmement variables, mais qui semblent en général assez lentes (entre 0.001 et 0.1 m/an) lorsque l'on se place à de longues échelles de temps (10^5-10^6 années) (e.g. Van Heijst and Postma, 2001 ; Figure 5). En transposant ces valeurs moyennes à de grands bassins versants, on obtient des durées de migration pour atteindre les limites amont du bassin versant comprises entre 10^6 et 10^8 années pour des rivières mesurant 100 Km, et comprises entre 10^7 et 10^9 années pour des rivières mesurant 1000 Km.

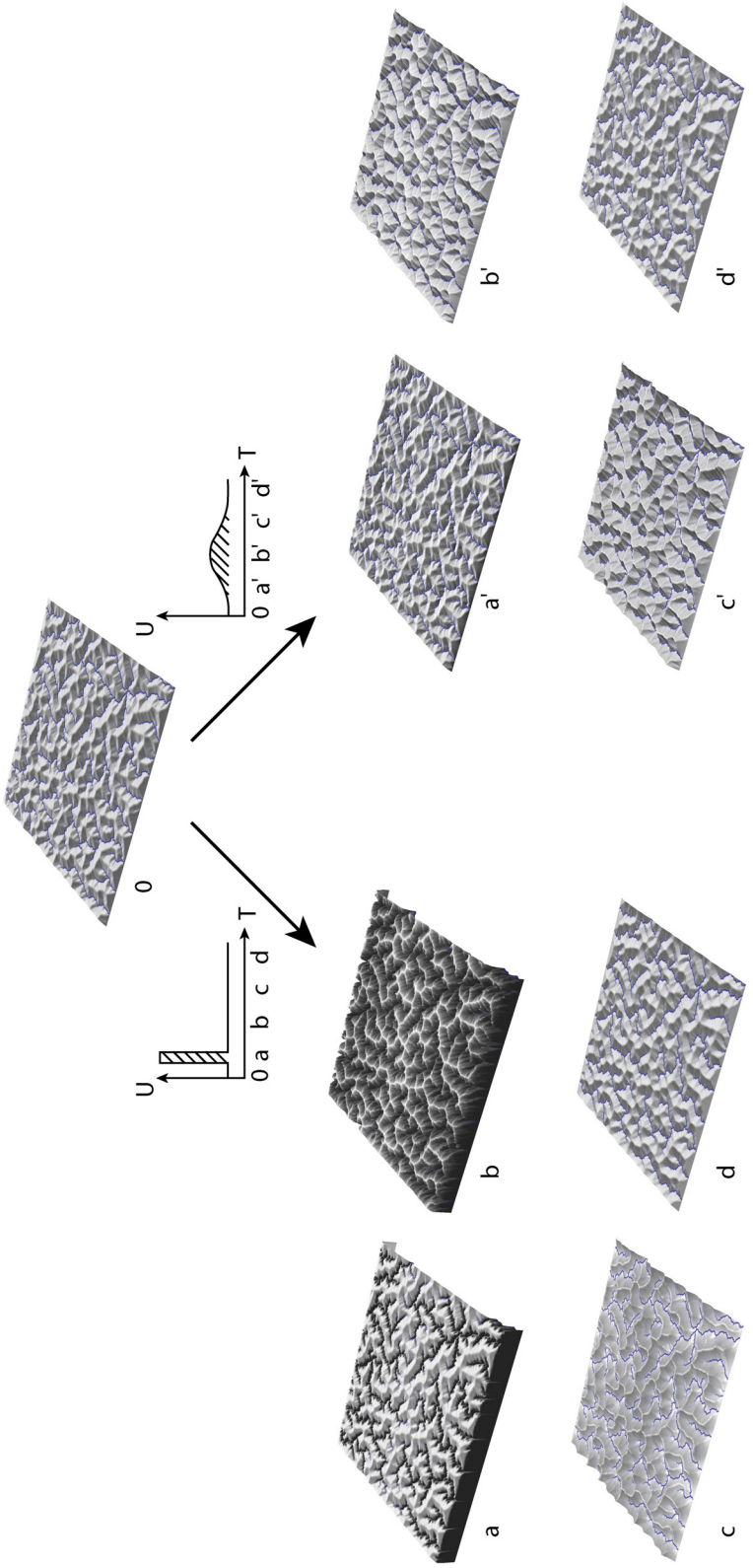

***Figure 3** : Simulations numériques représentant l'évolution d'un paysage pour une même quantité d'uplift introduite dans le modèle (hachures) mais à des vitesses différentes. Le modèle de gauche permet d'observer un rajeunissement marqué du paysage tandis que le modèle de droite présente un paysage qui s'adapte continuellement (modèle EROS développé par P.Davy).*

Ces temps de réponse sont excessifs puisque une grande partie des rivières mondiales présentent des profils de rivière globalement concaves, même dans les orogènes actives (Taïwan, Nouvelle Zélande). Les temps de réponse des rivières et des systèmes géomorphologiques estimées sont plutôt autour de 10^6 années (Tucker and Slingerland, 1996 ; Ellis et al., 1999 ; Whipple, 2001). Afin d'adapter leur profil d'équilibre, les grandes rivières disposent nécessairement de processus plus rapides que ce que l'on peut mesurer simplement à partir des vitesses de migration de knickpoints. Les variations eustatiques du Quaternaire semblent indiquer que les rivières peuvent répondre loin sans présenter de knickpoints dans les rivières (e. g. Van Heijst and Postma, 2001). Par exemple, le Mississippi a enregistré la migration d'une incision, consécutive à la chute eustatique de la dernière glaciation, estimée entre 300 Km et 1000 Km en amont de la ligne de côte actuelle (Fisk, 1944 ; Saucier, 1996). D'un autre côté, les canyons messiniens en Méditerranée ont migré sur des distances, en s'éloignant de leurs côtes respectives, allant de plusieurs dizaines de kilomètres dans le Languedoc, à 300 Km dans la vallée du Rhône jusqu'à plus de 1000 Km dans la vallée du Nil (Chumakov, 1973 ; Clauzon, 1982, Ambert, 1998). La période d'activité de ces canyons est estimée entre 10^5 et 3.10^5 années (Clauzon, 1996 ; Krijgsman, 1999) impliquant des vitesses de migration pouvant atteindre 1 à 3 m/an dans la vallée du Rhône et 3.3 à 10 m/an dans la vallée du Nil. La capacité de migration des incisions, à travers l'étude des knickpoints, est vraisemblablement sous estimée et les rivières sont capables de transmettre un signal très loin en amont (sur plusieurs centaines de kilomètres) dans un temps largement inférieur au million d'années, expliquant pourquoi la plupart des rivières mondiales présente des profils plus ou moins équilibrés.

Le retour à un profil d'équilibre total peut s'avérer, en revanche, un processus très long (plusieurs millions ou dizaines de millions d'années) si l'on se réfère à l'évolution des marges continentales en Afrique du Sud ou en Australie (Kooi and Beaumont, 1994 ; Brown et al., 2002 ; Van Der Beek et al., 2002). De la même manière, il ne faut pas confondre la notion de profil d'équilibre (graded profile) et l'équilibre dynamique, ce dernier étant un processus bien plus long, car il demande l'adaptation complète du réseau (rivières et versants).

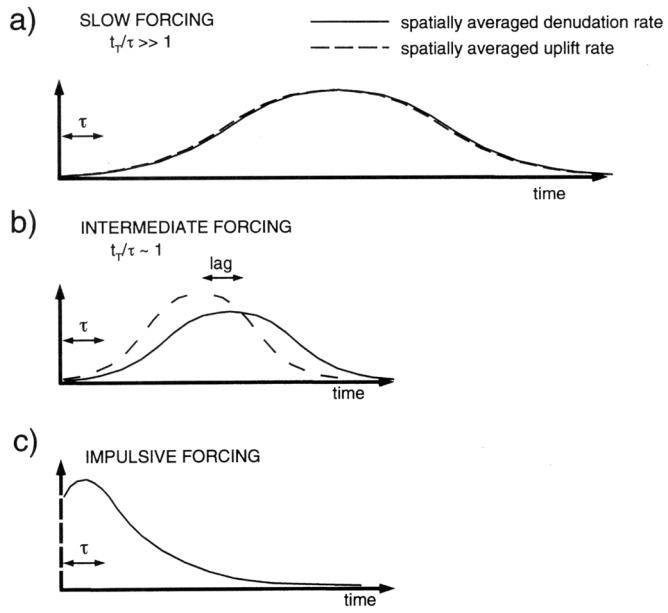

Figure 4 *: Influence du forçage tectonique sur la réponse du système géomorphologique (d'après Beaumont, 2000)*

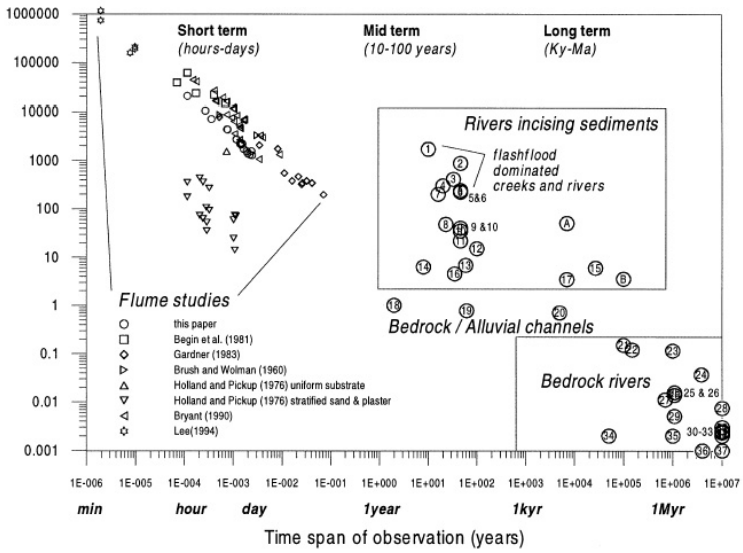

Figure 5 *: Vitesses de migration d'une incision suivant l'échelle de temps considérée (d'après Van Heijst and Postma, 2001).*

Average knickpoint migration rates plotted against the time scale of their occurrence (observation). The graph does not intend to show a numerical relation, but illustrates the order of magnitude of knickpoint migration rates in flumes and various rivers. In the graph we plotted average retreat rates, although it is known (Gardner, 1983; Leeder & Stewart, 1996) and also observed from our flume experiments that knickpoint migration rates decrease from an initially high value. Bedrock rivers typically adjust their profiles with knickpoint migration rates between 0.001 and 0.1 m yr^{-1} while short-term river adjustment indicates values between 100 and 1000 m yr^{-1}. Knickpoint migration rates on alluvial plain and shelves that accommodate 100-kyr glacio-eustatic sea-level changes are inferred to range from 1 to 70 km kyr^{-1}. The symbols represent data of flume studies (Brush & Wolman, 1960; Holland & Pickup, 1976; Begin *et al.*, 1981; Gardner, 1983; Bryan, 1990; Lee & Hwang, 1994). A and B are model estimates for knickpoint migration during the Wisconsin glaciation of the Mississippi River from Salter (1993) and Leeder & Stewart (1996), respectively. The numbers represent river data from: 1 West Tennessee channels (Simon, 1991); 2 Homochitto River (Yodis & Kesel, 1993); 3 Dry Creek (Begin, 1988); 4 Deep Creek (Schumm *et al.*, 1996); 5 St. Catharine Creek (Yodis & Kesel, 1993); 6 Homochitto tributaries (Yodis & Kesel, 1993); 7 Pechahalee Creek (Begin, 1988); 8 Crawfords Creek (Begin *et al.*, 1981); 9 St. Catharine Creek tributaries (Yodis & Kesel, 1993); 10 Harding Bayou (Yodis & Kesel, 1993); 11 Spanish Bayou (Yodis & Kesel, 1993); 12 Saikawa River (Begin, 1988); 13 Pleasant Valley, Nevada (Begin, 1988); 14 Oaklimiter Creek (Begin, 1988); 15 Indus (Leland *et al.*, 1998); 16 Wolf Creek (Eaton, 1991); 17 Mattole River (Pazzaglia *et al.*, 1998); 18 Blue Hills channels (Dick *et al.*, 1997); 19 Gully near Imlay, Nevada (Begin, 1988); 20 Niagara Falls (Wohl, 1998); 21 South River (Bank & Harbor, 1998); 22 Rio Jemez (Pazzaglia *et al.*, 1998); 23 Rappahannock River (Howard *et al.*, 1994); 24 Susquehanna (Pazzaglia *et al.*, 1998); 25 Swede (Stock & Montgomery, 1999); 26 French (Stock & Montgomery, 1999); 27 Amargosa River (Butler, 1984); 28 Tumut River (Young & McDougall, 1993); 29 Cowlet (Stock & Montgomery, 1999); 30 Tumbarumba Creek (Young & McDougall, 1993); 31 Wheeo Creek (Stock & Montgomery, 1999); 32 Shoalhaven River (Nott *et al.*, 1996); 33 Paddys River (Young & McDougall, 1993); 34 Dabang River (Yang & Li, 1988); 35 Maclean River (Weissel & Seidl, 1997); 36 Hawaiian channels (Seidl *et al.*, 1994); 37 Boggy Creek (Young & McDougall, 1993).

Stabilité et pérennité des réseaux de drainage

La chute du niveau de base d'une rivière permet de marquer l'empreinte du réseau de drainage dans laquelle cette dernière évoluait avant cet événement. Ceci pose indirectement la question de la durée de vie des paysages et des réseaux de drainage ainsi que leur pérennité à l'échelle des temps géologiques. La perspective humaine soulève un paradoxe quant à cette question. Tant à l'échelle humaine la déstabilisation d'un réseau hydrographique apparaît difficile à envisager, tant à l'échelle des temps géologiques (plusieurs millions d'années) la stabilité d'un réseau demeure délicate à démontrer. Cependant, l'enregistrement sédimentaire des bassins où se jettent les grands fleuves comme l'Amazone, le Mississipi, le Nil, le Gange tend à prouver que de nombreux systèmes de drainage sont en place depuis plusieurs millions d'années voire dizaines de millions d'années (e.g. Audley-Charles et al., 1977 ; Potter, 1978 ; Cox, 1989 ; Summerfield and Hulton, 1994 ; Potter, 1997 ; Hallet and Molnar, 2001)(Figure 6).

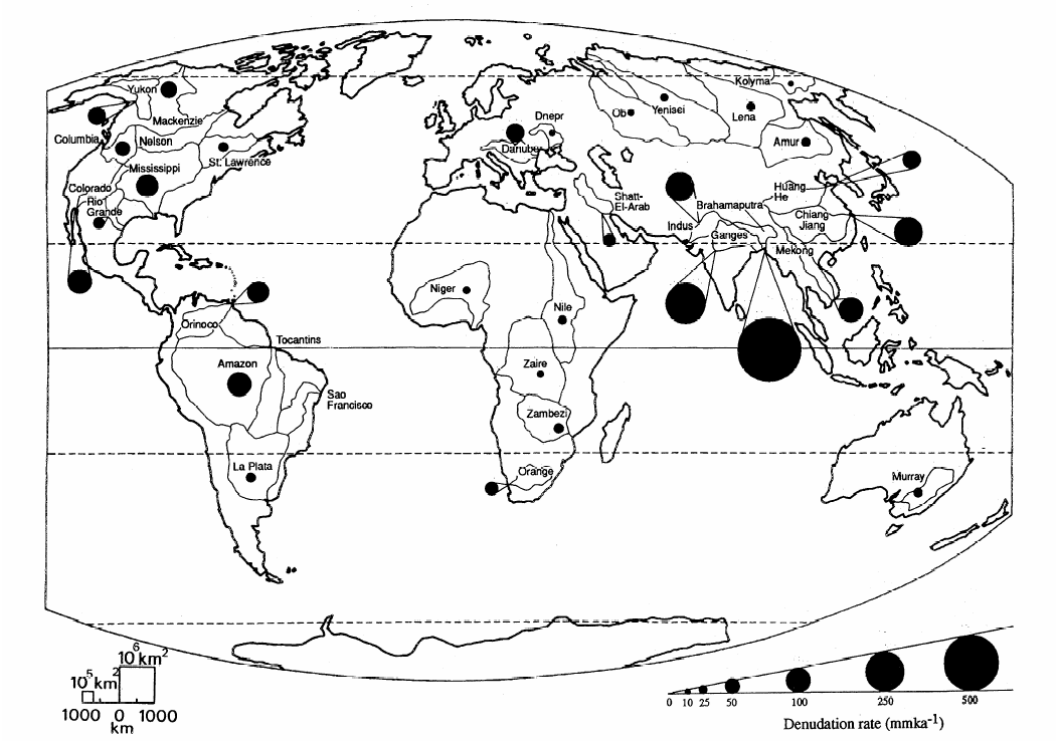

***Figure 6** : Localisation et estimation des taux de dénudation des grands bassins versants actuels. Ces valeurs sont, dans de nombreux endroits, comparables aux taux de dénudation à long terme estimés à partir de données de volumes sédimentaires et thermochronologiques renseignant ainsi sur l'âge des bassins versants (d'après Summerfield and Hulton, 1994).*

La période relative à l'origine d'une rivière peut être définie comme la date la plus précoce où une rivière permanente va s'installer (Potter, 1978). A l'échelle des temps géologiques, la position d'une rivière peut être assimilée au bassin versant originel, imposé par la tectonique, dans lequel cette rivière s'est installée. A tectonique constante, c'est-à-dire sans changement de direction de la ligne de plus grande pente, on peut dire que « la rivière va évoluer dans une dépression dont elle ne peut s'échapper » (Brunsden, 1993). Dans une vallée encaissée, cette notion est intuitive, elle l'est, en revanche, beaucoup moins dans une vallée très large (Figure 7). Quels sont alors les paramètres qui vont permettre à la rivière de « sortir » de son bassin versant initial ? La figure 8 montre diverses manières de déplacer transversalement une rivière. Trois schémas sont envisageables : (1) combler, (2) basculer ou (3) aplanir la vallée initiale.

(1) Le comblement est lié à une phase d'aggradation, c'est-à-dire d'une remontée du niveau de base. Ce phénomène peut avoir une extension régionale, notamment lors d'événements eustatiques, mais il faudrait alors envisager un ré ennoiement complet de tout le système continental afin d'aplanir totalement le relief (comme au Crétacé par exemple). Or, une partie du domaine continental reste généralement émergé, en particulier dans les chaînes de montagne. La pente régionale va très vite réimposer sa direction d'écoulement et le drainage va se réinstaller à proximité immédiate des vallées initiales ou même réemprunter son cours initial.

(2) Le basculement de la vallée est lié à des mouvements tectoniques dont l'amplitude doit être supérieur au relief de celle-ci. Si ce phénomène reste local, la vallée va se déplacer à proximité. En revanche, s'il s'agit d'un mouvement à grande échelle, la vallée va migrer au cours du temps de plus en plus loin par rapport à sa position initiale en enregistrant possiblement des modifications de son bassin de drainage (phénomènes de capture). A terme, si la ligne de plus grande pente se réoriente dans la même direction, les rivières vont se mettre à couler transversalement par rapport à leur direction initiale.

(3) L'aplanissement de la vallée consiste à détruire progressivement les lignes de crête qui la bordent pour aboutir à la genèse d'une pénéplaine dont l'altitude est proche du niveau de la mer (Davis, 1899). Ce processus est extrêmement long car la dégradation des crêtes est de loin le processus le plus long en géomorphologie. Néanmoins, la dynamique de ce processus peut être décuplée si intervient une calotte glaciaire. Si l'un des deux mouvements précédemment cités rentre alors en action, le réseau hydrographique pourra aisément être

modifié, même par des mouvements de faible amplitude. C'est ce que l'on enregistre par exemple dans le nord ouest de la France au cours du Plio-Pléistocène (Vilaine, Loire, Seine). Finalement, et ceci peut paraître comme paradoxal, les zones orogéniques (instables verticalement) présentent des réseaux plus stables à long terme que les zones pénéplanées (stables verticalement) car les rivières sont « prisonnières » de leur vallées primitives.

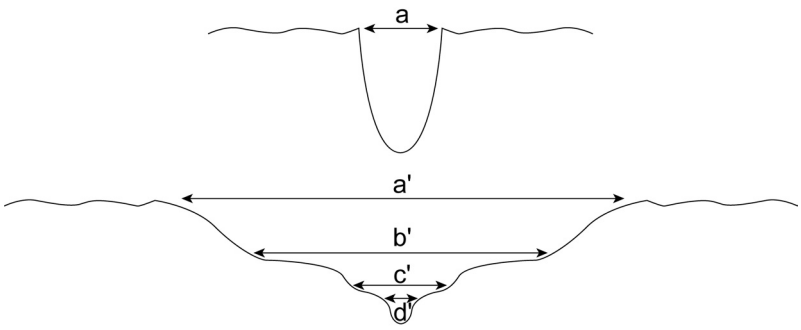

***Figure 7** : Détermination de la largeur de divagation d'une rivière. Une vallée encaissée définie une valeur maximale unique (a) tandis qu'une vallée large entrecoupée de niveaux de terrasses propose plusieurs largeurs (d', c', b', a'). Quelle est, à l'échelle des temps géologiques, la largeur la plus pertinente ?*

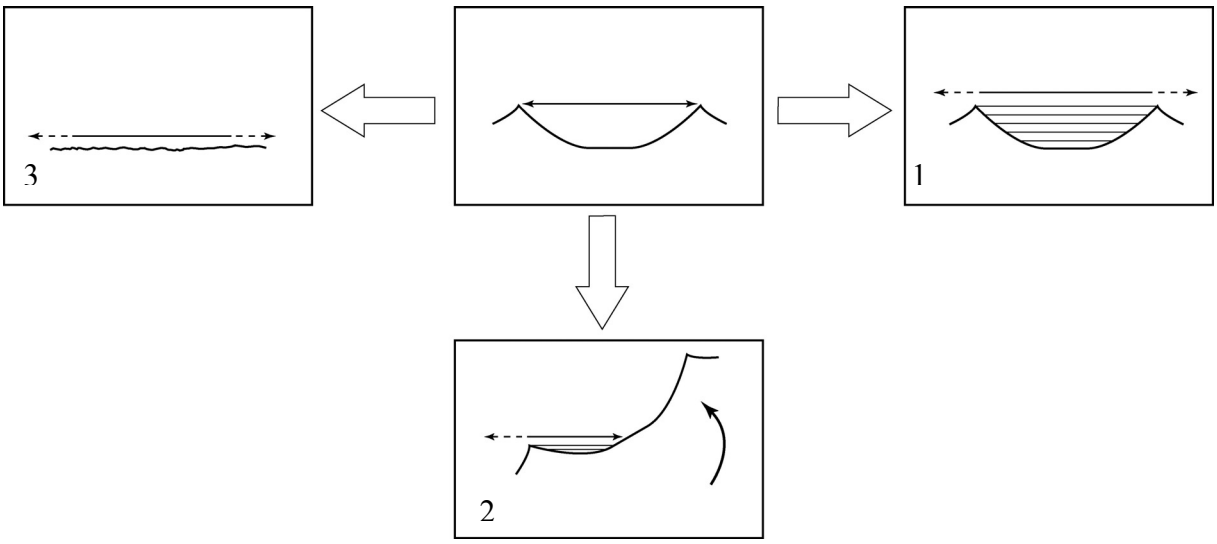

***Figure 8** : Mécanismes mis en jeu dans la migration transversale d'une rivière. 1-Comblement ; 2-Basculement ; 3- Aplanissement*

Le canyon du Rhône ennoiement et d'une manière générale, les canyons incisés du sud de la France, illustrent parfaitement ce paradoxe (Figure 9). Après avoir incisé sur plusieurs centaines de mètres, le canyon du Rhône a été entièrement comblé par des dépôts pliocènes suite à une remontée du niveau de base de plus de 1500 m. Pourtant, le Rhône actuel réemprunte quasiment le même tracé depuis Lyon jusqu'en Camargue, démontrant la contrainte établie par les pentes régionales (Alpes et Massif Central) sur l'évolution du réseau rhodanien depuis la fin du Miocène. Par conséquent, la vallée du Rhône peut être définie comme une zone morphologiquement stable depuis la fin du Miocène. A l'inverse, les canyons incisées qui ont incisé là où les pentes régionales ont fortement évolué depuis la fin du Miocène (Bétiques, Bassin de l'Ebre, Apennins) témoignent de peu d'affinité avec les réseaux actuels, du à des mouvements tectoniques à grande échelle issus de la convergence entre les plaques Afrique et Europe. Notamment, dans ces zones, les réseaux hydrographiques présentent toujours des phénomènes de capture. Nous les définirons comme des zones morphologiquement instables depuis la fin du Miocène.

Le présent mémoire s'organise en deux parties :

La première partie s'intéresse à la croissance des réseaux hydrographiques via l'étude d'incisions messiniennes dans des zones morphologiquement stables depuis le Miocène. Cette partie comprend deux articles en cours de soumission. S'appuyant sur une modélisation numérique, le premier article vise à comprendre le mode de propagation des incisions à grande échelle de temps (10^5-10^6 ans) et d'espace (plusieurs centaines de kilomètres) en se basant sur l'exemple du Rhône ennoiement Le second article s'intéresse plus particulièrement au contrôle de l'aire drainée amont sur la propagation des incisions, dans le cas des incisions messiniennes mais aussi dans un cadre plus général ;

La seconde partie a pour bout de montrer les conséquences de la chute ennoiement dans les zones morphologiquement instables. Le troisième article (sous presse) s'intéresse à la propagation de l'incision ennoiement au voisinage du détroit de Gibraltar (zone que l'on suppose plane, donc sans véritable pente régionale à la fin du Miocène). En s'appuyant sur une modélisation numérique, nous montrons que de façon quasi inévitable, un réseau de canyons se développe induisant la capture des eaux atlantiques et le ré ennoiement consécutif de la Méditerranée au début du Pliocène, constituant une alternative aux autres modèles proposés pour l'ouverture du détroit de Gibraltar (tectonique, eustatisme). Le quatrième article (accepté, en cours de correction) vise à évaluer la pertinence des autres modèles proposés, notamment l'hypothèse tectonique, pour l'ouverture du détroit de Gibraltar. Nous

montrons que, bien qu'étant une structure topographique majeure, aucune étude n'a montré que celle-ci correspondait à une quelconque structure tectonique précoce du Pliocène. Le cinquième article (soumis) s'intéresse aux modalités et à l'âge de la connexion du bassin de l'Ebre à la Méditerranée et le rôle de l'incision messinienne sur celle-ci. Il conclut à une connexion au cours du Pliocène.

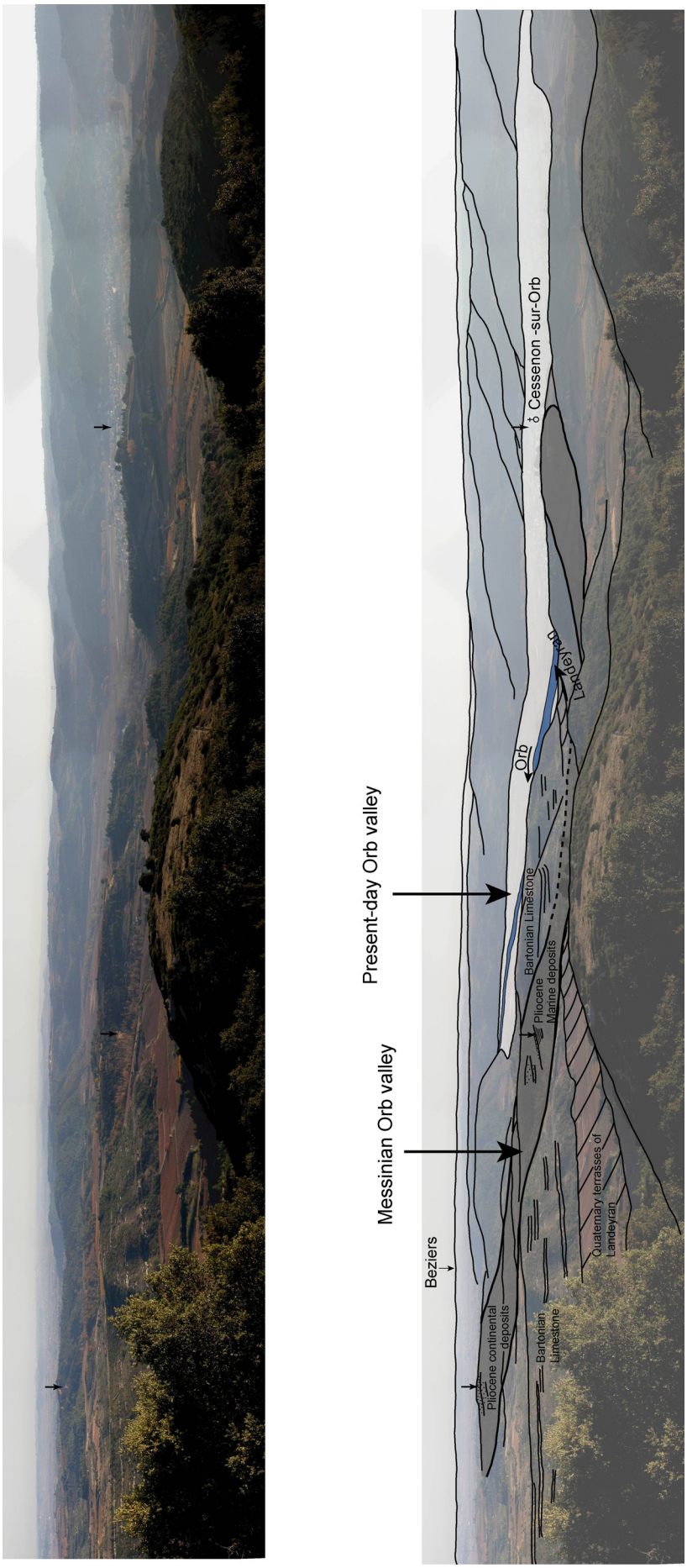

***Figure 9** : Exemple de juxtaposition des vallées messiniennes et des vallées actuelles dans la vallée de l'Orb montrant l'influence de la pente régionale sur le développement des vallées du Sud de la France depuis la fin du Miocène.*

Références

Ambert, P., Aguilar, J.P., and Michaux, J., 1998. Evolution géodynamique messinio-pliocène en Languedoc central : le paléo-réseau hydrographique de l'Orb et de l'Hérault (sud de la France). *Geodin. Acta*, **11**, 139–146.

Arrowsmith, J R., and Strecker, M. R., 1999. Seismotectonic range-front segmentation and mountain-belt growth in the Pamir-Alai region, Kyrgyzstan (India-Eurasia collision zone). *Geol. Soc. Am. Bull.*, **111**, 1665–1683.

Audley-Charles, M.G., Curray, J.R., and Evans, G., 1977. Location of major deltas. *Geology*, **5**, 341–344.

Azanon, J.M., Azor, A., Perez-Pena, J.V., and Carrillo, J.M., 2005. Late Quaternary large-scale rotational slides induced by river incision: The Arroyo de Gor area (Guadix basin, SE Spain). *Geomorphology*, **69**, 152–168.

Baulig, 1928. Le Plateau central de la France et sa bordure méditerranéenne, Thesis, Paris, 591 pp.

Beaumont, C., Kooi, H., and Willett, S., 2000. Coupled tectonic-surface process models with applications to rifted margins and collisional orogens. In *Geomorphology and global tectonics*, edited by Summerfield, M.A., John Wiley, pp. 29–55.

Brown, R.W., Summerfield M.A., and Gleadow A.J.W., 2002. Denudational history along a transect across the Drakensberg Escarpment of southern Africa derived from apatite fission track thermochronology. *J. Geophys. Res.*, **107 (B12)**, 2350, doi:10.1029/2001JB000745.

Brunsden, D., 1993. The persistence of landforms. *Z. Geomorphol. Suppl.*, **93**, 13–28.

Chumakov, I.S., 1973. Pliocene and Pleistocene deposits of the Nile valley in Nubia and upper Egypt. In: *Initial reports of the Deep Sea Drilling Project*, **13**, pp. 1242–1243, US Govern. Print. Office, Washington, DC.

Clauzon, G., 1982. Le canyon messinien du Rhône : une preuve désicive du "dessicated deep basin model" (Hsü, Cita et Ryan, 1973). *Bull. Soc. Géol. Fr.*, **24**, 231–246.

Clauzon, G., Suc, J.P., Gautier, F., Berger, A., and Loutre, M.F., 1996. Alternate interpretation of the Messinian salinity crisis : Controversy resoved? *Geology*, **24**, 363–366.

Cox, K.G., 1989. The role of mantle plumes in the development of continental drainage patterns. *Nature*, **342**, 873–877.

Davis, W.M., 1899. The geographical cycle. *Geogr. J.*, **14**, 481–504.

Ellis, M.A., Densmore, A.L. and Anderson, R.S. 1999. Development of mountainous topography in the Basin Ranges, U.S.A. *Basin Res*, **11**, 21–41.

Fisk, H.N., 1944. Geological Investigation of the Alluvial Valley of the Lower Mississippi River. Mississippi River Commission, Vicksburg.

Glock, W.S., 1931. The development of drainage systems: a synpotic view. *Geogr. Rev.*, **21**, 475–482.

Hack, 1960. Interpretation of erosional topography in humid temperature regions. *Am. J. Sci.*, **258-A**, 80–97.

Hallet, B., and Molnar, P., 2001. Distorted drainage basins as markers of crustal strain east of the Himalaya. *J. Geophys. Res.*, **106**(B7), 13,697–13,710.

Hasbargen, L.E. and Paola, C., 2000. Landscape instability in an experimental drainage basin. *Geology*, **28**, 1067–1070.

Horton, R.E., 1945. Erosional development of streams and their drainage basins: hydrophysical approach to quantitative morphology. *Geol. Soc. Am. Bull.*, **56**, 275–370.

Howard, A.D., 1971. Optimal angles of stream junction: geometric, stability to capture, and minimum power criteria. *Water Resour. Res*., **7**, 863–873.

Howard, A.D., and Kerby G., 1983. Channel changes in badlands. *Geol. Soc. Am. Bull.*, **94**, 739–752.

Howard, A.D., Dietrich, W.E., and Seidl, M.A., 1994. Modeling fluvial erosion on regional to continental scales. *J. Geophys. Res.*, **99**, 13,971–13,986.

Hsü, K.J., Cita, M.B., and Ryan, W.B.F., 1973a. The origin of the Mediterranean evaporites. In *Initial reports of the deep sea drilling project*, **13**, pp 1203–1231, US Govern. Print. Office, Washington, DC.

Hsü, K.J., Ryan, W.B.F., and Cita, M.B., 1973b. Late Miocene dessication of the Mediterranean. *Nature*, **242**, 240–244.

Hsü, K.J., 1983. *The Mediterranean was a Desert. A Voyage of the Glomar Challenger*. Princeton University Press, Princeton, NJ, 183 pp.

Kooi, H., and Beaumont C., 1994. Escarpment evolution on high-evelvation rifted margins: Insights derived from a surface processes model that combines diffusion, advection, and reaction. *J. Geophys. Res.*, **99**, 12,191–12,209.

Krijgsman, W., Hiigeni, F.J., Raffi, I., Sierro, F.J., and Wilson, D.S., 1999. Chronology, causes and progression of the Messinian salinity crisis. *Nature*, **400**, 652–655.

Parker, R.S., 1977. Experimental study of basin evolution and its hydrologic implications. *unpublished PhD dissertation*, Colorado State University, Fort Collins, 331 pp.

Pazzaglia, F.P., Gardner, T.W. and Merritts, D.J., 1998. Bedrock Fluvial incision and longitidinal profile development over geologic time scales determined by fluvial terraces. In *Rivers Over Rock: Fluvial Processes in Bedrock Channels*, *Geophys. Monogr. Ser.*, **107**, edited by K. J. Tinkler and E. E. Wohl, pp. 207–235, AGU, Washington, D. C.

Pelletier, J.D., 2003. Drainage basin evolution in the Rainfall Erosion Facility: dependence on initial conditions. *Geomorphology*, **53**, 183–196.

Penck, W., 1924. Die Morphologische Analyse: Ein Kapital der Physikalischen Geologie. Engelhorn, Stuttgart, Germany, 283 pp.

Potter, P.E. 1978. Significance and origin of big rivers. *J. Geol*, **86**, 13-33.

Potter, P.E., 1997. The Mesozoic and Cenozoic paleodrainage of South America: a natural history. *J. South Am. Earth Sci*., **10**, 331–344.

Powell, J.W. 1875. Exploration of the Colorado River of the West, US Government Printing Office, Washington, DC, 400 pp.

Rosenbloom, N.A., and Anderson, R.S., 1994. Hillslope and channel evolution in a marine terraced landscape, Santa Cruz, California. *J. Geophys. Res.*, **99**, 14,013–14,029.

Ryan, W.B.F., Hsü, K.J. et al., 1973. *Initial reports of the Deep Sea Drilling Project*, **13**, US Govern. Print. Office, Washington, DC., 1447 pp.

Saucier, R.T., 1996. A contemporary appraisal of some key Fiskian concepts with emphasis on Holocene meanderbelt formation and morphology. *Engineering Geol.*, **45**, 67–86.

Schumm, S.A., 1956. Evolution of drainage systems and slopes in badlands at Perth Amboy, New Jersey. *Geol. Soc. Am. Bull.*, **67**, 597–646.

Schumm, S.A., Mosley, M.P., and Weaver, W.E., 1987. *Experimental fluvial geomorpholgy*. New York, Wiley, 413 pp.

Schumm, S.A., 1993. River response to baselevel change: Implications for sequence stratigraphy. *J. Geology*, **101**, 279–294.

Seidl, M.A., Dietrich, W.E. and Kirchner J.W., 1994. Longitudinal profile development into bedrock: An analysis of Hawaiian channels. *J. Geol.*, **102**, 457–474.

Stock, J.D., and Montgomery, D.R., 1999. Geologic constraints on bedrock river incision using the strem power law. *J. Geophys. Res.*, **104**, 4983–4993.

Summerfield, M.A., and Hulton, N.J., 1994. Natural controls of fluvial denudation rates in major world drainage basins. *J. Geophys. Res.*, **99**, 13,871–13,883.

Tucker, G., and Slingerland R., 1996. Predicting sediment flux from fold and thrust belts. *Basin Res*., **8**, 329–349.

Van der Beek, P., Summerfield, M.A., Braun, J., Brown, R.W., and Fleming A., 2002. Modeling postbreakup landscape development and denudational history across the southeast African (Drakensberg Escarpment) margin. *J. Geophys. Res.*, **107 (B12)**, 2351, doi:10.1029/2001JB000744.

Van Heijst, M.W.I.M., and Postma G., 2001. Fluvial response to sea-level changes: a quantitative analogue, experimental approach. *Basin Res.*, **13**, 269–292.

Weissel, J.K., and Seidl M.A., 1998. Inland propagation of erosional escarpments and river profile evolution across the southeast Australian passive continental margin. In *Rivers Over Rock: Fluvial Processes in Bedrock Channels*, *Geophys. Monogr. Ser*., **107**, edited by K. J. Tinkler and E. E. Wohl, pp. 189–206, AGU, Washington, D. C.

Whipple, K.X., 2001. Fluvial landscape response time: How plausible is steady-state denudation? *Am. J. Sci*., **301**, 313–325.

Whipple, K.X., and Tucker, G.E., 1999. Dynamics of the stream-power river incision model: Implications for height limits of mountain ranges, landscape response timescales, and research needs. *J. Geophys. Res.*, **104**, 17,661–17,674.

Young, R.W., and McDougall, I., 1993. Long-term landscape evolution: Early Miocene and modern rivers in southern New South Wales, Australia. *J. Geol*., **101**, 35–49.

2. Dynamique de l'érosion messinienne : Propagation des incisions messiniennes en contexte morphologique « stable ».

Cette première partie s'intéresse à la dynamique de l'érosion fluviatile consécutive à une chute du niveau de base. Elle s'articule autour de deux articles:

Le premier a pour but de modéliser, à l'aide d'un simulateur numérique développé par P. Davy, la réponse d'une rivière messinienne consécutive à la chute de 1500m du niveau de la Méditerranée lors de la Crise de Salinité Messinienne. L'exemple choisi est la vallée du Rhône messinienne en raison de la remarquable préservation des canyons messiniens ainsi que de la densité des prospections effectuées depuis plus d'un siècle, permettant une reconstitution de l'incision messinienne.
La comparaison entre simulations numériques et données géologiques permet d'évaluer le rôle des paramètres influant sur la dynamique de l'érosion lors d'une phase de ré-incision d'un réseau hydrographique et de les quantifier.
Il en ressort que l'incision messinienne est dépendante non linéairement du flux d'eau (ou encore de l'aire drainée amont), ainsi que d'une faible longueur de transport des sédiments dans la rivière. Cette faible longueur de transport suggère que l'évolution du profil du Rhône s'est réalisée de manière diffusive, et que la rupture de pente initiale (knickpoint) consécutive à la chute du niveau de base n'a ainsi pas été préservée et s'est progressivement atténuée en progressant vers l'amont.
Le ré-ennoyage brutal de toute la Méditerranée au début du Pliocène a permis de fossiliser cette topographie en incision grâce à une sédimentation détritique en masse (Gilbert deltas), si bien que la durée de l'incision messinienne n'a pas excédé 90 à 300 ka. Cette tranche de temps représente un stade incrémental de l'évolution à long terme (plusieurs millions voire dizaines de millions d'années) d'escarpements kilométriques présents le long de marges continentales liées à un épisode de rifting. En s'appuyant sur l'exemple messinien, nous suggérons que le comportement précoce des marges continentales (~100 ka), consécutivement à une chute du niveau de base, est de nature diffusive et se transmet très loin dans le système amont.

Le second article s'intéresse à la propagation de l'incision messinienne à l'échelle de toute la Méditerranée. Nous montrons, à partir de la mesure de nombreuses incisions sur le pourtour méditerranéen, que la distance à laquelle se sont propagées ces incisions sont reliées par une loi de puissance aux aires drainées des bassins versants actuels dans lesquels elles apparaissent respectivement. Cette relation montre que la taille des bassins versants au

moment de la Crise de Salinité Messinienne était similaire à la taille des bassins versants actuels.

L'exemple messinien montre en outre que :

(1) La vitesse de propagation d'une incision est proportionnelle à la racine carrée de l'aire drainée amont ;

(2) l'aire drainée est le paramètre qui contrôle la distance de propagation des incisions. Les autres facteurs tels que la lithologie, la végétation ou les effets de seuil ne sont pas perceptibles aux échelles de temps et d'espace considérées (10^5ans, 10^3-10^6km²) ;

(3) les grandes rivières ont une capacité à transmettre un changement de conditions aux limites très en amont dans le système même sur un court laps de temps (~100 ka).

Simulation numérique de l'érosion enregistrée dans la vallée du Rhône lors de la chute du niveau de base de 1500 m de la Méditerranée pendant la Crise de Salinité Messinienne.

2.1. Propagation de l'incision en contexte morphologique stable : le bassin versant du Rhône.

Article :

Propagation of large length scale fluvial incision: Insight from the Messinian sea-level drop modelling.

Nicolas loget, Philippe Davy, and Jean Van Den Driessche

Géosciences Rennes, Campus de Beaulieu, 35042 Rennes cedex - France

Submitted to Journal of Geophysical Research

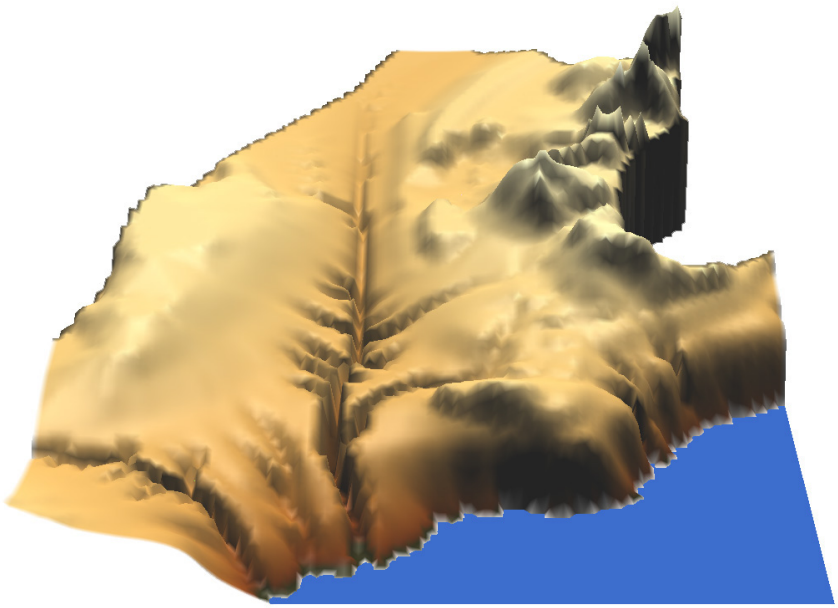

PROPAGATION OF LARGE LENGTH SCALE FLUVIAL INCISION: INSIGHT FROM THE MESSINIAN SEA-LEVEL DROP MODELLING.

N. Loget, P. Davy and J. Van Den Driessche
Géosciences Rennes, UMR 6118, Université de Rennes 1

ABSTRACT

After a base-level drop, rivers are first components of landscape to respond by incising topography. A base-level drop first results in a knickpoint in the down stream part of river longitudinal profiles. Whether knickpoints are preserved or erased during the upstream propagation of incision is still debated. These two end member processes work in natural systems at different time scales, different length scales, and different places. We show that the huge (1500 m) and fast (10's kyr) sea-level drop in the Mediterranean during the Messinian resulted in the fast propagation of incision far inland, especially in the Rhone valley (southern France). A numerical modeling of this event has been performed using the EROS model, which simulates both erosional and depositional processes in rivers. Best fit between numerical results and geological data is obtained for a non-linear relation between incision and drainage area, and for a small transport length of sediment. This small transport length, of two orders of magnitude lower than the length of the Rhone, suggests a rather diffusive-like propagation of incision, so that the initial knickpoint is not preserved. The short duration of incision (100's kyr), due to the reflooding of the Mediterranean in the early Pliocene and the subsequent preservation of the Messinian canyons by Pliocene sedimentation, may represent an incremental stage of the long-term evolution of large scale escarpments that develop during continental rifting. We finally conclude that long-term evolution of escarpment is a diffusive-like process when the drainage divide lies far from the initial knickpoint.

1. INTRODUCTION

Numerous models have attempted to further in the comprehension of erosion processes at continental scale, especially with regards to hillslope and fluvial erosion [e.g. *Pinet and Souriau*, 1988; *Chase*, 1992; *Willgoose et al.*, 1991; *Kooi and Beaumont*, 1994; *Crave and Davy*, 2001; *Tucker and Slingerland*, 1996; *Braun and Sambridge*, 1997]. At that scale, the parameterization of erosion and deposition laws is necessarily lumped into some very crude parameters chosen for both their physical relevance, accessibility, and the expected model resolution. The crudest "mean-field" model describes the history of the mean topographic elevation; it has been parameterized by a constant erosion time scale in its simplest version [*Pinet and Souriau*, 1988]. Nowadays most of the current landscape evolution models are a bit more sophisticated, and consider a spatially variable erosion pattern divided into two main spatial entities: hillslopes and a fluvial system represented by a network of 1D-structures [e. g. *Howard et al.*, 1994; *Whipple and Tucker*, 1999]. In this model framework, called LEM in the following, there is quite a large consensus to consider that the erosion and deposition laws depend on two main parameters: the local topographic slope and the drainage area, taken as a proxy for water discharge. However the nature of the constitutive erosion laws is yet an issue, with important consequences on the understanding of the physical geomorphological processes that prevails at such large length and time scales, and on the predictions that can be made on landscape dynamics, or on the coupling between erosion, tectonic and climate.

The parameters of these landscape evolution models can be constrained both by some theoretical considerations on the physics of erosion and sediment transport, and by natural examples for which the erosion can be quantified and fitted with models. This is the latter approach that we aim at developing in this paper, by studying one of the most striking geological examples of erosional dynamics: the Messinian sea level drop and its consequences on the carving of a huge canyon along the Rhone. The analysis of the canyon incision will be done in the framework of the landscape evolution models described above (in particular with 1D wired rivers).

The particular exercise of fitting net erosion patterns with erosion models was already achieved by a couple of studies in the past years. The main difficulty is the quantification of erosion, with a spatial resolution fine enough to make this inverse problem relevant. *Snyder et al.* [2000] and *Lague and Davy* [2003] used tectonic uplift as a reasonable estimate of erosion rates in areas where erosion and tectonic uplift are supposed to be at equilibrium. Within this assumption, a morphometric measure such as the slope-area relationship can be related to

model parameters. There is however a fundamental indetermination in this approach since various erosion equations can fit the same data. Transport-limited and detachment-limited models (see below) are known to fit both the observed power laws between slope and drainage areas. The only way to solve this indetermination is to study transient topographic evolution [*Whipple and Tucker*, 1999; *Tucker and Whipple*, 2002]. *Stock and Montgomery* [1999] and *van der Beek et al.* [2003] have make use of well-dated erosion surfaces to deduce the amount of erosion in some river profiles. This approach is potentially richer than the previous one because the disequilibrium history contains the very nature of the erosion-transport equation. The main limitation is in the quality of the dataset with regards to modeling. Both cited studies calculate the amount of erosion along river profile as the difference between terraces (taken as a paleo-river profile) and the contemporary river. The amount of erosion is generally small compared to the height difference along the river profile, making the signal-over-noise ratio quite large. The very detailed study of *van der Beek et al*. [2003] eventually end up to the frustrating conclusion that river profiles can be fitted by a couple of models with similar accuracy, which denotes the difficulty to deal with small erosion amplitudes, that is less than the height amplitude.

Here we investigate an outstanding example of huge sea-level drop that occurred in the Mediterranean during the Late Miocene. Indeed, the closure of marine gateways between the Atlantic and Mediterranean waters respectively resulted in the rapid desiccation of the Mediterranean Sea inducing a 1500 m sea level drop and the carving of deep canyons along the pre-existing drainage network. This event is called the Messinian Salinity Crisis (MSC) because desiccation was accompanied by the deposit of 1600 to 3200 m thick evaporites [*Hsü et al.*, 1973]. The MSC lasted about 600 kyr [e.g. *Krijgsman et al.*, 1999] and ended by the extremely rapid re-flooding of the desiccated basin during the early Pliocene [*Blanc*, 2002], allowing relief rejuvenation all around the Mediterranean region to be "frozen" by marine Pliocene sedimentation [e. g. *Chumakov*, 1973; *Clauzon*, 1982; *Clauzon*, 1996].

The Messinian erosion story can be viewed as the ultimate experiment of bedrock incision. We aim at modeling the erosion profile of the Rhone river for deriving the erosion-transport parameters. We use an original surface process model – €ros –, which introduces a transport-length parameter that encompasses both detachment-limited and transport-limited equations into one single formulation. In the following, we first describe the €ros model, then we present the geological data and the modeling approach. From our results, we finally discuss the insights that the MSC example provides into the question of how large scale fluvial propagates.

2. THE €ROS MODEL

We briefly present the principles used in the landscape evolution model €ros. It is a particle method where equivalent rain drops (called precipiton) are launched on top of an erodible grid. A preliminary version of the code has been published in [*Davy and Crave*, 2000; *Crave and Davy*, 2001]. In such models, the physics of the modelled phenomena is embodied in a series of rules that specify how the running droplets interact with the topographic grid. With simple interaction rule, it is possible to create complex auto-organized spatial patterns which own the same statistical properties than natural landforms [e.g., *Chase*, 1992; *Murray and Paola*, 1997].

In €ros, each precipiton is moving on top of the grid as water flows on top of the topography. It has a finite water volume but a variable discharge q that renders changes in water velocity, depth or width. The way of calculating water discharge according to the precipiton distribution is given in [*Crave and Davy*, 2001].

Precipitons transports the sediment load S and exchange matter with the topography h according to erosion-deposition rules. The consequent erosion and deposition fluxes depend on both water discharge, topographic gradients, and material erodability. In contrast with most of the models [*Chase*, 1992] erosion flux is qualitatively different from deposition flux. The former is given by the classical power-law relationship:

$$q_{\mathrm{E}} = K {q_w}^m s^n \tag{1}$$

where q_{E} is the erosion flux, q_{w} the water discharge, s the largest descending topographic slope, K a proxy for erodability, m and n the two classical power-law exponents. The deposition flux q_{D} is taken proportional to the sediment load S transported by the precipiton:

$$q_{\mathrm{D}} = \frac{S}{\tau},$$

where τ is a time constant, which quantifies the time spent by a particle within river. In €ros, the mass balance is calculated as the variation with distance of the sediment load carried by precipiton. This comes to use the Lagrangian referential that moves with precipitons. In this referential, the mass balance becomes:

$$\mathrm{d}S = (q_{\mathrm{E}} v \, \mathrm{d}x - \frac{S}{\xi} \mathrm{d}x), \tag{2}$$

where ξ is a transfer distance equal to the product of τ by the horizontal water velocity. ξ is a basic parameter that has been used in some landscape evolution models [*Beaumont et al.*, 1992; *Kooi and Beaumont*, 1994]. It represents the typical distance that a river particle runs before depositing. If ξ is small (compared to the grid size for instance), the topographic mass balance expresses as :

$$\frac{\partial h}{\partial t} = -\nabla(\xi q_{\mathrm{E}}) \tag{3}$$

If ξ is large, sediment never re-deposits and the topography mass balance contains only the erosion term:

$$\frac{\partial h}{\partial t} = -q_{\mathrm{E}} \tag{4}$$

It is intuitively sound to relate ξ to the sediment grain size via the vertical velocity term. The finest sediment grain tends to be transported very far from their erosion place, which means very large values of ξ; in contrast, larger sediment grains redeposit close to the place they were before eroding, and thus propagate from place to place by a kind of saltation process, which is typical of small transfer length values.

A complete description of the €ros model and of its parameters will be given in a further paper [*P. Davy*, in preparation].

At last, we mention a specific problem that is general for that kind of landscape evolution model: the river width issue. For rivers considered as 1D structure, erosion-transport equations such as (3) or (4) are normally integrated over the grid cell. If *h* is the average cell height, as it should be, the left-hand term is multiplied by the grid cell width d*x*. Since erosion is considered to be localized along river, the right-hand term is integrated over the river width *W*. There is thus a ratio *W*/d*x* that appears on the right-hand side of equations. The problem here is that we have no information on canyon width, so that it is not possible to calculate the average cell height. We thus consider that *h* is the river-profile height, and that the above erosion-transport equations are integrated over river width. Since *W* appears on both left and right sides of equations, it disappears and equations (3) and (4) represent both the local erosion-transport equation and its integrated formulation (the only exception is that the derivative of *W* should appear in the integrated formulation, but we consider that this term is negligible compared to the other).

3. THE MESSINIAN SEA-LEVEL DROP

During Messinian times, a dramatic sea-level fall took place in Mediterranean resulting in the closure of the gateways between Atlantic and Mediterranean [e.g. *Weijemars*, 1988; *Martìn et al.*, 2001]. This event is known as the Messinian Salinity Crisis (MSC) [e.g. *Hsü*, 1973]. The base-level drop is estimated at 1500 m [*Ryan*, 1976]. Such an amplitude is comparable to that of base-level variations induced by tectonic uplift (and one to two orders of magnitude higher that that induced by glacio-eustatism).

Following on this sea-level drop, the pre-MSC drainage network was strongly re-incised by regressive erosion all around the Mediterranean region (Figure 1). Many Messinian canyons have been documented that underlie current valleys such as in the Nile, Rhone and Var valleys [*Chumakov*, 1973; *Barber*, 1981; *Clauzon*, 1978; *Clauzon*, 1982]. Owing to a very fast, catastrophic reflooding during the early Pliocene, these canyons have been preserved by Pliocene marine infilling deposits [*Denizot*, 1952; *Chumakov*, 1973]. Incision is very deep in the downstream part of these canyons (more than 1000 m for the Rhone and Nile) and was propagated very far inland (several 100's km) (Figure 2). The corresponding incision rate is considerable, up to 10 mm y^{-1} such as in the downstream part of the Rhone. This rate is close to fluvial incision rate in tectonically active mountain belts as the Himalayas [2-12 mmy-1 e.g. *Burbank et al.*, 1996].

4. GEOLOGICAL DATA

In this study, we focus on the Messinian Rhone valley (Figures 2 and 3). The Rhone valley was first a Late Miocene valley [*Mandier*, 1988], that originated within the Alps and mainly developed between the Alps to the east and the French Massif Central to the west (Figure 3). The current Rhone is about 800 km long and its drainage basin is of 100,000 km². During the MSC, incision was propagated on more than 300 km [*Clauzon*, 1982]. Numerous pre-Messinian tributary valleys were also re-incised [e.g. *Ballesio*, 1972; *Mandier*, 1988; *Clauzon et al.*, 1995]. The Messinian Rhone valley is one of the best documented canyon, both onshore and offshore, with numerous boreholes and seismic data (Figure 3), allowing the longitudinal profile of the Messinian Rhone to be restored (Figure 2). Previous works have emphasized the convex-up shape of the downstream part of this profile that has been interpreted as resulting from a strong disequilibrium [*Clauzon*, 1982]. Remnants of pre-Messinian surfaces are present all along the current valley of the Rhone [*Clauzon*, 1982], thus

making possible the determination of the vertical incision that developed during the MSC (Figure 4).

Because the currently observable Messinian profile might have been affected by some post-Messinian tectonic deformation [*Steckler and Watts*, 1980; *Schlupp et al*., 2001], we consider hereafter the vertical incision recorded along the profile rather that the shape of the profile itself, to compare the results of the numerical modeling with the geological data. This allows post-Messinian tectonics or general subsidence to be overlooked and we refer hereafter to the variation of the vertical incision along the Messinian Rhone profile as the cumulative erosion curve (Figure 5).

We use the data published by *Clauzon* [1982] and *Guennoc et al.* [2000] to determine the vertical incision onshore and offshore, respectively (Figure 5).

The lowest Mediterranean shoreline during the MSC is considered to match the limits of the Messinian evaporites [*Rouchy and Saint Martin*, 1992]. In the downstream part incision is no more perceptible below the -2500m Messinian isobath [*Guennoc et al*., 2000]; we account this boundary to be the limit for aerial erosion. The Messinian incision headwater was not clearly identified in the Rhone valley. Near Lyon, the vertical incision is around 300 m, so the headwater is certainly located farther upstream, possibly up to St Jean de Losne, about 200 km north of Lyon [*Baumard*, 2001].

5. MODELING PROCEDURE

The general idea of this paper is to discuss the simplest – but not too simplistic –average erosion model that can be compared with Messinian erosion. We thus use a couple of simplifications compatible with both this objective of finding an average erosion model, with the geological knowledge described above, but also with the lack of knowledge intrinsic to such a large geological system.

The first assumption is about the pre-Messininan topography. Since the late Miocene, the stress field did not varied significantly in the studied area [e.g. *Bergerat*, 1987], so that regional slopes during pre-Messinian times were similar to the present ones. Remnants of pre-Messinian alluvial sedimentation all along the Rhone valley also show that a paleo-Rhone was flowing into the Mediterranean. Moreover, by looking to the length of preserved Messinian incisions around the Mediterranean, *Loget et al*. [2005] have argued for the similar size of most Messinian drainage areas to the size of present ones. Therefore the pre-MSC topography has been derived from the DEM GTOPO 30 by smoothing the contour lines on a

regional scale (Figure 6). In order to mimic the Messinian sea-level drop, the base-level of the model has been fixed to the -1500 m current isobath that roughly corresponds to the present-day, maximum lateral extent of the Messinian evaporites [*Rouchy and Saint Martin*, 1992]. Moreover, according to *Gorini* [1993], the morphology of the Gulf of Lions shelf was most probably comparable to the present-day one, including a similar location of the shelf break.

The second assumption is about the erosion law. That described in equation (1) is a mesoscale formulation, in the sense that it expresses the dependency of erosion and deposition fluxes with respect to some physical parameters which integrates local-scale complexity. The two parameters in equation (1) are local slope and water discharge. Local slope is defined at the resolution scale of calculation, which is about 1 km. Water discharge encompasses the flow variability within a river cross-section. The validity of the mesoscale approach is intimately related to the choice of the mesoscale parameters. For the erosion equation, the main discussion is about the use of water discharge as a proxy of the river shear stress over the river bed. This is partially justified by phenomenological and heuristic relationships [*Howard et al.*, 1994; *Whipple and Tucker*, 1999], but the reader has to be aware that the discussion is far to be closed even if most, if not all, landscape evolution models are built on this assumption.

In this paper, we also assume that the erosion parameters (K, m, n, and ξ) are homogeneous over the entire system, in a way consistent with the seek of the average fitting model. We could have considered two main departures of this homogeneous assumption: an erosion law that changes for small drainage area (according to the hillslope/channel dichotomy) or for large slopes (to include mass wasting processes), and a dependency with lithology. In the Messinian example, most, if not all, the erosion is concentrated into the fluvial system. The steepness of the Messinian valley flanks [e.g. *Clauzon et al*., 1995; *Schlupp et al*., 2001] shows that both incision and the subsequent filling by Pliocene sediments have been too fast for hillslopes to respond significantly. On the other hand, the Messinian incisions all around Mediterranean appear to be controlled by the above watershed areas whatever the variable nature of basement lithology in Mediterranean catchments [*Loget et al.*, 2005]. This could emphasize that fluvial incision is not as sensitive to lithology as hillslope erosion.

6. RESULTS

All runs were tested using the initial topography described above and with varying m, n, and ξ parameters. Each experimental curve represents the variation in space of the amount of incision for a given period of time (that is represented by a numerical dimensionless time that

depends on the average rainfall rate and on erodibility). Negative values of cumulative erosion mean that the experimental river aggrades. Experiments are stopped when experimental curves fit with the global shape of the geological cumulative erosion curve, or when significant parameters, such as maximum amount of incision or headwater position are similar in both the experiment and nature. The fit between geological data and numerical results is also appreciated with regards to 3D drainage pattern obtained in the experiments compared to the natural system.

Note that only ξ values larger than the grid cell (here 1 km), and smaller than system size, can be resolved. For large ξ, the erosion-transport equation (eq.4) does not depend on ξ. For small ξ, the erosion-transport equation is (3) meaning that ξ is just a proportional coefficient playing the same role than the time scale.

Effect of m and n parameters on the incision dynamics

We first investigate the effects of m and n on the incision pattern in the Rhone valley and for a fixed ξ value (1km) (Figure 7).

When n=1, an increase of m favors erosion in the large drainage areas according to equation (1). In a general way the time required to reach the peak of erosion decreases when m increases.

For n=1 and m=1 (that is the linear case), sedimentation occurs in the upstream part of the drainage area from the early stages onwards (t=2500) whereas erosion is distributed in the downstream part. At t=50.000, only the downstream part of the experimental curve is correlated with the geological one. The 3D drainage pattern does not display a localized narrow incision in the Rhone valley and tributaries as well.

For n=1 and m=2, t he peak of erosion is reached for a very short numerical time (0.15. Propagation of incision up to the headwater position requires additional time (t=0.4), but involves exceeding erosion, in particular between 200 km and 400 km. In 3D view, a narrow incision occurs within the Rhone valley but tributaries weakly developed.

For n=1 and m=1.5, the experimental curves fit rather well with the geological curve for $20<t<40$. 3D experimental pattern also resembles the natural system, characterized by the presence of a major drain in the Rhone valley and of several well-developed tributaries.

An increasing value of n to n=2 favors erosion along the steepest slopes and reduces the influence of the drainage area, according to equation (1), especially for $m>1$. In a general way, an increase of n, for a fixed value of m, raises the propagation rate of incision.

For n=2 and m=1, fluvial incision is restricted to the very downstream part of the drainage area whereas sedimentation occurs in the upstream part. The experiment was stopped at t=1250 and much more additional time would be required to reach both the headwater and the peak of erosion, whereas at t=500 the landscape is already smoothed.

For n=2 and m=1.5, the downstream part of the profile fits rather well with the geological profile at t=50, but sedimentation tends to develops while approaching the headwater. Moreover the 3D view shows that erosion is achieved through a denser drainage network with much more broad valleys than in the natural system.

For n=2 and m=2, the headwater is reached at $0.375<t<0.5$ but with an amount of erosion in excess with respect to geological data. In 3D view, although the drainage pattern as the whole resembles the natural system, incision has propagated too far inland, in regard to the tributaries.

In conclusion, for a transport length $\xi = 1$ km, best fit between the geological data and the experiment results is obtained for an exponent combination so that m=1.5 and n=1.

Effect of ξ parameter on the incision dynamics (Figures 8 and 9)

An increase of the transport length makes the river behavior evolve from an advective/diffusive model for low ξ toward a complete evacuation of the erosion products for large ξ [*Crave and Davy*, 2001]. In the numerical experiments, the larger is ξ, the faster is the propagation of erosion.

Hereafter, we focus on the effect of the transport length for two exponent combinations: m=1.5 and n=1, and m=1 and n=1 respectively. The second combination corresponds to the used linear case that corresponds to the "undercapacity model", and commonly used in other numerical simulations [e.g. *Kooi and Beaumont*, 1994].

For m=1.5 and n=1, an increase of ξ from 1 km up to 400 km moves the experimental curve away from the geological curve. For ξ= 40km, both curves yet show a similar whole geometry during the first stages in the downstream part, but much more erosion is needed to reach the headwater than in the natural system. For ξ=400 km the experimental curve cut across the geological curve as soon as the experiment starts and its shape never matches geological curve. Reaching the headwater would require a considerable amount of erosion.

In 3D view an increase of ξ inhibits the tributaries development and erosion concentrates within one major drain.

In the linear case (m=1, n=1), both the experimental curves and the 3D views show that an increase of ξ helps incision to propagate, although sedimentation occurs upstream for both ξ=1km and ξ= 40km, but does not allow a good fit with the geological data. As in the previous case (m=1.5, n=1), a large ξ (400km) needs much more erosion to reach the headwater.

Finally, testing the influence of the transport length reinforces the relevance of the exponent combination deduced from the first set of experiments, namely m=1.5, n=1 and ξ=1 km.

Evolution with time of the drainage for m=1.5, n=1 and ξ= 1km

The Figure 10 shows successive stages of the network growth during an experimental run for m=1.5, n=1 and ξ= 1km. Incision first develops on the edge of the emerged topography inside the Rhone valley (t=1). At t=10, two major drains have propagated far inland (in the Rhone valley and the Languedoc plain). At t=40, tributary incisions that initiated during the previous stages, now extend inland, whereas the major drains continue to propagate inland. Concerning erosion dynamics in the Rhone valley, the experimental curves show that incision develops very fast during the early stages in the downstream part (from t=0 to t=5). The headwater (Hd) propagates about 350 km inland wards whereas the peak of erosion, whose value reaches 650 m (Epy), is located only 70 km from the outlet (Epx). In the further stages, (from t=5 to t=40), the headwater migration slows down whereas the peak of erosion rises up to 1100 m. The best time interval confidence that account for the geological data is from t=20 to t=40. Finally, this evolution as a whole corresponds to a diffuse behavior of the river longitudinal profile, with time. This will also results in a nonlinear behavior of sedimentation, the bulk of the discharge being stored during the first stages (Figure 11).

7. DISCUSSION

Significance of the m,n and ξ parameters

The first set of experiments shows that a necessary condition to reproduce the Messinian erosion pattern, in the Rhone valley, is m>1 and m>n, emphasizing the crucial role of the drainage area in the propagation of the erosion. Experimental results have provided values of m and n of 1.5 and 1 respectively. These values are similar to that described in previous works assuming a transport limited case [*Murray and Paola*, 1997; *Crave and Davy*, 2001; *Whipple and Tucker*, 2002; *Lague and Davy*, 2003; *Clevis et al.*, 2004]. These values also

provide a concavity index of 0.5 (defined as $\theta' = m' - 1/n'$, in the transport limited case). Similar values ($0.4 < \theta < 0.7$) have been reported from natural drainage system [e.g. *Hack*, 1957; *Tarboton et al*., 1989; *Masson and Montgomery*, 2000]. As an example, the current Rhone basin provides a comparable value around 0.4 (Figure 12).

The second set shows that propagating the incision far inland, and confining most of erosion in the downstream valley as well, requires a small transport length ξ in order of 1km.

A decrease of the transport length tends to erase the initial break slope. Indeed in the experiments the largest (ξ=400 km) and the smallest (ξ=1km) transport lengths constitute two end-members modes of this knickpoint evolution, namely "knickpoint parallel retreat" or "knickpoint replacement" respectively (Figure 13) [e.g. *Gardner*, 1983].

A small transport length implies a transport-limited mode of fluvial erosion [e.g. *Kooi and Beaumont*, 1994]. In the present case, the transport length is at least two orders of magnitude smaller than the length–scale of the drainage system. This suggests that the response of the drainage system, subsequent to the Messinian base-level drop, was transport-limited, implying the diffusive-like evolution of the Rhone profile and the progressive replacement of the initial break slope.

Short- to long-term drainage evolution: Insight from the Messinian erosional pattern

The migration of knickpoints is usually interpreted as corresponding to transient stages in the evolution of the river profiles toward equilibrium. Conversely, the absence of knickpoint is considered to be symptomatic of a profile close to equilibrium. Although knickpoints do not occur along the Messinian Rhone profile, its convex-up shape shows that it did not reach equilibrium. On the other hand, due the short duration of the Messinian sea-level drop (10^5 years), the preserved Messinian Rhone profile can be considered as corresponding to a transient stage of an aborted river response to a base-level drop.

Similar river response, that is far inland river incision (10's to 100's km) without evidence of knickpoint propagation, has been reported from the study of Quaternary eustatic variations on comparable time scales, but for amplitudes lower of one order of magnitude (10^2m versus 10^3m for sea-level drop during the Quaternary and the Messinian, respectively) [e.g. *Van Heijst and Postma*, 2001].

Because of the very large amplitude of the Messinian sea level drop, the evolution of the Messinian Rhone profile may be compared to the escarpment evolution of high-elevation rifted margins. Indeed, great escarpments of 1km high and up to several hundreds kilometers

far from the coast line, as in southwest Africa, eastern Brazil and western India [e.g. *Ollier*, 1985] have been interpreted as resulting from the morphological evolution of passive continental margins [*Gilchrist et al*., 1994; *Kooi and Beaumont*, 1994; *Brown et al*., 2002; *van der Beek et al*., 2002; *Braun and van der Beek*, 2004]. The time scale of such an evolution is one to three orders of magnitude higher than that of the Messinian evolution (10^6 years to 10^8 years versus 10^5 years), so that this latter can be considered as an "incremental" stage of a long-term evolution. The Messinian Rhone example suggests that, long-term erosion of large scale escarpments is a diffusive-like process. Previous works have already described such an evolutionary model when the main drainage divide occurs far away from the initial break slope [*Kooi and Beaumont*, 1994; *Gilchrist et al*., 1994; *Brown et al*., 2002; *van der Beek et al*., 2002], as in the case of the Messinian Salinity Crisis.

Knickpoint retreat might have occurred during Messinian erosion, in particular just after the emersion of the shelf break. Indeed, several studies have shown that margin emersion is followed by knickpoint retreat from a regressive canyon created at the base of the shelf break, but this knickpoint dissipates in the upstream drainage area during the further stages of regressive erosion [e.g. *Koss et al.*, 1994; *Fagherazzi et al*., 2004]. This stage is generally very short (several ka). It corresponds to a period during which the shelf break is disconnected from the upstream drainage network resulting in a time lag between sea-level drop and inland propagation of incision [Butcher, 1990]. If knickpoint retreat stage occurred after the Messinian sea-level drop, the knickpoint will have erased considering the duration of the Messinian Salinity Crisis (90 ka to 300 ka). Finally, few works have addressed the evolution of drainage pattern on different time scales (10^3 to 10^6 a) after a base-level drop. The figure 14 described such an evolution as suggested by the Messinian example.

8. CONCLUSION

The modeling of the Messinian Rhone valley provides new insights on the comprehension of the migration of the incision subsequent to a base-level drop. First, the values obtained for the exponents *m* and *n* of the erosion are concordant with those obtained from the analysis of natural systems and from previous experimental studies. The drainage area and the sediment transport length in rivers are two predominant parameters during the response of a drainage network to the fall of its base-level. Concentration and propagation of incision require a non linear exponent *m* (*m*=1.5) of drainage area. A very low value of ξ (1 km order) makes it possible the incision to propagate very far inland (up to 500 km) without knickpoint

migration. Such a behavior may be considered as a diffuse process at large length scale. This was already suspected in the case of Quaternary eustatism variations whose vertical amplitude does not exceed some ten's of meter on a similar time duration as the Messinian Salinity Crisis. Finally, propagation of fluvial incision appears to be very fast at the geological time scales, but a long-term restoration of equilibrium profile is needed because of the diffusive-like behavior response of rivers after a base-level fall.

References

Ballesio, R. (1972), Etude stratigraphique du Plioène rhodanien, *Doc. Lab. Géol. Fac. Sci. Lyon, 53*, 333 p.

Barber, P.M. (1981), Messinian subaerial erosion of the Proto-Nile delta. *Mar. geol.*, *44*, 253–272.

Baumard, B. (2001), Valorisation de données pour l'étude de la crise messinienne dans le Gard rhodanien et la moitié est de la France, *PhD thesis*, Ecole des Mines de Paris, 260 pp.

Beaumont, C., P. Fullsack, and J. Hamilton (1992), Erosional control of active compressional orogens, in *Thrust Tectonics*, edited by K. R. McClay, pp. 1– 18, Chapman and Hall, New York.

Begin, Z. (1988), Application of a diffusion-erosion model to alluvial channels which degrade due to base-level lowering, *Earth Surf. Processes Landforms*, *13*, 487–500.

Bergerat, F. (1987), Stress fields in the european platform at the time of Africa-Eurasia collision, *Tectonics*, *6*, 99–132.

Blanc, P.L. (2002), The opening of the Plio-Quaternary Gibraltar Strait: assessing the size of a cataclysm, *Geodinamica Acta*, *15*, 303–317.

Braun, J., and M. Sambridge (1997), Modelling landscape evolution on geological time scales: A new method based on irregular spatial discretization, *Basin Res.*, *9*, 27–52.

Braun, J., and P. van der Beek (2004), Evolution of passive margin escarpments: What can we learn from low-temperature thermochronology?, *J. Geophys. Res.*, *109*, doi:10.1029/2004JF000147.

Brown, R. W., M. A. Summerfield, and A. J. W. Gleadow (2002), Denudational history along a transect across the Drakensberg Escarpment of southern Africa derived from apatite fission track thermochronology, *J. Geophys. Res.*, *107*(B12), 2350, doi:10.1029/2001JB000745.

Burbank, D. W., J. Leland, E. Fielding, R. S. Anderson, N. Brozovic, M. R. Reid, and C. Duncan (1996), Bedrock incision, rock uplift and threshold hillslopes in the northwestern Himalayas, *Nature*, *379*, 505–510.

Butcher, S.W. (1990), The Nickpoint Concept and its Implications Regarding Onlap to the Stratigraphic Record, In: *Quantitative Dynamic Stratigraphy* (Ed. By T.A. Cross), pp. 375-385, Prentice Hall, Englewood Cliffs, NJ.

Campillo, A., A. Maldonado and A. Mauffret (1992), Stratigraphic and tectonic evolution of the western Alboran sea: Late Miocene to recent: *Geo-Mar Lett*., *12*, 165–172.

Chase, C. G. (1992), Fluvial landsculpting and the fractal dimension of topography, *Geomorphology*, *5*, 39–57.

Chumakov, I.S. (1973), Pliocene and Pleistocene deposits of the Nile valley in Nubia and upper Egypt. In: Initial reports of the Deep Sea Drilling Project, 13, pp. 1242-1243, US Govern. Print. Office, Washington, DC.

Clauzon, G. (1978), The Messinian Var canyon (Provence, Southern France). Paleogeographic implications, *Mar. geol*., *27*, 231–246.

Clauzon, G. (1982), Le canyon messinien du Rhône : une preuve décisive du "dessicated deep basin model" (Hsü, Cita et Ryan, 1973). *Bull. Soc. Géol. Fr.*, *24*, 231–246.

Clauzon G., J.L Rubino and B. Savoye (1995), Marine Pliocene Gilbert-type fan deltas along the French Mediterranean coast. A typical infill feature of preexisting subaerial Messinian canyons, In: *5ème congrès français de sédimentologie*, *23*, ASF, Paris, 254 pp.

Clauzon, G., J. P. Suc, F. Gautier, A. Berger, and M. F. Loutre (1996), Alternate interpretation of the Messinian salinity crisis : Controversy resoved?, *Geology*, *24*, 363–366.

Clevis, Q., P.L. De Boer, and W. Nijman (2004), Differentiating the effect of episodic tectonism and eustatic sea-level fluctuations in foreland basins filled by alluvial fans and axial deltaic systems: insights from a three-dimensional stratigraphic forward model, *Sedimentology*, *51*, 809–835.

Crave, A., and P. Davy (2001), A stochastic ''precipiton'' model for simulating erosion/sedimentation dynamics, *Comput. Geosci*., *27*, 815–827.

Davy, P., and A. Crave (2000), Upscaling local-scale transport processes in large-scale relief dynamics, *Phys. Chem. Earth*, *Part A*, *25*(*6–7*), 533–541.

Denizot, G. (1952), Le Pliocène dans la vallée du Rhône, *Rev. Géogr. Lyon*, *27*, 327–357.

Escutia, C., and A. Maldonado (1992), Paleogeographic implications of the Messinian surface in the Valencia trough, northwestern Mediterranean Sea, *Tectonophysics*, *203*, 263–284.

Fagherazzi, S., A. D. Howard, and P. L. Wiberg (2004), Modeling fluvial erosion and deposition on continental shelves during sea level cycles, *J. Geophys. Res.*, *109*, F03010, doi:10.1029/2003JF000091.

Field, M.E., and J.V. Gardner (1991), Valencia gorge : Possible Messinian refill channel for the western Mediterranean Sea, *Geology*, *19*, 1129–1132.

Garcia-Castellanos, D., J. Vergés, J. Gaspar-Escribano, and S. Cloetingh (2003), Interplay between tectonics, climate, and fluvial transport during the Cenozoic evolution of the Ebro Basin (NE Iberia), *J. Geophys. Res.*, *108*(B7), 2347, doi:10.1029/2002JB002073.

Gardner, T.W. (1983), Experimental study of knickpoint and longitudinal profile evolution in cohesive, homogeneous material, *Geol. Soc. Am. Bull.*, *94*, 664–672.

Gilchrist, A. R., H. Kooi, and C. Beaumont (1994), The post-Gondwana geomorphic evolution of southwestern Africa: Implications for the controls on landscape development from observations and numerical experiments, *J. Geophys. Res*., *99*, 12,211–12,228.

Gorini, C. (1993), Géodynamique d'une marge passive: Le Golfe du Lion (Méditerranée occicentale), *Phd Thesis*, Université Paul Sabatier de Toulouse III, 264 pp.

Guennoc, P., C. Gorini, and A. Mauffret (2000), Histoire geologique du golfe du Lion et cartographie du rift oligo-aquitanien et de la surface messinienne, *Geol. France*, *3*, 67–97.

Hack, J. T. (1957), Studies of longitudinal stream profiles in Virginia and Maryland, *U.S. Geol. Surv. Prof. Pap*., *294-B*, 97 pp.

Howard, A. D., and G. Kerby (1983), Channel changes in badlands, *Geol. Soc. Am. Bull.*, *94*, 739–752.

Howard, A. D., W. E. Dietrich, and M. A. Seidl (1994), Modeling fluvial erosion on regional to continental scales, *J. Geophys. Res*., *99*, 13,971–13,986.

Hsü, K.J., M.B. Cita, , and W.B.F. Ryan (1973), The origin of the Mediterranean evaporites. In Initial reports of the deep sea drilling project, 13, pp 1203–1231, US Govern. Print. Office, Washington, DC.

Kooi, H., and C. Beaumont (1994), Escarpment evolution on high-evelvation rifted margins: Insights derived from a surface processes model that combines diffusion, advection, and reaction, *J. Geophys. Res.*, *99*, 12,191–12,209.

Koss, J.E., F.G. Ethridge, and S.A. Schumm (1994), An experimental study of the effecs of base-level change on fluvial, coastal plain and shelfs systems, *Jour. Sed. Res*., *B64*, 90–98.

Krijgsman, W., F.J. Hiigeni, I. Raffi, F.J. Sierro, and D.S. Wilson (1999), Chronology, causes and progression of the Messinian salinity crisis, *Nature*, *400*, 652–655.

Lague, D., and P. Davy (2003), Constraints on the long-term colluvial erosion law by analyzing slope-area relationships at various tectonic uplift rates in the Siwaliks Hills (Nepal), *J. Geophys. Res*., *108*(B2), 2129, doi:10.1029/2002JB001893.

Loget, N., J. Van Den Driessche and P. Davy (2005), How did the Messinian Salinity Crisis end ?, *Terra Nova*, *17*, 414–419.

Mandier, P. (1988), Le relief de la moyenne vallée du Rhône au Tertiaire et au Quaternaire. Essai de synthèse paléogéographique, *Doc. BRGM*, *151*.

Martín, J.M., J. C. Braga, and C. Betzler (2001), The Messinian Guadalhorce corridor : the last northern, Atlantic-Mediterranean gateway, *Terra Nova*, *13*, 418–424.

Murray, A.B., and C. Paola (1997), Properties of a cellular braided-stream model, *Earth Surf. Processes Landforms*, *22*, 1001–1025.

Ollier, C.D., (1995), Morphotectonics of continental margins with great escarpments, in *Tectonic Geomorphology, Binghamton Symp. Geomorphol. Int. Ser.*, vol. 15, edited by M. Morisawa and J.T. Hack, pp.3–25, Allen and Unwin, Boston, Mass.

Pinet, P., and M. Souriau (1988), Continental erosion and large-scale relief, *Tectonics*, 7, 563–582.

Rouchy, J. M., and J. P. Saint Martin (1992), Late Miocene events in the Mediterranean as recorded by carbonate-evaporite relations, *Geology*, *20*, 629–632.

Ryan, W.B.F. (1976), Quantitative evaluation of the depth of the western Mediterranean before, during and after the late Miocene salinity crisis, *Sedimentology*, *23*, 791–813.

Schlupp, A., G. Clauzon, and J. P. Avouac (2001), Mouvement post-messinien sur la faille de Nîmes: implications pour la sismotectonique de la Provence, *Bull. Soc. Géol. Fr.*, *172*, 697–711.

Schoorl, J.M., and A. Veldkamp (2003), Late Cenozoic landscape development and its tectonic implications for the Guadalhorce valley near Alora (Southern Spain), *Geomorphology*, *50*, 43–57.

Schumm, S. A., M. P. Mosley, and W. E. Weaver (1987), *Experimental Fluvial Geomorphology*, John Wiley, New York.

Seidl, M.A., W.E. Dietrich, and J.W. Kirchner (1994), Longitudinal profile development into bedrock: An analysis of Hawaiian channels, *J. Geol.*, *102*, 457–474.

Snyder, N. P., K. X. Whipple, G. E. Tucker, and D. J. Merritts (2000), Landscape response to tectonic forcing: DEM analysis of stream profiles in the Mendocino triple junction region, northern California, *Geol. Soc. Am. Bull.*, *112*(*8*), 1250–1263.

Steckler, M.S., and A. B. Watts (1980), The gulf of Lion: subsidence of a young continental margin, *Nature*, *287*, 425–429.

Tucker, G., and R. Slingerland (1996), Predicting sediment flux from fold and thrust belts, *Basin Res.*, *8*, 329–349.

Tucker, G. E., and K. X. Whipple (2002), Topographic outcomes predicted by stream erosion models: Sensitivity analysis and intermodel comparison, *J. Geophys. Res.*, *107*, 2179, doi:10.1029/2001JB000162.

van der Beek, P., M. A. Summerfield, J. Braun, R. W. Brown, and A. Fleming (2002), Modeling postbreakup landscape development and denudational history across the southeast African (Drakensberg Escarpment) margin, *J. Geophys. Res.*, *107*(B12), 2351, doi:10.1029/2001JB000744.

van der Beek, P., and P. Bishop (2003), Cenozoic river profile development in the Upper Lachlan catchment (SE Australia) as a test of quantitative fluvial incision models, *J. Geophys. Res.*, *108*(B6), 2309, doi:10.1029/2002JB002125.

Van Heijst, M.W.I.M., and G. Postma (2001), Fluvial response to sea-level changes: a quantitative analogue, experimental approach, *Basin Res.*, *13*, 269–292.

Weissel, J. K., and M. A. Seidl (1998), Inland propagation of erosional escarpments and river profile evolution across the southeast Australian passive continental margin, in *Rivers Over Rock: Fluvial Processes in Bedrock Channels*, *Geophys. Monogr. Ser.*, vol. 107, edited by K. J. Tinkler and E. E. Wohl, pp. 189–206, AGU, Washington, D. C.

Whipple, K. X., and G. E. Tucker (1999), Dynamics of the stream-power river incision model: Implications for height limits of mountain ranges, landscape response timescales, and research needs, *J. Geophys. Res.*, *104*(*B8*), 17,661–17,674.

Whipple, K. X., and G. E. Tucker (2002), Implications of sediment-flux-dependent river incision models for landscape evolution, *J. Geophys. Res.*, *107*(B2), 2039, doi:10.1029/2000JB000044.

Willgoose, G. R., R. L. Bras, and I. Rodriguez-Iturbe (1991), Results from a new model of river basin evolution, *Earth Surf. Processes Landforms*, *16*, 237–254.

FIGURES

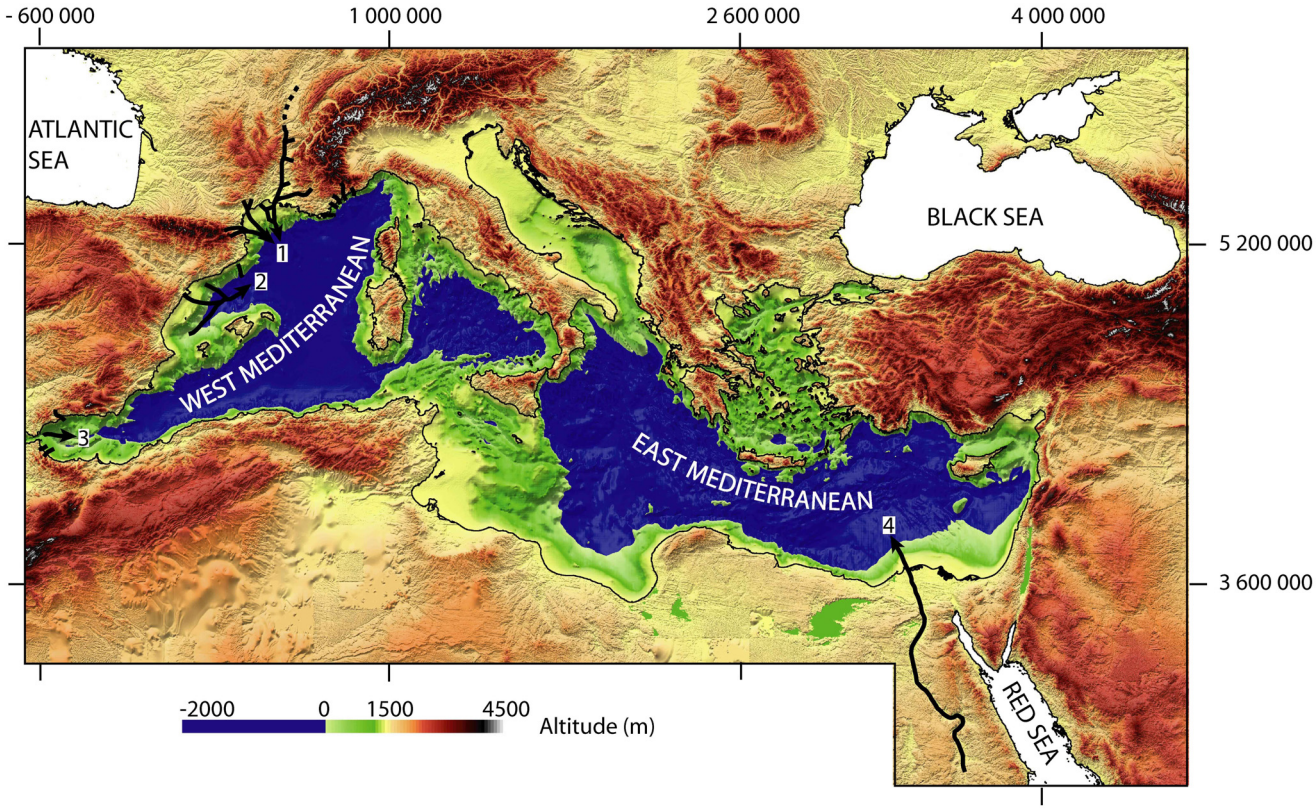

Figure 1.

Digital elevation model of the Mediterranean region during the Messinian Salinity Crisis (GTOPO 30 and ETOPO 2).

The shoreline (thin black line) has been dropped down to the present-day -1500 m isobath to account for the Messinian sea-level fall. Main Messinian drainage systems are shown (thick black lines). 1: Rhone-Pyrenean-Languedocian-Ligure [e. g. *Clauzon et al*., 1995; *Guennoc et al*, 2000]; 2: Valencia-Ebro [*Field and Gardner*, 1991; *Escutia and Maldonado,* 1992]; 3: Alboran [*Campillo et al*., 1992; *Schoorl and Veldkamp*, 2003; *Loget et al*., 2005]; 4: Nil [*Chumakov*, 1973; *Barber*, 1981]

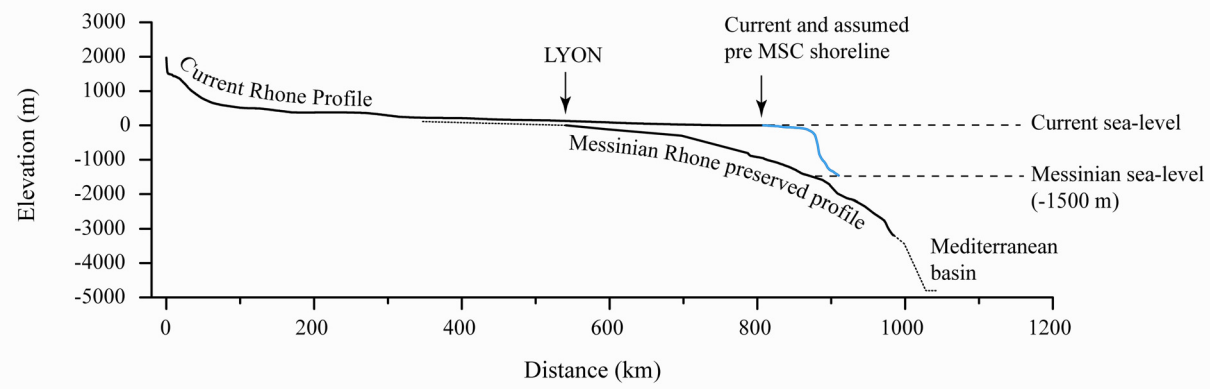

Figure 2.

Present-day and Messinian profiles in the Rhone valley and their respective base-levels. Note the marked convex shape of the Messinian profile indicating a state of strong disequilibrium.

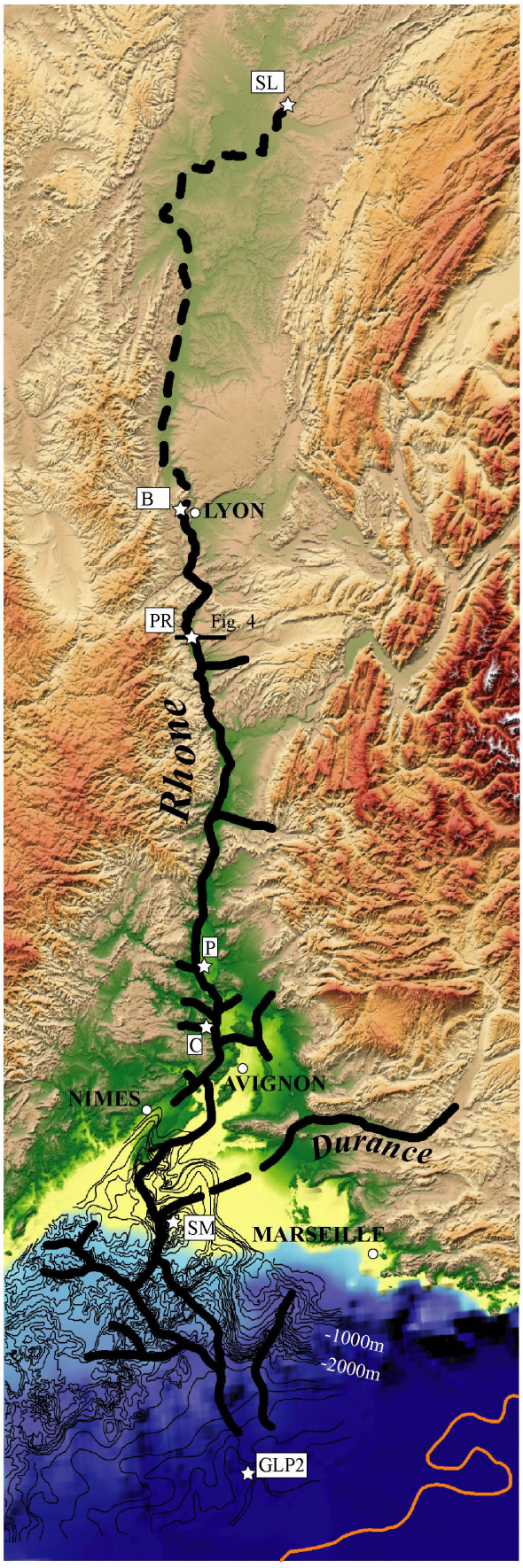

Figure 3. Digital elevation model of southern France showing the Messinian drainage pattern. Stars: boreholes where Messinian erosional surface is identified (SL: Saint Jean de Losne, BA: Belle Allemande, PR: Peage du Roussilon, P: Pierrelate, SM: Saintes Marie); black solid lines: contour lines of the Messinian surface [after *Guennoc et al.*, 2000]; grey solid line: limit of the Messinian evaporites (lowest Messinian shoreline)

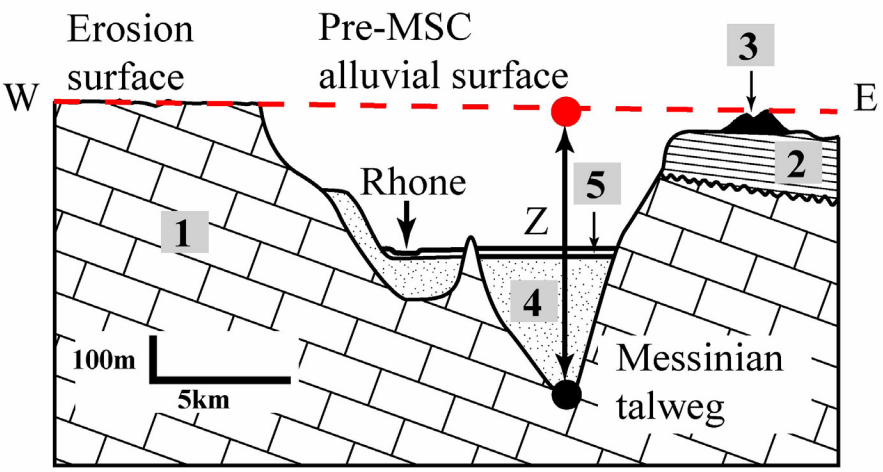

Figure 4.

Method for determining vertical incision in the Rhone valley during MSC [modified after *Clauzon*, 1982]. (see location in Figure 3).

1- Mesozoic; 2- Miocene; 3- Remnants of pre-MSC alluvial surface; 4- Pliocene fill; 5- Quaternary alluvial deposits; Z- Calculated incision.

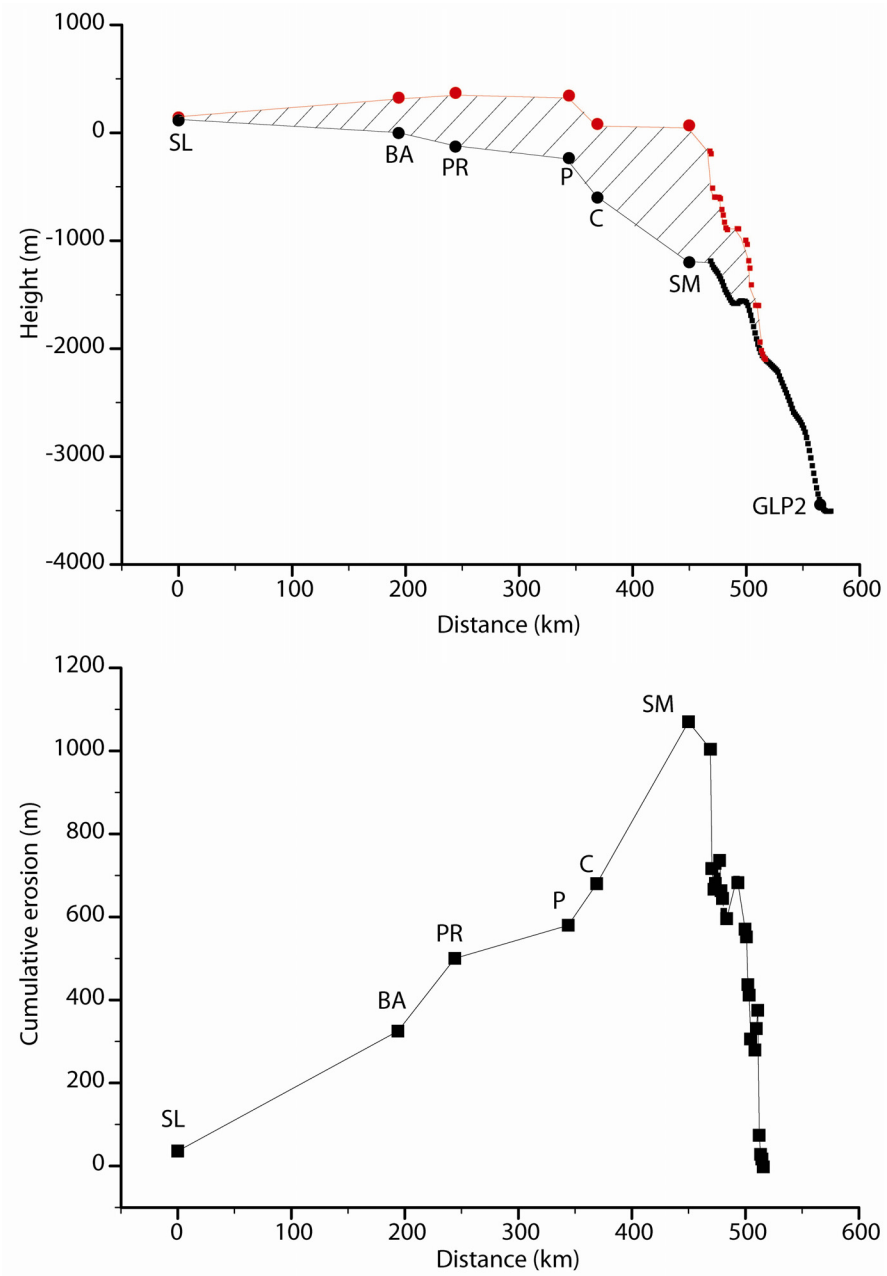

Figure 5.

Vertical incision along the Messinian Rhone valley. A- Reconstruction of Messinian (black) and pre-MSC profiles (grey) [data after *Clauzon*, 1982; *Guennoc et al.*, 2000; *Baumard*, 2001]. Circles: bore holes; square: seismic data; hatched: amount of material removed. B- Calculated cumulative erosion curve.

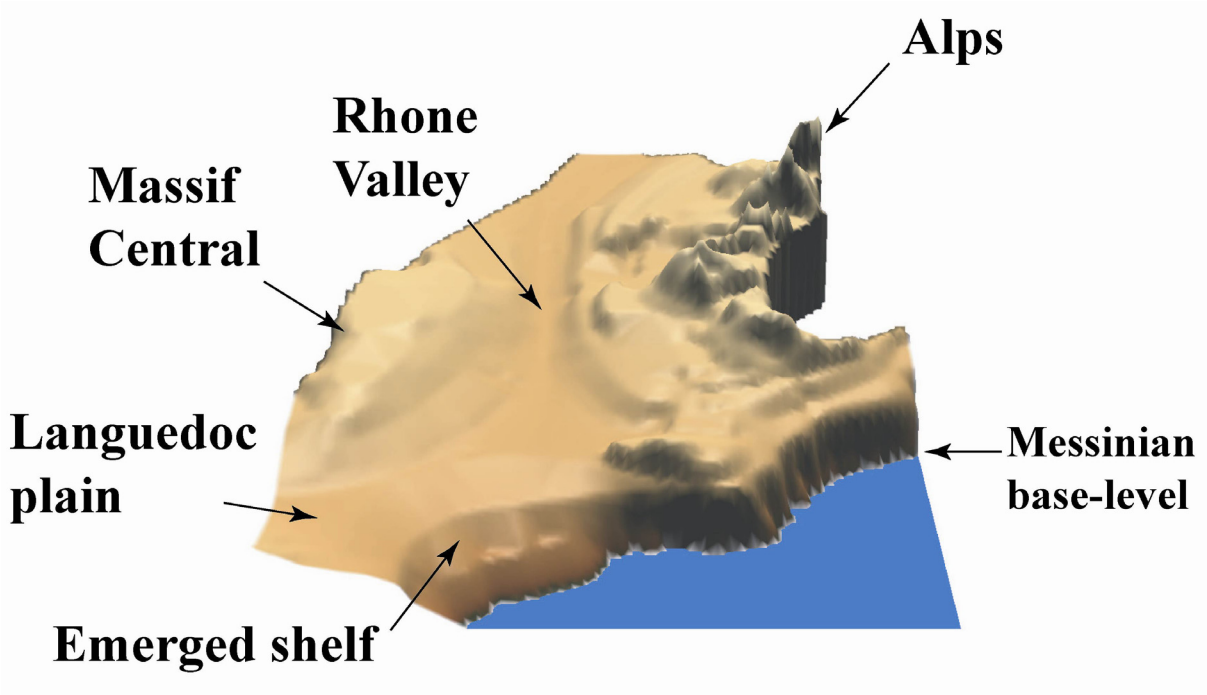

Figure 6

Initial topography used in the modeling.

The topography is obtained by smoothing the present-day topography and by fixing the sea-level to the present-day -1500m isobath (vertical dilatation x 32).

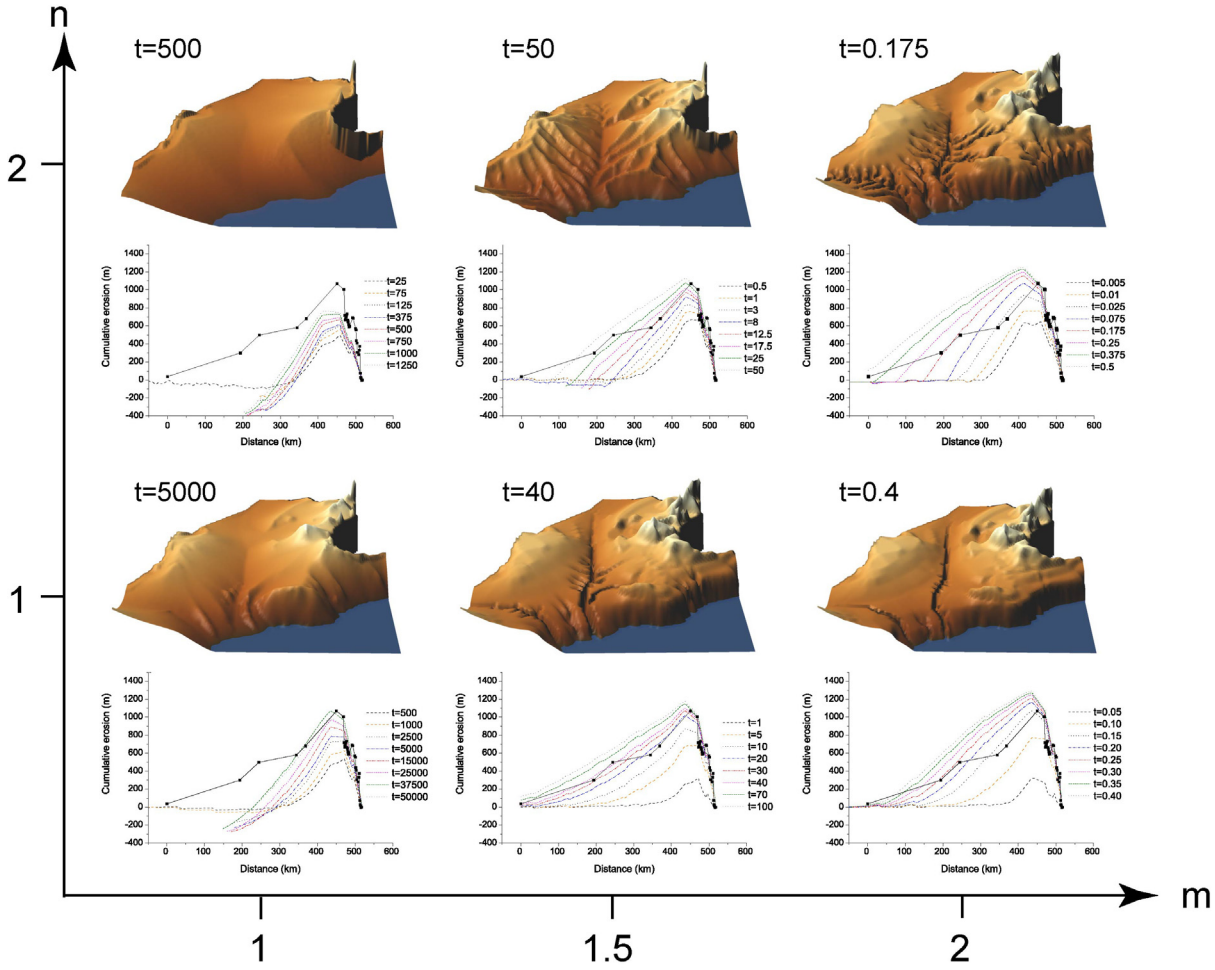

Figure 7

Numerical modeling showing the effect of *m* and *n* variations on Messinian erosion pattern for ξ= 1 km (pixel size=1km).

Top: 3D view of the models (vertical dilatation x 32). Bottom: experimental cumulative erosion curves at different times (colored lines) and geological data (black line). Best fit between numerical results and geological data is obtained for *m*=1.5 and *n*=1 (see text for explanation).

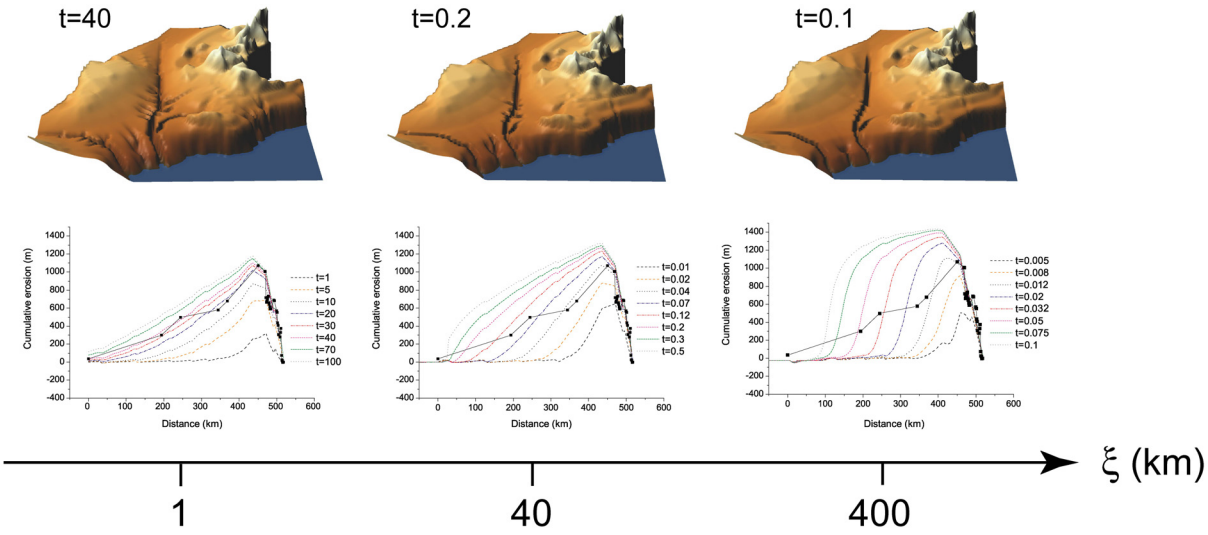

Figure 8

Numerical modeling showing the effect of an increasing transport length (ξ) on Messinian erosion pattern for *m*=1.5 and *n*=1.

Top: 3D view of the models (vertical dilatation x 32). Bottom: experimental cumulative erosion curves at different times (colored lines) and geological data (black line) (see text for explanation).

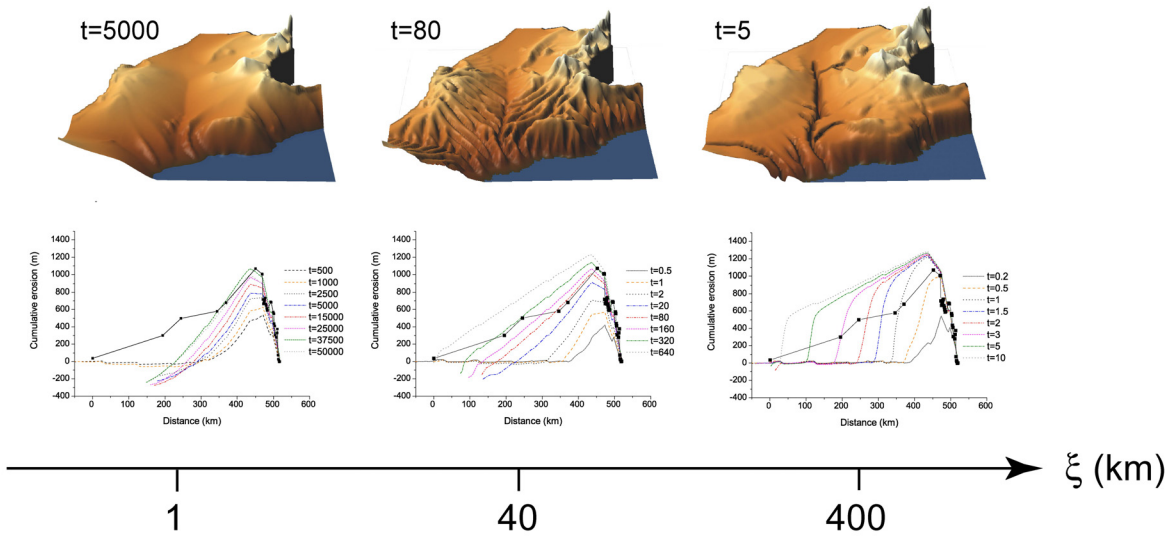

Figure 9

Numerical modeling showing the effect of an increasing transport length (ξ) on Messinian erosion pattern for *m*=1 and *n*=1 (linear case).

Top: 3D view of the models (vertical dilatation x 32). Bottom: experimental cumulative erosion curves at different times (colored lines) and geological data (black line) (see text for explanation).

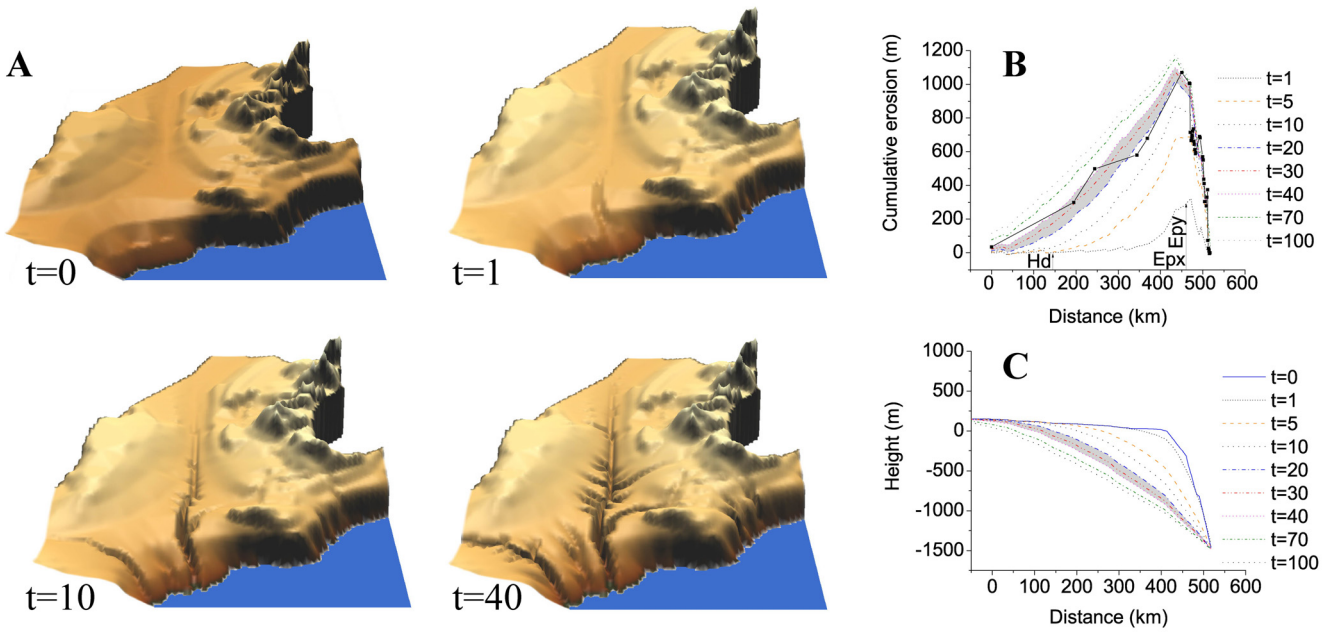

Figure 10

Run of a numerical experiment using the best combination of parameters (m=1.5, n=1, ξ= 1 km). A- 3D views. B- Experimental curve at different time (colored) compared to the geological curve (black). C- Evolution of the longitudinal profile with time. The numerical time interval confidence (t=20 to t=40) is deduced from the best fit with geological data (grey area) (see text for explanation).

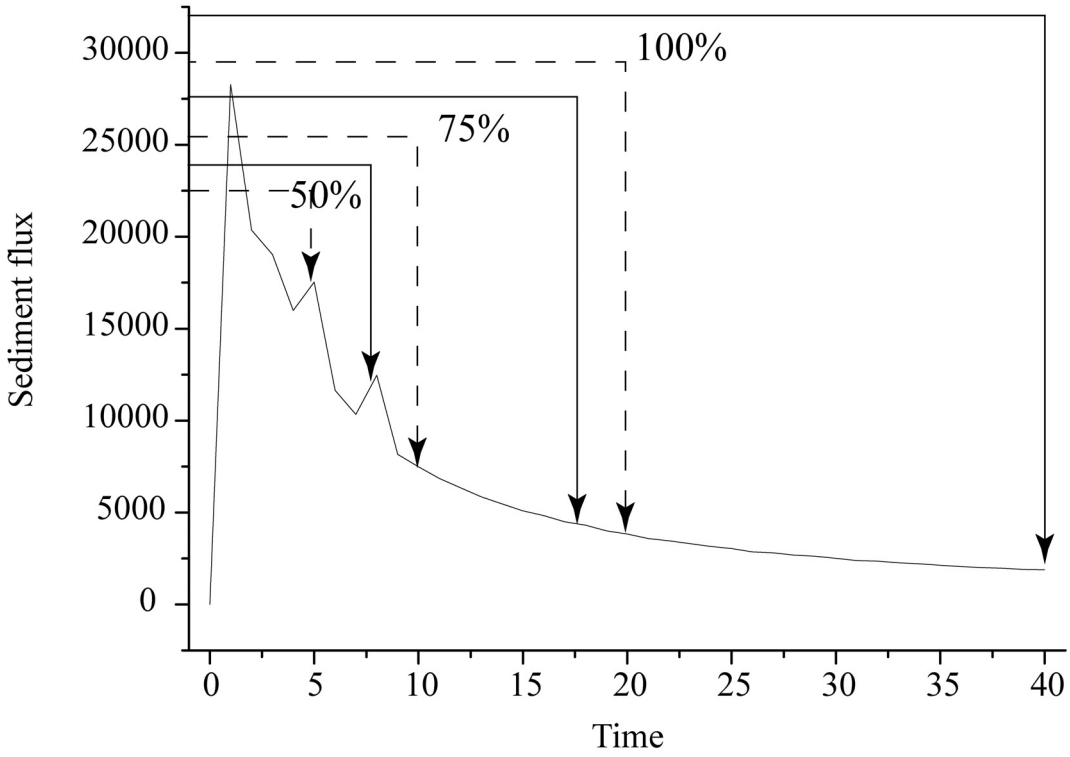

Figure 11

Variation of the flux of removed material in the modeled Rhone valley.

The amount of total erosion is indicated in percent. The solid and dashed lines correspond to the percentage of sediments removed at a given time for the two experiment durations that correspond to the limits of the numerical time interval confidence, t=20 and t=40, respectively. Note that most of sediment is evacuated in early stages in both cases.

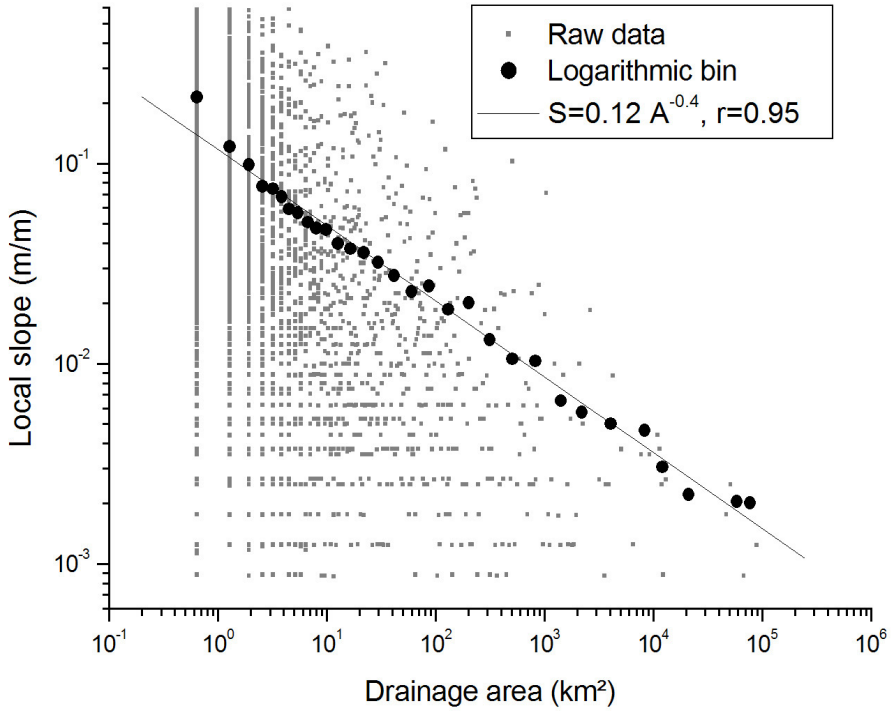

Figure 12

Area-slope relationship for the whole drainage basin of the current Rhone.

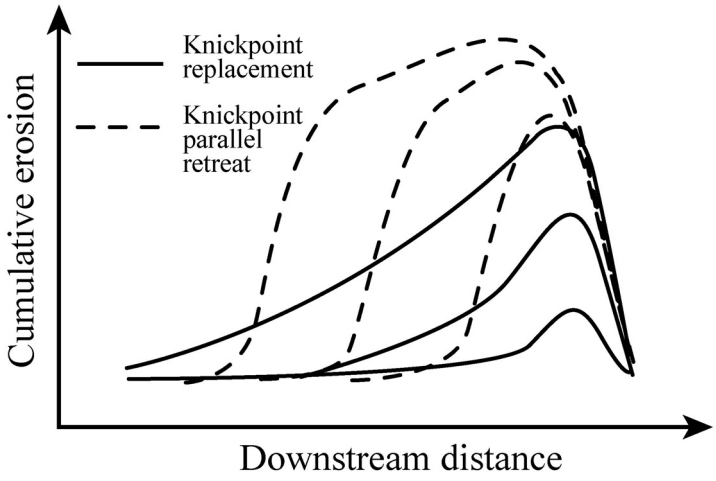

Figure 13

Significance of the shape of the cumulative erosion curve with regard to large and small values of ξ respectively.

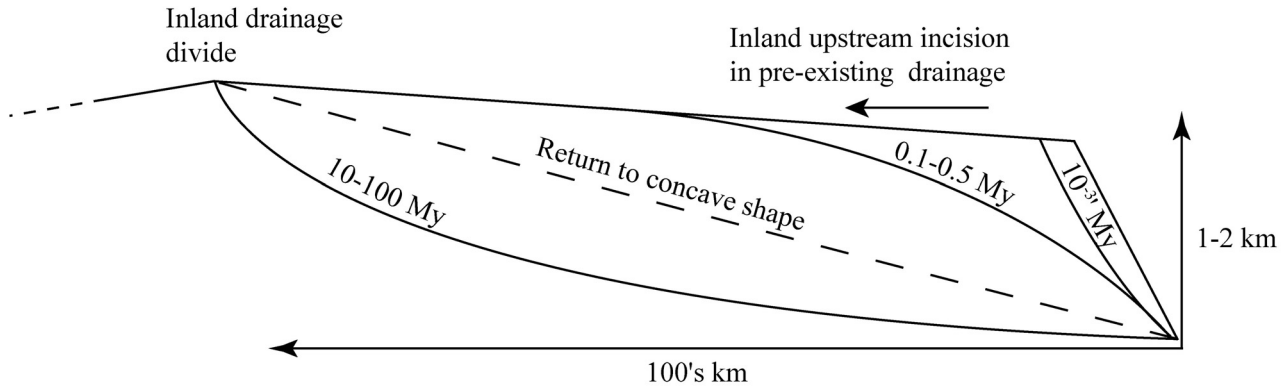

Figure 14

A model of the evolution of continental escarpments lying far away from a drainage divide. Very first stages (10^{-3} My) profile adjustment is mainly achieved by knickpoint retreat. During the following stages (0.1 to 0.5 My), erosion propagates far inland in a diffuse-like pattern resulting in a convex shape of the adjusting profile. The return to a concave equilibrium profile requires a much longer time (10 to 100 My) (see text for further explanation).

Modèle Numérique de Terrain de la Méditerranée représentant la situation pendant la Crise de Salinité Messinienne, à savoir un niveau de base situé 1500m en contrebas du niveau actuel

2.2. Dynamique de l'érosion messinienne à l'échelle de la Méditerranée : Contrôle des aires drainées sur la propagation des incisions.

Article :

Drainage area control on fluvial incision: The case of the Mediterranean Messinian Salinity Crisis.

Nicolas loget[1], Jean Van Den Driessche[1], Sébastien Castelltort[2] and Julien Babault[1]

[1]Géosciences Rennes, Université de Rennes 1, UMR 6118, Campus de Beaulieu, 35042 Rennes cedex, France.

[2]Geology Institute, ETH Zurich, 8092 Zurich, Switzerland.

Submitted to Geology

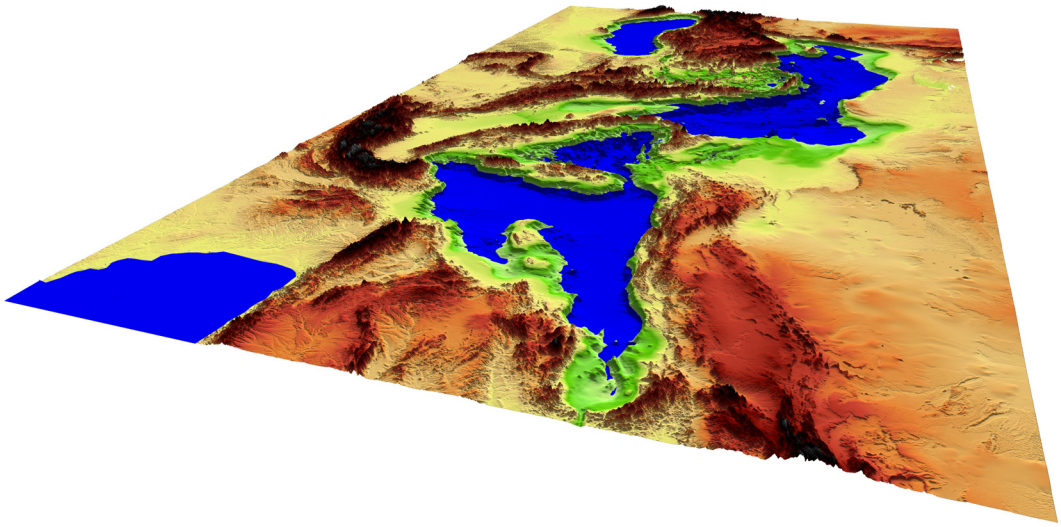

DRAINAGE AREA CONTROL ON FLUVIAL INCISION: THE CASE OF THE MEDITERRANEAN MESSINIAN SALINITY CRISIS.

Nicolas Loget[1]
Jean Van Den Driessche[1]
Sébastien Castelltort[2]
Julien Babault[1]

[1]Géosciences Rennes, Université de Rennes 1, UMR 6118, Campus de Beaulieu, 35042 Rennes cedex, France.
[2]Geology Institute, ETH Zurich, 8092 Zurich, Switzerland.

Abstract

Rivers respond to a drop of their base level by incising. Incision migration is thought to depend on several parameters such as the drainage area, lithology, or base level drop amplitude. Here we investigate the case of the Messinian Salinity Crisis that was characterized by the huge base level fall (1500m) of the Mediterranean Sea at the end of the Miocene. By looking at the response of drainage areas of three orders of magnitude (10^3 to 10^6 km^2) we conclude to the prevailing role of the drainage area in controlling river incision propagation after a base level fall. The mean rate of incision propagation for time durations ranging from 10 years to 10^7 years appears to be proportional to the square root of the upstream drainage area.

Keywords: Messinian Salinity Crisis, Mediterranean, sea-level fall, fluvial erosion, incision propagation, drainage area.

Introduction

How fast a drainage network responds to a lowering of its base level is hardly documented in natural settings because of the transient nature of the potential markers of such event (terraces, knickpoints, landslides…). What governs this response is also questionable. The migration rate of knickpoints is a first approximation of the rate at which a network can return to equilibrium after a base level drop. Rates of knickpoints migration generally range between 0.001 and 0.1 my^{-1} (e.g. Van Heijst and Postma, 2001) with exceptional values greater than 1 my^{-1} as for Niagara Falls or active orogens (Wohl, 1998; Crosby and Whipple, in press). Such migration rates are too low to account for a complete response of large rivers (10^2 to 10^3 tens of kilometers) because knickpoints tend to be smoothed during upstream migration (Gardner, 1983). Several field and experimental works have emphasized the correlation that exists between the rate of knickpoint migration and the upstream drainage area (Parker, 1977; Schumm et al., 1987; Rosenbloom et al., 1994; Crosby and Whipple, in press; Bishop et al., 2005). Gully growth studies (e.g. Seginer, 1966) have provided an exponential relationship between the gully advance (R) and the drainage area (A) such as:

$$R=CA^b \qquad with\ b\sim0.5$$

Here we investigate this topic by looking at a huge base level lowering that occurred in the Mediterranean region during the Late Miocene. The base level drop of the Mediterranean during the Messinian Salinity Crisis (hereafter referred as MSC) triggered the incision of the rivers that were flowing into the Mediterranean during this period (e.g. Hsü et al., 1973). This event gives the opportunity to investigate the response of a large range of drainage areas (10^3 to 3.10^6 km²) to a base level fall.

The Messinian Mediterranean sea level drop

The closure of the gateways between the Atlantic Ocean and the Mediterranean Sea at the end of the Miocene has induced a sea level fall of the later of about 1500 m (Hsü et al., 1973; Clauzon et al., 1996). This event was called the Messinian Salinity Crisis because of the up to 2000 m-thick deposit of evaporites in the desiccated Mediterranean basin (Hsü et al., 1973). This sea level fall was responsible for the development of a regional erosional surface and of the strong incision of the pre-MSC drainage network, resulting in the formation of deep canyons (Hsü et al., 1973; Barber, 1981; Clauzon, 1982). The base level fall of the Mediterranean Sea during the Late Miocene was already deduced long before by Depéret

(1895) and Baulig (1928) from the infilling of canyons by Pliocene sediments along the French Mediterranean coast. Indeed, the sudden reflooding of the Mediterranean during the early Pliocene caused the very fast rise of the sea level up to the present 80 m contour line and the *en masse* deposition of the suspended charge of the Messinian rivers in Gilbert deltas (e. g. Clauzon et al., 1995). The incision migration was inhibited and the morphology of the canyons was largely preserved. The duration of the erosional phase is estimated between 90 000 and 300 000 years (Clauzon et al., 1996; Krijgsman et al., 1999).

Messinian incisions versus current drainage areas

According to experimental works, for a given time duration shorter than the time necessary to recover river profile equilibrium, the length of the incisions that developed after a base level lowering is related to the pre-existing drainage area (Parker, 1977; Schumm et al., 1987). We therefore suspect that the length of the incisions that developed during the MSC was related to the pre-MSC drainage areas as already suggested by Baulig (1928) who wrote: "… the dimensions and the shape of each incision are in close relation with the importance of the corresponding river…"

As, since the late Miocene, the far-field stress state did not change markedly in the considered areas (i.e., southern France, north-eastern Spain and Egypt) (e.g. Bergerat, 1987), the pre-MSC regional deformation pattern was likely similar to the present one, then the pre-MSC regional slopes were dipping as the present-day slopes. We make the a priori hypothesis that the pre-MSC drainage areas were similar to the present-day drainage areas. On the other hand, such an assumption is sustained by regional studies. According to Griffin (2002), the river Nile feed the Mediterranean at the end of the Miocene with a drainage basin of about 2.10^6 km². The upstream part of the Nile drainage would have been set up since the Oligocene (Pik et al., 2003). The Rhone started to drain the Western Alps toward the Mediterranean from the end of the Tortonian (Ballesio, 1972; Mandier, 1988; Sissingh, 2001) whereas the Durance drained the Southern Alps before the MSC (Ballesio, 1972). Regional slopes that shaped the drainage of the Languedoc rivers (Orb, Hérault) set up during the Middle and Late Miocene (Langhian to Messinian) (Séranne et al., 2002). The French Pyrenean rivers (Tech and Têt Rivers) flowed already into the Mediterranean during the upper Miocene (Clauzon et al., 1987).

Eventually, most of the preserved Messinian incisions are observable within the current valleys around the Mediterranean.

As mentioned above, the incisions have been only partly preserved, so that the determination of the whole incision length is not straightforward, especially for the largest drainage areas, i.e., the Rhone and the Nile drainage areas (10^5 and 3.10^6 km^2, respectively) (Figs 1 and 2, Table 1). Hereafter the incision lengths have been first estimated from the occurrence of marine to continental Pliocene sedimentary fills.

For example, in the Rhone valley, the Messinian incision reaches about 300 m at Lyon, i.e., 300 km from the present-day coastline. The incision propagates most probably northwards, following the current Bresse depression up to 200 km north of Lyon where a slight incision still occurs and marks the northernmost propagation of the Messinian Rhone response (Baumard, 2001). In the Nile valley, a Messinian incision of nearly 80 m has been identified at Aswan, i.e., 1000 km from the present coastline (Chumakov, 1973). By extending the Messinian palaeo-slope of the Nile, Chumakov (1973) evaluated to 2000 km the upstream maximum extension of the incision.

For the smaller drainage areas (10^3 to 10^4 km^2) the maximum propagation of incision has been deduced from the upstream progressive thinning of the sedimentary Pliocene fills of the paleovalleys. For example, in the Orb valley, the upstream limit of the incision is considered to be about 35 km upstream of the present-day coastline where there are no more Pliocene filling or Messinian erosional surfaces (Ambert et al., 1998). This layout was found in most of valleys of the South of France (Hérault, Tech, Têt, Var, and Durance) (Clauzon, 1978; Clauzon, 1979; Clauzon et al., 1987; Ambert et al., 1998).

The plot of the incision lengths (L) versus the respective present-day areas (A) provides the following relation (Fig. 2):

$$L=\alpha A^h \quad \text{with } 0.64<\alpha<1.3 \text{ and } 0.45<h<0.55 \quad \text{(Equation 1)}$$

This relation shows that the propagation of the Messinian incision was controlled by the size of the pre-MSC drainage areas. Only the point that corresponds to the Ebro does not plot on the curve. Indeed, the Ebro basin was not connected to the Mediterranean before the MSC and accordingly no Messinian incision has developed within this foreland basin of the Pyrenees (Babault et al., 2005).

This relation is of the same form that the relation between the propagation rate of incision and the upstream drainage area described in Parker's experimental work. It is also closed to the Hack's law (Hack, 1957), which postulates that the length of a drain is related to its drainage area following a power law such as:

$$L \propto A^h$$

where h is close to 0,5 (Montgomery and Dietrich, 1992). Using the present-day drainage areas and their respective main drain in the studied area provides the following relation:

$$L = 2.5\ A^{0.52}$$

That the curve of the Messinian incisions versus the current drainage areas lies beneath the curve of the current main drains versus their respective drainage areas is interpretable in two different ways, depending on whether incision has propagated or not up to the headwater of the pre-MSC watersheds. In the first case, this means that the size of the pre-MSC watersheds was smaller than the current ones in the same proportion for each of the watersheds. This interpretation appears unlikely as it does not rely on any physical or geological explanations. In the second case, the short duration of the MSC did not allow the incision to propagate up to the headwater of the pre-MSC watersheds and each incision length was depending on the respective size of the watershed. Reaching the headwater would have required a longer time.
In the other hand, translating equation (1) into migration rates (V) provides a similar relationship such as:

$$V=CA^{b} \text{ (Equation 2)}$$

where C is a coefficient of retreat efficiency ($L^{(1-2b)}T^{-1}$). This relation is classically compared to a celerity wave equation with regard to knickpoints propagation (e.g. Rosenbloom et al., 1994; Whipple and Tucker, 1999). As the exponent b is 0.5, the equation 2 can be written:

$$V = C\sqrt{A} \text{ (Equation 3)}$$

By plotting others examples of incision migration, on different length and time scales, and for various amplitudes of base level drop, a similar general trend can be drawn for different orders of the time duration of incision migration (Fig. 3). A value of 0.5 for the exponent b appears to be a multi-scale value, as well as for gullies development than for long-lived knickpoints migration.

Discussion and Conclusion

The MSC example shows that, for drainage areas ranging from 10^3 to 10^6 km^2, the upstream drainage basin controls the distance up to which the incision propagates after a base level fall. The value of the exponent of the power law, which links the current drainage areas with the respective Messinian incision lengths, is close to that of the Hack's law (~ 0.5) suggesting that during the Messinian erosional stage, the geometry of the incisions was homothetic to that of the current drainage networks.

In the case of the MSC, we did not formally identify knickpoint propagation. According to Loget et al. (2005), river profiles have evolved following a diffusive-like mode after the base level drop of the Mediterranean Sea. On the other hand, experimental and field works have shown that upstream migration of knickpoints is also controlled by the upstream drainage area (Schumm et al., 1987; Rosenbloom et al., 1994; Bishop et al., 2005; Crosby and Whipple, in press). This is challenged by the work of Weissel and Seidl (1998) who proposed that the propagation of the incision with knickpoints is rather controlled by the intensity and the frequency of rock failure mechanisms in the gorge head vicinity. These two conclusions are not necessarily contradictory, but they probably depend on the scale of observation. Weissel and Seidl's work is concerned with drainage areas of 10^2 to 10^3 km², i.e., one to three orders of magnitude smaller than the ones considered here. The MSC example shows that drainage areas as large as 10^3 km^2 are the determinant parameter on incision migration. Indeed, the Messinian incisions have developed in different basement lithology ranging from sedimentary rocks to metamorphic or plutonic rocks, and through various basement tectonic structures as well (Table 1). This predominant control of the drainage area, with regard to lithology, was already advanced in other studies (e.g. Bishop and Cowell, 1997; Bishop et al., 2005). For smaller drainage areas than 10^3 km^2, others parameters such as lithology, vegetation or threshold effects are likely to prevail over drainage area in controlling incision migration.

The deduced mean rates of incision migration for the MSC range from 0.1 to 1 myr^{-1} for the drainage areas ranging from 10^3 to 10^4 km², respectively (Table 1). Migration rates reach 2.65 to 10 myr^{-1} for the Rhone and Nile drainage areas, respectively (Table 1). These mean rates are very high compared with those of knickpoints migration for the same time scales (10^5-10^6 years) described in literature (e.g. Van Heijst and Postma, 2001). They reflect the capacity that the large rivers have to respond very fast to a base level drop. Short response times were already suspected with regard to the far inland response (100's km) of large rivers such as the Mississippi and the Colorado to eustatic sea level drops during the Quaternary (Fisk, 1944; Blum, 1993; Saucier, 1996). In a general way, the Messinian pattern may reflect a general scheme concerning migration rate in natural systems whatever the processes involved (pure knickpoint retreat or knickpoint degradation). The comparison between the figure 2 and 3 suggests that at each step of incision migration, the Hack's law is verified. Finally, the relationship that exists between the Messinian incision lengths and the present-day drainage areas argue for similar respective Messinian drainage areas. As a general rule, the present plot could be a good test in order to track the drainage basins which potentially

varied since the end of Miocene in Mediterranean, due in particular to regional deformation induced by the convergence between Africa and Europe plates.

References

Ambert, P., Aguilar, J.P., and Michaux, J., 1998, Evolution géodynamique messinio-pliocène en Languedoc central : le paléo-réseau hydrographique de l'Orb et de l'Hérault (sud de la France): Geodinamica Acta, v. 11, p. 139–146.

Babault, J., Van Den Driessche, J., Bonnet, S., Castelltort, S., and Crave, A., 2005, Origin of the highly elevated Pyrenean peneplain: Tectonics, v. 24, TC2010 doi:10.1029/2004TC001697.

Ballesio, R., 1972, Etude stratigraphique du Pliocène rhodanien: Document du laboratoire de géologie de la Faculté des Sciences de Lyon, v. 53, 333 p.

Barber, P.M., 1981, Messinian subaerial erosion of the Proto-Nile delta: Marine Geology, v. 44, p. 253–272.

Baulig, 1928, Le Plateau central de la France et sa bordure méditerranéenne, Thesis, Paris, 591 p.

Baumard, B., 2001, Valorisation de données pour l'étude de la crise messinienne dans le Gard rhodanien et la moitié est de la France, PhD Thesis, Ecole des Mines de Paris, 260 p.

Bergerat, F., 1987, Stress fields in the european platform at the time of Africa-Eurasia collision: Tectonics, v. 6, p. 99–132.

Betts, H.D., and DeRose, R.C., 1999, Digital elevation models as a tool for monitoring and measuring gully erosion: JAG, v. 1, p. 91–101.

Bishop, P., and Cowell, P., 1997, Lithological and drainage network determinants of the character of drowned, embayed coastlines: Journal of Geology, v. 105, p. 685–699.

Bishop, P., Hoey, T.B., Jansen, J.D., and Artza I.L., 2005, Knickpoint recession rate and catchment area: the case of uplifted rivers in eastern Scotland: Earth Surface Processes and Landforms, v. 30, p. 767–778.

Blum, M.D., 1993, Genesis and Architecture of Incised Valley Fill Sequences: A Late Quaternary Example from the Colorado River, Gulf Coastal Plain of Texas In: Siliciclastic Sequence Stratigraphy, Recent Developments and Applications (Ed. by P. Weimer & H.W. Posamentier), Am. Ass. Petrol. Geol. Mem., v. 58, 259–283.

Brocard, G.Y., Van der Beek, P.A., Bourles, D.L., Siame, L.L., and Mugnier, J.L., 2003, Long-term fluvial incision rates and postglacial river relaxation time in the French Western Alps from 10Be dating of alluvial terraces with assessment of inheritance, soil development and wind ablation effects: Earth and Planetary Science Letters, v. 209, p. 197–214.

Chumakov, I.S., 1973, Pliocene and Pleistocene deposits of the Nile valley in Nubia and upper Egypt: in Initial reports of the Deep Sea Drilling Project, v.13: Washington, D. C., U. S. Government Printing Office, p. 1242–1243.

Clauzon, G., 1978, The Messinian Var canyon (Provence, Southern France). Paleogeographic implications: Marine Geology, v. 27, p. 231–246.

Clauzon, G., 1979, Le canyon messinien de la Durance (Provence, France): une preuve paléogéographique du bassin profond de dessication: Palaeogeography, Palaeoclimatology, Palaeoecology, v. 29, p. 15–40.

Clauzon, G., 1982, Le canyon messinien du Rhône: une preuve désicive du "dessicated deep basin model" (Hsü, Cita et Ryan, 1973): Bulletin de la Société Géologique de France, v. 24, p. 231–246.

Clauzon, G., Aguilar, J.P., and Michaux, J., 1987, Le bassin pliocene du Roussillon (Pyrenees-Orientales, France): exemple d' evolution geodynamique d' une ria mediterraneenne consecutive a la crise de salinite messinienne: Comptes-Rendus de l'Académie des Sciences de Paris, v. 304, p. 585–590.

Clauzon, G., Rubino, J.L. and Savoye, B., 1995, Marine Pliocene Gilbert-type fan deltas along the French Mediterranean coast. A typical infill feature of preexisting subaerial Messinian canyons: In: IAS-16th Regional Meeting of Sedimentology, Field Trip Guide Book, ASF Ed., Paris, v. 23, p. 145–222.

Clauzon, G., Suc, J.P., Gautier, F., Berger, A., and Loutre, M.F., 1996, Alternate interpretation of the Messinian salinity crisis : Controversy resoved?: Geology, v. 24, p. 363–366.

Crosby, B.T., and Whipple K.X., In press, Knickpoint Initiation and Distribution within Fluvial Networks: 236 waterfalls in the Waipaoa River, North Island, New Zealand: Geomorphology: The Bedrock Channels Special Issue.

Depéret, C., 1895, Aperçu sur la structure générale et l'histoire de la formation de la vallée du Rhône, Annales de Géographie, vol. 4, p. 432–452.

Derricourt, R.M., 1976, Retrogression rate of the Victoria falls and the Batoka gorge: Nature, v. 264, p. 23–25.

Fisk, H.N., 1944, Geological Investigation of the Alluvial Valley of the Lower Mississippi River: Mississippi River Commission, Vicksburg.

Gardner, T.W., 1983, Experimental study of knickpoint and longitudinal profile evolution in cohesive, homogeneous material: Geological society of America Bulletin, v. 94, p. 664–672.

Griffin, D.L., 2002, Aridity and humidity: two aspects of the late Miocene climate of North Africa and the Mediterranean: Palaeogeography, Palaeoclimatology, Palaeoecology, v. 182, p. 65–91.

Hack, J.T., 1957, Studies of longitudinal stream profiles in Virginia and Maryland, U. S. Geological Survey Professional Paper, v. 294-B, p. 45–97.

Hassan, M.A., and Klein, M.U., 2002, Fluvial adjustment of the Lower Jordan River to a drop in the Dead Sea level: Geomorphology, v. 45, p. 21–33.

Hayakawa, Y., and Matsukura, Y., 2003, Recession rates of waterfalls in Boso peninsula, Japan, and a predictive equation: Earth Surface Processes and Landforms, v. 28, p. 675–684.

Hsü, K.J., Cita, M.B., and Ryan, W.B.F., 1973, The origin of the Mediterranean evaporites: in Initial reports of the deep sea drilling project, v.13: Washington, D. C., U. S. Government Printing Office, p. 1203–1231.

Irr, F., 1984, Paléoenvironnements et evolution géodynamique néogènes et quaternaries de la bordure nord du bassin méditerranéen occidental, un système de pente de la paléo-marge liguro-provençale: Thesis, 464 p.

Krijgsman, W., Hilgen, F.J., Raffi, I., Sierro, F.J., and Wilson, D.S., 1999, Chronology, causes and progression of the Messinian salinity crisis: Nature, v. 400, p. 652–655.

Loget, N., Van Den Driessche, J., and Davy, P., 2005, How did the Messinian Salinity Crisis end?: Terra Nova v. 17, 414–419

Mandier, P., 1988, Le relief de la moyenne vallée du Rhône au Tertiaire et au Quaternaire. Essai de synthèse paléogéographique: Document BRGM, 151.

Montgomery, D.R., and Dietrich, W.E., 1992, Channel initiation and the problem of landscape scale: Science, v. 255, p. 826–830.

Parker, R.S., 1977, Experimental study of basin evolution and its hydrologic implications: unpublished PhD dissertation, Colorado State University, Fort Collins, 331 p.

Pazzaglia, F.P., Gardner, T.W., and Merrits, D.J., 1998, Bedrock Fluvial incision and longitudinal profile development over geologic time scales determined by fluvial terraces, in Tinkler, K. J., and Wohl, E. E., eds., Rivers over rock: fluvial processes in bedrock channels: American Geophysical Union Geophysical Monograph 107, p. 207–235.

Pik, R., Marty, B., Carignan, J., and Lavé, J., 2003, Stability of the Upper Nile drainage network (Ethiopia) deduced from (U–Th)/He thermochronometry: implications for uplift and erosion of the Afar plume dome: Earth and Planetary Science Letters, v. 215, p. 73–88.

Rosenbloom, N.A., and Anderson, R.S., 1994, Hillslope and channel evolution in a marine terraced landscape, Santa Cruz, California: Journal of Geophysical Research, v. 99, p. 14,013–14,029.

Saucier, R.T., 1996, A contemporary appraisal of some key Fiskian concepts with emphasis on Holocene meanderbelt formation and morphology: Engineering Geology, v. 45, 67–86.

Schumm, S.A., Mosley, M.P., and Weaver, W.E, 1987, Experimental fluvial geomorphology: New York, Wiley, 413 p.

Seginer, I., 1966, Gully development and sediment yield: Journal of Hydrology, v. 4, p. 236–253.

Seidl, M.A., Dietrich, W.E., and Kirchner, J.W., 1994, Longitudinal profile development into bedrock: An analysis of Hawaiian channels: J. Geol., v. 102, p. 457–474.

Séranne, M., Camus, H., Lucazeau, F., Barbarand, J., and Quinif, Y., 2002, Surrection et érosion polyphasées de la bordure cévenole. Un exemple de morphogenèse lente: Bulletin de la Société Géologique de France, v. 173, p. 97–112.

Sissingh, W., 2001, Tectonostratigraphy of the West Alpine foreland: correlation of Tertiary sedimentary sequences, changes in eustatic sea-level and stress regimes: Tectonophysics, v. 333, p. 361–400.

Van Heijst, M.W.I.M., and Postma, G., 2001, Fluvial response to sea level changes: a quantitative analogue, experimental approach: Basin Research, v. 13, p. 269–292.

Weissel, J.K. and Seidl, M.A., 1998, Inland Propagation of Erosional Escarpments and River Profile Evolution Across the Southeast Australian Passive Continental Margin In: K.J. Tinkler and E.E. Wohl (Editors), Rivers Over Rock: Fluvial Processes in Bedrock Channels, American Geophysical Union, Washington, D. C., pp. 189–206.

Whipple, K.X., and Tucker, G.E., 1999, Dynamics of the stream-power river incision model: Implications for height limits of mountain ranges, landscape response timescales, and research needs: Journal of Geophysical Research, v. 104, p. 17661–17674.

Wohl, E. E. 1998, Bedrock channel morphology in relation to erosional processes, in Tinkler, K. J., and Wohl, E. E., eds., Rivers over rock: fluvial processes in bedrock channels: American Geophysical Union Geophysical Monograph 107, p. 133–151.

Young, R.W., and McDougall, I., 1993, Long-term landscape evolution: Early Miocene and modern rivers in southern New South Wales, Australia: Journal of Geology, v. 101, p. 35–49.

FIGURES

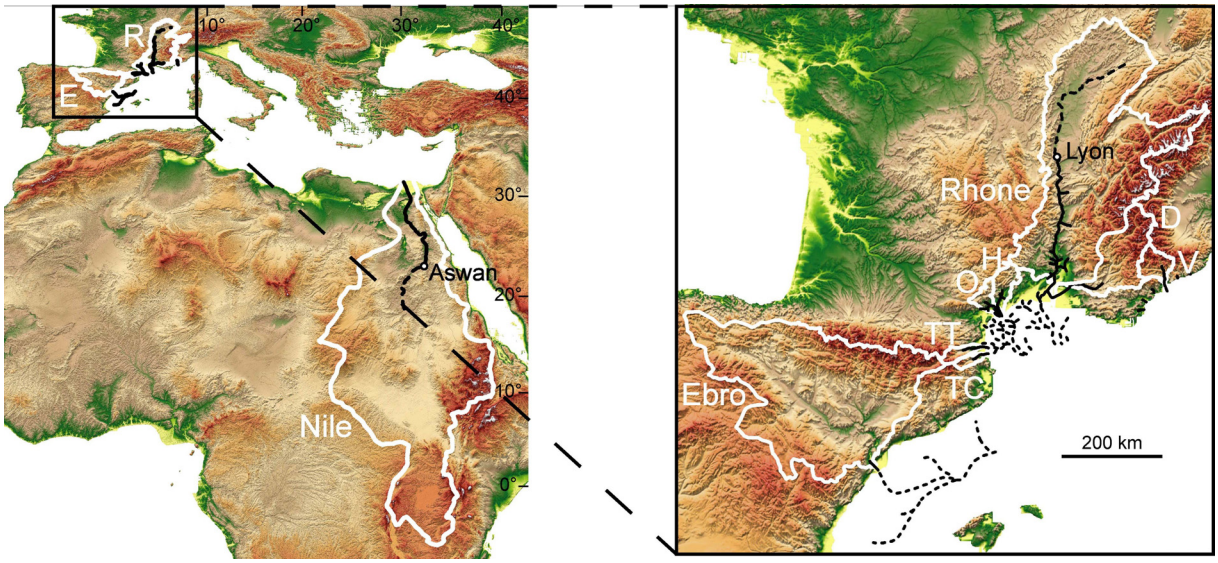

Figure 1

Digital Elevation Model showing the Messinian incisions and the corresponding current drainage areas (source: GTOPO30).

Thick black lines-Onshore incisions; Dotted black lines-Offshore incisions; Dashed black lines-Possible maximum extension.

D-Durance ; E-Ebro ; O-Orb ; H-Herault ; R-Rhone ; TC-Tech ; TT-Tet ; V-Var.

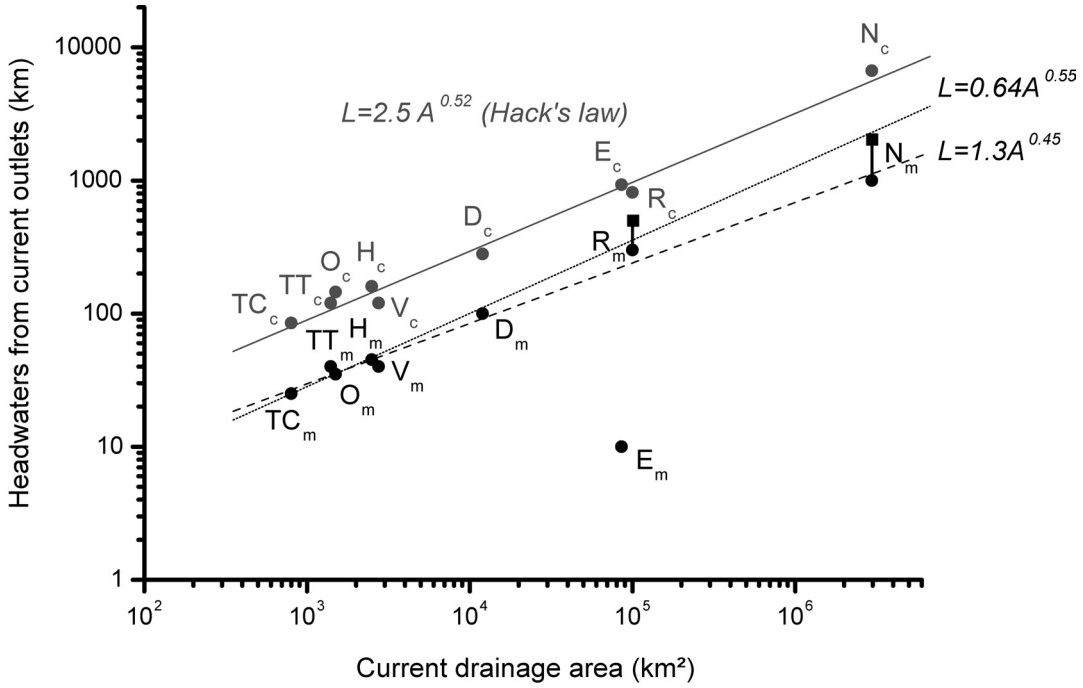

Figure 2

Black (thick and dashed): Lengths of the Messinian incisions (measured from the present coast line) versus the corresponding present-day drainage areas (see text for further explanation)

Grey: present-day river lengths versus their respective drainage areas.

Index c and m refer to current rivers and Messinian incisions respectively.

D-Durance ; E-Ebro ; O-Orb ; H-Herault ; N- Nile; R-Rhone ; TC-Tech ; TT-Tet ; V-Var.

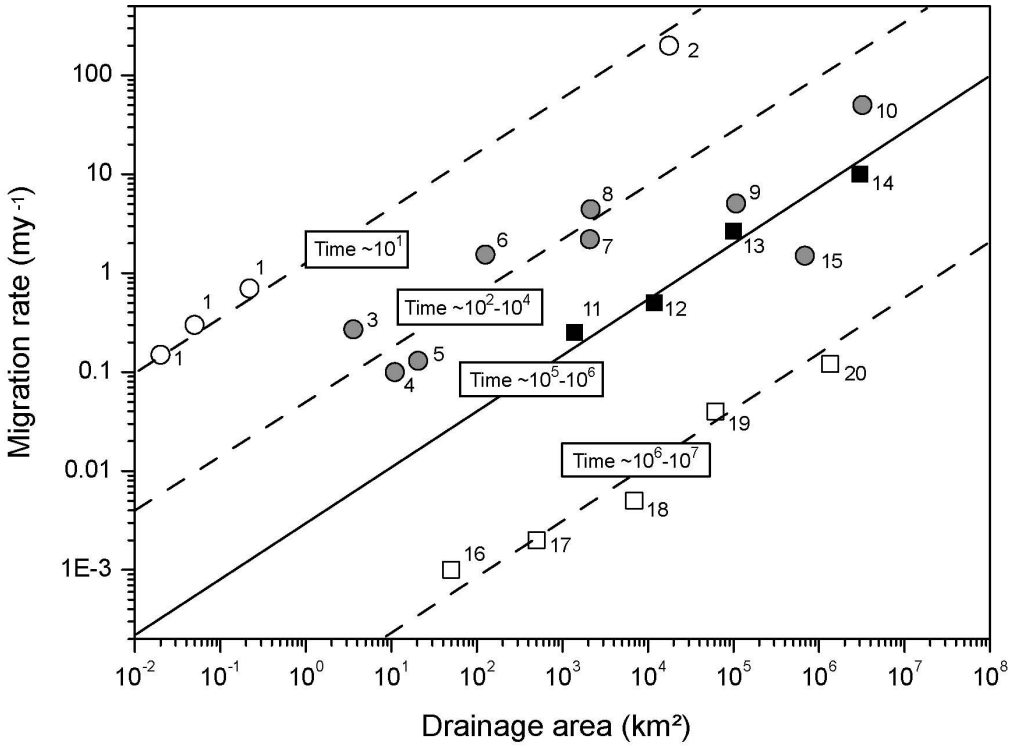

Figure 3

Average migration rates of incisions versus drainage areas. Four domains can be determined with regards to the time scale (10^1 yrs: white circle; 10^2-10^4 yrs: grey circle; 10^5-10^6 yrs: black square; 10^6-10^7: white square) which boundaries correspond to the equation $V=C\sqrt{A}$

1- Waipaoa gullies (Betts and Derose, 1999); 2- Jordan river (Hassan and Klein, 2002); 3- Sanagowa falls (Hayakawa and Matsukura, 2003); 4- Zenzen falls (Hayakawa and Matsukura, 2003); 5- Catterline Burn (Bishop et al., 2005); 6- Bervie Water (Bishop et al., 2005); 7- Drac river (Brocard et al., 2003); 8- Waipaoa river (Crosby and Whipple, in press); 9- Colorado river (Blum, 1993); 10- Mississippi river (Fisk, 1944); 11- Tech river (this study); 12- Durance river (this study); 13- Rhone river (this study); 14- Nile river (this study); 15- Niagara falls (Wohl, 1998); 16- Hawaïan rivers (Seidl et al., 1994); 17- McCleay river (Weissel and Seidl, 1998); 18- Shoalhaven river (Young and McDougall, 1993) ; 19- Susquehanna river (Pazzaglia et al., 1998); 20- Victoria falls (Derricourt, 1976).

River	Current Drainage area [km²]	Current Length [km]	Lengths of messinian incisions from the current shoreline [km]	Migration rate [my^{-1}]	Lithology	References
Nile	2960000	6671	1000 2000	3.3-10 6.6-20	Sedimentary rocks, Granitic rocks	Chumakov, 1973 Barber, 1981
Rhone	99000	812	300 500	1-3 1.6-5	Sedimentary rocks (sanstone, limestone), Grantic rocks	Clauzon, 1982 Mandier, 1988 Baumard, 2001
Ebro	85820	930	10	0.033-0.1	Granitic rocks, Metamorphic rocks	Maestro et al., 2002
Durance	12000	280	100	0.33-1	Sedimentary rocks (sanstone, limestone)	Clauzon, 1979
Var	2758	120	40	0.13-0.4	Sedimentary rocks (sanstone, limestone)	Clauzon, 1978 Irr, 1984
Herault	2500	160	45	0.15-0.45	Sedimentary rocks (sanstone, limestone)	Ambert, 1998
Orb	1758	145	35	0.12-0.35	Sedimentary rocks (sanstone, limestone)	Clauzon et al., 1995 Ambert, 1998
Tet	1400	120	40	0.13-0.4	Sedimentary rocks (sanstone, limestone), Grantic rocks, Metamorphic rocks	Clauzon et al., 1995
Tech	800	85	25	0.08-0.25	Sedimentary rocks (sanstone, limestone), Grantic rocks, Metamorphic rocks	Clauzon et al., 1995

Table 1

Morphological features and geological settings of several Messinian incisions and the corresponding present-day drainage basins. The two-end member migration rate values are deduced from the time range of the Messinian erosional stage (after Clauzon et al., 1996; Krijgsman et al., 1999).

2.3. Annexes à la partie 2

2.3.1. Caractéristiques morphologiques des canyons messiniens.

2.3.2 Simulations numériques complémentaires

2.3.3. Rebond isostatique lié à l'assèchement de la Méditerranée et conséquences sur le niveau de base messinien.

2.3.1. Caractéristiques morphologiques des canyons messiniens

Le Canyon messinien du Rhône

Ce canyon s'étend sur plus de 300 km depuis la Camargue jusqu'au nord de Lyon (Ballesio, 1972 ; Clauzon, 1982). Sa découverte remonte à la fin du XIX^{ème} siècle grâce aux travaux de Fontannes (1882). L'origine de sa formation, à savoir une chute du niveau de base méditerranéen pendant le Messinien, a été proposé par Denizot (1952), puis Clauzon (1973, 1982) suite à la découverte des évaporites en Méditerranée (Leg 13).

Le canyon messinien du Rhône traverse les terrains tertiaires puis secondaires, avant d'atteindre le socle hercynien à partir de Valence (Figure a1). Il met en évidence le réseau qui préfigurait le Rhône actuel, à la fin du Miocène. Ce réseau était déjà composé d'un drain principal Nord-sud collectant la partie occidentale des Alpes et la partie orientale du Massif Central, de manière très analogue au Rhône actuel. Les tributaires du Rhône étaient également présents, les plus développés étant les tributaires alpins. La Durance confluait avec le Rhône beaucoup plus au Sud qu'actuellement, traversant les Alpilles et empruntant le même cours qu'actuellement plus en amont (Clauzon, 1979). Plus au nord, deux affluents alpins (paléo-Aigues et paléo-Ouvèze) ainsi que deux affluents rive droite (paléo-Cèze et paléo-Ardèche) se jetaient dans le Rhône au Nord d'Avignon. L'affluent le plus septentrional qui drainait le Nord des Alpes (qui préludait l'Isère actuelle) confluait avec le Rhône dans la région de la Bièvre-Valloire. La partie avale, aujourd'hui ennoyée et préservée sous la plate-forme du golfe du Lion actuelle, a été densément prospecté (e.g. Gennesseaux and Lefebvre, 1980 ; Séranne et al., 1995 ; Guennoc et al., 2000) (Figure a2). L'incision au niveau de la Camargue dépasse le millier de mètres avec un canyon large d'environ 5km (Gennesaux and Lefebvre, 1980 ; Clauzon, 1982).

Le canyon messinien du Rhône a été fossilisé par la ré inondation pliocène, consécutive à l'ouverture du détroit de Gibraltar (Gentil, 1909 ; Hsü et al., 1973 ; Campillo et al., 1992 ; Blanc, 2002). Le retour au niveau 0 de la Méditerranée conjugué au haut eustatique Pliocène (+80 m) (Haq et al., 1987) a permis à la mer de s'engouffrer dans la vallée du Rhône jusqu'à Lyon en séparant les Alpes du Massif Central de la même manière qu'un fjord ou une ria (Figure a3). Les dépôts détritiques qui ont remplis la ria rhodanienne sont liés à la mise en place d'un Gilbert delta (Gilbert, 1885) (Figure a4 et a5).

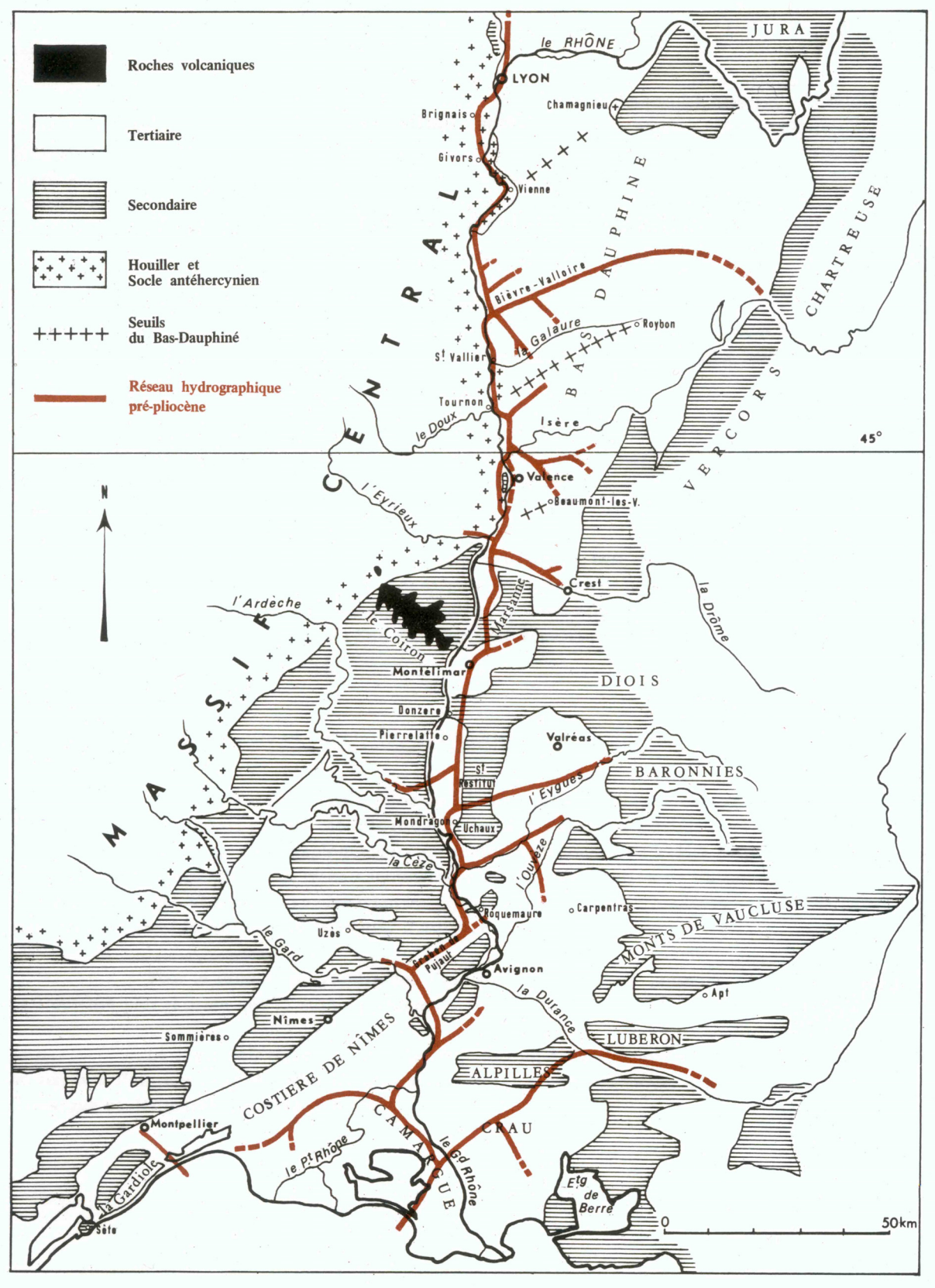

Figure a1 *: Cartographie du réseau messinien dans le bassin rhodanien (d'après Ballésio, 1972)*

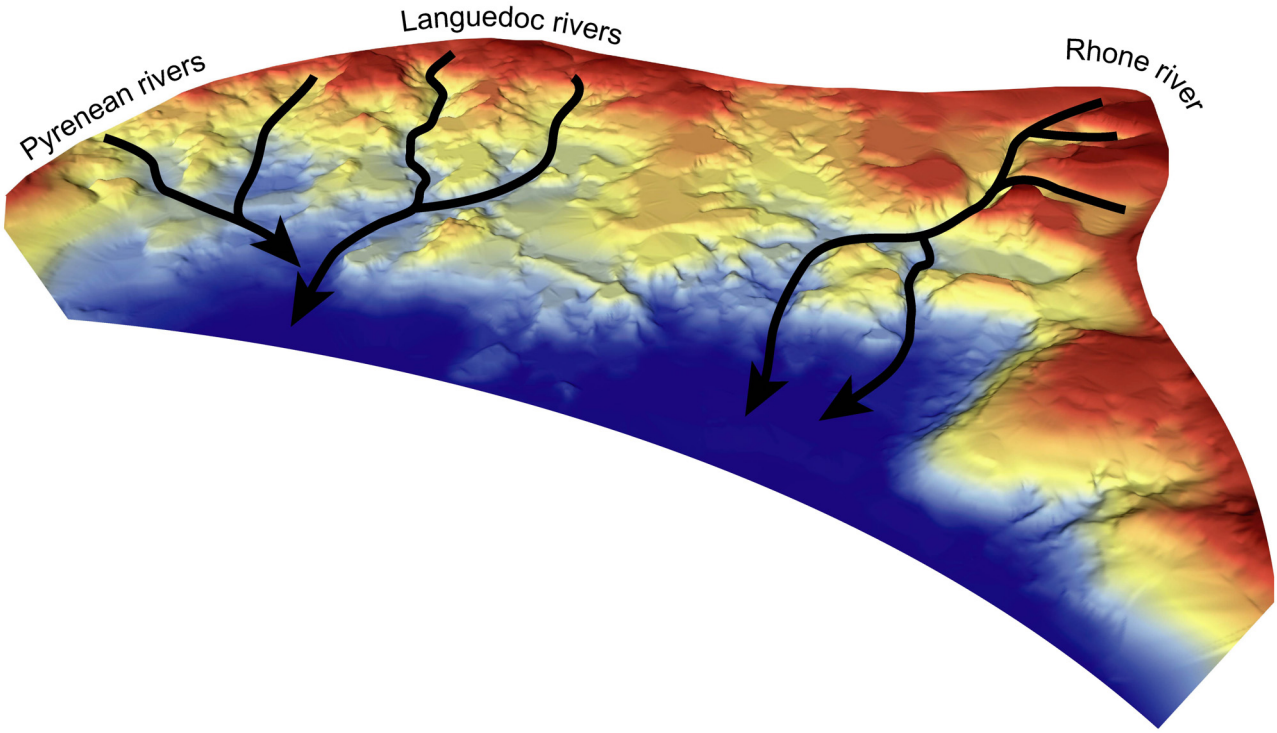

Figure a2 *: Modèle Numérique de Terrain de la surface messinienne préservée sous la plate-forme du Golfe du Lion montrant la position des canyons messiniens au débouché des rivières actuelles (réalisé à partir des données publiées par Guennoc et al., 2000).*
Notez la très forte incision du Rhône comparée aux autres rivières méridionales.

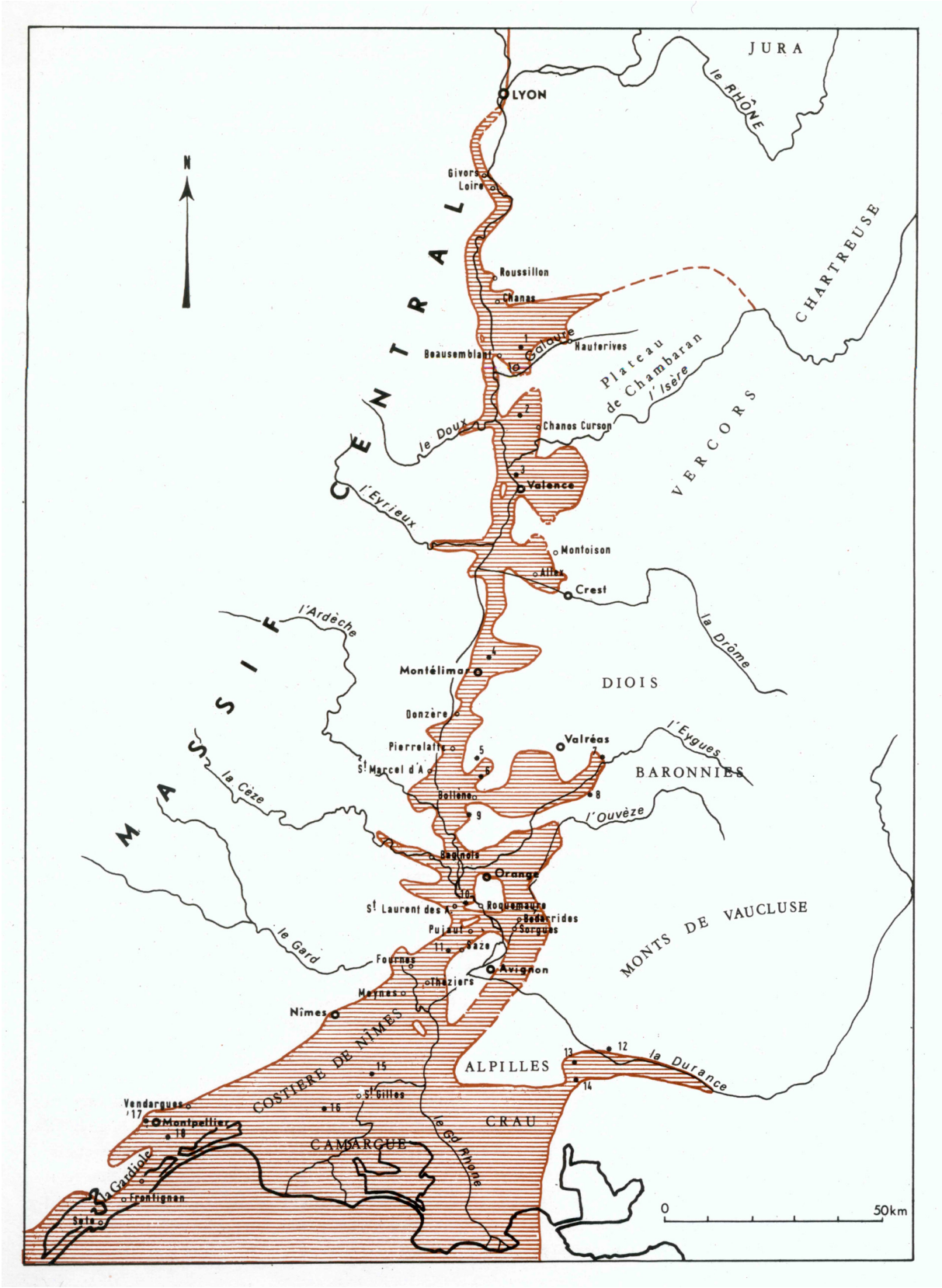

Figure a3 *: Cartographie de la ria pliocène dans le bassin rhodanien (d'après Ballésio, 1972)*

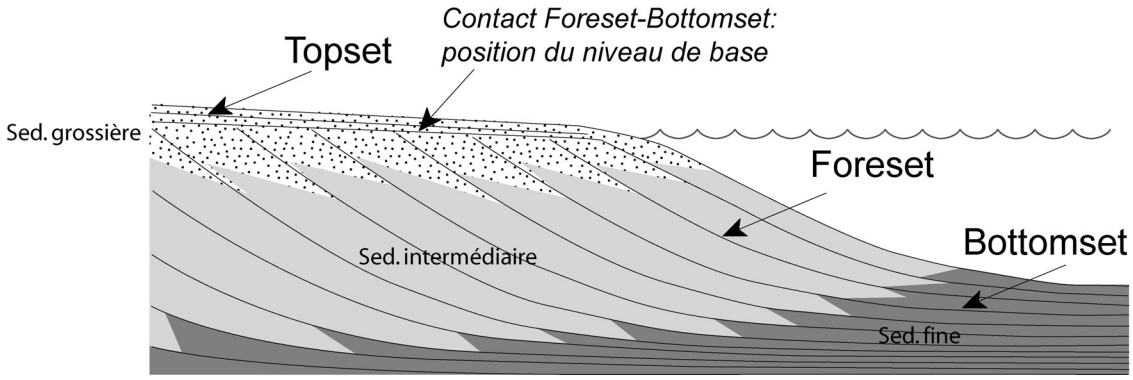

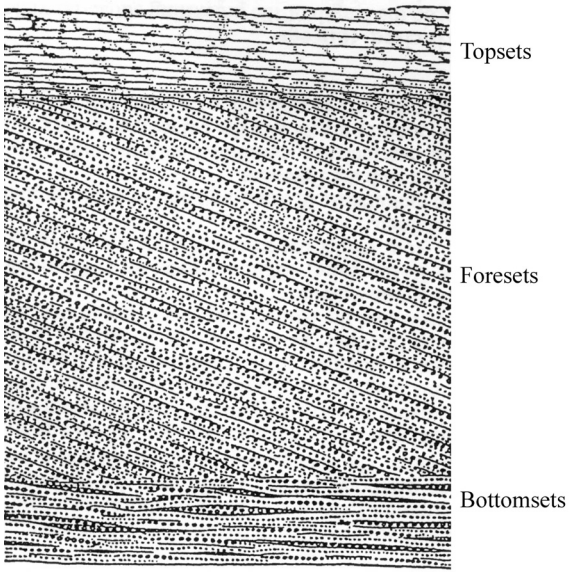

Figure a4 *: Mise en place et structure d'un "Gilbert delta".*
Ce type de delta a été pour la première fois décrit dans les dépôts pléistocènes du lac Bonnevile aux USA par Gilbert (1885) (figure de gauche).
Le gilbert delta peut être assimilé à un eventail deltaïque se déposant en milieu profond (type fjord ou lac périglaciaire).
Il se distingue de son homologue de plate-forme par un angle de progradation des structures sédimentaires très prononcé (10° à 35°) ainsi qu'une sédimentation plus grossière.
La géométrie du dépôt peut être subdivisé en 3 parties distinctes (figure du haut): une série sub aquatique penté (foresets), une série profonde tangentielle plus fine (bottomsets) et une série sub aquatique à subaérienne (topsets).
Les foresets et les topsets sont séparés par une surface horizontale qui représente le niveau de la mer ou du lac pendant le remplissage.

Figure a5 *: Exemple d'un "Gilbert delta" dans la vallée du Roussillon. Notez au centre de l'image le pendage prononcé des structures sédimentaires ou foresets (photo : J. Lofi).*

Le Canyon Messinien du Nil

La découverte du canyon messinien du Nil remonte aux travaux de Chumakov (1967) suite aux travaux entrepris pour la construction du barrage d'Assouan. Ces travaux ont révélé l'existence d'une incision dans le substratum granitique remplie par des sédiments marins pliocènes. L'origine de cette incision est restée inconnue jusqu'à la découverte des évaporites messinniennes en Méditerranée, Chumakov (1973) reliant alors la découverte de cette incision à la chute du niveau de base consécutive à la Crise de Salinité Messinienne (Figure a6).
Par la suite, les travaux de Barber (1981) vont directement confirmer la présence d'une telle incision en révélant l'existence d'un canyon profond de plus de 1000m dans sa partie avale entre Alexandrie et le Caire (Figure a7).

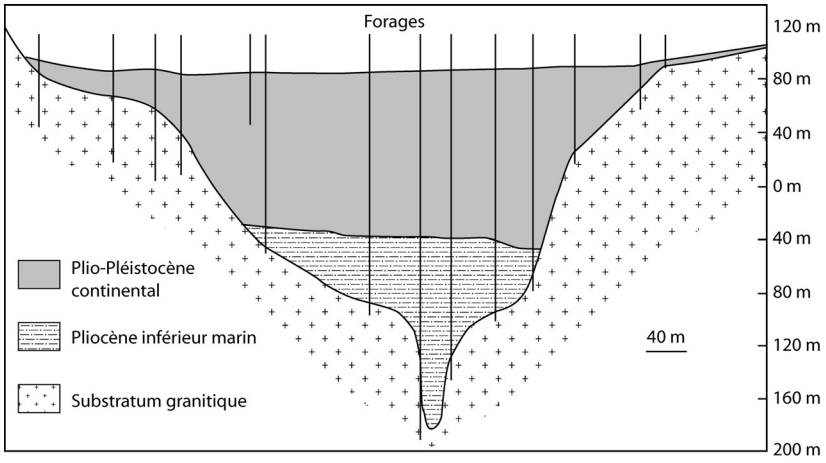

Figure a6 *: Coupe transverse au niveau de Assouan montrant l'incision messinienne du Nil enregistrée à plus de 1000 km de la ligne de côté, et où se sont déposés les sédiments marins pliocènes consécutif au remplissage de la Méditerranée (d'après Chumakov, 1973).*

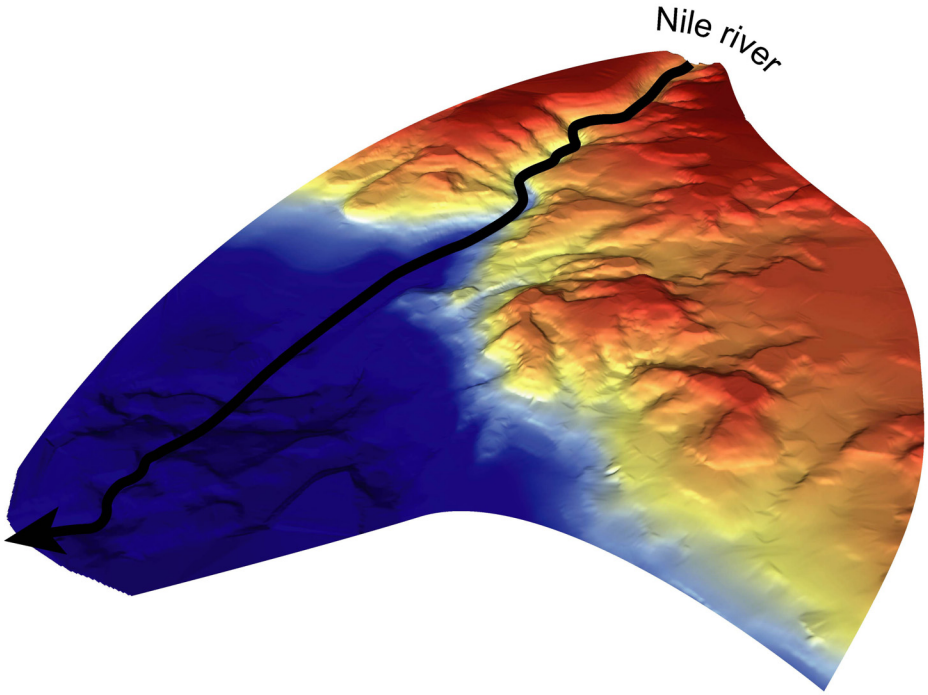

***Figure a7** : Modèle Numérique de Terrain de la surface messinienne dans la parie avale du bassin du Nil. (D'après les données isobathes publiées par Barber, 1981).*
Notez la très forte incision du Nil qui se prolonge jusqu'à Assouan (1000 km en amont).

Le canyon de l'Ebre-Valence

La découverte de ce canyon remonte au leg 13 (Ryan et al., 1973) qui avait mis en évidence une surface d'érosion. La présence et la géométrie d'un canyon aérien (Figure a8) ont par la suite été démontré suite aux nombreuses campagnes sismiques qui ont eu lieu dans la fosse de Valence (e.g. Stampfli and Höcker, 1989 ; Field and Gardner, 1990 ; Escutia and Maldonado, 1992 ; Maillard, 1993).

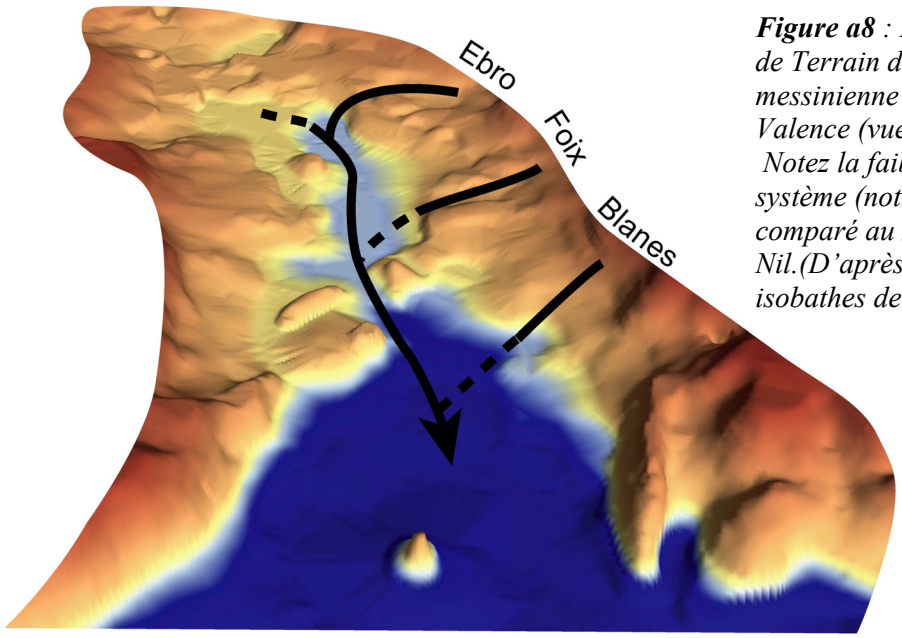

***Figure a8** : Modèle Numérique de Terrain de la surface messinienne dans la fosse de Valence (vue vers le Sud).*
Notez la faible incision de ce système (notamment l'Ebre) comparé au système Rhône ou Nil.(D'après les données isobathes de Maillard, 1993)

2.3.2 Simulations numériques complémentaires

Cette annexe illustre les expériences citées dans l'article : "Propagation of large length scale fluvial incision: Insight from the Messinian sea-level drop modelling."
Pour chacune d'elle a été reporté plusieurs stades de croissance du réseau de drainage (vues 3D) ainsi que l'évolution de l'érosion enregistrée au niveau de la vallée du Rhône. L'évolution de la courbe d'érosion cumulée (graphique de droite) comparée aux données géologiques (points noirs) ainsi que l'évolution du profil longitudinal (graphique de gauche) ont également été reportés. Le temps, comparable entre les différentes simulations numériques, est un temps numérique correspondant à un temps réel compris entre 90 et 300 Ka (Clauzon et al., 1996 ; Kijgsman et al., 1999).

	Paramètres		
Numéro de l'expérience	m	n	ξ (km)
1	1	1	1
2	1.5	1	1
3	2	1	1
4	1	2	1
5	1.5	2	1
6	2	2	1
7	1.5	1	40
8	1.5	1	400
9	1	1	40
10	1	1	400

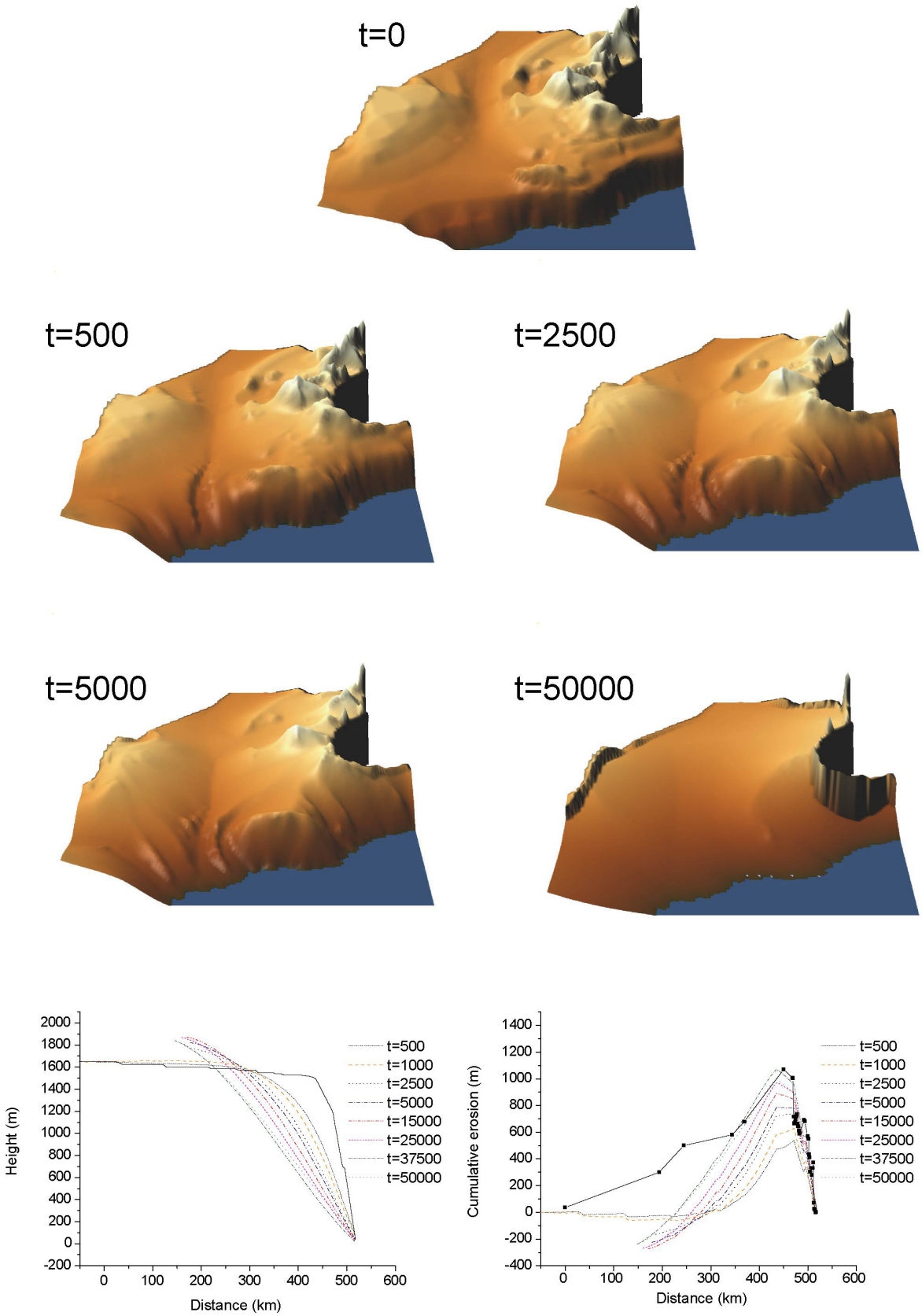

Figure a9 : Expérience 1

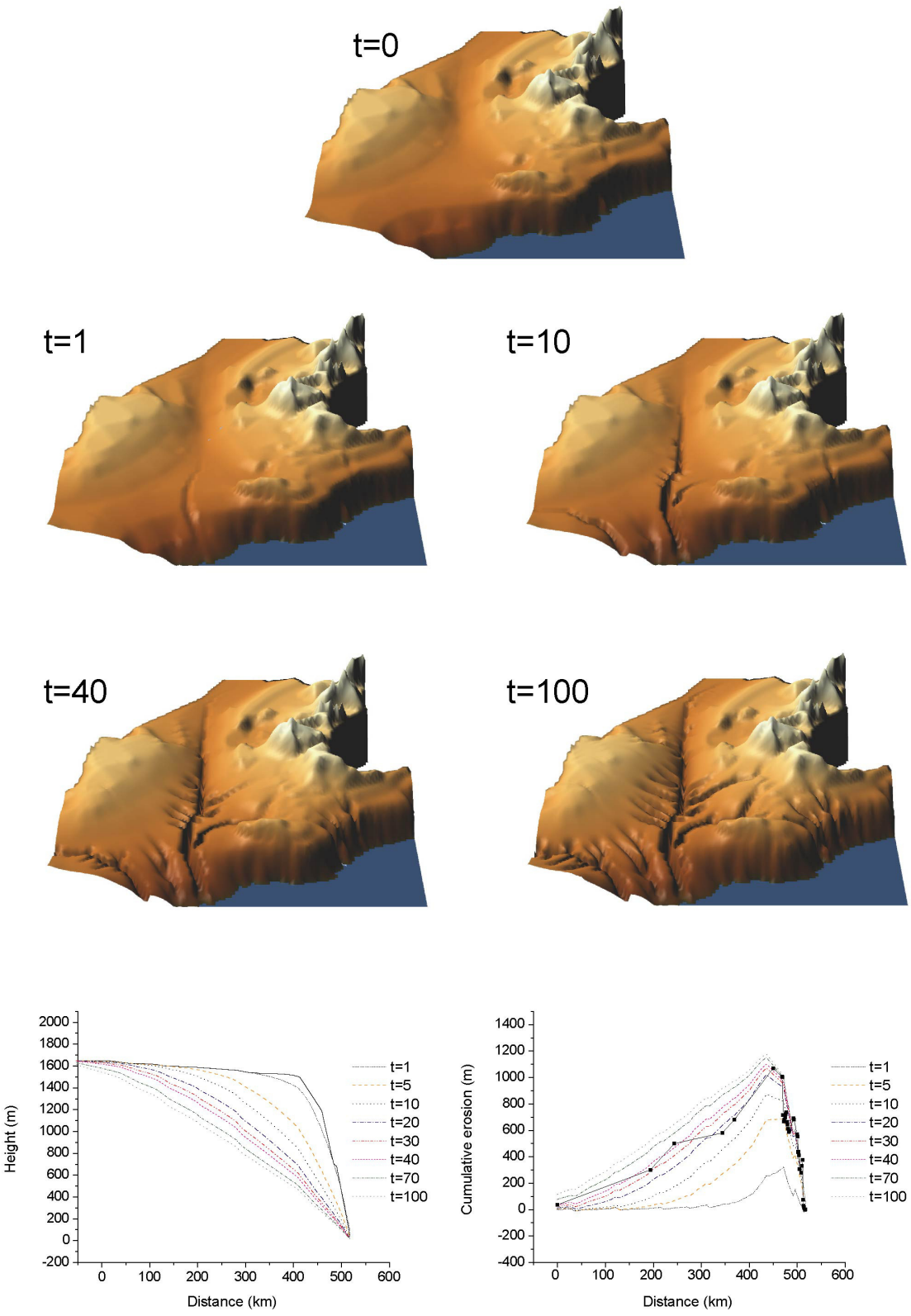

Figure a10 : Expérience 2

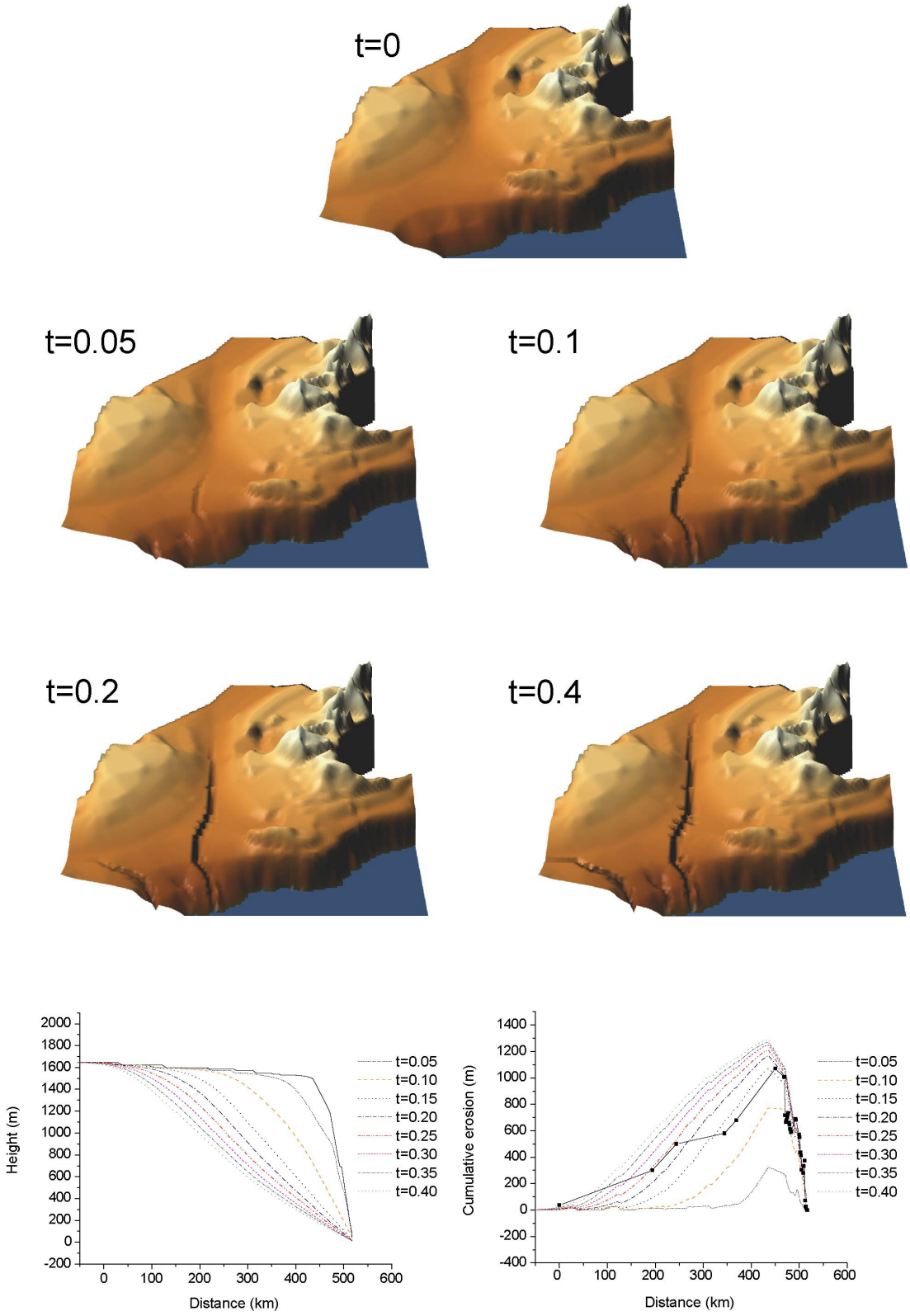

Figure a11 : Expérience 3

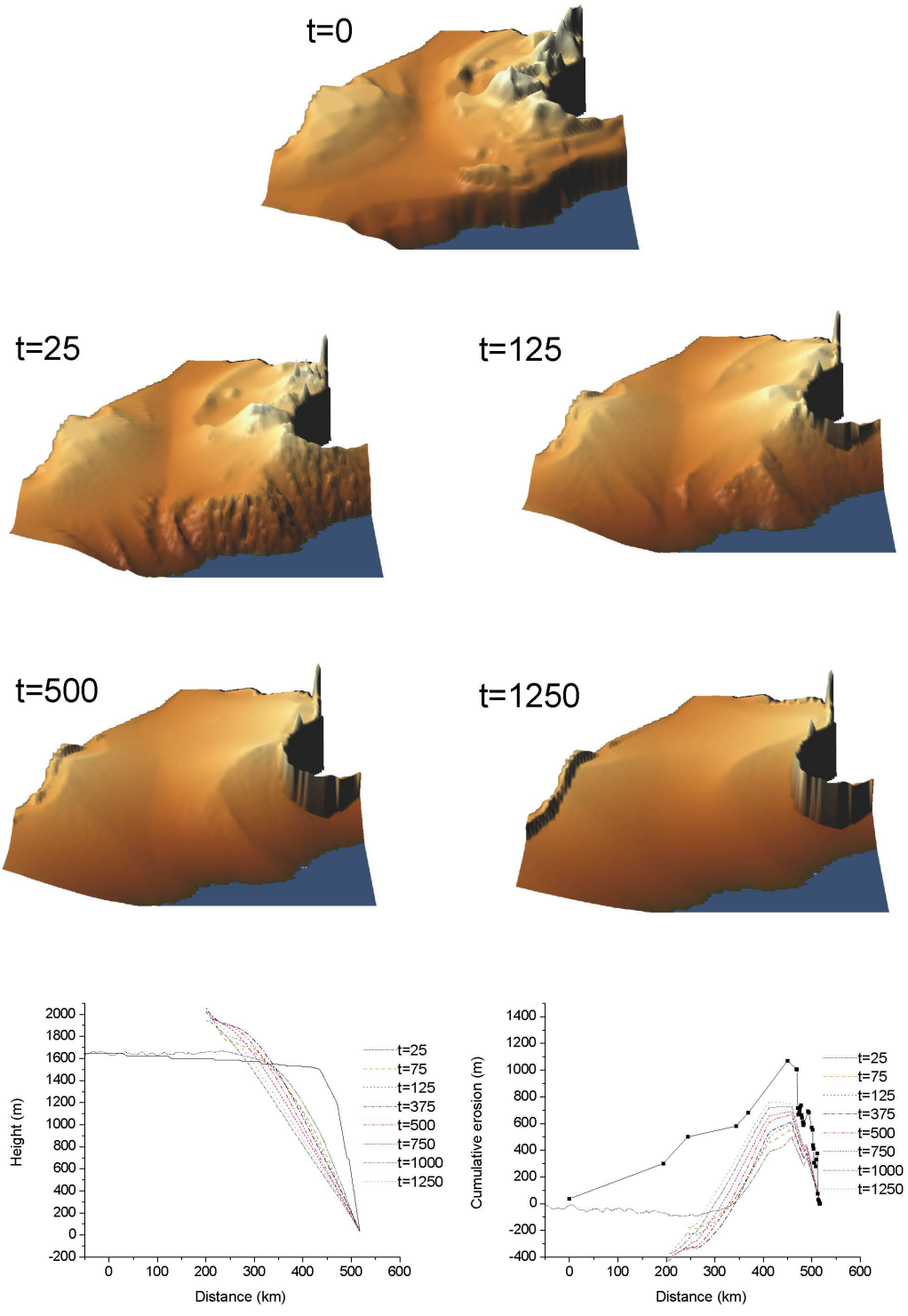

Figure a12 : Expérience 4

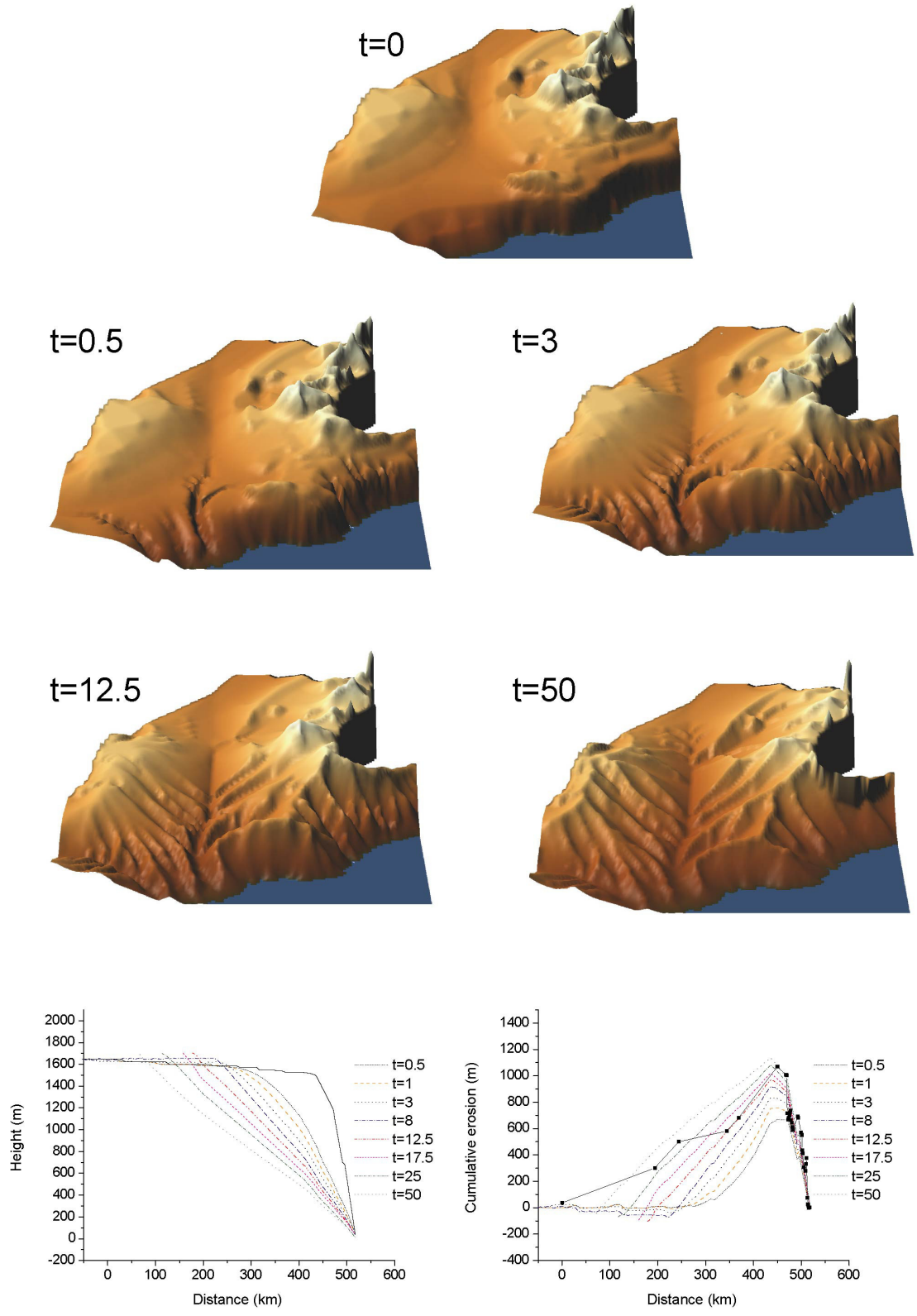

Figure a13 : Expérience 5

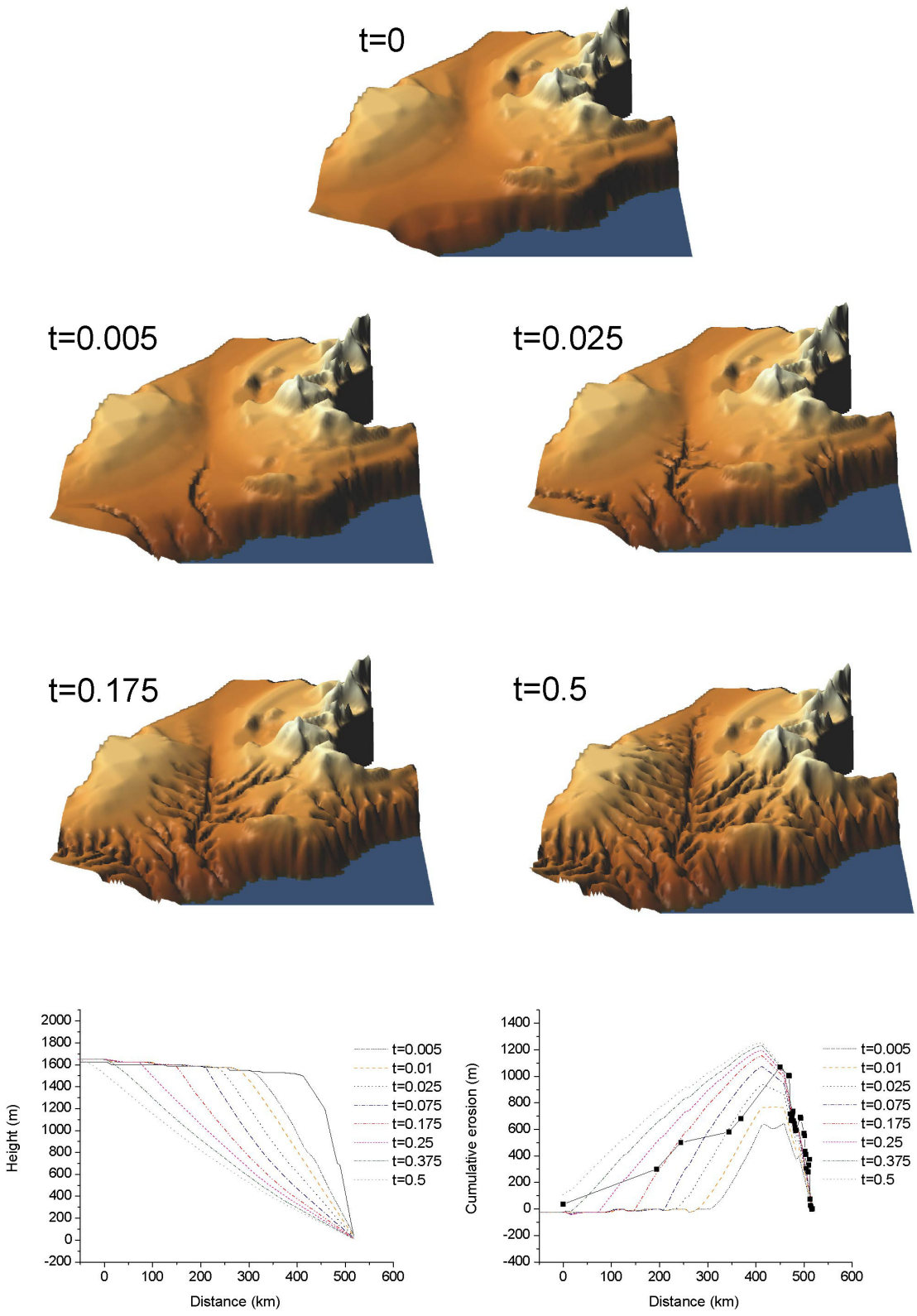

Figure a14 : Expérience 6

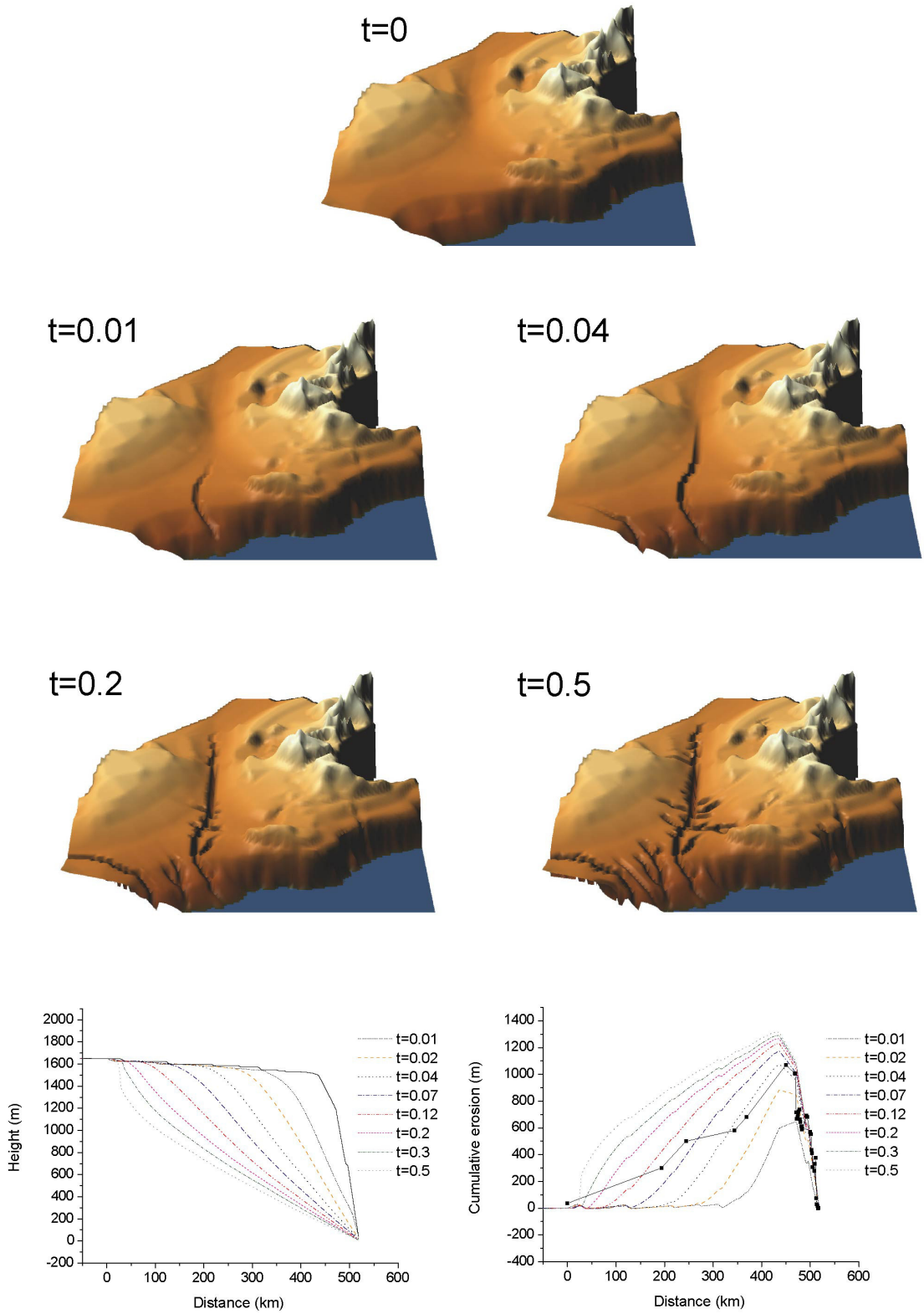

Figure a15 : Expérience 7

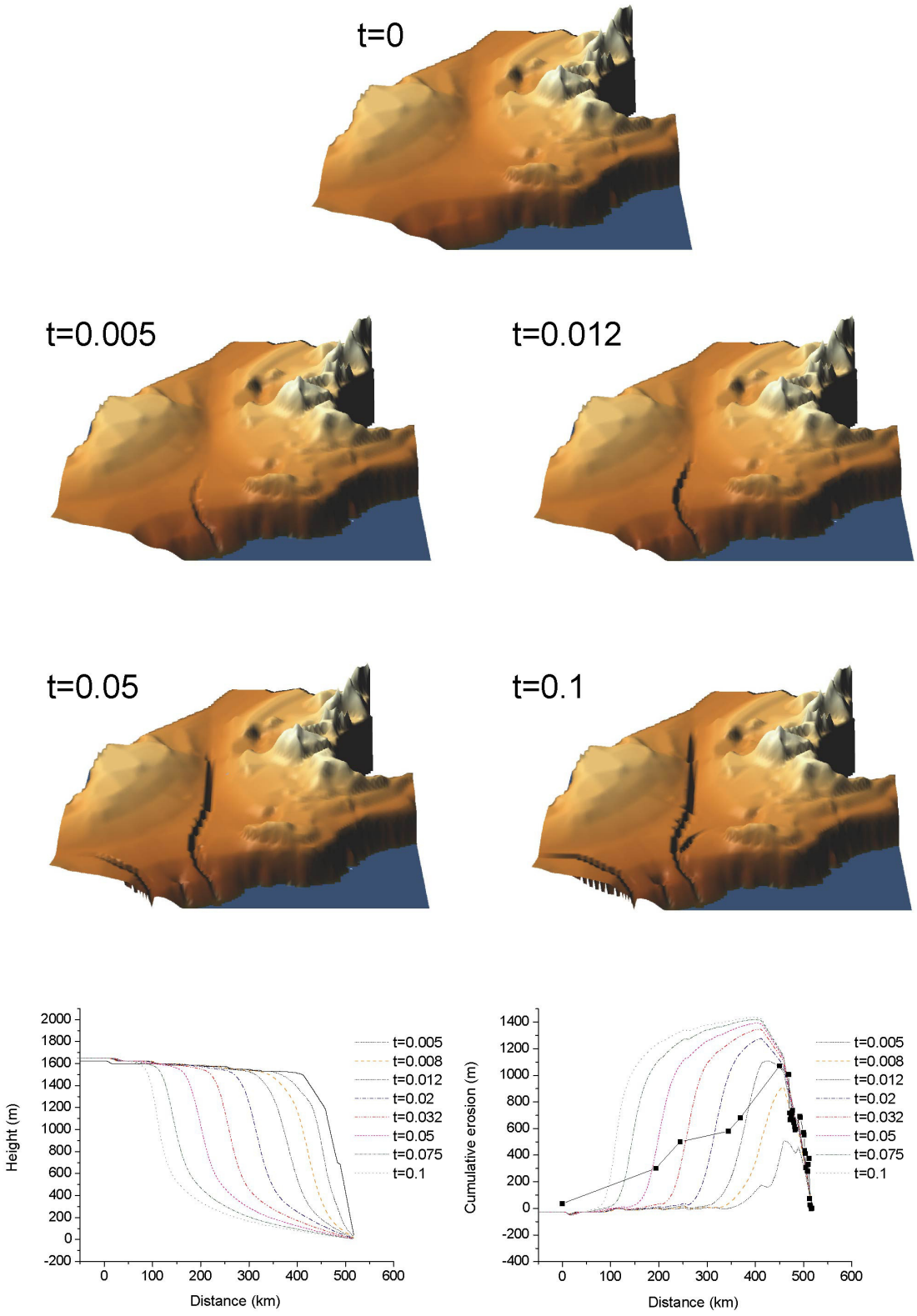

Figure a16 : Expérience 8

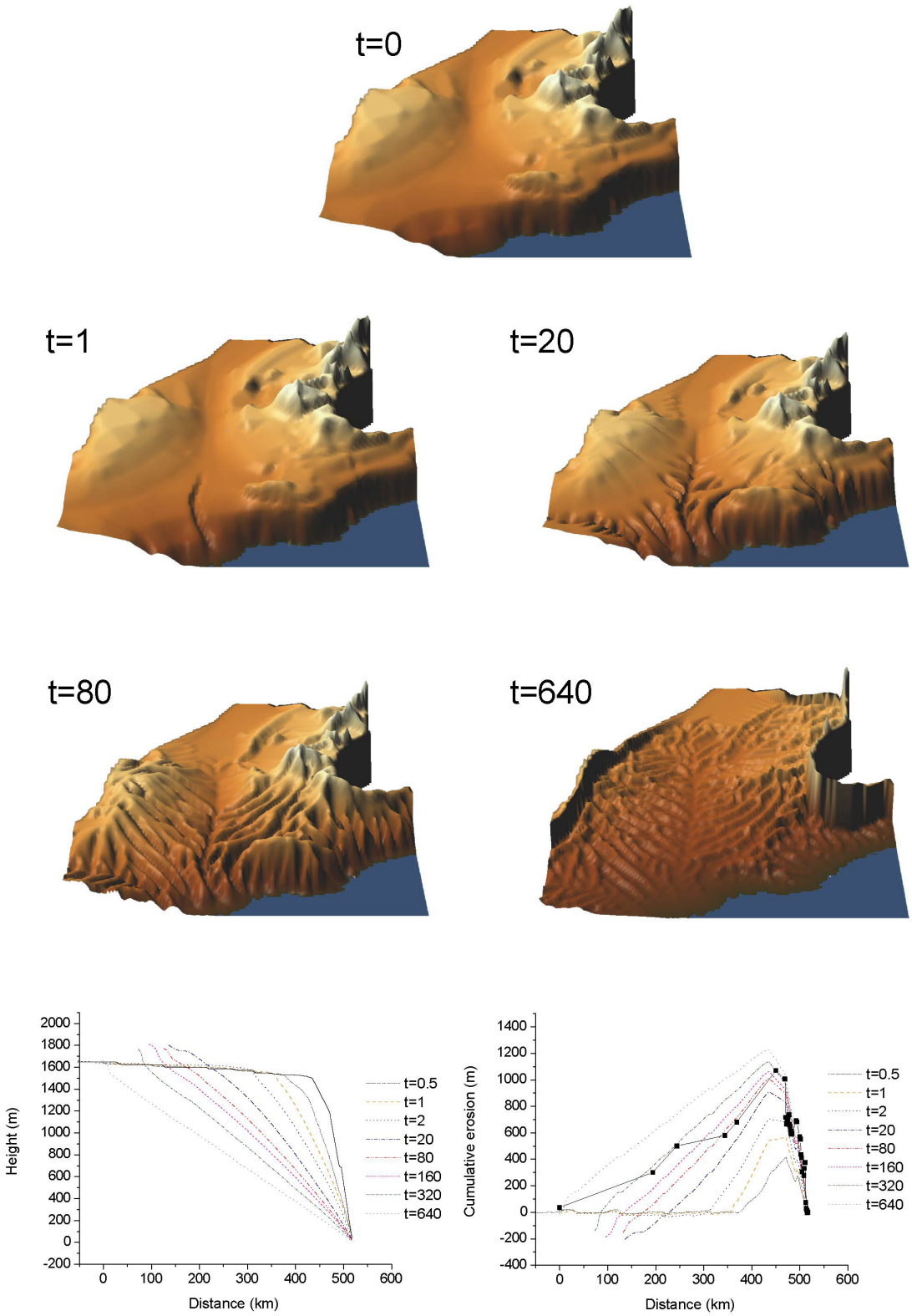

Figure a17 : Expérience 9

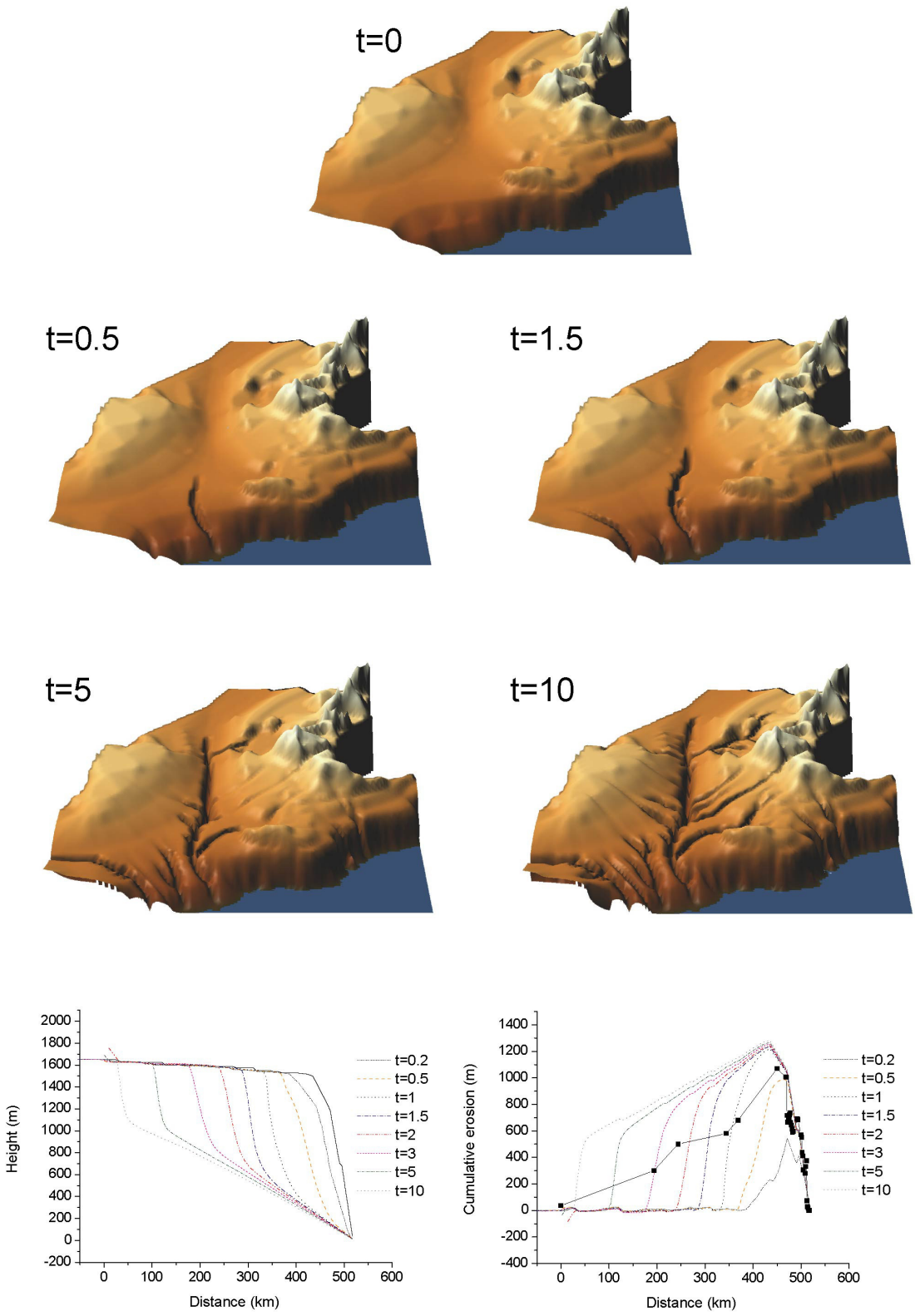

Figure a18 : Expérience 10

2.3.3. Rebond isostatique lié à l'assèchement de la Méditerranée et conséquences sur le niveau de base messinien.

Norman et Chase (1986) ont montré que l'évaporation de la Méditerranée a vraisemblablement provoqué un rebond isostatique dans le bassin ainsi que sur tout le littoral méditerranéen (Figure a19). En simulant une évaporation totale de la Méditerranée actuelle, ils en déduisent que l'assèchement de la Méditerranée a provoqué une remontée du substratum de l'ordre de 1000m dans le bassin, et de plusieurs dizaines voire centaines de mètres sur le rivage méditerranéen. En soustrayant la subsidence liée aux dépôt d'évaporites qu'ils considèrent comme tardifs dans l'histoire de la Crise Messinienne, ils déduisent une remontée de plus de 2000m du substratum dans le centre du bassin et de plusieurs centaines de mètres sur le rivage. Les conséquences sur le développement des incisions sont alors majeures puisque une partie de l'incision enregistrée en aval serait liée à un uplift du rivage. Norman et Chase (1986) proposent que ce mouvement aurait même pu inverser les réseaux de drainage qui n'auraient pas eu la capacité d'inciser.

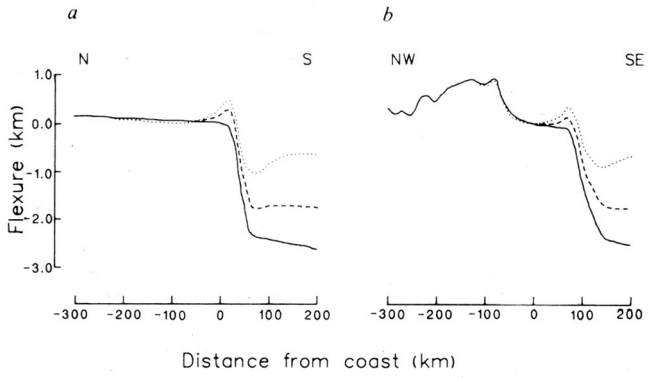

Flexural effects combined with present topography, giving a regionally compensated palaeotopography profile from 200 km offshore to 300 km onshore, assuming $D = 10^{23}$ N m. Solid line, present profile; broken line, latest Messinian palaeotopography, calculated by removal of water load; dotted line, early Messinian palaeotopography, calculated by removing both water and salt loads (density 2,200 kg m^{-3}). *a*, N7E through Rhone Valley, slight uphill gradient. *b*, N38W through Cape d'Agde, moderate uphill gradient.

Figure a19 *: Modèle numérique simulant le rebond isostasique du bassin méditerranéen consécutif à l'assèchement de la Méditerranée pendant la Crise de Salinité Messinienne (d'après Norman et Chase, 1986)*

Le dépôt d'évaporites va jouer un rôle important sur la réponse isostatique car la densité du sel est plus importante que celle de l'eau (2.2 à 2.4). De plus, la quantité de sel produite dans le bassin (plus de 1500m) est beaucoup plus importante que ce que peut produire l'évaporation d'une colonne d'eau de 1500m : l'évaporation d'une colonne d'eau par exemple

de 1000m possédant une concentration en sel de 35‰ ne produit que 14m de sel (Seibold and Berger, 1982). Dans le cas du Messinien l'accumulation de plus de 1500m de sel est due à différentes incursions marines en provenance de l'Atlantique (Hsü et al., 1973 ; Rouchy et Saint-Martin, 1992 ; Schackleton et al, 1995).

Rapporté au scénario proposé par Norman et Chase (1986), ceci suppose que le rebond isostatique précède le dépôt massif d'évaporites, car ce dernier aura tendance à contrebalancer voire inverser ce mouvement (subsidence). Or la mise en place des évaporites reste sujette à caution en ce qui concerne le dépôt des évaporites dites « inférieures » (500 à 700m d'épaisseur). Krijgsman et al (1999) ont en effet proposé que leur dépôt ne soit lié qu'à une faible chute initiale du niveau de la Méditerranée (~200m) au début de la Crise Messinienne plutôt qu'à des répétitions assèchement/réinondation après la chute de 1500m de la Méditerranée. Dans ce cas, il faudrait envisager non pas un rebond isostasique du à l'évaporation (négligeable si l'on considère une chute du niveau de la mer de 200m) mais plutôt une subsidence progressive qui au final annulerait et supplanterait ce rebond.

Dans tous les cas de figures, la sédimentation évaporitique aura effacé les effets liés au soulèvement créé par le rebond isostatique consécutif à l'assèchement de la Méditerranée. Deux scenarii limites sont possible:

(1) soit la sédimentation évaporitique surcompense à chaque instant le rebond, entraînant à terme la subsidence du bassin profond.

(2) soit la sédimentation évaporitique se développe imédiatement après l'assèchement de la Méditerranée, auquel cas, le rebond isostatique qui a pu se développer, aura été compensé et effacé par le dépôt des évaporites.

3. Dynamique de l'érosion messinienne :
Conséquences sur les zones morphologiquement « instables »

Cette seconde partie s'intéresse aux conséquences de la dynamique de l'érosion messinienne dans les zones où les pentes régionales ont été modifiées ou ont été créés depuis la fin du Miocène, autrement dit dans des zones morphologiquement instables. Cette partie s'articule autour de trois articles et leurs annexes respectives. Les deux premiers articles visent à comprendre quelle est la part de l'érosion fluviatile dans la fin de la Crise de Salinité Messinienne liée à l'ouverture du détroit de Gibraltar. Le troisième article s'intéresse à l'âge de la connexion de l'Ebre au bassin Méditerranéen, en particulier quel a été le rôle de l'érosion messinienne dans l'histoire de cette connexion tardive.

Le premier article traite du rôle de l'érosion régressive quant à l'ouverture du détroit de Gibraltar qui a mis fin à la Crise de Salinité Messinienne en Méditerranée. Les causes de l'assèchement de la Méditerranée ont été très largement débattues alors que les causes du ré-ennoyage restent obscures, même si depuis longtemps on sait que l'ouverture du détroit de Gibraltar est le facteur déclenchant de cet évènement au début du Pliocène (e.g. Gentil, 1909). Un grand nombre de travaux attribue une cause externe à cette ouverture, i.e. une cause tectonique (un graben ou un bassin en pull-apart) ou une cause eustatique (remontée du niveau mondial des océans) ou encore une combinaison des deux. Bien qu'un des traits majeurs de la chute du niveau de base messinien en Méditerranée soit la formation de canyons profonds sur tout le pourtour méditerranéen, ce forçage « interne » n'a été que rarement invoqué comme une cause possible de l'ouverture du détroit.
Nous montrons à partir d'une modélisation numérique, dont les paramètres sont dérivés de la modélisation de l'évolution du Rhône messinien développée précédemment, que ce scénario est vraisemblablement le plus pertinent. L'érosion régressive d'une rivière au niveau du seuil de Gibraltar aurait ainsi induit la capture des eaux atlantiques mettant ainsi fin à la crise messinienne en Méditerranée. Autrement dit la Crise de Salinité Messinienne aurait d'une certaine manière induite sa propre fin via la réponse du système fluviatile.

Le second article aborde le même thème que l'article précédent, à la différence près que nous avons ici testé la solidité des autres modèles de ré-ennoyage de la Méditerranée, notamment l'hypothèse d'une tectonique pliocène au niveau de Gibraltar. Il en ressort qu'aucune structure tectonique n'a été mise en évidence pouvant expliquer l'ouverture du détroit de Gibraltar.

Le troisième article concerne l'âge de la connexion du bassin de l'Ebre à la Méditerranée suivant un scénario comparable à l'ouverture du détroit de Gibraltar. Le raisonnement s'appuie sur la singularité de l'incision messinienne dans le bassin de l'Ebre au regard des autres bassins versants méditerranéens, en particulier celui du Rhône dont la taille est du même ordre de grandeur que celui de l'Ebre. En s'appuyant sur des arguments géologiques ainsi que sur une modélisation numérique dont les paramètres sont dérivés de la modélisation du Rhône, nous montrons que le bassin de l'Ebre n'était pas connecté pendant la Crise Messiniennne. Sa connexion telle qu'elle existe aujourd'hui est la conséquence d'une érosion fluviatile régressive, postérieure à cet événement et datée vraisemblablement du Pliocène.

Dessin anachronique de Guy Billout représentant le réenoyage de la Méditerranée au niveau du détroit de Gibraltar à la fin de la Crise de Salinité Messinienne
(Reproduit avec l'aimable autorisation de l'auteur)

3.1. Propagation de l'incision messinienne dans le détroit de Gibraltar

3.1.1. Comment s'est terminé la Crise de Salinité Messinienne ?

Article :

How did the Messinian Salinity Crisis end?

Nicolas Loget, Jean Van Den Driessche and Philippe Davy

Géosciences Rennes, Campus de Beaulieu, 35042 Rennes cedex - France

Terra Nova (October 2005)

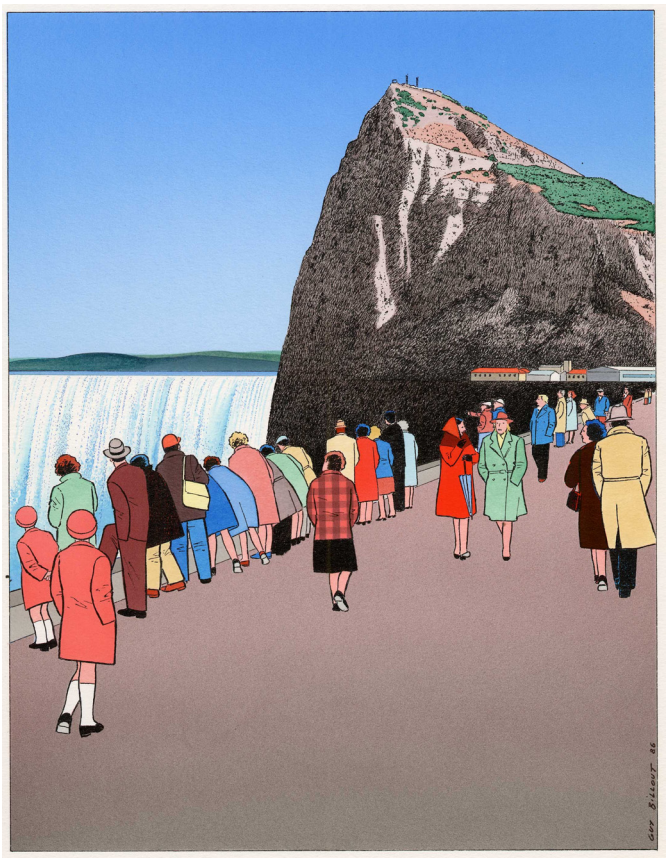

Nous remercions Blackwell Publishing de nous avoir autorisé à publier l'article Loget *et al*., « How did the Messinian Salinity Crisis end ? » Terra Nova, Vol **17**, No 5, 414–419.

doi: 10.1111/j.1365-3121.2005.00627.x

How did the Messinian Salinity Crisis end?

Nicolas Loget, Jean Van Den Driessche and Philippe Davy
Géosciences Rennes, Université de Rennes 1, UMR 6118, Campus de Beaulieu, 35042 Rennes cedex, France

ABSTRACT

The cause of the desiccation of the Mediterranean Sea during the Messinian Salinity Crisis has been widely debated, but its re-flooding remains poorly investigated. Interpretations generally involve tectonic collapse of the Strait of Gibraltar or global sea-level rise, or even a combination of both. The dramatic sea-level fall in the Mediterranean has induced deep fluvial incision all around the desiccated basin. We investigate erosion dynamics related to this base level drop by using the numerical simulator EROS. We show that intense regressive erosion develops inevitably in the Gibraltar area eventually inducing the piracy of the Atlantic waters by an eastward-flowing stream and the subsequent re-flooding of the Mediterranean.

Terra Nova, 17, 414–419, 2005

Introduction

The Messinian Salinity Crisis (MSC) is the most catastrophic base-level fluctuation ever recorded by the Earth's surface during geological times (Ryan *et al*., 1973). Between 5.96 Ma and 5.33 Ma, isolation of the Mediterranean Sea from the Atlantic Ocean resulted in an initial a sea-level drop of approximately 1500 m (Hsü *et al*., 1973; Ryan, 1976; Clauzon *et al*., 1996; Krijgsman *et al*., 1999a). This induced strong incision of the continental surface by rivers and the creation of deep canyons (e.g. Clauzon *et al*., 1996). The phase of maximum erosion lasted 90–300 kyr (Gautier *et al*., 1994; Clauzon *et al*., 1996; Krijgsman *et al*., 1999a). The subsequent opening of the Strait of Gibraltar (Fig. 1) caused the catastrophic re-flooding of the desiccated Mediterranean basin, stopping rivers incising and causing the infill of the inland canyons with early Pliocene marine deposits (Denizot, 1952; Chumakov, 1973).

Models proposed up to now to explain the initiation as well as the end of the MSC involve external forcing, i.e. tectonics (Weijermars, 1988; Krijgsman *et al*., 1999a; Duggen *et al*., 2003) combined in a more or less complex way with eustatism (Kastens, 1992; Hodell *et al*., 1994; Clauzon *et al*., 1996; Krijgsman *et al*., 1999a). Despite a major effect of the Mediterranean sea-level drop being the dramatic increase of erosional activity, this 'internal forcing' as a plausible cause for the end of the MSC has been seldom considered (Hsü *et al*., 1973; Blanc, 2002). Recently, Blanc (2002) proposed, by examining the morphological evolution of the Strait of Gibraltar, that its opening was achieved through retrogressive erosion by a Messinian stream flowing towards the east. In this paper, we test such a scenario by using a surface process model (EROS) (Davy and Crave, 2000; Crave and Davy, 2001). First, we model the morphological evolution of the Rhone valley, which is the best documented example of Messinian canyons (Clauzon, 1982), in order to calibrate the parameters of the erosion law used in the EROS model. Starting from a realistic pre-Messinian topography, we simulate the morphological evolution of the Strait of Gibraltar. We show that, using pertinent parameters, the 'internal forcing' hypothesis is viable.

Correspondence: Nicolas Loget, Géosciences Rennes, Université de Rennes 1, UMR 6118, Campus de Beaulieu, 35042 Rennes cedex, France. Tel.: 00 33 2 23 23 66 30; fax: 00 33 2 23 23 67 80; e-mail: nicolas.loget@univ-rennes1.fr

Geological constraints

Relation between current and pre-MSC catchments

The Messinian sea-level fall induced the formation of deep canyons, which have incised the pre-existing drainage network by regressive erosion all around the Mediterranean region (Fig. 1). Messinian incision was later preserved because of the fast sea-level rise and the resulting detrital sedimentation during the Early Pliocene (Denizot, 1952; Chumakov, 1973). Nowadays these overfilled Messinian valleys are re-incised by the current drainage network.

In the Nile and Rhone valleys, fluvial incision has propagated at least 1000 and 300 km, respectively, towards inland areas, with the depth of incision reaching more than 1000 m in the downstream parts of the canyons (e.g. Barber, 1981; Clauzon, 1982). Fluvial incision is more limited for smaller rivers as along the French, Spanish and Moroccan coasts (Clauzon, 1978; Clauzon *et al*., 1987; Morel, 1987; Ambert *et al*., 1998; Schoorl and Veldkamp, 2003).

Assuming that the coastline before the MSC was close to the present one, we have plotted the length of the Messinian incisions vs. the current drainage areas (Fig. 2). The plot shows an exponential relation where Messinian upstream incision is proportional to the above current watershed area. A similar relation has been obtained in experimental studies in which base level lowering produces upstream incision proportional to the 'above watershed area' (Schumm *et al*., 1987). In the present case, this suggests that the size of the pre-MSC catchments were either proportional, or similar to, the current ones.

The Messinian Rhone profile

Figure 3 shows a reconstruction of the Messinian Rhone longitudinal profile. The shoreline at the maximum of the Messinian sea level fall is considered to roughly follow the limits of the Messinian evaporites (Rouchy and Saint Martin, 1992; Fig. 1). The profile appears unusually 'juvenile', with a strongly convex-up shape of its downstream part. Remnants of pre-Messinian surfaces all along the current

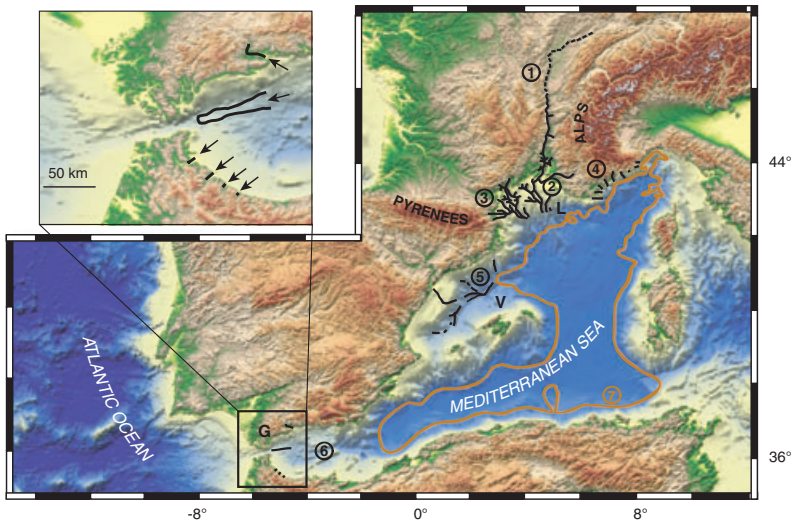

Fig. 1 Digital Elevation Model image of the western Mediterranean region (source: http://edcdaac.usgr.gov/gtopo30/gtopo30.asp) showing the main Messinian rivers. 1, Rhone (after Clauzon, 1982; Clauzon *et al*., 1995; Baumard, 2001); 2, Gulf of Lion shelf (after Guennoc *et al*., 2000); 3, Languedoc (after Clauzon *et al*., 1987; Ambert *et al*., 1998); 4, Var and Ligure (after Clauzon, 1978); 5, Valence (after Field and Gardner, 1991); 6, Western Alboran Sea (after Morel, 1987; Campillo *et al*., 1992; Schoorl and Veldkamp, 2003); 7, Limit of the Messinian evaporites (after Rouchy and Saint Martin, 1992). L, Gulf of Lions; V, Valence trough; G, Gibraltar strait.

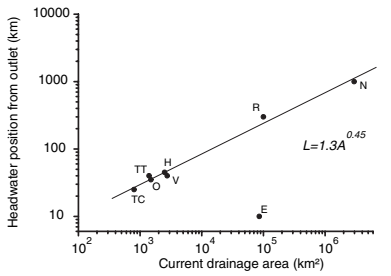

Fig. 2 Lengths of Messinian incisions, measured from the present coast line vs. respective current drainage areas for several Mediterranean rivers. N-Nil; R-Rhone; E-Ebro; H-Herault; O-Orb; TT-Têt; TC-Tech. The plot shows an exponential relationship suggesting that incision pattern is similar for at least three orders of magnitude. This also suggests that the size of the pre-MSC catchments were either proportional or similar to the current ones. Note that the relation is not verified for the Ebro river implying that the pre-MSC Ebro catchment had a rather different configuration (e.g. Coney *et al*., 1996).

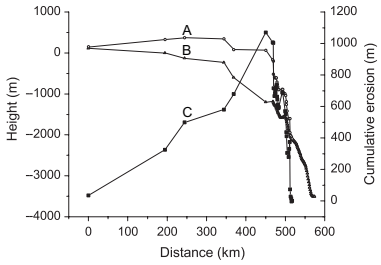

Fig. 3 Erosion pattern of the Messinian Rhone valley. (A) Reconstruction of the Pre-Messinian topography; (B) reconstruction of the Messinian talweg (data after Clauzon, 1982; Guennoc *et al*., 2000; Baumard, 2001) and (C) calculated cumulative erosion curve.

valley make it possible to restore the pre-Messinian Rhone profile (Clauzon, 1982). The present-day onshore part of the pre-Messinian profile has been refined by seismic data (Guennoc *et al*., 2000). The vertical incision is deduced from the difference in elevation between both profiles (Fig. 3). We refer hereafter to this difference as the cumulative erosion. By looking at the cumulative erosion curve rather than the shape of the profile, deformation by either tectonics or general subsidence can be ignored.

Numerical modelling

Principles

Firstly, we suppose that, for the Messinian period, the laws of erosion were similar to those used to describe the current topography. Secondly, we consider that, on a regional scale, hillslope erosion can be minimized and that erosion is mainly achieved by rivers. Indeed the steepness of the valley flanks (e.g. Clauzon *et al*., 1995; Schlupp *et al*., 2001) shows that incision was too fast for hillslopes to be able to respond. The dynamics of erosion resulting from the Messinian sea-level drop is modelled using the numerical simulator EROS, which is a versatile particle-based numerical method (Davy and Crave, 2000; Crave and Davy, 2001). The model incorporates a generic stream power law in which the erosion flux e depends on the local slope S and on the drainage area A, which is used as a proxy for the water flow, such that: $e = kA^mS^n - e_c$ where m and n are two exponents which are known to affect the time-length scaling (Howard *et al*., 1994; Whipple and Tucker, 1999), and where k and e_c are two constants which depend on rock strength properties. As discussed previously, the Messinian incisions are controlled by the above watershed areas, whatever the basement rocks. We therefore consider k and e_c as homogeneous and negligible respectively on a regional scale. Deposition flux is proportional, by $1/\xi$, to the sediment concentration in the stream, with ξ defined as a characteristic transport length of sediments (Beaumont *et al*., 1992; Crave and Davy, 2001). If ξ is very small, the model comes to the transport-limited case where the elevation of the channel bed varies proportionally to the gradient of the erosion flux e. In contrast, if ξ is very large, rivers can carry all the eroded sediment out of the system, which corresponds to the detachment-limited case. By changing the transfer length of sediments, the EROS model makes it possible to reproduce the three main types of rivers, i.e. alluvial, bedrock and mixed.

Pre-Messinian topography

Since the late Miocene, the stress field did not vary significantly in the studied area (e.g. Bergerat, 1987). We thus consider that the regional slopes during pre-Messinian times were similar to the current slopes. Remnants of pre-Messinian alluvial sedimentation

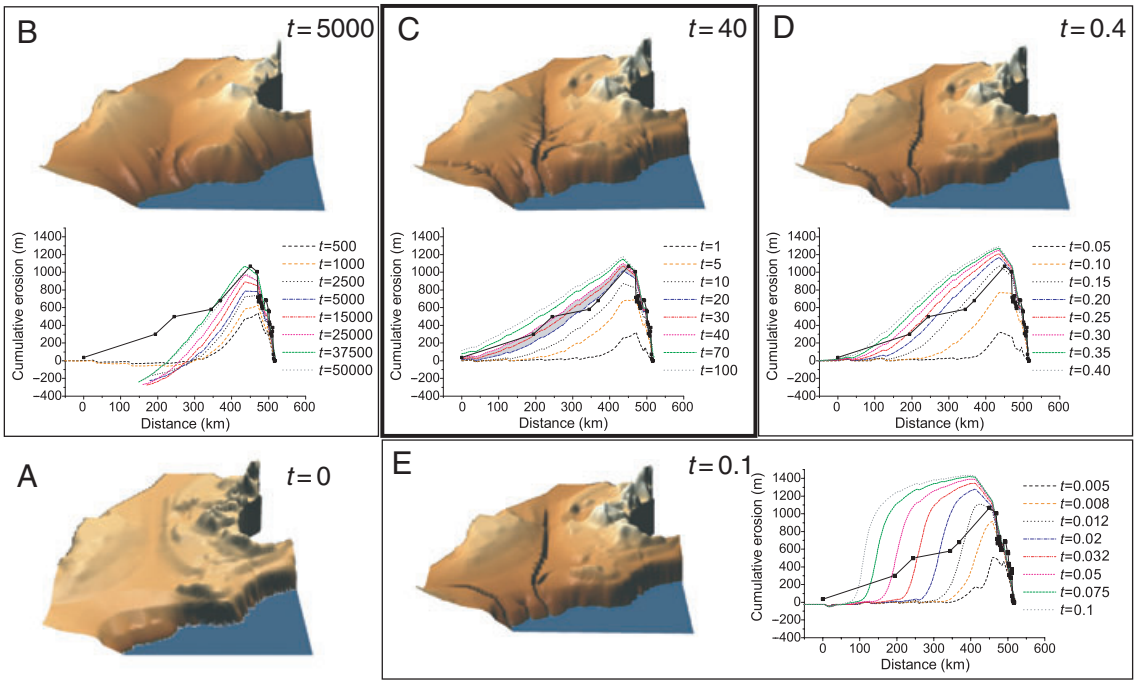

Fig. 4 Modelling of a 1500 m sea-level drop on the evolution of the Messinian Rhone valley compared with geological data (dark points) and corresponding view of the models at different t (vertical dilatation ×32). (A) initial topography; (B–D) influence of the parameter m on the Rhone erosion pattern (B = 1, C = 1.5, D = 2) with $n = 1$ and $\xi < 1$ km fixed values; (E) influence of a higher value of the parameter ξ (400 km) with $m = 1.5$ and $n = 1$. Best fit is obtained for $m = 1.5$, $n = 1$ and $\xi < 1$ km (model C). Time interval confidence ($t = 20$ to $t = 40$) is deduced from the best fit with geological data (grey area).

in the Rhone valley show that a palaeo-drainage system already existed with a more or less similar course since the Tortonian (e.g. Mandier, 1988). Hence, the pre-Messinian topography has been derived from the DEM GTOPO 30 (Fig. 1) by smoothing the contour lines on a regional scale (Fig. 4A). To simulate the Messinian sea-level drop, the base level of the model has been fixed to the −1500 m isobath, which roughly follows the limit of current extension of the Messinian evaporites. During pre-Messinian times, the Gibraltar area was above sea level whereas the Atlantic Ocean and the Mediterranean Sea were connected by two major gateways through Spain and Morocco, respectively (e.g. Martìn *et al.*, 2001). According to Blanc (2002), the continental slope on the Mediterranean side reached several percent.

On the contrary, the huge thickness of evaporites requires episodic overflowing of the Atlantic waters into the desiccated Mediterranean basin during the MSC (e.g. Hsü *et al.*, 1973; Rouchy and Saint Martin, 1992; Hodell *et al.*, 1994; Shackleton *et al.*, 1995; Clauzon *et al.*, 1996). As the Spanish and Moroccan pre-Messinian gateways were closed during the MSC (Weijermars, 1988; Krijgsman *et al.*, 1999b; Martìn *et al.*, 2001), it has been suggested that overflowing, because of eustatic sea level rise, occurred through the Gibraltar area (Krijgsman *et al.*, 1999b). As the amplitude of these eustatic changes did not exceed several tens of meters during the MSC (Aharon *et al.*, 1993; Braga and Martin, 1996; Hodell *et al.*, 2001), this implies the existence of an inherited topographic low in the Gibraltar area. Consequently, in our model, the pre-Messinian morphology of the Gibraltar threshold is depicted by a rather flat topographical surface between the Atlantic and Mediterranean domains (Figs 5 and 6).

Results

Figure 4 shows four models of the development of fluvial incision in the Rhone valley. A specific combination of the parameters m, n and ξ has been tested for each model (Loget *et al.*, 2003). For example, models 4B, 4C and 4D display the crucial effect of the parameter m on the network growth. An increase of the transport length (ξ) does not significantly affect the drainage pattern, but it results in a different behaviour of the Messinian Rhone profile with time (model 4E). The best fit with the Messinian Rhone profile, and the drainage pattern as well, is obtained for $m = 1.5$, $n = 1$ and $\xi < 1$ km (model 4C). Such values are similar to those obtained from the analysis of current drainage systems or used in experimental simulations (e.g. Murray and Paola, 1997; Crave and Davy, 2001; Whipple and Tucker, 2002; Clevis *et al.*, 2003; Lague *et al.*, 2003). The low ξ value, compared with the length of the Messinian Rhone river (in order of several hundreds of kilometres), implies that its profile has evolved according to a rather diffusive mode after the Messinian sea-level drop. In early stages ($t = 0$ to $t = 5$) erosion is extremely fast, the headwater propagates inland whereas the peak of erosion remains localized close to the downstream

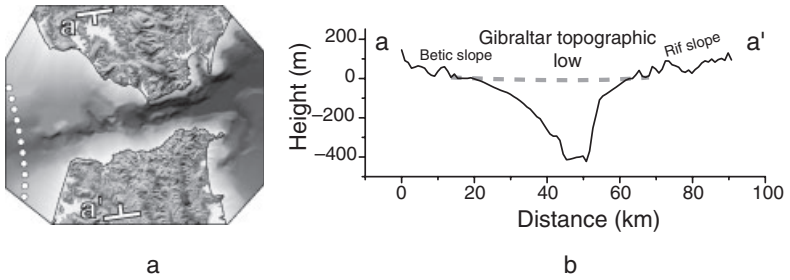

Fig. 5 Morphology of the Gibraltar area. (a) Digital Elevation Model of the Gibraltar area (land topography: SRTM90 DEM data; Strait of Gibraltar bathymetry extracted from Sanz *et al.*, 1991). Dotted line: possible position of the lowest Atlantic sea-level during the MSC (After, Blanc, 2002). (b) Cross-section trough the western part of the Strait of Gibraltar and the adjacent areas (Betics and Rif). Dashed line: probable morphology of the Gibraltar threshold before the MSC.

part. In the later stages ($t = 20$ to $t = 100$), the headwater propagation decreases dramatically whereas the peak of erosion, whose position does not shift significantly, reaches 1100 m. According to the geological data, the confidence interval of numerical time ranges between 20 and 40 (Fig. 4). The duration of the phase of maximum erosion during the MSC (Clauzon *et al.*, 1996; Krijgsman *et al.*, 1999a) provides t real values ranging from 90 kyr to 300 kyr for the present modelling. By using the parameters deduced from the Rhone valley modelling, we simulate the effect of the sea-level drop on the Gibraltar area.

We have argued previously that the response of the rivers to the sea level drop was determined by the size of their drainage. We consider consequently, and at first approximation, the same values for the parameters (m, n, ξ) of the erosion law, whatever the size of the drainage area, thus allowing us to study the dynamics of fluvial erosion in other parts of the Mediterranean region.

Concerning the Gibraltar area, numerical modelling shows that a drainage system develops, which strongly incises the threshold (Fig. 6). Within the confidence interval of time ($t = 20$ to $t = 40$), a 'Gibraltar stream' has cut in the threshold over a distance of 10–40 km. Vertical incision ranges from 50 m to 250 m. At $t = 40$, the incision eventually reached the Atlantic coast line, breaking through the initial topographical barrier between the Atlantic Ocean and the desiccated Mediterranean basin.

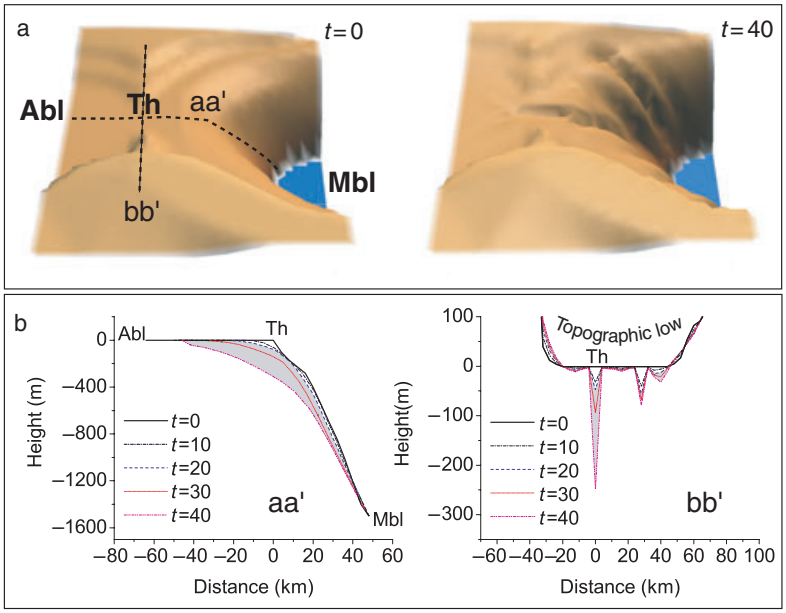

Fig. 6 Evolution of the topography of the Gibraltar threshold after the 1500 m Mediterranean sea-level drop. The eastern slope of the strait, just after the sea-level drop, has been fixed to 3%. The topography integrated in the Gibraltar area appears as a topographic low (see text for explanations). (a) Views looking to the north of the model ($t = 0$ and $t = 40$) (vertical dilatation ×32); (b) longitudinal and transverse sections (aa′ and bb′ respectively). Abl, Atlantic base level; Mbl, Mediterranean base-level; Th, Gibraltar threshold. Grey area, time interval confidence deduced from the Rhone valley modelling (show Fig. 4).

Discussion and conclusion

Previous studies suggested that the re-flooding of the dried Mediterranean basin through the Strait of Gibraltar was caused either by tectonics, or eustasy, or a combination of both (Weijermars, 1988; Kastens, 1992; Hodell *et al.*, 1994), but without providing indisputable evidence. Duggen *et al.* (2003) proposed that re-flooding might have a mantle-related origin. Uplift consecutive to mantle dynamics beneath the western margin of the Gibraltar arc would have induced large scale slumping that, coupled with faulting, would have opened a marine gateway in the Strait of Gibraltar. In a more general way, many studies have invoked faulting, either strike-slip or normal faulting or combination of both (pull-apart) as the main cause of the opening of the Strait of Gibraltar (Campillo *et al.*, 1992; Maldonado *et al.*, 1999).

However, to our knowledge, no study has yet documented early Pliocene normal faults, inducing graben collapse, in the Gibraltar area that could support such a hypothesis. Moreover, during the Pliocene, the regional stress field in this area was corresponding to roughly N-S compression (Philip, 1987). On the contrary, Hodell *et al.* (2001) have argued that the maximum sea-level rise was reached 170 kyr prior to the re-flooding. Shackleton *et al.* (1995) and Hodell *et al.* (2001) suggested that 'there

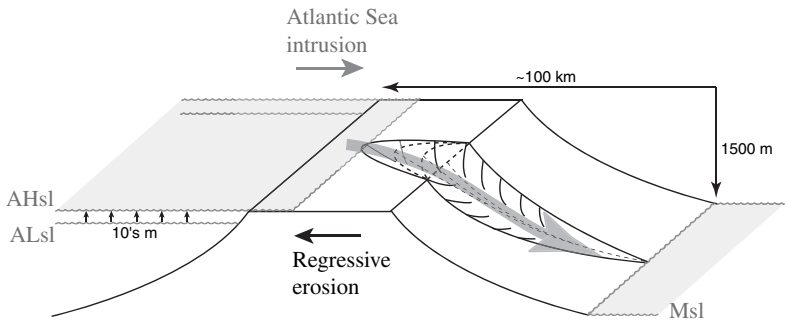

Fig. 7 Proposed scenario for the re-flooding of the desiccated Mediterranean basin by an eastwards flowing stream (see text for explanation). AHsl, High Atlantic sea-level (corresponding to either episodic or final reflooding); ALsl, Low Atlantic sea-level (corresponding to periods of separation between Atlantic and Mediterranean domains); dashed line, initial and transient stages; solid line, final stage.

was not enough erosion of the sill separating the Mediterranean and Atlantic to prevent desiccation until 5.32 My'. Hence, the eustatic rise alone cannot explain the re-flooding of the Mediterranean.

Although a significant consequence of the Messinian sea-level drop was the spectacular inland incision by rivers of the Mediterranean region, in particular in Spain and in Morocco close to the Strait of Gibraltar (Fig. 1), regressive erosion has been a surprisingly underestimated process with which to explain the re-flooding. It was recently considered by Blanc (2002) who thoroughly examined the morphological evolution of the Strait of Gibraltar. However, seismic investigation in the westernmost end of the Alboran Sea has revealed the presence of E-W directed canyons in the eastward, downslope continuation of the Strait of Gibraltar (e.g. Campillo *et al*., 1992). Figure 7 shows a possible scenario, based on this modelling, in which the sea-level drop of the Mediterranean induces the regressive erosion of the Gibraltar threshold by a river running towards the east. As the modelling relates only to fluvial erosion, we do not exclude that landslide or sapping on the eastern side of the Strait of Gibraltar, because of steep slopes and episodic overflowing, could help to erode the threshold. Let us suppose a situation as described in Fig. 7 and corresponding to the model of Fig. 6. The deep cut will act as a spillway during the episodic rise of the Atlantic Ocean sea-level. If a residual topographical barrier still existed, such a flow would most likely destroy it, so that the spillway turns into a permanent gateway, inducing the complete re-flooding of the desiccated Mediterranean basin.

Insofar as the Messinian sea level drop involved the dramatic re-incision of the drainage network in the Mediterranean region, such that a new gateway opened in the Gibraltar area, we propose here that the MSC caused its own end.

Acknowledgements

We thank two anonymous referees for constructive remarks. We also thank Sébastien Castelltort and Kaj Hoernle for comments of an earlier version. We are indebted to Mimi Hill who greatly improved the English. Financial support was provided by Centre National de la Recherche Scientifique INSU 'Programme Relief de la Terre' and 'Programme Eclipse'.

References

Aharon, P., Goldstein, P., Wheeler, C.W. and Jacobson, G., 1993. Sea-level events in the South Pacific linked with the Messinian salinity crisis. *Geology*, **21**, 771–775.

Ambert, P., Aguilar, J.-P. and Michaux, J., 1998. Evolution géodynamique messinio-pliocène en Languedoc central: le paléo-réseau hydrographique de l'Orb et de l'Hérault (sud de la France). *Geodin. Acta*, **11**, 139–146.

Barber, P.M., 1981. Messinian subaerial erosion of the Proto-Nile delta. *Mar. Geol.*, **44**, 253–272.

Baumard, B., 2001. *Valorisation de données pour l'étude de la crise messinienne dans le Gard rhodanien et la moitié est de la France*. PhD thesis, Ecole des Mines de Paris, 260 pp.

Beaumont, C., Fullsack, R. and Hamilton, J., 1992. Erosional control of active compressional orogens. In: *Thrust Tectonics* (K.R. McClay, ed.), pp. 1–18. Chapman & Hall, New York.

Bergerat, F., 1987. Stress fields in the European platform at the time of Africa-Eurasia collision. *Tectonics*, **6**, 99–132.

Blanc, P.L., 2002. The opening of the Plio-Quaternary Gibraltar Strait: assessing the size of a cataclysm. *Geodin. Acta*, **15**, 303–317.

Braga, J.C. and Martin, J.M., 1996. Geometries of reef advance in response to relative sea-level changes in a Messinian (uppermost Miocene) fringing reef (Cariatiz reef, Sorbas Basin, SE Spain). *Sed. Geol.*, **107**, 61–81.

Campillo, A., Maldonado, A. and Maufret, A., 1992. Stratigraphic and tectonic evolution of the western Alboran Sea. Late Miocene to recent. *Geomar. Lett.*, **12**, 165–172.

Chumakov, I.S., 1973. Pliocene and Pleistocene deposits of the Nile valley in Nubia and upper Egypt. In: *Initial Reports of the Deep Sea Drilling Project* (W.B.F. Ryan, K.J. Hsü, *et al.*, eds), Vol. 13, pp. 1242–1243. US Govern. Print. Office, Washington, DC.

Clauzon, G., 1978. The Messinian Var canyon (Provence, Southern France). Paleogeographic implications. *Mar. Geol.*, **27**, 231–246.

Clauzon, G., 1982. Le canyon messinien du Rhône: une preuve dèsicive du "dessicated deep basin model" (Hsü, Cita et Ryan, 1973). *Bull. Soc. Géol. Fr.*, **24**, 231–246.

Clauzon, G., Aguilar, J.P. and Michaux, J., 1987. Le bassin pliocene du Roussillon (Pyrenees-Orientales, France): exemple d' evolution geodynamique d' une ria mediterraneenne consecutive a la crise de salinite messinienne. *C. R. Acad. Sci. (Paris)*, **304**, 585–590.

Clauzon, G., Rubino, J.-L. and Savoye, B., 1995. Marine Pliocene Gilbert-type fan deltas along the French Mediterranean coast. A typical infill feature of preexisting subaerial Messinian canyons. In: *IAS-16th Regional Meeting of Sedimentology, Field Trip Guide Book*, Vol. 23, pp. 145–222. Publication ASF, Paris.

Clauzon, G., Suc, J.-P., Gautier, F., Berger, A. and Loutre, M.-F., 1996. Alternate interpretation of the Messinian salinity crisis: controversy resolved? *Geology*, **24**, 363–366.

Clevis, Q., de Boer, P. and Wachter, M., 2003. Numerical modelling of drainage basin evolution and three-dimensional alluvial fan stratigraphy. *Sed. Geol.*, **163**, 85–110.

Coney, P.J., Munoz, J.A., McKlay, K.R. and Evenchick, C.A., 1996. Syntectonic burial and post-tectonic exhumation of the Southern Pyrenees foreland fold-

thrust belt. *J. Geol. Soc. Lond.*, **153**, 9–16.
Crave, A. and Davy, P., 2001. A stochastic "precipiton" model for simulating erosion/sedimentation dynamics. *Comput. Geosci.*, **27**, 815–827.
Davy, P. and Crave, A., 2000. Upscaling Local-Scale Transport Processes in Large-Scale Relief Dynamics. *Phys. Chem. Earth (A)*, **25**, 533–541.
Denizot, G., 1952. Le Pliocène dans la vallée du Rhône. *Rev. Géogr. Lyon*, **27**, 327–357.
Duggen, S., Hoernle, K., Van Den Bogaard, P., Rupke, L. and Morgan, J.P., 2003. Deep roots of the Messinian salinity crisis. *Nature*, **422**, 602–606.
Field, M.E. and Gardner, J.V., 1991. Valencia gorge: possible Messinian refill channel for the western Mediterranean Sea. *Geology*, **19**, 1129–1132.
Gautier, F., Clauzon, G., Suc, J.P., Cravatte, J. and Violanti, D., 1994. Age et duree de la crise de salinite messinienne. *C. R. Acad. Sci. (Paris)*, **318**, 1103–1109.
Guennoc, P., Gorini, C. and Mauffret, A., 2000. Histoire geologique du golfe du Lion et cartographie du rift oligo-aquitanien et de la surface messinienne. *Geol. Fr.*, **3**, 67–97.
Hodell, D.A., Benson, R.H., Kent, D., Boersma, A. and Rakic-El Bied, K., 1994. Magnetostratigraphic, biostratigraphic, and stable isotope stratigraphy of an upper Miocene drill core from the Salé Briqueterie (northwest Morocco): a high resolution chronology for the Messinian stage. *Paleoceanography*, **9**, 835–855.
Hodell, D.A., Curtis, J.H., Sierro, F.J. and Raymo, M.E., 2001. Correlation of late Miocene to early Pliocene sequences between the Mediterranean and North Atlantic. *Paleoceanography*, **16**, 164–178.
Howard, A.D., Dietrich, W.E. and Seidl, M.A., 1994. Modeling fluvial erosion on regional to continental scales. *J. Geophys. Res.*, **99**, 13,971–13,986.
Hsü, K.J., Cita, M.B. and Ryan, W.B.F., 1973. The origin of the Mediterranean evaporites. In: *Initial Reports of the Deep Sea Drilling Project* (W.B.F. Ryan, K.J. Hsü, *et al.*, eds), Vol. 13 pp. 1203–1231. US Government Printing Office, Washington, DC.
Kastens, K.A., 1992. Did glacio-eustatic sea level drop trigger the Messinian salinity crisis? New evidence from ocean drilling program site 654 in the Tyrrhenian Sea. *Paleoceanography*, **7**, 333–356.
Krijgsman, W., Hiigeni, F.J., Raffi, I., Sierro, F.J. and Wilson, D.S., 1999a. Chronology, causes and progression of the Messinian salinity crisis. *Nature*, **400**, 652–655.
Krijgsman, W., Langereis, C.G., Zachariasse, W.J., Boccaletti, M., Moratti, G., Gelati, R., Iaccarino, S., Papani, G. and Villa, G., 1999b. Late Neogene evolution of the Taza-Guercif Basin (Rifian Corridor, Morocco) and implications for the Messinian salinity crisis. *Mar. Geol.*, **153**, 147–160.
Lague, D., Crave, A. and Davy, P., 2003. Laboratory experiments simulating the geomorphic response to tectonic uplift. *J. Geophys. Res.*, **108** (B1), 2008 doi:10.1029/2002JB001785.
Loget, N., Davy, P. and Van Den Driessche, J., 2003. Large scale erosion processes and parameters derived from a modelling of the Messinian Salinity Crisis. *Geo. Res. Abstr.*, **5**, 10718.
Maldonado, A., Somoza, L. and Pallares, L., 1999. The Betic orogen and the Iberian-African boundary in the Gulf of Cadiz: geological evolution (central North Atlantic). *Mar. Geol.*, **155**, 9–43.
Mandier, P., 1988. Le relief de la moyenne vallée du Rhône au Tertiaire et au Quaternaire. Essai de synthèse paléogéographique. *Doc. BRGM*, **151**.
Martin, J.M., Braga, J.C. and Betzler, C., 2001. The Messinian Guadalhorce corridor: the last northern, Atlantic-Mediterranean gateway. *Terra Nova*, **13**, 418–424.
Morel, J.L., 1987. *Evolution récente de l'orogène rifain et de son avant-pays depuis la fin de la mise en place des nappes (Rif, Maroc)*. PhD Thesis, University of Paris-Sud, 583 pp.
Murray, A.B. and Paola, C., 1997. Properties of a cellular braided-stream model. *Earth Surf. Process. Land.*, **22**, 1001–1025.
Philip, H., 1987. Plio-Quaternary evolution of the stress field in Mediterranean zones of subduction and collision. *Annu. Geophys.*, **5B**, 301–320.
Rouchy, J.-M. and Saint Martin, J.-P., 1992. Late Miocene events in the Mediterranean as recorded by carbonate-evaporite relations. *Geology*, **20**, 629–632.
Ryan, W.B.F., Hsü, K.J., *et al*, 1973. *Initial reports of the Deep Sea Drilling Project*, Vol. 13, US Government Printing Office, Washington, DC, 1447 pp.
Ryan, W.B.F., 1976. Quantitative evaluation of the depth of the western Mediterranean before, during and after the late Miocene salinity crisis. *Sedimentology*, **23**, 791–813.
Sanz, J.L., Acosta, J., Herranz, P., Palomo, C. and San Gil, C., 1991. *Mapa Batimétrico del Estrecho de Gibraltar*, scale 1:100 000. Instituto Español de Oceanografía, Publ. Espec. Inst. Esp. Oceangr., Madrid.
Schlupp, A., Clauzon, G. and Avouac, J.-P., 2001. Mouvement post-messinien sur la faille de Nîmes: implications pour la sismotectonique de la Provence. *Bull. Soc. Géol. Fr.*, **172**, 697–711.
Schoorl, J.M. and Veldkamp, A.U., 2003. Late Cenozoic landscape development and its tectonic implications for the Guadalhorce valley near Alora (Southern Spain). *Geomorphology*, **50**, 43–57.
Schumm, S.A., Mosley, M.P. and Weaver, W.E., 1987. *Experimental Fluvial geomorphology*. Wiley, New York, 413 pp.
Shackleton, N.J., Hall, M.A. and Pate, D., 1995. Pliocene stable isotope stratigraphy of site 846. *Proc. ODP Sci. Results*, **138**, 337–355.
Weijermars, R., 1988. Neogene tectonics in the Western Mediterranean may have caused the Messinian Salinity Crisis and an associated glacial event. *Tectonophysics*, **148**, 211–219.
Whipple, K.X. and Tucker, G.E., 1999. Dynamics of the stream-power river incision model: Implications for height limits of mountain ranges, landscape response timescales, and research needs. *J. Geophys. Res.*, **104**, 17,661–17,674.
Whipple, K.X. and Tucker, G.E., 2002. Implications of sediment-flux-dependent river incision models for landscape evolution. *J. Geophys. Res.*, **107** (B2), 2039 10.1029/2000JB00004.

Received 30 October 2004; revised version accepted 18 March 2005

Photographie du détroit de Gibraltar (vue vers le Maroc)

3.1.2. Sur l'origine du détroit de Gibraltar.

Article :

On the Origin of the Strait of Gibraltar

Nicolas Loget and Jean Van Den Driessche

Géosciences Rennes, Campus de Beaulieu, 35042 Rennes cedex - France

Accepted to Sedimentary Geology

ON THE ORIGIN OF THE STRAIT OF GIBRALTAR

Nicolas Loget* and Jean Van Den Driessche

Géosciences Rennes, Université de Rennes 1, UMR 6118, Campus de Beaulieu,

35042 Rennes cedex, France.

Abstract.

Most interpretations of the Early Pliocene opening of the Strait of Gibraltar involve a tectonic process. However, no tectonic structure of this age has been unequivocally documented that could account for such a hypothesis. On the other hand, the sea-level drop of the Mediterranean during the Messinian Salinity Crisis has dramatically enhanced continental erosion and in particular regressive fluvial erosion. We show that such erosional process inevitably developed in the Gibraltar area. We finally propose that regressive fluvial erosion was at the origin of the opening of the Strait of Gibraltar.

Keywords: Strait of Gibraltar**,** Messinian sea-level drop, Fluvial erosion, Pliocene re-flooding

*Corresponding author: nicolas.loget@univ-lr.fr

1. Introduction

The Strait of Gibraltar is an E-W narrow neck, 58 km long with a mean depth of about 350 m. Its width ranges from 13 km to the east, to 43 km at the western entrance (Fig. 1). The strait ensures the only water communication between the Atlantic and the Mediterranean. This exchange is crucial for the Mediterranean to compensate the negative hydrological balance with loss through evaporation exceeding the input of water through runoff and precipitation. Nowadays, closing of the Strait of Gibraltar would trigger a complete desiccation of the Mediterranean in about 1000 years (Hsü et al., 1973a).

Before the opening of the Strait of Gibraltar, the Atlantic and Mediterranean waters were connected through the Betic and Rif gateways, which were progressively uplifted and finally closed during the Miocene (e.g. Weijemars, 1988; Benson et al., 1991; Krijgsman et al., 1999b; Martìn et al., 2001; Duggen et al., 2003). This triggered the desiccation of the Mediterranean, inducing the so-called Messinian Salinity Crisis (MSC) (Hsü et al., 1973a).

The opening of the Strait of Gibraltar in the Early Pliocene allowed restoring the water exchange between the Atlantic and Mediterranean waters. Surprisingly, the origin of this opening is not so much of concern to the geological community. Because the Strait of Gibraltar is situated in a long-lived tectonic region, most works have considered that its opening was induced by the collapse of a narrow graben related either to regional extension or strike-slip faulting (pull-apart basin) (e.g. Hsü et al., 1973b; Campillo et al., 1992; Kastens, 1992; Maldonado et al., 1999; Hodell et al., 2001;). But, to our knowledge, no major normal faults have been documented on both sides of the Strait of Gibraltar to support these interpretations.

On the other hand, the desiccation of the Mediterranean during the Messinian has induced a dramatic sea-level drop that has been estimated up to 1500m below the current sea-level (Hsü et al., 1973a; Clauzon et al., 1996). A major consequence of this base-level drop was the strong re-incision of the rivers that were flowing into the Mediterranean, resulting in the cutting of deep canyons by regressive erosion all around the Mediterranean region, including the Alboran Sea (e. g. Clauzon et al., 1996). Blanc (2002) proposed, by analysing the morphology of the Strait of Gibraltar, that regressive erosion by an eastwards-flowing stream in the Gibraltar area was the main process by which the Strait of Gibraltar opened.

In the present paper we aim to show there are no tectonic structures that could account for the opening of the strait by reviewing the previous works that were concerned with tectonics in the Gibraltar area and surrounding regions. Then we discuss the consequences of the sea-level drop on erosion dynamics during the MSC. We present a numerical modelling that shows how fluvial regressive erosion has developed in the Gibraltar area, following the scenario first proposed by Blanc (2002). The erosional parameters used in this modelling have been deduced from a previous study concerning erosion dynamics in the Messinian Rhone valley (Loget et al., 2005) and are succinctly presented here. We finally discuss our results compared to previous interpretations. We conclude that the Strait of Gibraltar most probably originated in a Messinian pirate valley within which a stream flowing eastwards has eventually captured the Atlantic waters, inducing their re-connection with the Mediterranean Sea.

2. Which evidences for tectonically-driven reflooding through the Strait of Gibraltar?

2. 1. Geological setting

The Strait of Gibraltar marks the limit between the Atlantic and the westernmost Mediterranean, namely the Alboran Sea, to the west and to the east respectively (Fig. 1). The Alboran Sea is bounded by the Betics to the north and the Morocco Rif to the south. They connect through the Gibraltar area, shaping an arcuate orogenic belt, the so-called Gibraltar Arc (e.g. Michard et al., 2002). Farther east, the Alboran Sea connects to the Balearic basin and more generally to the Mediterranean basin.

The Gibraltar Arc results from the convergence between the African and European plates (Fig. 2) (e.g. Dewey et al., 1989). This motion started during the Upper Cretaceous and continued throughout the Cenozoic. Lithospheric shortening generated a complex pattern of Neogene thrust belts and extensional basins throughout the Mediterranean (e.g. Lonergan and White, 1997) (Fig. 3). The Gibraltar Arc is the westernmost end of a thrust belt extending from the Balearics up to the northern Apennines, through the Calabrian Arc to the east (e. g. Tapponnier, 1977; Faccenna et al., 2004).

The Betic-Rif orogen is classically divided into three structural zones (Fig. 4) that straddle the Strait of Gibraltar (e.g. Wildi, 1983; Lonergan and White, 1997; Comas et al., 1999; Platt et al., 2003; Frizon de Lamotte et al., 2004). (1) The external zone corresponds to the South Iberian and Maghrebian paleo-margins, formed of Mesozoic and Tertiary sediments. Crustal

shortening was accompanied by the development of Iberian and African foreland basins (the Guadalquivir and Rharb basins respectively). (2) The intermediate zone consists of the Flysch Nappes that are composed of Early Cretaceous to Early Miocene marine clastic deposits. (3) The internal zone is constituted by metamorphic basement rocks that belong to the Alboran crustal domain, and by Neogene intermontane basins.

The history of the Gibraltar arcuate belt started during Late Oligocene- Early Miocene times when the Alboran domain was overthrusted onto the South Iberian and Maghrebian continental margins (e.g. Comas et al., 1999). Further thrusting toward the west in the external zones led to the formation of the Gibraltar Arc during the Middle Miocene and Late Miocene (e.g. Faccenna et al., 2004). Thrusting and crustal shortening in the external zone was contemporaneous with extension and crustal thinning in the previously thickened, internal zone, namely the Alboran domain (e. g. Platt and Vissers, 1989, Vissers et al.,1995; Garcìa- Dueñas et al., 1992; Balanyá et al., 1997; Chalouan et al., 1997; Martínez-Martínez and Azañón, 1997; Comas et al., 1999; Platt et al., 2003). The relative motion between Africa and Iberia involved about 200 km, N-S convergence from the Middle Oligocene to the Late Miocene (Dewey et al., 1989). From the Late Tortonian onward around 50 km, NW-SE oblique convergence (Dewey et al., 1989) was responsible for a compressive regime characterized by folding, and reverse and strike-slip faulting within the Alboran Sea and onshore as well (e.g. Woodside and Maldonado, 1992; Watts et al., 1993). Neotectonic and seismotectonic studies show that compression is still active (e.g. Morel and Meghraoui, 1996).

A striking feature of the Betic-Rif orogen is the considerable crustal extension that occurred within the Alboran domain, while thrusting and crustal thickening were developing in the external zone (e.g. Platt and Vissers, 1989).

To explain this paradox, several tectonic models have been proposed including past or present subduction, or delamination of overthickened continental lithosphere (Platt and Vissers, 1989; Seber et al., 1996; Lonergan and White, 1997; Zeck, 1997; Calvert et al., 2000). Using tomographic, seismic or volcanic data, several authors have recently argued about the existence of an active east-dipping subduction zone beneath Gibraltar (Gutscher et al., 2002; Duggen et al., 2004, Faccenna et al., 2004). Following the subduction model, a westward slab rollback would induce back arc extension that could account for synchronous extension and contraction, and the westward advance of the Gibraltar Arc as well.

2. 2. Opening of Gibraltar strait in the Early Pliocene

During the formation of the Betic-Rif orogen, the Atlantic and the Mediterranean waters were communicating, except during a short period at the end of the Miocene. The closure of the Betic and Rif gateways triggered the desiccation of the Mediterranean, resulting in the Messinian Salinity Crisis (MSC) (Hsü et al., 1973a). The MSC did not last more than 600 Ky (Krijgsman et al., 1999a) before the opening of the Strait of Gibraltar, in the Early Pliocene, allowed the re-connection of the Mediterranean with the Atlantic. That the re-flooding of the Mediterranean has been achieved through the Strait of Gibraltar has been known for long, but the cause and mode of rupture of this threshold remain questionable. The different hypotheses involve either the eustatic rise of the Atlantic, or the topographic lowering of the threshold by tectonic collapse or superficial erosion, or the combination of both (Hsü et al., 1973a; 1973b; Campillo et al., 1992; Kastens, 1992; Maldonado et al., 1999; Hodell et al., 2001; Blanc, 2002) (Fig. 5).

Atlantic sea-level rise

To explain the very thick evaporite deposits during the MSC, most works put forward the episodic overflowing of the Atlantic waters into the desiccating Mediterranean basin (e.g. Hsü et al., 1973a; Rouchy and Saint Martin, 1992; Hodell et al., 2001; Shackleton et al, 1995; Clauzon et al., 1996), but none of these episodes have succeeded in rupturing definitively the threshold of Gibraltar (e.g. Hsü et al., 1973a). According to Hodell et al. (2001), the most prominent decrease in benthic $\delta^{18}O$ occurred at 5.5 Ma, that is 170 Ky prior to the Miocene-Pliocene boundary, suggesting that the Atlantic sea-level began to rise before the end of the MSC. The hypothesis that only eustatic rise would have resulted in the re-flooding of the Mediterranean, is therefore unlikely (e.g. Kastens, 1992; Shackelton et al., 1995; Hodell et al., 2001).

Graben collapse

The Strait of Gibraltar is nowadays a remarkable topographic feature at regional scale, but whether it corresponds to some major structural feature has never been demonstrated (Fig. 2 and Fig. 3). Many works presuppose the presence of normal or strike-slip faults within or in the vicinity of the Strait of Gibraltar (Fig. 6) : (1) normal faults (Giermann, 1961; Olivet et al., 1973; Groupe de recherche néotectonique de l'Arc de Gibraltar, 1977; Platt and Vissers, 1989; Vissers et al., 1995; Lonergan and White, 1997; Carminati et al., 1998; Michard et al., 2002);

(2) strike-slip faults (Didon, 1973; Leblanc and Olivier, 1984; Campillo et al., 1992; Comas et al., 1999; Maldonado and Nelson, 1999). Regarding the compressive regime that prevails during the Late Miocene in this area and the southward tilting of the Tanger peninsula, Morel (1987) has suggested that the strait could have originated in a crestal collapse graben on the top of an anticline, but without providing further evidence.

Onshore investigations

Geological mapping by Didon (1969; 1973), IGME (1994) and Suter (1980a; 1980b) along the Spanish and Morocco edges respectively does not reveal any major Early Pliocene faults that could explain a tectonic collapse in this area (Fig. 7). Morel (1987) has suggested that the steep flanks of the narrow troughs along the Mediterranean coast of Morocco, between Ceuta and Djeba, which are filled with Pliocene sediments (Wildi and Wernli, 1977) could correspond to normal faults. But microstructures on the surface flanks that could support this interpretation are not observed by Morel (1987). An alternative interpretation is to consider that these troughs corresponded to Messinian canyons, later filled as rias during the Early Pliocene transgression (Fig. 7) (see below).

Offshore investigations

Numerous offshore investigations have been carried out on both the Atlantic side and the Alboran side (e.g. Campillo et al., 1992; Woodside and Maldonado, 1992; Comas et al., 1999; Maldonado and Nelson, 1999).

Seismic investigations in the Alboran Sea have revealed that the rifting stage was completed during the Late Tortonian and was followed by a roughly N-S compressional regime (Bourgois et al., 1992; Comas et al., 1992; Maldonado et al., 1992; Mauffret et al., 1992; Watts et al., 1993; Morel and Meghraoui, 1996; Chalouan et al., 1997; Comas et al., 1999).

In the east of the Alboran Sea, this compressional regime induced folding, reverse and strike-slip faulting. Inland deformation along the Jehba fault in Morocco and along the Carboneras-Palomeras fault system corresponds to this event (Fig. 4) (e.g. Woodside and Maldonado, 1992; Morel and Meghraoui, 1996).

Campillo et al. (1992) has suggested that this compressional regime would have also induced a strike-slip fault system in the west of the Alboran Sea. Development of small pull-apart basins along this wrench zone would have resulted in the opening of the Strait of Gibraltar, an interpretation that is supported by other works (e.g. Mulder and Parry, 1977; Kastens, 1992; Maldonado and Nelson, 1999).

However, in the immediate vicinity of the Strait of Gibraltar, in Morroco, Chalouan et al. (1997) do not observe any strike-slip faults and note that "none post-Messinian normal faults bear witness to any significant crustal extension". More recently, a thorough geomorphologic investigation within the Strait of Gibraltar by Blanc (2002) has shown the presence of post – reflooding, large-scale slumping, but no evidence of high angle normal faults related to extensional deformation (Fig. 7).

Pliocene faults have been indeed documented, but father west of the Strait of Gibraltar in the Gulf of Cadiz, in the Atlantic (Maldonado and Nelson, 1999; Maldonado et al., 1999).

To conclude, no work has provided unequivocal evidences of Early Pliocene extensional deformation within or in the immediate vicinity of the Strait of Gibraltar that could account for its opening at this period.

On the other hand, numerous erosional channels, buried under Plio-Quaternary sediments, have been mapped along the Rif coast (Rampnoux et al., 1979; Morel, 1987; Chalouan et al., 1997), along the Betic coast (Schoorl and Veldkamp, 2003), in the eastern part of the Strait of Gibraltar (Mulder and Parry, 1977; Campillo et al., 1992; Watts et al., 1993) or within the strait itself (Blanc, 2002). This suggests that erosion can be an alternative mechanism for the opening the Strait of Gibraltar.

3. Arguments for the origin of the opening of the Strait of Gibraltar by regressive fluvial erosion.

3.1. Evidences of Messinian pervasive erosion in the Mediterranean

Since the pioneer work of Denizot (1952), who first suggested that a dramatic sea-level drop occurred in the Mediterranean during the Messinian, an interpretation that was later demonstrated by Hsü et al. (1973b), Ryan et al. (1973), Cita and Ryan (1978), Barber (1981) and Clauzon (1982), it has been recognized that this sea-level drop enhanced subaerial erosion, inducing strong re-incision of the pre-Messinian drainage system and deep cutting of the newly emerged margins.

Figure 8 shows a possible configuration of the Mediterranean during the MSC that has been traced from a current DEM, after the sea-level has been dropped by 1500 m.

Because of the very fast re-flooding of the Mediterranean, these incisions were "frozen" by detrital sedimentation during the Pliocene (Denizot, 1952; Chumakov, 1973).

In the Eastern Mediterranean, the most prominent Messinian incision developed in the Nile valley. Indeed, the proto-Nile River cuts down more than 1000m deep (Barber, 1981) beneath the current Nile delta and extends to more than 1000 km upstream (Chumakov, 1973). Many evidences of Messinian fluvial incisions have been reported all along the Mediterranean coast e.g. Libya (Barr and Walker, 1973), Greece (Delrieu et al., 1993), Turkey (Poisson et al., 2003), Cyprus (Orszag-Sperber et al., 2000) and Israel (Druckman et al., 1995).
In the Western Mediterranean basin as well, numerous Messinian fluvial incisions have been identified all along the coast (Cita and Ryan, 1978; Clauzon, 1978; Clauzon et al. 1987; Cita and Corselli, 1990; Field and Gardner, 1990; Savoye and Piper, 1991; Escutia and Maldonado, 1992; Martín and Braga, 1994; Butler et al., 1995; Clauzon et al., 1995; Ambert et al., 1998; Riding et al., 1999; Fortuin et al., 2000). The most prominent incision reaches 1000 m depth just beneath the current Rhone outlet and extends to more than 300 km upstream (Clauzon, 1982).

3. 2. Did a Messinian drainage network develop in the Alboran area?

The lack of evaporites in the Alboran basin (e.g. Comas et al., 1999) shows that, during the MSC, the Alboran Sea was emerged and subjected to erosion. Therefore it is most likely that similar fluvial erosion was developing in the Alboran basin as in the rest of the Mediterranean region. Loget et al. (2005) have shown that a power law, similar to the Hack's law, relies the Messinian incision length to the present-day drainage area, ranging from 10^2 to 3.10^6 km^2 and whatever the basement rocks. This indicates that Messinian drainage areas were similar to the present ones. Therefore it is likely that fluvial incision also developed in the Gibraltar area and the surroundings. Indeed, all along the Mediterranean Rif coast, Pliocene detrital sediments are trapped within narrow troughs that nowadays outcrop within wadis (Fig. 7 and Figs 9A–B) (e.g. Oued Martil, Oued Laou, Oued Tihissasse, Oued Amter and in the Melilla basin). This suggests that during the Pliocene reflooding, these troughs were rias (Wildi and Wernli, 1977; Rampnoux et al., 1979; Morel, 1987).
Along the Spanish coast, Messinian fluvial incisions, which have propagated far inland, are also preserved by Pliocene fills (Fig. 7 and Fig. 9C), as for example beneath the present Guadalhorce valley (Schoorl and Veldkamp, 2003).
As mentioned before, Mulder and Parry (1977), Campillo et al. (1992) have described a Messinian-Pliocene deep canyon at the eastern entrance of the Strait of Gibraltar (Fig. 7).

According to Mulder and Parry (1977) this canyon results from submarine erosion while Campillo et al. (1992) suggest a tectonic origin. According to Watts et al. (1993), fault structures as inferred by Campillo et al (1992), would result from strong submarine erosion rather than regional tectonics.

However the emersion of the western Alboran Sea during the Messinian suggests an alternative explanation. Recently, Blanc (2002) has mapped remnants of a paleo-canyon within the Strait of Gibraltar that he imputes to fluvial erosion during the MSC (Fig. 7). Indeed, regressive fluvial erosion, which resulted in the development of deep canyons all around the Mediterranean, had to inevitably affect the emerged Alboran domain including the Gibraltar area. We therefore suggest that the canyons described in the Alboran domain were also produced by fluvial incision consecutively to the Messinian sea-level drop rather than by any other suggested processes for which there is no unequivocal evidence (Fig. 10).

4. Numerical modeling of Messinian erosion dynamics in the Gibraltar area

4.1. Pre-Messinian topography

A first striking feature concerning the Messinian incisions is that the present rivers follow the Messinian network, as for example in the Rhone and Nile valleys. As rivers flow along the slope line, this shows that the regional slopes during the Messinian were similar to the present-day slopes, what is in agreement with the fact that the stress field did not vary significantly since the Late Miocene (e.g. Bergerat, 1987). As mentioned before, the pre-MSC drainage areas were very similar to the current ones, except for the Ebro basin, which was not connected to the Mediterranean before the MSC (Babault et al., 2005; Loget et al., 2005).

We thus model the pre-Messinian topography of the Gibraltar surrounding areas by smoothing the present-day topography. This relies also on two arguments. First, as our model is concerned with regional scale, topographic roughness, that is local slope, does not influence the whole erosional pattern as shown by Loget et al. (2005). Secondly, it has been argued (e. g. Molnar and England, 1990; Peizhen et al., 2001; Babault et al., 2005) that the present-day topographic roughness is to relate to the high-frequence variability of Pliocene-Quaternary climate, so that relief during the Messinian was most probably smoother than the present-day

one. The resulting topography on the east side of the future strait provides a minimum potential drainage area in the order of 5.10^2 km²,

To simulate the Messinian sea-level drop, we fix the Messinian shoreline at the present-day, -1500m isobath that roughly tracks the maximum lateral extent of the Messinian evaporites (Rouchy and Saint Martin, 1992).

According to many works (Hsü et al., 1973b; Rouchy and Saint Martin, 1992; Clauzon et al., 1996; Hodell et al., 2001), episodic overflowing of the Atlantic waters into the Mediterranean occurred during the MSC. As both the Betics and Rif gateways between the Atlantic and the Mediterranean were closed during the MSC, it was suggested that overflowing was achieved through the Gibraltar area (Krijgsman et al., 1999b). These episodic overflows were resulting from eustatism whose amplitude does not exceed some tens of meters during the Late Miocene and the Early Pliocene (Aharon et al., 1993; Braga and Martín, 1996; Hodell et al., 2001). This suggests the occurrence of an inherited topographic low in the Gibraltar area during the MSC, resembling the present-day emerged morphology (Fig. 11). Thus in our model the pre-Messinian topography is described by a saddle with a rather flat bottom.

4.2. Principles of modelling

We used the numerical model €ROS (Davy and Crave, 2000; Crave and Davy, 2001) in which "precipitons", corresponding to rainfall events (Chase, 1992), are randomly sent onto an initial topography (pixels grid). Precipitons simulate a water flow across a landscape, that will erode or not the topography (for details of the algorithm see Crave and Davy (2001)). The numerical procedure of the EROS model calculates the runoff water discharge as a function of the return period of elementary walking elements. This procedure generates water flux distribution at each point of the system that depends on the drainage area, and on the water rainfall, and that are statistically analogous to natural river discharge distribution (further explanation can be found in Crave and Davy (2001)).The pertinence of the input parameter is deduced by comparing the erosional pattern obtained in the model with the natural system. Changing this parameter will change the modelled morphology and/or the numerical time required to obtain the best fit between the model and the geological data (see Loget et al, 2005). As the determination of the real amount of precipitation during Messinian time is illusive (climate was rather dry, possibly resembling present-day climate in Red Sea region (Suc and Bessais, 1990)), this is a pertinent way to proceed in such a modelling.

In €ROS, erosion dynamics is simulated by a generic equation of the classic power-law framework where the incision rate (e) is a function of the local slope (S) and of the water flux (Q) such as $e=KQ^mS^n-e_c$. In this formulation, m and n is a pair of exponents that affect the time-length scaling of the erosional processes (Howard et al., 1994; Whipple and Tucker, 1999), and K and e_c are two constants depending on rock strength. As discussed previously, the nature of basement in the pre-MSC watershed areas was not a determinant parameter in the re-incision pattern after the Mediterranean sea-level drop. Consequently K and e_c can be considered as homogeneous and negligible, respectively, on a regional scale. As sedimentation may or not occur in the immediate neighbourhood of the eroding area (that is deposition or transfer, respectively), the model integrates a transport length (ξ) of sediment in the river (Beaumont et al., 1992; Crave and Davy, 2001).

4.3. Results

Several combinations of the parameters m, n and ξ have been tested in a previous work about erosion dynamics in the Rhone valley during the Messinian (Loget et al., 2005) (Fig. 12). Best fit between geological data and experiments has been obtained for m=1.5, n=1 and $\xi \sim$ 1km, values that are roughly similar to those obtained from the analysis of the topography or used in other experimental results (e. g. Murray and Paola, 1997; Crave and Davy, 2001; Whipple and Tucker, 2002; Clevis et al., 2003; Lague et al., 2003).

To investigate erosion dynamics in the Gibraltar area, we applied both the same parameters and the same confidence interval for numerical time as Loget et al. (2005), ranging between 20 and 40. During the MSC, maximum erosion lasted between 90 Ky and 300 Ky (Clauzon et al., 1996; Krijgsman et al., 1999a), thus providing real time values for our modeling. Starting from pre-MSC topography described above, the modeling shows that a drainage network develops in the Gibraltar area that could corresponds to the present-day preserved Messinian canyons (Fig. 13). However, the erosion pattern is somewhat different from that of the Rhone considering that the drainage surface is smaller. Indeed the incisions are weak marked at t=10, but at t= 40 regressive erosion has developed all around the Gibraltar area and has also attacked up to the flat floor of the pre-Messinian topographic low. Within the confidence interval of time (t=20 to t=40), the length and the depth of the incision reach 10 to 40 km and 50 to 250 m respectively, within the pre-Messinian "Gibraltar saddle" that separates the Atlantic from the Mediterranean (Fig. 13B). The difference between the modelled fluvial

incision and the present-day mean depth and width of the strait is likely attributable to later erosion by marine currents, which are nowadays among the strongest in the world.

5. CONCLUDING REMARKS

To our opinion, all previous studies did not provide really convincing proof for the crucial role of tectonics in the opening of the Strait of Gibraltar during the Early Pliocene. Whereas the Gibraltar area is a topographic low, that this one corresponds to some structural feature (i. e., graben, pull-apart basin or syncline) was never proved. Indeed, numerous, contradictory fault mappings have been proposed that rely on regional tectonic interpretations but apparently not on field observations in the Gibraltar area itself. Deformation on a lithospheric scale such as roll-back subduction, producing surface uplift and subsequent gravity-induced slumping, has been also put forward as a possible cause of the opening of the strait (e.g. Duggen et al., 2003), but whatever the reality of such a process, it requires the occurrence of a topographic low in the Gibraltar area that this process does not explain. Considering that the reflooding of the desiccated Mediterranean basin cannot be ascribed to the Atlantic sea-level rise alone, especially not during the Early Pliocene (e.g. Hodell et al., 2001), this suggests an alternative process.

On the other hand, it has been recognized long before that the desiccation of the Mediterranean during the Messinian has produced a vigorous re-incision of the drainage networks that were flowing into the Mediterranean. Whatever the size of their pre-MSC catchments, all valleys were cut, the larger the catchments, the longer and deeper the incisions.

It would be very unlikely that such rejuvenation did not also develop in the future strait, while even small catchments display a significant re-incision, as it has been documented in the surrounding areas.

Numerical modeling of erosion dynamics during the MSC verifies that the regressive fluvial erosion hypothesis (e.g. Blanc, 2002) is viable, i.e. that drainage network may develop in the Gibraltar area. Using pertinent parameters, it shows that fluvial regressive erosion is able to penetrate within the flat bottom of a saddle to eventually capture the Atlantics waters.

We therefore propose that the deep cut into the threshold of Gibraltar was due to the regressive erosion of a stream that was flowing toward the desiccated Mediterranean basin, resulting in the opening of the "Strait of Gibraltar".

Acknowledgements

Financial support was provided by Centre National de la Recherche Scientifique INSU, "Programme Eclipse", and by the Ministère de l'Education, de la Recherche et de la Technologie, who funded Nicolas Loget's PhD. Reviews by Laurent Jolivet and an anonymous referee greatly improved the manuscript. We acknowledge Philippe Davy for his invaluable help to us in numerical modelling, and Peter van der Beek, Jacques Deverchère and J.-M. Rouchy for their constructive remarks on this work.

REFERENCES

Aleria Group, 1980. Le canal de Corse et les bassins nord-tyrrhéniens au Miocène supérieur et terminal (Messinien); leur évolution plio-quaternaire. Géologie méditerranéenne 7, 5–12.

Aharon, P., Goldstein, P., Wheeler, C.W., Jacobson, G., 1993. Sea-level events in the South Pacific linked with the Messinian salinity crisis. Geology 21, 771–775.

Ambert, P., Aguilar, J.P., Michaux, J., 1998. Evolution géodynamique messinio-pliocène en Languedoc central: le paléo-réseau hydrographique de l'Orb et de l'Hérault (sud de la France). Geodinamica Acta 11, 139–146.

Babault, J., Van Den Driessche, J., Bonnet, S., Castelltort, C., Crave, A., 2005. Origin of the highly elevated Pyrenean peneplain. Tectonics 24, TC2010, doi:10.1029/2004TC001697.

Balanyá, J.C., García-Dueñas, V., Azañón, J.M., Sánchez-Gómez, M., 1997. Alternating contractional and extensional events in the Alpujarride nappes of the Alboran Domain (Betics, Gibraltar Arc). Tectonics 16, 226–238.

Barber, P.M., 1981. Messinian subaerial erosion of the Proto-Nile delta. Marine Geology 44, 253–272.

Barr, F.T., Walker, B.R., 1973. Late Tertiary channel system in Northern Lybia and its implications on Mediterranean sea-level changes. In: Ryan, W.B.F., Hsü, K.J., et al. (Eds.), Initial Reports of the Deep Sea Drilling Project, vol. 13. U.S. Government Printing Office, Washington, DC, pp. 1244–1250.

Beaumont, C., Fullsack, P., Hamilton, J., 1992. Erosional control of active compressional orogens, in Thrust Tectonics, edited by K. R. McClay, pp. 1– 18, Chapman and Hall, New York.

Benson, R.H., Rakic-El Bied, K., Bonaduce, G., 1991. An important current reversal (influx) in the Rifian Corridor (Morocco) at the Tortonian-Messinian boundary: the end of the Tethys ocean. Paleoceanography, 6, 164–192.

Bergerat, F., 1987. Stress fields in the european platform at the time of Africa-Eurasia collision. Tectonics 6, 99–132.

Blanc, P.L., 2002. The opening of the Plio-Quaternary Gibraltar Strait: assessing the size of a cataclysm. Geodinamica Acta 15, 303–317.

Bourgois, J., Mauffret, A., Ammar, A., Demnati, N.A., 1992. Multichannel seismic data imaging of inversion tectonics of the Alboran Ridge (Western Mediterranean Sea). Geo-Marine Letters 12, 117–122.

Braga, J.C., Martín, J.M., 1996. Geometries of reef advance in response to relative sea-level changes in a Messinian (uppermost Miocene) fringing reef (Cariatiz reef, Sorbas Basin, SE Spain). Sedimentary Geology 107, 61–81.

Butler, R.W., Lickorish, W.H., Grasso, M., Pedley, H.M., Ramberti, L., 1995. Tectonics and sequence stratigraphy in Messinian basins, Sicily: Constraints on the initiation and termination of the Mediterranean salinity crisis. Geological Society of America Bulletin 170, 425–439.

Calvert, A., Sandvol, E., Seber, D., Barazangi, M., Roecker, S., Mourabit, T., Vidal, F., Alguacil, G., Jabour, N., 2000. Geodynamic evolution of the lithosphere and upper mantle beneath the Alboran region of the western Mediterranean: Constraints from travel time tomography. Journal of Geophysical Research 105, 10,871–10,898.

Campillo, A.C., Maldonado, A., Mauffret, A., 1992. Stratigraphic and tectonic evolution of the Western Alboran Sea: Late Miocene to Recent. Geo-Marine Letters 12, 165–172.

Carminati, E., Wortel, M.J.R., Meijer, P.T., Sabadini, R., 1998. The two-stage opening of the western-central Mediterranean basins: a forward modeling test to a new evolutionary model. Earth and Planetary Science Letters 160, 667–679.

Chalouan, A., Saji, R., Michard, A., Bally, A.W., 1997. Neogene tectonic evolution of the southwestern Alboran basin as inferred from seismic data off Morocco. American Association of Petroleum Geologists Bulletin 81, 1161–1184.

Chase, C.G., 1992. Fluvial landsculpting and the fractal dimension of topography: Geomorphology 5, 39–57.

Chumakov, I.S., 1973. Pliocene and Pleistocene deposits of the Nile valley in Nubia and upper Egypt. In: Ryan, W.B.F., Hsü , K.J., et al. (Eds.), Initial Reports of the Deep Sea Drilling Project, vol. 13. U.S. Government Printing Office, Washington, DC, pp. 1242–1243.

Cita, M.B., Ryan, W.B.F., eds., 1978. Messinian erosional surfaces in the Mediterranean. Marine Geology 27, pp. 366.

Cita, M.B., Corselli, C., 1990. Messinian paleogeography and erosional surfaces in Italy : an overview. Palaeogeography, Palaeoclimatology, Palaeoecology 77, 67–82.

Clauzon, G., 1978. The Messinian Var canyon (Provence, Southern France). Paleogeographic implications. Marine Geology 27, 231–246.

Clauzon, G., 1982. Le canyon messinien du Rhône : une preuve désicive du "dessicated deep basin model" (Hsü, Cita et Ryan, 1973). Bulletin de la Société Géologique de France 24, 231–246.

Clauzon, G., Aguilar, J.P., Michaux, J., 1987. Le bassin pliocène du Roussillon (Pyrénéées-orientales, France): exemple d' évolution géodynamique d'une ria méditerranéenne consécutive à la crise de salinité messinienne. Comptes-Rendus de l'Académie des Sciences de Paris 304, 585–590.

Clauzon, G., Rubino, J.-L., Savoye, B., 1995. Marine Pliocene Gilbert-type fan deltas along the French Mediterranean coast. A typical infill feature of preexisting subaerial Messinian canyons. In: IAS-16th Regional Meeting of Sedimentology, Field Trip Guide Book 23, ASF Ed., Paris, pp. 145–222.

Clauzon, G., Suc, J.-P., Gautier, F., Berger, A., Loutre, M.F., 1996. Alternate interpretation of the Messinian salinity crisis : Controversy resoved? Geology 24, 363–366.

Clevis, Q., de Boer, P., Wachter, M., 2003. Numerical modelling of drainage basin evolution and three-dimensional alluvial fan stratigraphy. Sedimentary Geology 163, 85–110.

Comas, M.C., García-Dueñas, V., Jurado, M.J., 1992. Neogene tectonic evolution of the Alboran Basin from MCS data. Geo-Marine Letters 12, 157–164.

Comas, M.C., Platt, J.P., Soto, J.I, Watts, A.B., 1999. The origin and tectonic history of the Alboran Basin: insights from Leg 161 results. In: Zahn, R., Comas, M.C., Klaus, A. (Eds.), Proc. ODP, Sci. Results, vol. 161. Ocean Drilling Program, College Station, TX, pp. 555–580.

Crave, A., Davy, P., 2001. A stochastic "precipiton" model for simulating erosion/sedimentation dynamics. Computers & Geosciences 27, 815–827.

Davy, P., Crave, A., 2000. Upscaling Local-Scale Transport Processes in Large-Scale Relief Dynamics. Physics and Chemistry of the Earth (A) 25, 533–541.

Delrieu, B., Rouchy, J.-M., Foucault, A., 1993. The latest Messinian erosional surface in central Crete (Greece) and around the Mediterranean: relations with the Mediterranean salinity crisis. Comptes-Rendus de l'Académie des Sciences de Paris 316 (II), 527–533.

Denizot, G., 1952. Le Pliocène dans la vallée du Rhône. Revue de géographie de Lyon 27, 327–357.

Dewey, J.F., Helman, M.L., Turco, E., Hutton, D.H.W., Knott, S.D., 1989. Kinematics of the western Mediterranean. In: Coward, M. (Ed.), Alpine Tectonics. Special Publication Geological Society of London 45, 265–283.

Didon, J., 1969. Etude géologique du Campo de Gibraltar (Espagne méridionale). Thèse, Faculté des Sciences, Paris, 539 pp.

Didon, J., 1973. Accidents transverses et coulissages longitudinaux dextres dans la partie N de l'arc de Gibraltar (Cordillères bétiques occidentales–Espagne). Bulletin de la Société Géologique de France 15, 121–127.

Druckman, Y., Buchbinder, B., Martinotti, G.M., Tov, R.S., Aharon, P., 1995. The buried Afiq Canyon (eastern Mediterranean, Israel): a case study of a Tertiary submarine canyon exposed in Late Messinian times. Marine Geology 123, 167–185.

Duggen, S., Hoernle, K., Van Den Bogaard, P., Rupke, L., Morgan, J.P., 2003. Deep roots of the Messinian salinity crisis. Nature 422, 602–606.

Duggen, S., Hoernle, K., van den Bogaard, P., Harris, C., 2004. Magmatic evolution of the Alboran region: The role of subduction in forming the western Mediterranean and causing the Messinian Salinity Crisis. Earth and Planetary Science Letters 218, 91–108.

Escutia, C., Maldonado, A., 1992. Paleogeographic implications of the Messinian surface in the Valencia trough, northwestern Mediterranean Sea. Tectonophysics 203, 263–284.

Faccenna, C., Piromallo, C., Crespo-Blanc, A., Jolivet, L., Rossetti, F., 2004. Lateral slab deformation and the origin of the western Mediterranean arcs. Tectonics 23, doi:10.1029/2002TC001488.

Field, M.E., Gardner, J.V., 1990. Pliocene-Pleistocene growth of the Rio Ebro margin, northeast Spain: A prograding-slope model. Geological Society of America Bulletin 102, 721–733.

Fortuin, A.R., Krijgsman, W., Hilgen, F.J., Sierro, F.J., 2000. Late Miocene Mediterranean desiccation: topography and significance of the 'Salinity Crisis' erosion surface on-land in southeast Spain: a comment. Sedimentary Geology 133, 167–174.

Frizon de Lamotte, D., Crespo-Blanc, A., Saint-Bézar, B., Comas, M.C., Fernàndez, M., Zeyen, H., Ayarza, P., Robert-Charrue, C., Chalouan, A., Zizi, M., Teixell, A., Arboleya, M. L., Alvarez-Lobato, F., Julivert, M., Michard, A., 2004. Transect I: Iberia-Meseta - Guadalquivir Basin - Betic Cordillera - Alboran Sea - Rif - Moroccan Meseta - High Atlas - Sahara Domain. In The TRANSMED Atlas - The Mediterranean region from crust to Mantle, edited by W. Cavazza, F.M. Roure, W. Spakman, G.M. Stampfli and P.A.Z. (eds), Springer, Berlin, Heidelberg.

García-Dueñas, V., Balanyá, J.C., Martínez-Martínez, J.M., 1992. Miocene extensional detachments in the outcropping basement of the northern Alboran basin (Betics) and their tectonic implications. Geo-Marine Letters 12, 88–95.

Giermann, G., 1961. Erläuterungen zur bathymetrischen Karte der Strasse von Gibraltar. Bull. Inst. Océanogr. Monaco 58 (1218 A), 28 pp.

Groupe de recherche néotectonique de l'Arc de Gibraltar, 1977. L'histoire néotectonique récente (Tortonien à Quaternaire) de l'Arc de Gibraltar et des bordures de la mer d'Alboran. Bulletin de la Société Géologique de France 19, 575–614.

Gutscher, M.A., Malod, J., Rehault, J.P., Contrucci, I., Klingelhoefer, F., Mendes-Victor, L., Spakman, W., 2002. Evidence for active subduction beneath Gibraltar. Geology 30, 1071–1074.

Hodell, D.A., Curtis, J.H., Sierro, F.J., Raymo, M.E., 2001. Correlation of late Miocene to early Pliocene sequences between the Mediterranean and North Atlantic. Paleoceanography 16, 164–178.

Howard, A.D., Dietrich, W.E., Seidl, M.A., 1994. Modeling fluvial erosion on regional to continental scales. Journal of Geophysical Research 99, 13,971–13,986.

Hsü, K.J., Ryan, W.B.F., Cita, M.B., 1973a. Late Miocene dessication of the Mediterranean. Nature 242, 240–244.

Hsü, K.J., Cita, M.B., Ryan, W.B.F., 1973b. The origin of the Mediterranean evaporites. In: Ryan, W.B.F., Hsü, K.J., et al. (Eds.), Initial Reports of the Deep Sea Drilling Project, vol. 13. U.S. Government Printing Office, Washington, DC, pp. 1203– 1231.

Instituto Geologico y Minero de Espana (IGME), 1994. Mapa Geologico de la Peninsula Iberica, y Canarias, scale 1:1.000.000.

Jiménez-Munt, I., Negredo, A.M., 2003. Neotectonic modelling of the western part of the Africa-Eurasia plate boundary: from the Mid-Atlantic ridge to Algeria. Earth and Planetary Science Letters 205, 257–271.

Kastens, K.A., 1992. Did glacio-eustatic sea level drop trigger the messinian salinity crisis? New evidence from ocean drilling program site 654 in the Tyrrhenian Sea. Paleoceanography 7, 333–356.

Krijgsman, W., Hiigeni, F.J., Raffi, I., Sierro, F.J., Wilson, D.S., 1999a. Chronology, causes and progression of the Messinian salinity crisis. Nature 400, 652–655.

Krijgsman, W., Langereis, C.G., Zachariasse, W.J., Boccaletti, M., Moratti, G., Gelati, R., Iaccarino, S., Papani, G., Villa, G., 1999b. Late Neogene evolution of the Taza-Guercif Basin (Rifian Corridor, Morocco) and implications for the Messinian salinity crisis. Marine Geology 153, 147–160.

Lague, D., Crave, A., Davy, P., 2003, Laboratory experiments simulating the geomorphic response to tectonic uplift. Journal of Geophysical Research 108(B1), doi:10.1029/2002JB001785.

Leblanc, D., Olivier, P., 1984. Role of strike-slip faults in the Betic-Rifian orogeny. Tectonophysics 101, 345–355.

Loget, N., Van Den Driessche, J., Davy, P., 2005. How did the Messinian Salinity Crisis end? Terra Nova 17, 414–419.

Lonergan, L., White, N., 1997. Origin of the Betic-Rif mountain belt. Tectonics 16, 504–522.

Maldonado, A., Nelson, C.H., 1999. Interaction of tectonic and depositional processes that control the evolution of the Iberian Gulf of Cadiz margin. Marine Geology 155, 217–242.

Maldonado, A., Campillo, A.C., Mauffret, A., Alonso, B., Woodside, J., Campos, J., 1992. Alboran Sea late Cenozoic tectonic and stratigraphic evolution. Geo-Marine Letters 12, 179–186.

Maldonado, A., Somoza, L., Pallares, L., 1999. The Betic orogen and the Iberian-African boundary in the Gulf of Cadiz: geological evolution (central North Atlantic). Marine Geology 155, 9–43.

Martín, J.M., Braga, J.C., 1994. Messinian events in the Sorbas Basin in southeastern Spain and their implications in the recent history of the Mediterranean. Sedimentary Geology 90, 257–268.

Martín, J.M., Braga, J.C., Betzler, C., 2001. The Messinian Guadalhorce corridor : the last northern, Atlantic-Mediterranean gateway. Terra Nova 13, 418–424.

Martínez-Martínez, J.M., Azañón, J.M., 1997. Mode of extensional tectonics in the southeastern Betics (SE Spain): Implications for the tectonic evolution of the peri-Alborán orogenic system. Tectonics 16, 205–225.

Mauffret, A., Maldonado, A., Campillo, A.C., 1992. Tectonic framework of the Eastern Alboran and Western Algerian Basins, Western Mediterranean. Geo-Marine Letters 12, 104–110.

Michard, A., Chalouan, A., Feinberg, H., Goffé, B., Montigny, R., 2002. How does the Alpine belt end between Spain and Morocco? Bulletin de la Société Géologique de France 173, 3–15.

Molnar, P., England, P., 1990. Late Cenozoic uplift of mountain ranges and global climatic change: Chicken or egg? Nature 346, 29–34.

Montenat, C., Ott d'Estevou, P. La Chapelle, G., 1990. Le bassin de Nijar–Carboneras et le couloir du Bas-Andarax. In: Les bassins néogenes du domaine bétique oriental (Espagne) (Ed. C. Montenat). Documents et Travaux de l'IGAL 12–13, pp. 129–164.

Morel, J.L., 1987. Evolution récente de l'orogène rifain et de son avant-pays depuis la fin de la mise en place des nappes (Rif, Maroc). Thèse d'Etat, Université Paris-Sud, 583 pp.

Morel, J.L., Meghraoui, M., 1996. Goringe-Alboran-Tell tectonic zone: A transpression system along the Africa-Eurasia plate boundary. Geology 24, 755–758.

Mulder, C.J., Parry, G.R., 1977. Late Tertiary evolution of the Alboran Sea at the eastern entrance of the Straits of Gibraltar. In: International Symposium on the Structural History of the Mediterranean Basins (Ed. By B. Biju-Duval and L. Montadert), Editions Technip, Paris, pp. 401–410.

Murray, A.B., Paola, C., 1997. Properties of a cellular braided-stream model. Earth Surface Processes and Landforms 22, 1001–1025.

Olivet, J.L., Auzende, J.M., Bonnin, J., 1973. Alboran Sea structural framework. In: Ryan, W.B.F., Hsü, K.J., et al. (Eds.), Initial Reports of the Deep Sea Drilling Project, vol. 13. U.S. Government Printing Office, Washington, DC, pp. 1417– 1430.

Orszag-Sperber, F., Rouchy, J.M., Blanc-Valleron, M.M., 2000. La transition Messinien – Pliocène en Méditerranée orientale (Chypre): la période du Lago-Mare et sa signification. Comptes-Rendus de l'Académie des Sciences de Paris 2 (331), 490–493.

Peizhen, Z., Molnar, P., Downs, W.R. 2001. Increased sedimentation rates and grain sizes 2-4 Myr ago due to the influence of climate change on erosion rates. Nature 410, 891–897.

Platt, J.P., Vissers, R.L.M., 1989. Extensional collapse of thickened continental lithosphere: A working hypothesis for the Alboran Sea and Gibraltar arc. Geology 17, 540–543.

Platt, J.P., Whitehouse, M.J., Kelley, S.P., Carter, A., Hollick, L., 2003. The ultimate arc: differential displacement, oroclinal bending, and vertical axis rotation in the External Betic-Rif arc. Tectonics 22, 1017, doi: 10.1029⁄2001TC001321.

Poisson, A., Wernli, R., Kemal Saular, E., Temz, H., 2003. New data concerning the age of the Aksu Thrust in the south of the Aksu valley, Isparta Angle (SW Turkey): consequences for the Antalya Basin and the Eastern Mediterranean. Geological Journal 38, 311–327.

Rampnoux, J.P., Angelier, J., Colleta, B., Fudral, S., Guillemin, M., Pierre, G., 1979. Sur l'évolution néotectonique du Maroc septentrional. Géologie Méditerranéenne 6, 439–464.

Riding, R., Braga, J.C., Martìn, J.M., 1999. Late Miocene Mediterranean desiccation: topography and significance of the 'Salinity Crisis' erosion surface on-land in southeast Spain. Sedimentary Geology 123, 1–7.

Rouchy, J.M., Saint Martin, J.P., 1992. Late Miocene events in the Mediterranean as recorded by carbonate-evaporite relations. Geology 20, 629–632.

Rouchy, J.M., Pierre, C., Et-Touhami, M., Kerzazi, K., Caruso, A., Blanc-Valleron, M.M., 2003. Late Messinian to Early Pliocene paleoenvironmental changes in the Melilla Basin (NE Morocco) and their relation to Mediterranean evolution. Sedimentary Geology 163, 1–27.

Ryan, W.B.F., Hsü, K.J. et al., 1973. Initial reports of the Deep Sea Drilling Project, vol. 13. U.S. Government Printing Office, Washington, DC, pp. 1447.

Savoye, B., Piper, D.J.W., 1991. The Messinian event on the margin of the Mediterranean Sea in the Nice area, southern France. Marine Geology 97, 279–304.

Schoorl, J.M., Veldkamp, A., 2003. Late Cenozoic landscape development and its tectonic implications for the Guadalhorce valley near Alora (Southern Spain). Geomorphology 50, 43–57.

Shackleton, N.J., Hall, M.A., Pate, D., 1995. Pliocene stable isotope stratigraphy of site 846. Proceedings of the Ocean Drilling Program, Scientific Results 138, 337–355.

Seber, D., Barazangi, M., Ibenbrahim, A., Demnati, A., 1996. Geophysical evidence for lithospheric delamination beneath the Alboran Sea and Rif- Betic Mountains. Nature 379, 785–791.

Suc, J.P., Bessais, E., 1990. Pérennité d'un climat thermo-xérique en Sicile avant, pendant, après la crise de salinité messinienne. Comptes-Rendus de l'Académie des Sciences de Paris 310, 1701–1707.

Suter, G., 1980a. Carte géologique de la chaine rifaine au 1/500 000. Notes et mémoires Service géologique du Maroc 245a.

Suter, G., 1980b. Carte structurale de la chaine rifaine au 1/500 000. Notes et mémoires Service géologique du Maroc 245b.

Tapponnier, P., 1977. Evolution tectonique du système alpin en Méditerranée : poinçonnement et écrasement rigide-plastique. Bulletin de la Société Géologique de France 19, 437–460.

Vissers, R.L.M., Platt, J.P., van der Wal, D., 1995. Late orogenic extension of the Betic Cordillera and the Alboran Domain: a lithospheric view. Tectonics 14, 786–803.

Watts, A.B., Platt, J.P., Buhl, P., 1993. Tectonic evolution of the Alboran Sea basin. Basin research 5, 153–177.

Weijermars, R., 1988. Neogene tectonics in the Western Mediterranean may have caused the Messinian Salinity Crisis and an associated glacial event. Tectonophysics 148, 211–219.

Whipple, K.X., Tucker, G.E., 1999. Dynamics of the stream-power river incision model: Implications for height limits of mountain ranges, landscape response timescales, and research needs. Journal of Geophysical Research 104, 17,661–17,674.

Whipple, K.X., Tucker, G.E., 2002. Implications of sediment-flux-dependent river incision models for landscape evolution. Journal of Geophysical Research 107 (B2), 10.1029/2000JB00004.

Wildi, W., 1983. La chaine tello-rifaine (Algérie, Maroc, Tunisie): Structure, stratigraphie et évolution du Trias au Miocène, Revue de Géologie Dynamique et de Géographie Physique 24, 201–297.

Wildi, W., Wernli, R., 1977, Stratigraphie et micropaléontologie des sédiments pliocènes de l'Oued Laou (côte méditerranéenne marocaine). Archives des Sciences de Genève 30, 213–228.

Woodside, J.M., Maldonado, A., 1992. Styles of compressional neotectonics in the Estearn Alboran Sea. Geo-Marine Letters 12, 111–116.

Zeck, H.P., 1997. Mantle peridotites outlining the Gibraltar Arc: Centrifugal extensional allochthons derived from the earlier Alpine, westward subducted nappe pile. Tectonophysics 281, 195–207.

FIGURES

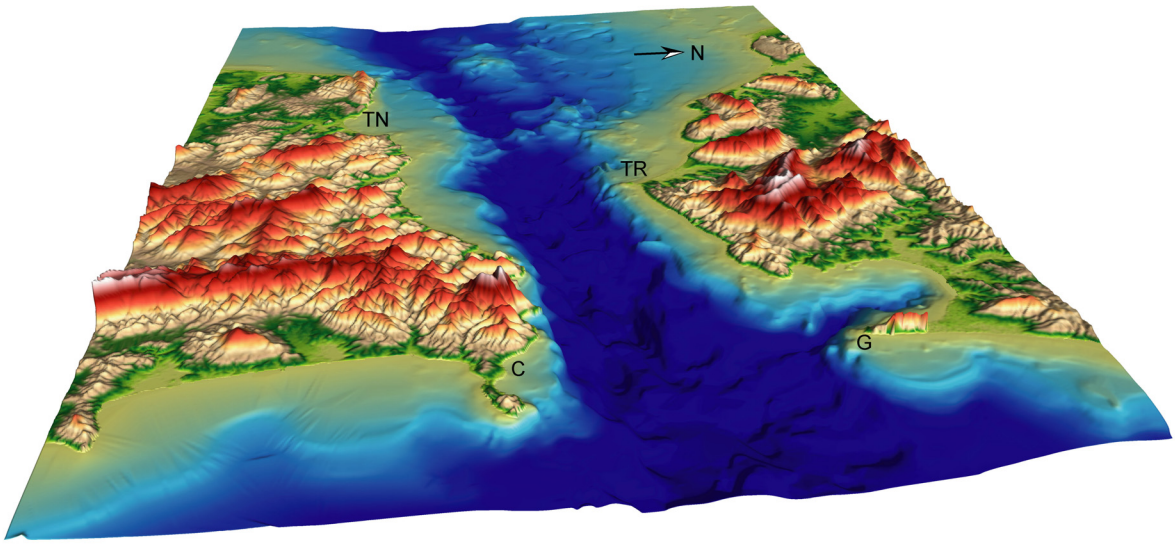

Figure 1

Digital Elevation Model (view toward the west) of the Gibraltar Strait (land topography: SRTM90 DEM data; Gibraltar Strait bathymetry: isobaths from Giermann, 1961). The strait is 58 km long and narrows to 13 km in width between Point Marroquí, Spain, and Point Cires, Morocco.

C:Ceuta ; G:Gibraltar; TN: Tanger; TR: Tarifa.

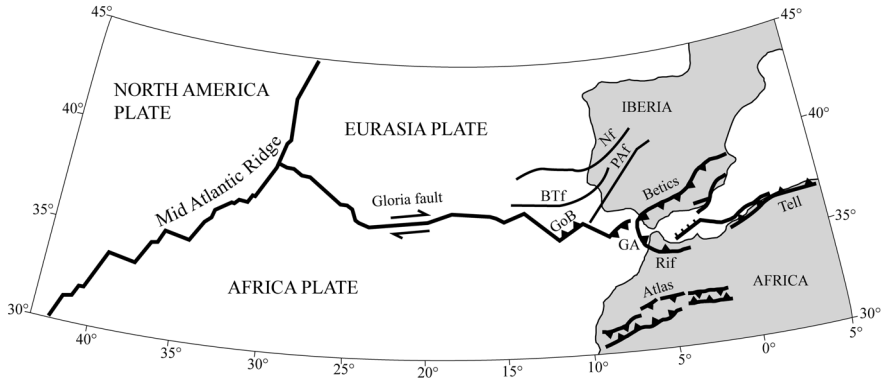

Figure 2

Plate tectonics framework of the Gibraltar area (modified after Jiménez-Munt and Negredo, 2003). The Gibraltar area is part of the diffuse plate boundary between Africa and Eurasia. Note that no major fault zone follows the Strait of Gibraltar itself.

GA: Gibraltar Arc; GoB: Gorringe Bank; BTf: Bato-Tajo fault; Nf: Nazare fault; PAf: Plasencia-Alentejo fault.

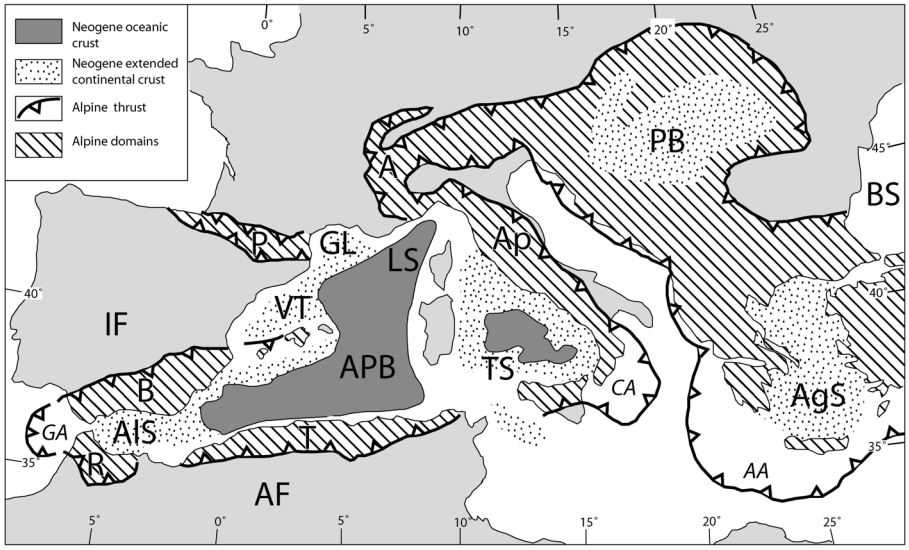

Figure 3

Map of the Mediterranean region showing the Neogene extensional basins and the external front of the Alpine thrusts (After Lonergan and White, 1997). *AA*- Aegean Arc; *CA*- Calabrian Arc; *GA*- Gibraltar Arc; A- Alps; AgS- Aegean Sea; AF- African Foreland; AlS- Alboran Sea; Ap- Apennines; APB- Algerian Provencal basin; B- Betics; BS- Black Sea; GL- Gulf of Lion; IF- Iberian Foreland; LS- Ligurian Sea; P- Pyrenees; PB- Pannonian basin; R- Rif; T- Tell; TS- Tyrrhenian Sea; VT- Valencia trough.

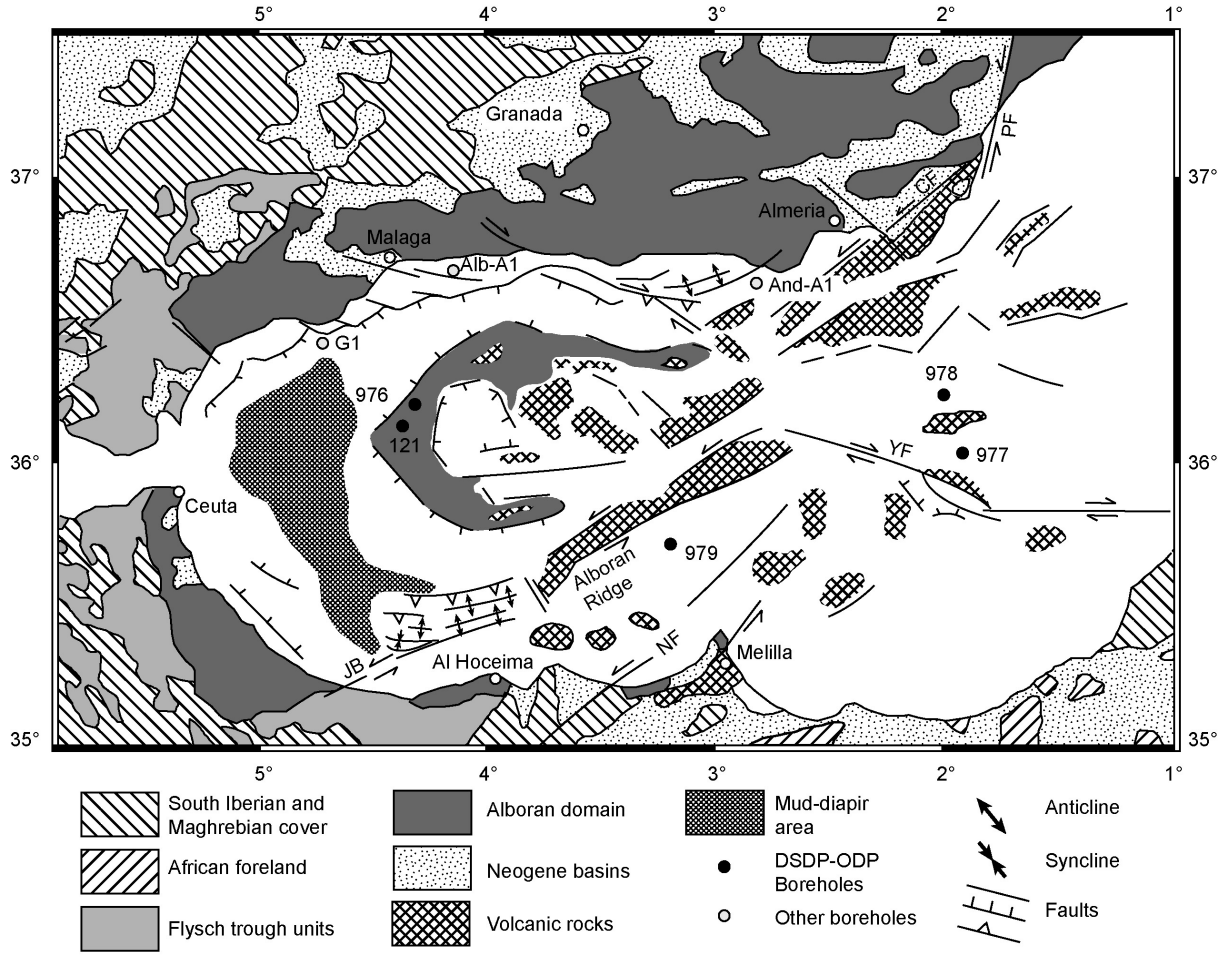

Figure 4

Geological map of the Arc of Gibraltar showing the Betic and the Rif, to the north and to the south respectively, separated by the Alboran basin (modified after Comas et al., 1999). CF- Carboneras Fault; JB- Jebha Fault; NF- Nekor Fault; PF- Palomares Fault; YF- Yussuf Fault.

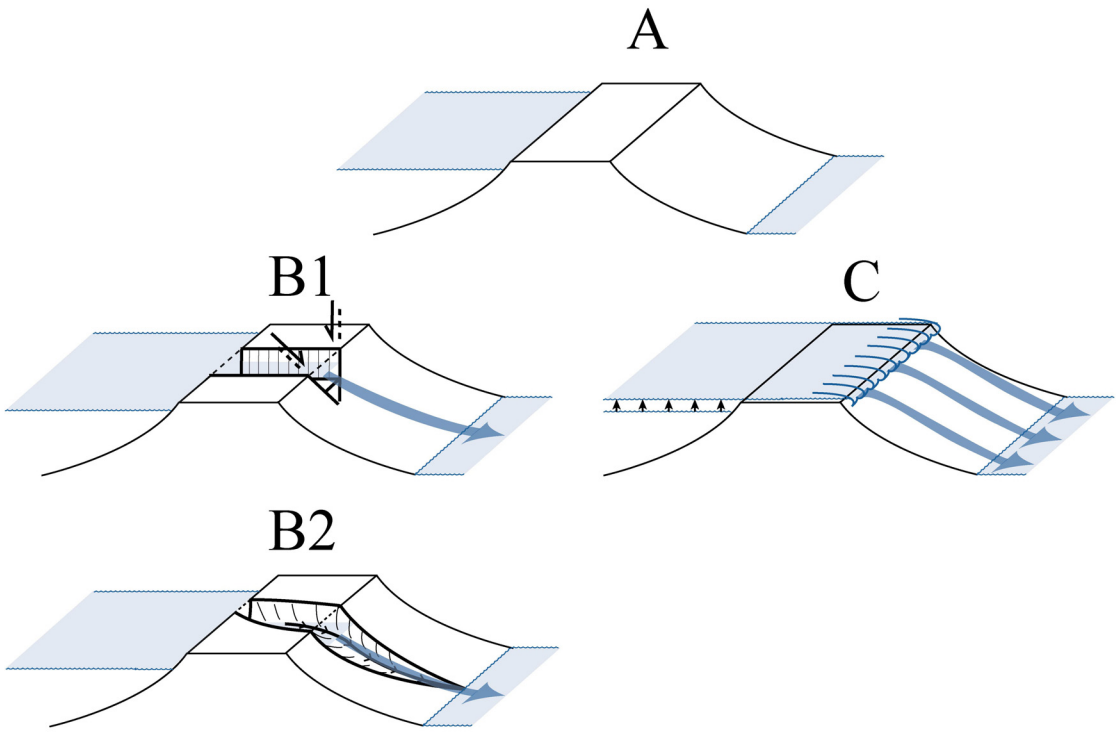

Figure 5

Different hypotheses for the breakdown of the threshold in Gibraltar area. A- Initial configuration during the MSC; B1 and B2 - Topographic lowering of the threshold by tectonic collapse or regressive fluvial erosion respectively; C- Overflowing of the Atlantic waters due to eustatism.

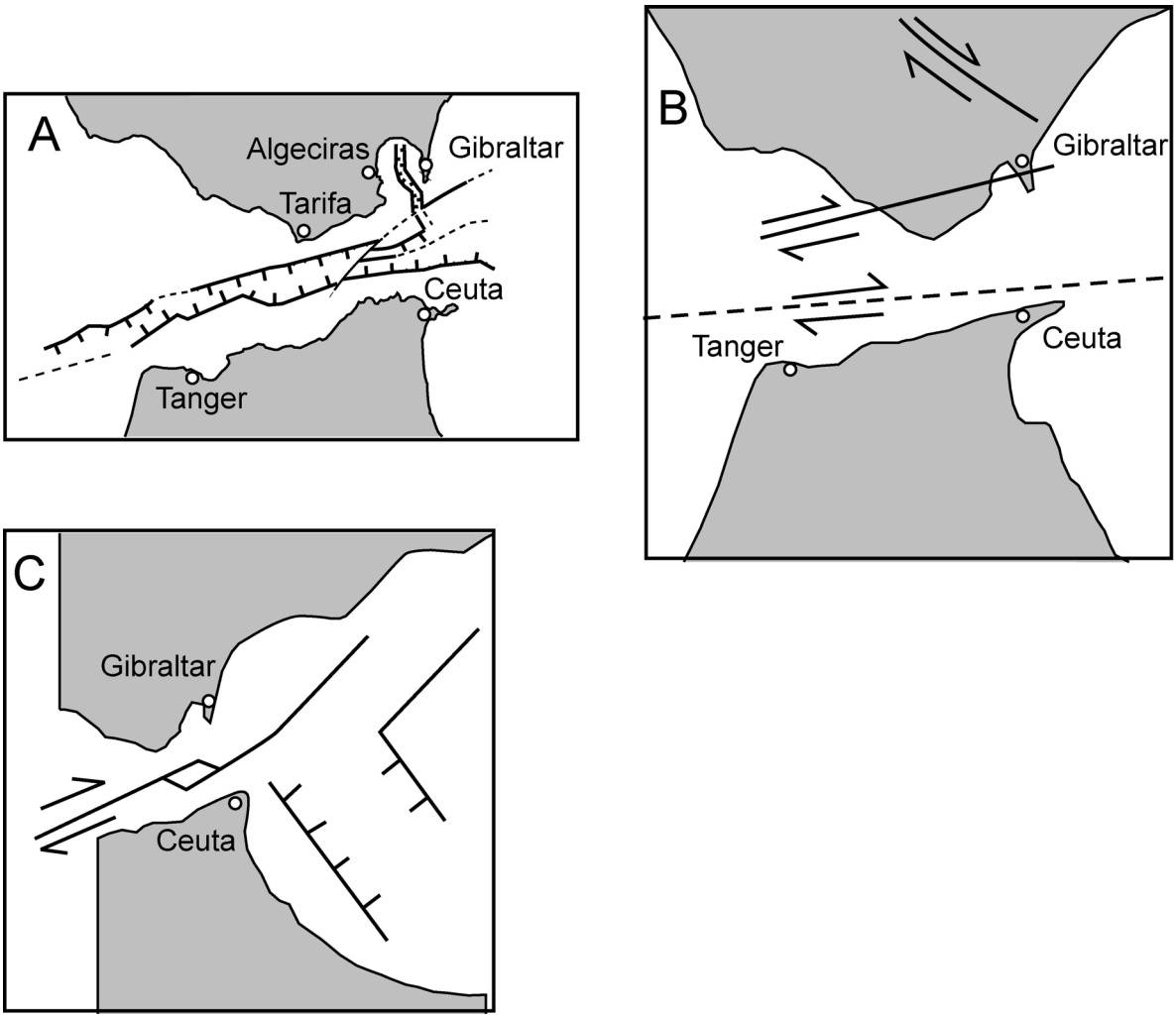

Figure 6

Different tectonic hypotheses for the origin of the Strait of Gibraltar. A- Normal faulting (after Giermann, 1961); B- Strike-slip faults (after Didon, 1973); C- Pull-apart basin (after Campillo et al., 1992).

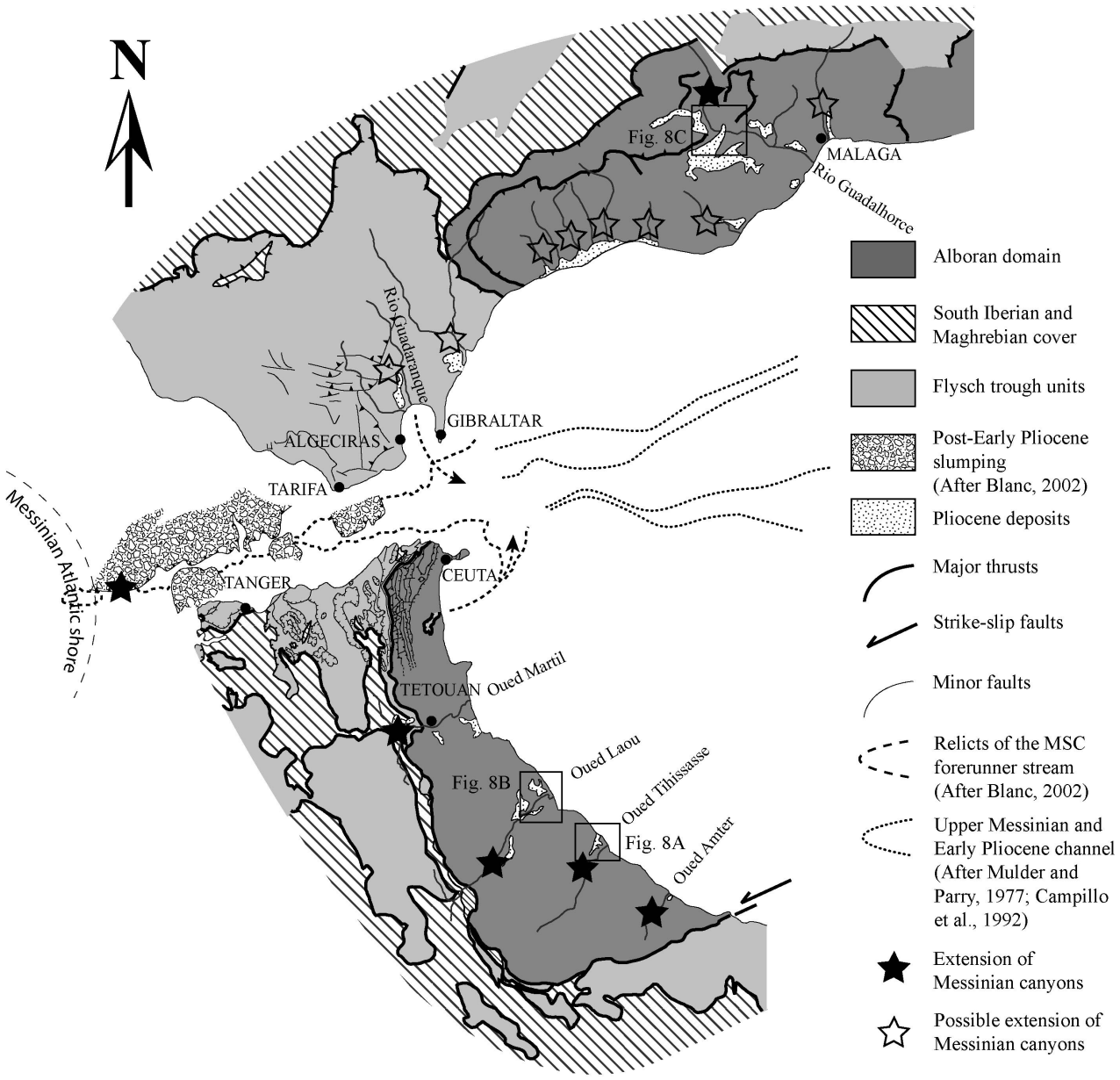

Figure 7

The main structural units of the Gibraltar Arc and the location of Pliocene rias (see text for further explanation) (modified after Suter, 1980a and 1980b and IGME, 1994).

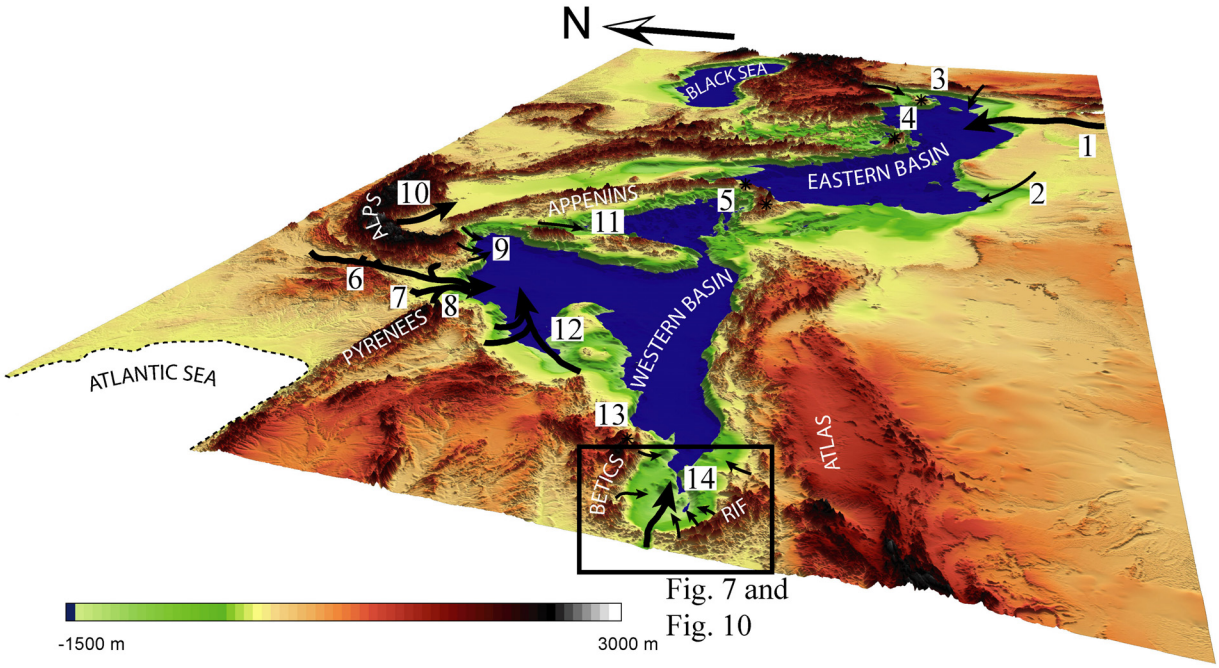

Figure 8

Digital Elevation Model of the Mediterranean region (land topography: GTOPO30 DEM data; Mediterranean Sea bathymetry: ETOPO2 DEM data). The coastline has been drop to the -1500 m isobath to mimic the Messinian sea-level fall. Note that in such a configuration, the Alboran domain is emerged. Main features related to Messinian erosion are shown. Black arrows: drainage systems; crossbars: occurrence of aerial erosional surfaces.

Eastern basin: 1- Nile (Chumakov, 1973; Barber, 1981); 2- Lybian sahabi channel (Barr and Walker, 1973); 3- Israel from Turkish coast (Druckman et al., 1995; Poisson et al., 2003); 4- Erosion surface in Cyprus and Crete (Delrieu et al., 1993; Orszag-Sperber et al., 2000). Western basin: 5- Local erosion in Sicily and south Italia (Butler et al., 1995); 6- Rhone (Clauzon, 1982); 7- Languedoc (Ambert et al., 1998); 8- Pyrenean (Clauzon et al., 1987); 9- Var/Ligure (Clauzon, 1978; Savoye and Piper, 1991; Clauzon et al., 1995); 10- Po and Italian coast (e.g. Cita and Corselli, 1990); 11- Corsica channel (Aleria Group, 1980) 12- Valencia trough (Field and Gardner, 1990; Escutia and Maldonado, 1992); 13- Erosion surface in Sorbas basin (e.g. Martín and Braga, 1994; Riding et al., 1999; Fortuin et al., 2000) 14- Alboran domain; thick arrow after the present work (Fig. 7 and Fig. 10 for more details).

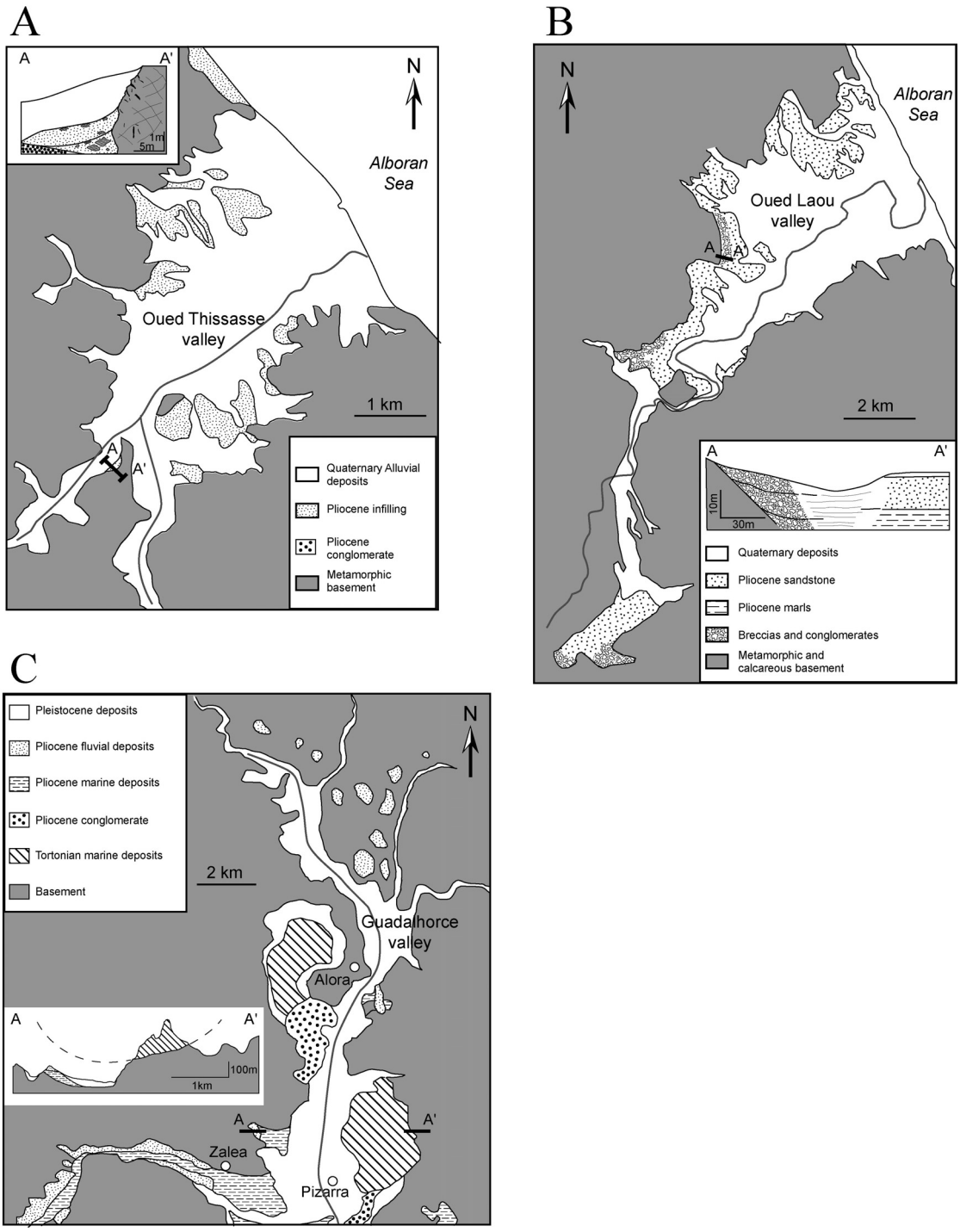

Figure 9

Western Pliocene rias on the Alboran Sea coast (see location figure 7). A- Oued Thissasse valley (after Morel, 1987); B- Oued Laou valley (after Wildi and Wernli, 1977); Guadalhorce valley (after Schoorl and Veldkamp, 2003).

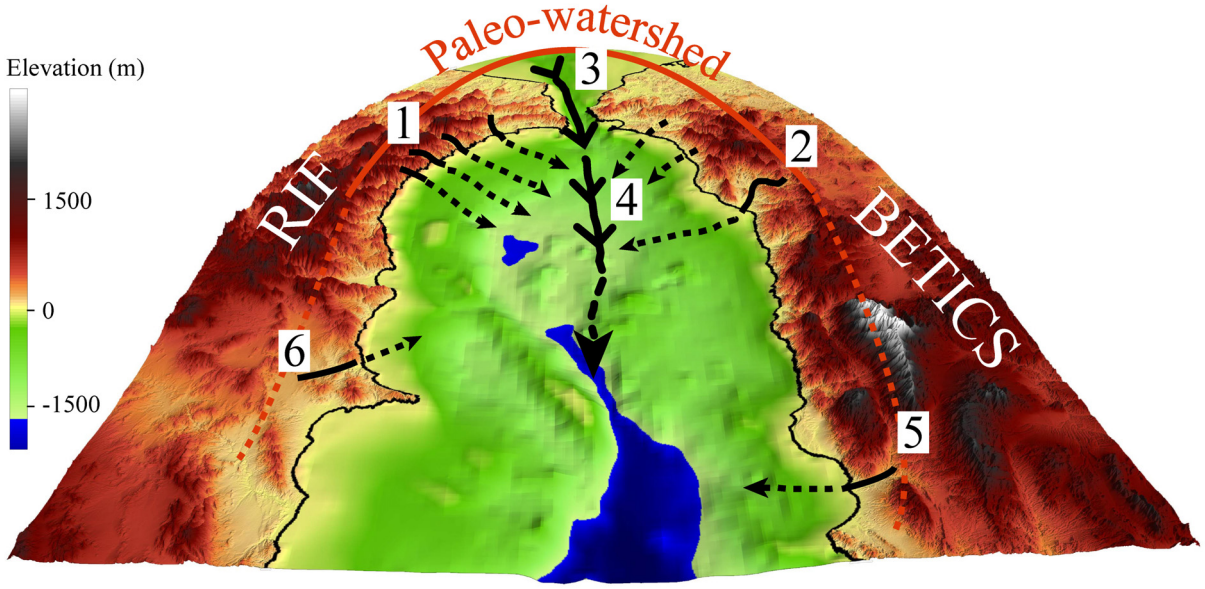

Figure 10

Digital Elevation Model (looking to the west) showing the drainage pattern during the MSC in the Alboran area as proposed in this work (land topography: SRTM90 DEM data; Alboran Sea bathymetry: ETOPO2 DEM data).

1- Rif coast (Rampnoux et al., 1979; Morel, 1987; Chalouan et al., 1997); 2- Betic coast (Schoorl and Veldkamp, 2003); 3- Strait of Gibraltar (Blanc, 2002); 4- Eastern entrance of the Strait of Gibraltar (Mulder and Parry, 1977; Campillo et al., 1992); 5- Andarax (Montenat et al. 1990); 6- Mellila (Rouchy et al., 2003). Black arrows: Messinian canyons; dashed arrows: possible extension of Messinian canyons.

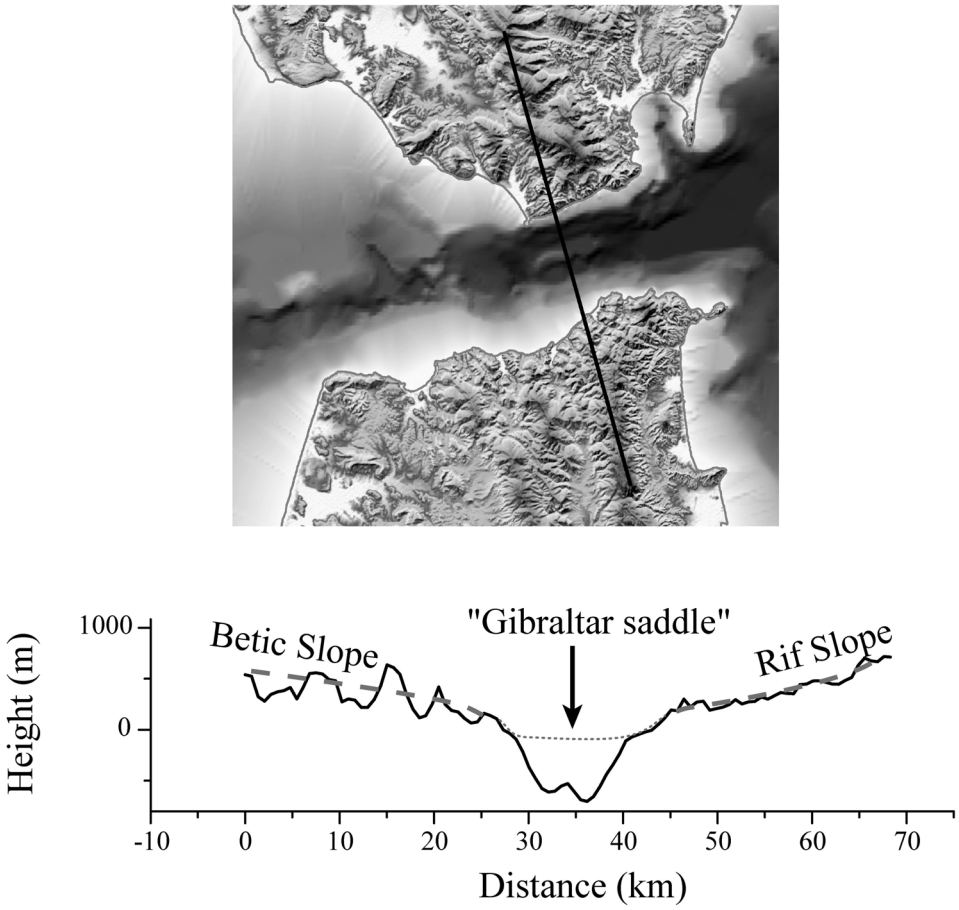

Figure 11

Cross section through the Strait of Gibraltar and the adjacent areas (Betics and Rif).

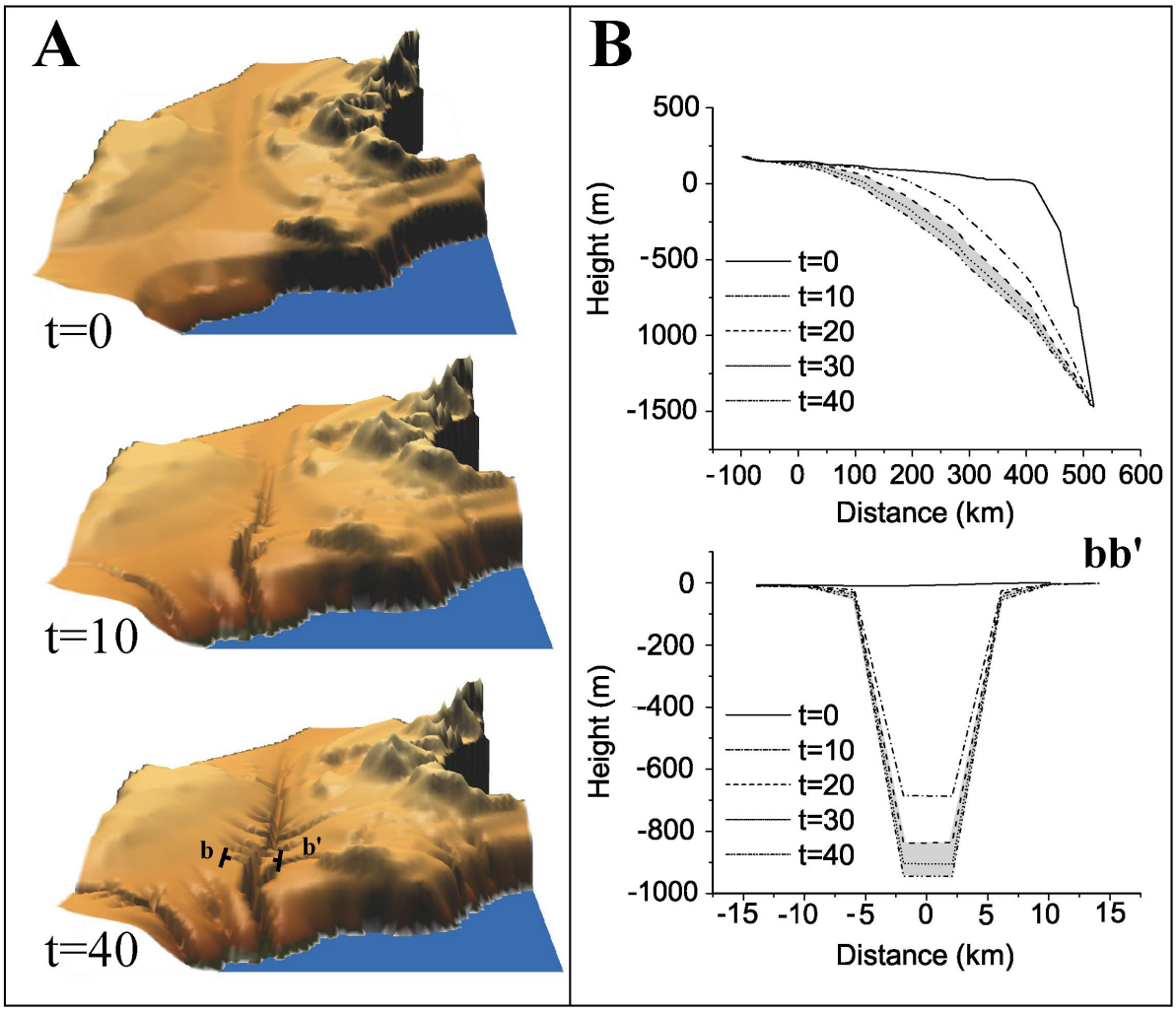

Figure 12

Numerical experiment (EROS model) simulating the evolution of the topography in the Rhone valley after the 1500m Mediterranean sea-level drop. A- Oblique views of the model at three successive stages (t=0 corresponds to the initial topography; vertical dilatation x 32) B- B- Longitudinal profile (top) and transverse section (bottom). The maximum width of the canyon is around 5km and the maximum depth is around 1000m in the downstream part, values that fit with geological data (Clauzon, 1982) Grey area: best fit between experimental curves and the geological data (see Loget et al., 2005 for further discussion).

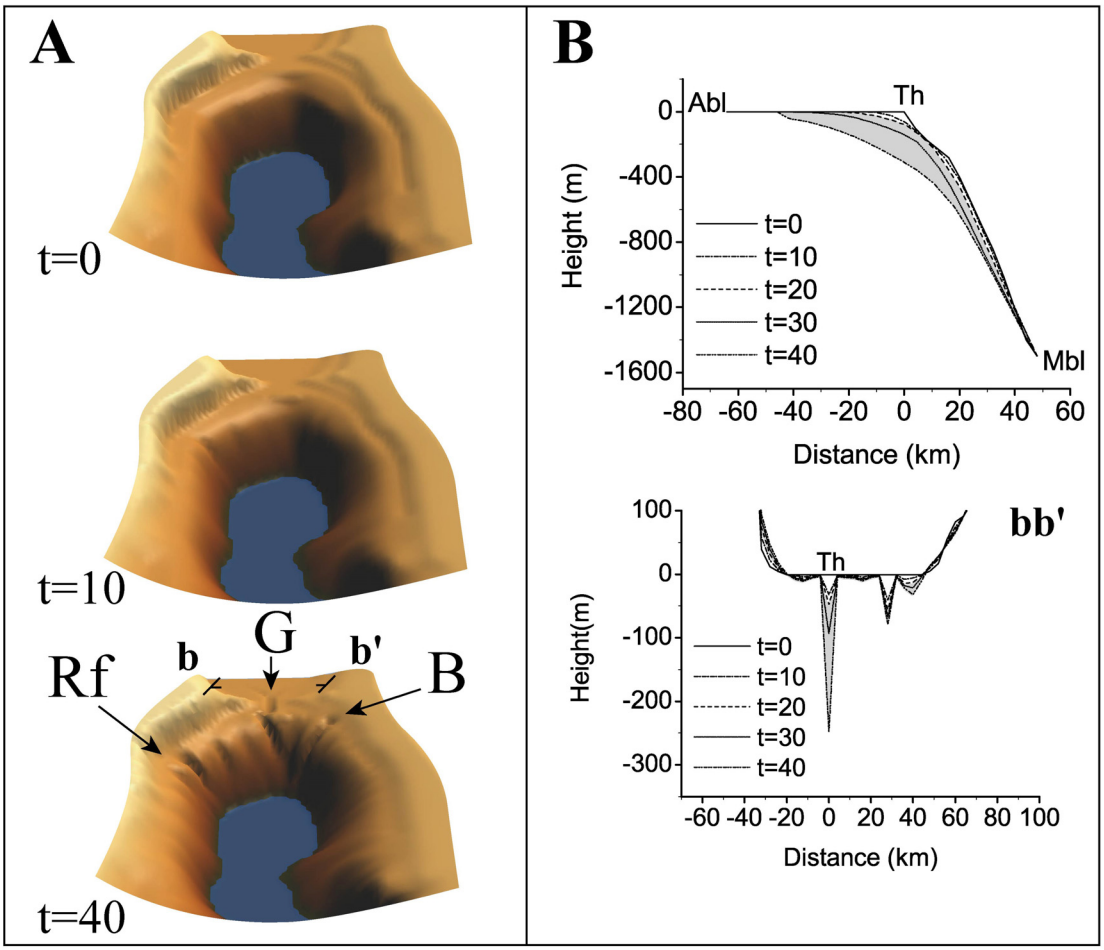

Figure 13

Numerical experiment (EROS model) simulating the evolution of the topography of the Gibraltar area after the 1500m Mediterranean sea-level drop. A- Oblique views of the model at three successive stages (t=0 corresponds to the initial topography, vertical dilatation x 32) B- Longitudinal profile (top) and transverse section (bottom). Note that both horizontal and vertical scales are different from figure 12. The width of the main canyon to the right is about 5km and maximum depth reaches 250m.

Abl- Atlantic base level; Mbl- Mediterranean base-level; Th- Gibraltar thrershold; G, Rf and B: Gibraltar, Rif and Betic experimental rivers respectively (compare with figure 10). Grey area: time interval confidence deduced from the Rhone valley modelling.

Incision de l'Ebre au niveau de la chaîne Catalane (quelques dizaines de kilomètres en amont du delta de l'Ebre). Aucune trace d'incision messinienne n'a été mise en évidence dans cette région.

3.2. Propagation de l'incision messinienne dans le bassin de l'Ebre

---

Article :

Does the Ebro River connect to the Mediterranean before the Messinian Salinity Crisis?

Julien Babault[1], Nicolas loget[1], Jean Van Den Driessche[1], Sébastien Castelltort[2] and Philippe Davy [1]

[1]Géosciences Rennes, Université de Rennes 1, UMR 6118, Campus de Beaulieu, 35042 Rennes cedex, France.

[2]Geology Institute, ETH Zurich, 8092 Zurich, Switzerland.

Submitted to Journal of the Geological Society, London

DOES THE EBRO RIVER CONNECT TO THE MEDITERRANEAN BEFORE THE MESSINIAN SALINITY CRISIS?

Julien Babault[1], Nicolas loget[1], Jean Van Den Driessche[1] and Sébastien Castelltort[1]

[1]Géosciences Rennes, Université de Rennes 1, UMR 6118, Campus de Beaulieu, 35042 Rennes cedex, France.

[2]Geology Institute, ETH Zurich, 8092 Zurich, Switzerland.

Abstract

The connection of the Ebro river to the Mediterranean is supposed to have played a major role in the relief rejuvenation of northern Spain and especially of the South-Pyrenees by lowering the initial base level of the Ebro internal drainage area down to the sea level. However, the timing and causes of this connection are still debated. A fundamental question is: was the Ebro river connected to the Mediterranean before or after the Messinian Salinity Crisis? Morphologic analysis and landscape evolution numerical modelling show that this connection did not exist before the Messinian Salinity Crisis but is effective from the Pliocene onward due to progressive regressive erosion.

Keywords: Ebro basin opening, Messinian Salinity Crisis, Sea level fall, Surface process model.

Introduction

The Ebro Basin in NE Spain corresponds to the southern foreland basin of the Pyrenees with a Tertiary sedimentary fill. Until the end of the Eocene, the basin was open towards the Atlantic Ocean. Further tectonic shortening along the Pyrenees and the Iberian Range closed this western marine connection, resulting in internal drainage and lacustrine sedimentation during the Oligocene and the Miocene (Birot 1937, Reille 1971, Riba et al. 1983). At present the Ebro Basin is drained through the Ebro river toward the Mediterranean Sea and both the Ebro basin and the Pyrenees are deeply dissected by the current drainage network.

When the opening of the interior Miocene Ebro basin started is still the subject of debate. This is a key point in the understanding of both continental erosion dynamics and submarine sedimentation in NE Spain and NW Mediterranean respectively.

According to Roca (2001), and Evans and Arche (2002), the presence of a thick succession of deposits in the adjacent offshore Valencia Trough of Middle to Late Miocene age indicates a considerable flux presumably supplied by a proto Ebro river of a considerable size. For Riba et al (1983) and Serrat (1992) the opening of the interior basin started during the Miocene and was a combined result of lake capture by a Mediterranean stream and sediment overfilling of the basin. Quantitative validation of this mechanism by numerical modelling (Garcia-Castellanos et al. 2003) provides ages between 13 Ma and 8.5 Ma for the basin opening toward the Mediterranean. Field and Gardner (1990) observe a change of the sedimentary record from clays to prograding sandstones in the Valencia Trough, which they attribute to the capture of the Ebro basin during the Quaternary. Coney et al. (1996) state that the capture could result from either the Miocene rifting in the Valencia Trough or regressive erosion during the Messinian Salinity Crisis, or a combination of these two processes that would have led the Ebro river to erode across the Catalan Coastal Ranges.

From the analysis of erosion dynamics in the western Mediterranean and sedimentation pattern along the eastern Spanish margin from Miocene to Quaternary times, we argue hereafter that the Ebro basin was not connected to the Mediterranean Sea before the Pliocene.

The Messinian fluvial incisions

During the Late Messinian, the sea-level of the Mediterranean dropped dramatically (about 1500 m) consecutive to its isolation from the Atlantic waters and its subsequent desiccation (Hsü et al. 1973, Ryan 1976). This base- level fall induced the rejuvenation of the continental Mediterranean landscape, and especially the strong incision of the pre-Messinian drainage network. Deep canyons developed along most of the present day valleys around the Mediterranean. This event, which lasted from 5.96 Ma to 5.32 Ma (Krijgsman et al. 1999), is called the Messinian Salinity Crisis (MSC) because of the concomitant deposit of a thick layer of evaporites. These incisions have been largely preserved due to the sudden reflooding of the Mediterranean during the Early Pliocene (Denizot 1952, Chumakov 1973, Clauzon 1982). A remarkable feature is the relation that exists at first order between the length of the Messinian incisions and the present-day drainage areas, so that the larger the drainage area, the longer the incision length (Fig. 1).

As a general rule, following the base-level fall of a drainage network, the length of river incision is related by a power law to the upstream drainage area (e. g. Schumm et al. 1987, Rosenbloom & Anderson 1994, Bishop et al. 2005). According to Loget et al (2005), in most of the Mediterranean region, the regional slopes and the size of the pre-Messinian drainage areas were similar to the present-day ones, so that the relation between the present-day drainage areas and the Messinian incisions reflects fluvial erosion dynamics during the MSC. A notable exception to this relation concerns the Ebro drainage area, the dimensions of which are of the same order (10^5 km²) of the Rhone ones (Fig. 1). Indeed in the Rhone valley, fluvial incision propagated more than 300 km inland and the canyon depth reached more than 1000 m in the downstream part (Gennesaux & Lefebvre 1980, Clauzon 1982). Therefore, if the Ebro basin was connected to the Mediterranean before the onset of the MSC, then a similar canyon would have incised far inland within the basin.

In fact offshore deep Messinian canyons do exist along the Spanish Mediterranean shelf, but their depth does not exceed 400 m (Farran & Maldonado 1990, Nelson & Maldonado 1990, Estcutia & Maldonado 1992, Frey-Martinez et al. 2004). To our knowledge, no Messinian canyon has been positively documented onshore. Some studies (Agustí et al. 1983, Martinell 1988, Arasa Tuliesa 1990, Maillard 1993) have reported an Early Pliocene, marine to continental lithological succession that is identical to that observed in the infilling of inland Messinian canyons elsewhere around the Mediterranean. These series are separated from the underlying basement by a Late Messinian irregular erosional surface. This suggests

that the offshore canyons could have propagated inland, but only a short distance from the present-day coastline. For example, a paleotopography is buried by Early Pliocene marine to continental sediments in the downstream Ebro valley, suggesting that incision had propagated only a few kilometers distance, from the coastline to near Tortosa (Agustí et al. 1983, Martinell 1988, Arasa Tuliesa 1990, Maestro et al. 2002).

Mass balance between eroded volume in the Ebro basin and coeval deposits in the Valencia Trough since the Pliocene.

According to Nelson (1990), most of the sediments transported by the Ebro river are deposited in the Valencia Trough and the deep-sea Valencia fan (Fig. 2). Therefore the volume of sediments in these areas must be correlated to the upstream eroded volume in the Ebro drainage basin, whatever the age of the connection (Miocene or later) to the Mediterranean Sea, via the Ebro River.

We estimate a maximum eroded volume in the Ebro basin by restoring the Miocene paleotopography (Fig. 3). This paleotopography is computed by fitting a smooth surface between all the summits of the surrounding mountains (Pyrenees, Iberian Range, Catalan Coastal Range) and the top of the Miocene sediment remnants within the Ebro basin. The present-day maximum elevation of these lacustrine deposits is 860 m (Arenas 1993), providing a minimum elevation for the Miocene basin paleotopography. On the margins of the basin, Miocene sediments reach a minimum elevation of about 1000m (e.g. Babault et al. 2005). For the Iberian Range and the Coastal Range, where current mean elevation is in the order of 1300 m respectively, the surface is directly fitted between the summits and the basins. Concerning the northern margin of the basin, i.e. along the southern flank of the Pyrenees, Oligocene sediments reach up to an elevation of 2000 m. According to Babault et al. (2005) these sediments attest for a highly-elevated piedmont with a paleoslope of order $1.25° \pm 0.25$ (Fig. 3 and Fig. 4), a value compatible with that of chains surrounded by internal basins (e.g. Smith 2000). This highly-elevated piedmont that developed from the Oligocene was responsible for the inhibition of upstream erosion resulting in a highly elevated Pyrenean peneplain. The presence of relics of this peneplain at high elevation (up to 2500 m) strongly suggests that summit erosion since the Miocene was rather weak. Fitting the surface between the surrounding ranges and the basin implies that no Miocene valley existed, an unlikely

statement, but one that provides a maximum estimate of 37800 ± 800 km^3 of eroded material (Fig. 4).

We estimate the volume of sediments that were deposited during the Pliocene-Quaternary within the Valencia trough to be 25 700 km^3, from the difference between the Messinian top-surface (Maillard 1993) and the current bathymetry (Fig. 2). On the other hand Nelson (1990) has estimated the volume of post-Messinian detrital sediments that are discharged by the Ebro river in the Valencia fan to be 6300 km^3. This provides a total amount of post-Messinian sediments of 32 000 km^3. Keeping in mind that (1) we probably overestimated the eroded volume by neglecting the likely occurrence of Miocene valleys and (2) we probably underestimate the deposited offshore volume, because the whole extent of the offshore sedimentation area is uncertain, we conclude that both estimates are similar, precluding the pre-Messinian connection of the Ebro basin to the Mediterranean.

Numerical modelling

Principles

The principle of the modelling has been described elsewhere (Davy & Crave 2000, Crave & Davy 2001, Loget et al., 2005). It assumes that erosion laws in the past were similar to that deduced from the analysis of current topography. It also considers that erosion on a regional scale is almost entirely achieved by rivers so that hillslope erosion can be minimized (Loget et al. 2005). The numerical simulator EROS incorporates a generic stream power law such as:

$$e = kQ^m S^n - e_c \,,$$

where e is the erosional flux, Q is the water flow, S is the local slope, k and e_c are two constants depending on material strength properties, and m and n two exponents related to the time-length scaling (Howard et al. 1994, Whipple & Tucker 1999). Deposition flux is proportional by $1/Lt$ to the sediment concentration in the stream, where Lt is the characteristic transport length of sediments (Beaumont et al. 1992, Crave & Davy 2001). The elevation of the channel bed corresponds to the balance between these two fluxes. Therefore when Lt is small, the model comes to the transport-limited case and the elevation of the channel bed varies proportionally to the gradient of the sediment flux. By contrast, when Lt is large, rivers

carry all the eroded sediment out of the system and the elevation is only controlled by the detachment flux (detachment-limited model).

In the present modelling, the values of the different parameters (m = 1.5, n = 1, Lt <1 km) are deduced from previous modelling of the Messinian Rhone valley (Loget et al. 2005). The parameters k and e_c are considered homogeneous and negligible, respectively, on a regional scale (Loget et al. 2005). Numerical times that correspond to the duration of the Messinian Salinity Crisis range from 20 to 40. All the rivers around the Mediterranean flowed on very different terranes during the sea-level drop, but were all incised by deep canyons. Therefore, the threshold e_c is considered as negligible at the regional scale and the bedrock erodibility k is set as unity and spatially homogeneous.

Pre-Messinian topography.

We test four scenarios with regard to the morphology of the eastern edge of the Ebro basin. Except for this eastern edge, the slope of the basin margins has been deduced from the present-day morphology by smoothing the contour lines derived from the current DEM GTOPO 30 (Fig. 5). Indeed, since the late Miocene the stress field and resulting regional deformation did not vary significantly in the area (Bergerat 1987, Herraiz et al. 2000) and therefore regional slopes were dipping as the present ones.

The first case considers that the Ebro River was already connected to the Mediterranean Sea before the onset of the MSC. The second configuration assumes that the eastern edge of the Ebro basin corresponded to a high elevated, flat topography, due to the overfilling of the internal basin up to 1000 m (Coney et al. 1996). In the third case, the Ebro basin is separated from the Mediterranean Sea by a topographic barrier that would correspond to the Catalan Coastal Ranges. The fourth experiment involves the same basin configuration as in the second experiment, but without a sea-level drop, that is, the base level is considered to be similar to the present one.

Results

In all the experiments represented on figure 5, when topographic profiles lie below initial profiles it means that streams incise, and conversely if topographic profiles lie above, streams deposit sediment.

Experiment 1 shows that a deep canyon (up to 750 m) develops after t = 40 and rapidly propagates inland (about 300 km with regard to the present coast line) in a similar way

as canyons did in many pre-Messinian valleys around the Mediterranean, in particular in the Rhone valley (Clauzon 1982, Loget et al. 2005).

In experiment 2, a stream starts to incise the eastern edge, but it propagates on a distance that is much shorter than in experiment 1 after the same time (about 150 km for t=40). The maximum incision is about 500 m. The period required for incision to propagate as far as in experiment 1 is t = 100, i.e. 2.5 times the period needed with the configuration of experiment 1, that represents the real duration of the MSC.

Experiment 3 shows that if a relief existed between the basin and the Mediterranean Sea, no stream could have cut through it and entered the basin.

As mentioned before, the configuration of experiment 4 is similar to experiment 2, but it does not involve a sea-level drop. The results of experiment 4 show that even in this case, the stream eventually enters the basin.

Discussion

No fluvial incision has been identified within the Ebro basin. All rivers that were flowing to the Mediterranean incised their basement, whatever the lithology and the Mediterranean climatic environment after the Messinian sea-level fall (Loget et al. 2005). Except for experiment 3, all the experiments show more or less deep incisions of the Ebro basin. Following experiment 1, if the Ebro basin was already connected to the Mediterranean Sea before the MSC, a deep canyon would have deeply incised onshore and entered within the Ebro basin, up to a distance near Zaragoza. Experiment 3 suggests that if any relief was overhanging the eastern edge of the Ebro basin, no stream flowing toward the Mediterranean could have entered the basin. However, the present modelling only addresses fluvial erosion and does not take into account hillslope surface processes, such as landslide, or groundwater-sapping effects as well. Therefore, we cannot exclude that this would have induced the breaking of a possible topographic barrier, but to our knowledge, there is to date no evidence of such processes in the sediment record. There is also no evidence for tectonic processes such as NW-SE directed normal faulting that could explain the breaking of a topographic barrier at the onset of the MSC.

On the other hand the experiments 2 and 4 show that regressive erosion could result in Ebro basin capture if this latter was overfilled "to the brim", that is, the western flank of the Catalan Coastal Ranges were buried under sediments. These experiments suggest that the sea-

level during the MSC was not a *sine qua non* condition to induce the capture of the Ebro basin although this could have favoured it (see also Garcia-Castellanos et al. 2003).

The only explanation to the lack of Messinian fluvial incision in the Ebro basin is to consider that it was not connected to the Mediterranean. The current Ebro drainage area is comparable to that of the current Rhone. There is no reason for post-Messinian erosion to have completely erased any remnant of such incision in the Ebro basin. Strong erosion would require tectonic uplift and/or climate change. This would result also in the re-incision of the Pliocene rias. It would be very unlikely that Pliocene terraces did not develop as Quaternary terraces did in uplifting active mountain belts such the Himalayas or the Alps. Moreover, large remnants of the Var Pliocene ria are found at an elevation up to 1000 m in the southern French Alps (Clauzon 1978).

Yet, our results are contrary to recent interpretations suggesting that the Ebro basin was already connected via the Ebro river to the Mediterranean Sea before the Messinian. Such interpretations rely on (1) mass balance between eroded materials coming from the Ebro basin and the surrounding ranges, and coeval sediments within the Valencia trough and (2) the presence of pre-Messinian, prograding detrital sediments in the Ebro delta and the significance of the Castellon group.

(1) Mass balance

Using a similar type of calculation to us, Garcia-Castellanos et al. (2003) reach a different conclusion, considering, as we do, that the Ebro basin incision was triggered by its opening toward the Mediterranean. They conclude that the post-Messinian delta estimated by Nelson (1990) (27000 km^3) does not account for this post-opening complete incision.

Firstly, our estimate of sediment budget in the Ebro delta, from recent offshore seismic data on the top-Messinian surface (Maillard 1993), is larger than that provided by Nelson's work who used borehole interpolation, leading to a total budget of 32 000 km^3 of sediments for the Ebro delta and Valencia trough.

Secondly, our estimate of the eroded volume in the Axial zone since the Late Miocene is only 4000 km^3, compared with the 10000 km^3 suggested by Garcia-Castellanos et al. (2003). Their calculation is based on local denudation rate estimates that are deduced from a thermochronology study, implying up to 2-3 km of denudation within this area since the Miocene (Fitzgerald et al. 1999). It is beyond the scope of the present paper to discuss in detail such an estimate, but we would like to stress that it has long been recognized that a major morphological characteristic of the Pyrenean Axial Zone, is the occurrence of a high elevated (more than 2000 m), low relief, Miocene erosional surface, now dissected by the

recent drainage network (Birot 1937, de Sitter 1952). This suggests that erosion since the Miocene within the Axial Zone mainly corresponds to the present dissection of this erosional palaeosurface (see figure 4) and that local denudation rates deduced from thermochronology are far overestimated when applied at regional scale in the present case.

Although we agree with Garcia-Castellanos (2003) that such type of calculations remains rough, our estimate of volume balance challenges theirs and shows that the assumption of a post-Messinian dissection of the Ebro basin and the surrounding reliefs is likely.

(2) Significance of the Castellon group

Evans and Arche (2002) have suggested that the presence of a pre-Messinian succession of prograding detrital deposits, the Castellon group, in the Valencia Trough, as observed by Bartrina et al. (1992), was presumably indicative of the connection of the Ebro basin to the Mediterranean. These authors consider that a river with a catchment limited to the Catalan Coastal Ranges can hardly provide such an amount of sediment, but they did not provide any quantification. They acknowledge that conclusive confirmation of an origin from the Ebro basin requires additional studies. For Bartrina et al. (1992) the Castellon group may result from the reworking of pre-Serravallian terrigeneous deposits initially trapped in the onshore active half-grabens, when the older paleohighs where overlain under high sea-level conditions. Post-Langhian prograding terrigeneous systems, with basal unconformity, also developed just before the MSC in the Gulf of Lion (Gorini et al., Gorini 1993), whereas no major change in the drainage basin pattern is observed (Loget et al. 2005). Therefore the Castellon group in the Valancia trough does not appear as a specific sedimentary event that would be related to the opening of the Ebro basin.

Conclusion

The sea-level fall of the Mediterranean during the Messinian was responsible for the strong fluvial incision of the pre-Messinian drainage networks. Incision propagation was directly controlled by the pre-existing drainage areas. These incisions were later sealed by Early Pliocene sedimentation all around the Mediterranean region. If the Ebro basin, as observed today, was connected to the Mediterranean, similar strong incision would have developed and would have been preserved as in the case of the present Rhone drainage area.

Therefore, the lack of Messinian incision within the Ebro basin shows that it was not connected to the Mediterranean before the Messinian Salinity Crisis.

References

Agustí, J., Anadón, P. & Julia, R. 1983. Nuevos datos sobre el Plioceno del Baix Ebre. Aportación a la correlación entre las escalas marina y continental. *Acta Geologica Hispanica*, **18**, 123-130.

Ambert, P., Aguilar, J.-P. & Michaux, J. 1998. Evolution géodynamique messinio-pliocène en Languedoc central : le paléo-réseau hydrographique de l'Orb et de l'Hérault (sud de la France). *Geodinamica Acta*, **11**, 139-146.

Arasa Tuliesa, A. 1990. El terciario del Baix Ebre: Aportaciones estratigráficas y sedimentológicas. *Acta Geologica Hispanica*, **25**, 271-287.

Arenas, C. 1993. *Sedimentología y paleogeografía del Terciario del margen pirenaico y sector central de la cuenca del Ebro (zona aragonesa occidental)*.PhD, Universidad de Zaragoza, Zaragoza, Spain.

Babault, J., Van Den Driessche, J., Bonnet, S., Castelltort, S. & Crave, A. 2005. Origin of the highly elevated Pyrenean peneplain. *Tectonics*, **24**, TC2010, doi:10.1029/2004TC001697.

Bartrina, M. T., Cabrera, L., Jurado, M. J., Guimerà, J. & Roca, E. 1992. Evolution of the central Catalan margin of the Valencia Trough (Western Mediterranean). *Tectonophysics*, **203**, 219-247.

Beaumont, C., Fullsack, P. & Hamilton, J. 1992. Erosional control of active compressional orogens. *In:* McClay, K. R. (eds) *Thrust Tectonics*, 1-18.

Bergerat, F. 1987. Stress fields in the european platform at the time of Africa-Eurasia collision. *Tectonics*, **6**, 99-132.

Birot, P. 1937. *Recherches sur la morphologie des Pyrénées orientales franco-espagnoles*.Doctorat Ès Lettres, Paris

Bishop, P., Hoey, T. B., Jansen, J. D. & Lexartza Artza, I. 2005. Knickpoint recession rate and catchment area: the case of uplifted rivers in Eastern Scotland. *Earth Surface Processes and Landforms*, **30**, 767-778.

Chumakov, I. S. 1973. Pliocene and Pleistocene deposits of the Nile valley in Nubia and upper Egypt. *In:* Kaneps, A. G. (eds) *Initial reports of the Deep Sea Drilling Project*, **13**. U. S. Government Printing Office, Washington, D. C., 1242-1243.

Clauzon, G. 1978. The Messinian Var canyon (Provence, Southern France). Paleogeographic implications. *Mar. Geol.*, **27**, 231-246.

Clauzon, G. 1982. Le canyon messinien du Rhône : une preuve désicive du "dessicated deep basin model" (Hsü, Cita et Ryan, 1973). *Bull. Soc. Geol. France*, **24**, 231-246.

Clauzon, G., Aguilar, J. P. & Michaux, J. 1987. Le bassin pliocene du Roussillon (Pyrenees-Orientales, France): exemple d' evolution geodynamique d' une ria mediterraneenne consecutive a la crise de salinite messinienne. *C. R. Acad. Sc. Paris*, **304**, 585-590.

Coney, P. J., Muñoz, J. A., McClay, K. R. & Evenchick, C. A. 1996. Syntectonic burial and post-tectonic exhumation of the southern Pyrenees foreland fold-thrust belt. *Journal of the Geological Society London*, **153**, 9-16.

Crave, A. & Davy, P. 2001. A stochastic "precipiton" model for simulating erosion/sedimentation dynamics. *Computers & Geosciences*, **27**, 815-827.

Davy, P. & Crave, A. 2000. Upscaling Local-Scale Transport Processes in Large-Scale Relief Dynamics. *Phys. Chem. Earth (A)*, **25**, 533-541.

de Sitter, L. U. 1952. Pliocene uplift of Tertiary mountain chains. *American Journal of Science*, **250**, 297-307.

Denizot, G. 1952. Le Pliocène dans la vallée du Rhône. *Rev. geogr. Lyon*, **27**, 327-357.

Estcutia, C. & Maldonado, A. 1992. Paleogeographic implications of the Messinian surface in the Valencia trough, northwerstern Mediterranean Sea. *Tectonphysics*, **203**, 263-284.

Evans, G. & Arche, A. 2002. The flux of siliciclastic sediment from the Iberian Peninsula, with particular reference to the Ebro. *In:* Jones, S. J. & Frostick, L. E. (eds) *Sediment Flux to Basins: Causes, Controls and Consequences*, **191**. Geological Society, London, Special Publications, 199-208.

Farran, M. & Maldonado, A. 1990. The Ebro continental margin shelf: Quaternary seismic stratigraphy and growth patterns. *Marine Geology*, **95**, 289-312.

Field, M. E. & Gardner, J. V. 1990. Pliocene-Pleistocene growth of the Rio Ebro margin, northeast Spain: A prograding-slope model. *Geological Society of America Bulletin*, **102**, 721-733.

Fitzgerald, P. G., Muñoz, J. A., Coney, P. J. & Baldwin, S. L. 1999. Asymmetric exhumation across the Pyrenean orogen: implications for the tectonic evolution of a collisional orogen. *Earth and Planetary Science Letters*, **173**, 157-70.

Frey-Martinez, J. M., Cartwright, J. A., Burgess, P. M. & Vicente Bravo, J. 2004. 3D seismic interpretation of the Messinian Unconformity in the Valencia Basin, Spain. *In:* Davies, R. J., Cartwright, J., Stewart, S. A., Lappin, M. & Underhill, J. R. (eds) *3D Seismic Technology: Application to the Exploration of Sedimentary Basins*. *Geological Society Memoir*, **29**. Geological Society, London, 91-100.

Garcia-Castellanos, D., Vergés, J., Gaspar-Escribano, J. & Cloetingh, S. 2003. Interplay between tectonics, climate and fluvial transport during the Cenozoic evolution of the Ebro Basin (NE Iberia). *Journal of Geophysical Research*, **108**, 2347-2364.

Gennesseaux, M. & Lefebvre, D. 1980. Le Golfe du Lion et le Paléo-Rhône messinien. *Géologie Méditerranéenne*, **VII**, 71-80.

Gorini, C. 1993. *Géodynamique d'une marge passive: Le Golfe du Lion (Méditerranée occicentale)*.Phd. Thesis, Université Paul Sabatier, Toulouse III, Toulouse.

Gorini, C., Lofi, J., Duvail, C., Dos Reis, A. T., Guennoc, P., Lestrat, P. & Mauffret, A. 2005. The Late Messinian salinity crisis and Late Miocene tectonism: Interaction and consequences on the physiography and post-rift evolution of the Gulf of Lions margin. *Marine and Petroleum Geology*, **22**, 695-712.

Hack, J. T. 1957. Studies of longitudinal stream profiles in Virginia and Maryland. *U. S. Geol. Surv. Prof. Pap.*, **294**, 45-94.

Herraiz, M., De Vicente, G., Lindo-Naupari, R., Giner, J., Simón, J. L., González-Casado, J. M., Vadillo, O., Rodríguez-Pascua, M. A., Cicuéndez, J. I., Casas, A., Cabañas, L., Rincón, P., Cortés, A. L., Ramírez, M. & Lucini, M. 2000. The recent (upper Miocene to Quaternary) and present tectonic stress distributions in the Iberian Peninsula. *Tectonics*, **19**, 762-786.

Howard, A. D., Dietrich, W. E. & Seidl, M. A. 1994. Modeling fluvial erosion on regional to continental scales. *J. Geophys. Res.*, **99**, 13,971-13,986.

Hsü, K. J., Cita, M. B. & Ryan, W. B. F. 1973. The origin of the Mediterranean evaporites. *In:* Kaneps, A. G. (eds) *Initial reports of the deep sea drilling project*, **13**. U. S. Government Printing Office, Washington, D. C., 1203-1231.

Krijgsman, W., Hiigeni, F. J., Raffi, I., Sierro, F. J. & Wilson, D. S. 1999. Chronology, causes and progression of the Messinian salinity crisis. *Nature-London*, **400**, 652-655.

Loget, N., Van Den Driessche, J. & Davy, P. 2005. How did the Messinian Salinity Crisis end? *Terra Nova*, **17**, 414-419.

Maestro, A., Barnolas, A., Somoza, L., Lowrie, A. & Lawton, T. 2002. Geometry and structure associated to gas-charged sediments and recent growth faults in the Ebro Delta (Spain). *Marine Geology*, **186**, 351-368.

Maillard, A. 1993. *Structure et riftogénèse du Golfe de Valence (Méditerranée Nord-Occidentale)*.Thèse de Doctorat, Université Pierre et Marie Curie, Paris 6, Paris.

Martinell, J. 1988. An overview of the marine Pliocene of N.E. Spain. *Géologie Méditerranéenne*, **XV**, 227-233.

Montgomery, D. R. & Dietrich, W. E. 1992. Channel initiation and the problem of landscape scale. *Science*, **255**, 826-830.

Nelson, C. H. 1990. Estimated post-Messinian supply and sedimentation rates on the Ebro continental margin, Spain. *Marine Geology*, **95**, 395-418.

Nelson, C. H. & Maldonado, A. 1990. Factors controlling late Cenozoic continental margin growth from the Ebro Delta to the western Mediterranean deep sea. *Marine Geology*, **95**, 419-440.

Reille, J. L. 1971. *Les relations entre tectorogénèse et sédimentation sur le versant sud des Pyrénées centrales d'après l'étude des formations terciaires essentiellement continentales*.Doct. Etat Sci., USTL, Montpellier.

Riba, O., Reguant, S. & Villena, J. 1983. Ensayo de síntesis estratigráfica y evolutiva de la cuenca terciaria del Ebro. *In:* Comba, J. (eds) *Libro Jubilar J. M. Ríos, Geología de España*, **2**. Instituto Geológico y Minero de España, Madrid (Spain), 131-159.

Roca, E. 2001. The Northwest Mediterranean Basin (Valencia Trough, Gulf of Lions and Liguro-Provençal basins); structure and geodynamics evolution. *In:* Ziegler, P. A., Cavazza, W., Robertson, A. H. F. & Crasquin, S. S. (eds) *Peri-Tethys memoir 6; Peri-Tethyan rift/wrench basins and passive basins*. *Mémoires du Muséum National d'Histoire Naturelle*, **186**, 671-706.

Rosenbloom, N. A. & Anderson, R. S. 1994. Hillslope and channel evolution in amarine terraced landscape, Santa Cruz, California. *J. Geophys. Res.*, **99**, 14,013-14,029.

Ryan, W. B. F. 1976. Quantitative evaluation of the depth of the western Mediterranean before, during and after the late Miocene salinity crisis. *Sedimentology*, **23**, 791-813.

Schumm, S. A., Mosley, M. P. & Weaver, W. E. 1987. *Experimental fluvial geomorphology*. John Wiley and Sons, New York.

Serrat, D. 1992. La xarxa fluvial dels Països Catalans. In: *História Natural dels Països Catalans* (edited by Catalana, E.) **Geologia II**, Barcelona, 375– 389.

Smith, G. A. 2000. Recognition and significance of streamflow-dominated piedmont facies in extensional basins. *Basin Research*, **12**, 399-411, doi:10.1046/j.1365-2117.2000.00125.x.

Whipple, K. X. & Tucker, G. E. 1999. Dynamics of the stream-power river incision model: Implications for height limits of mountain ranges, landscape response timescales, and research needs. *J. Geophys. Res.*, **104**, 17,661-17,674.

Figures

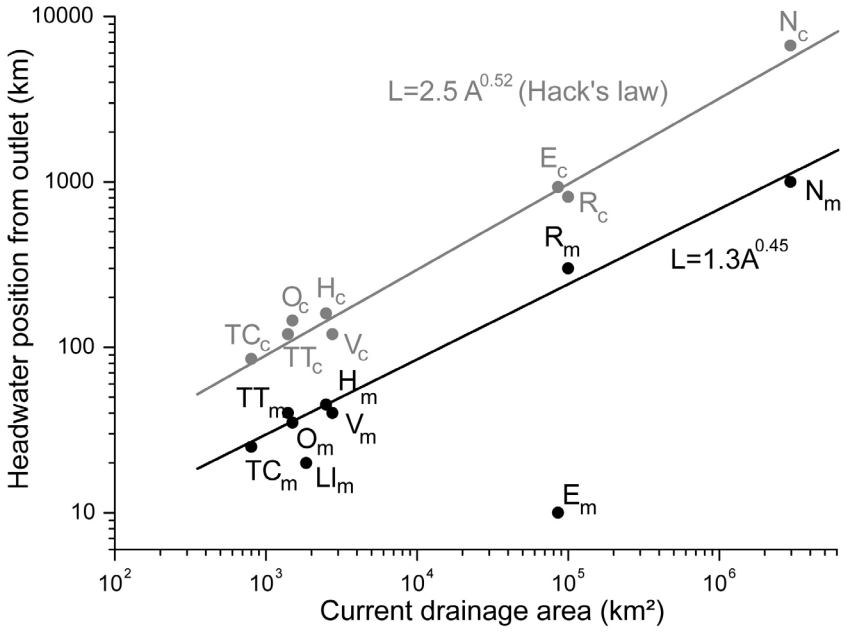

Figure 1: Distance of headwater position from the present outlet (river length) vs. current drainage area for some Mediterranean rivers.

Grey circles: present headwater position; black circles: Messinian headwater incision. N-Nil; R-Rhone; E-Ebro; H-Herault; O-Orb; TT-Têt; TC-Tech; m and c: index for Messinian and current respectively (Database compiled after (Chumakov 1973, Clauzon 1978, 1982, Clauzon et al. 1987, Ambert et al. 1998).

The length of current rivers is a function of drainage area, such as $L=2.5A^{0.5}$, which corresponds to Hack's law (Hack 1957, Montgomery & Dietrich 1992). When plotted against current drainage areas, lengths of Messinian canyons follow a similar law such as $L=1.3A^{0.45}$, except for the Ebro. This strongly suggests that (1) the pre-Messinian drainage areas were similar to the present ones, (2) the duration of the Messinian sea-level drop was not long enough for fluvial incision to propagate up to pre-Messinian headwaters, and (3) the pre-Messinian drainage area of the "proto-Ebro" river was much less extensive than the present one or (4) the Ebro basin was not yet connected to the Mediterranean. (see text for further discussion).

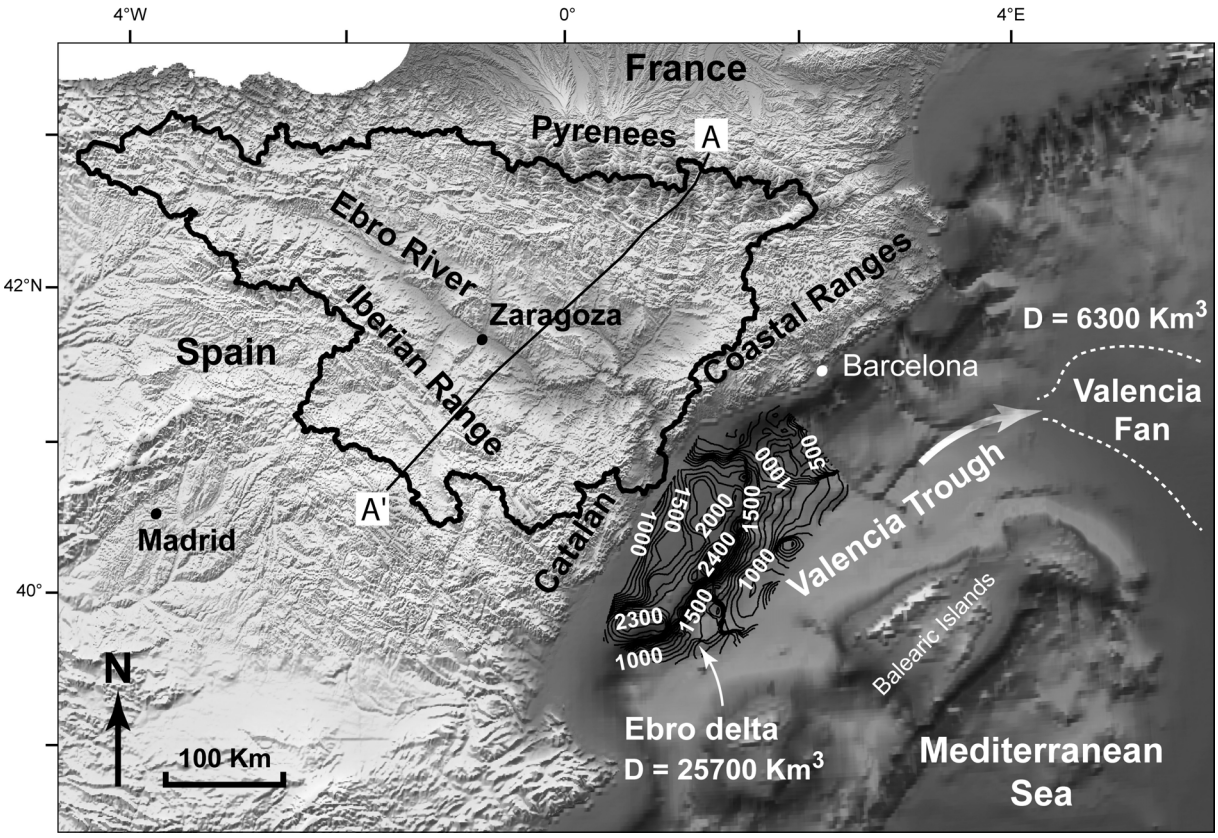

Figure 2: Estimate of the deposited volume in the Valencia Trough since the Pliocene. Topography of NE Spain (SRTM90). Black line onshore: location of the topographic profile (Figure 4). Black lines offshore: isobaths of Pliocene and Quaternary deposits. The Catchment of the Ebro river is also shown. The volume of post-Messinian detrital sediments within the Valencia trough has been determined to be 25700 km^3 from the difference between the Messinian top-surface and the current bathymetry (Accurate reconstruction of the top-Messinian surface is from Maillard (1993)). Nelson (1990) estimated the volume of post-Messinian detrital sediments that are discharged by the Ebro river in the Valencia fan as 6300 km^3. This provides a total amount of post-Messinian sediment of 32 000 km^3.

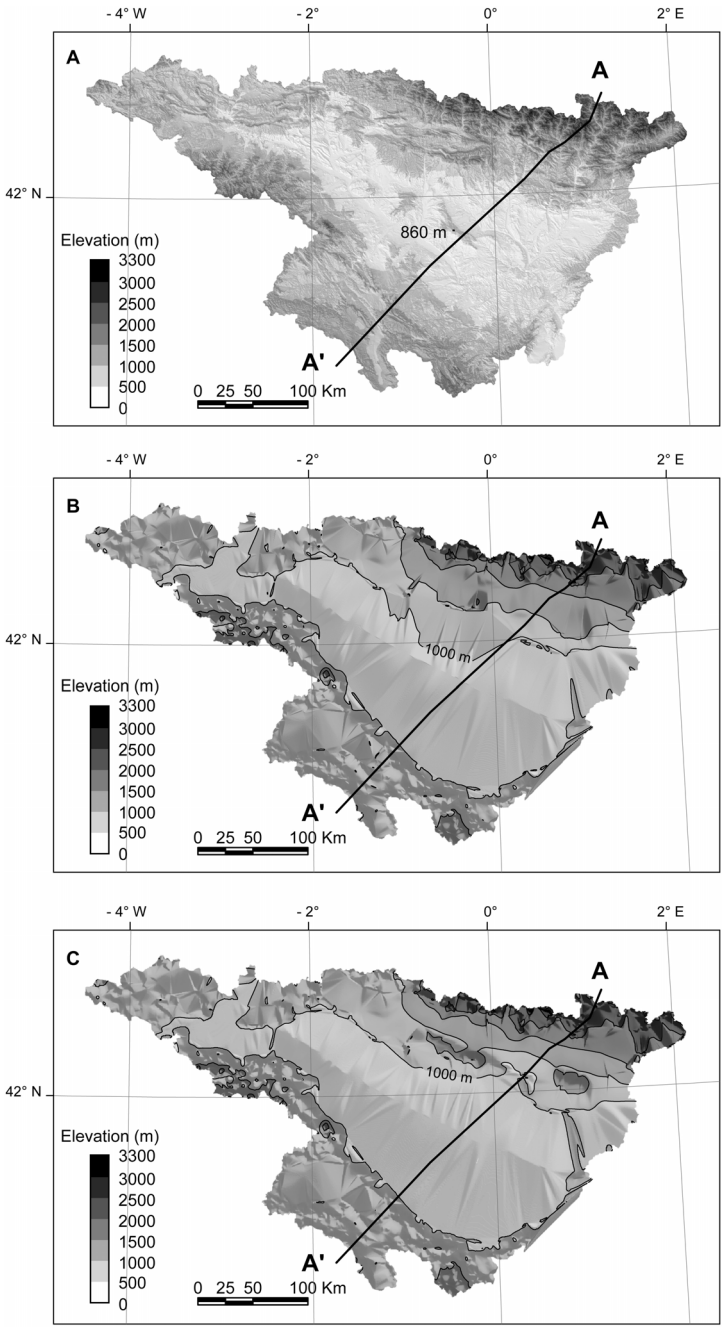

Figure 3: Miocene paleotopography.

A: Current topography of the Ebro drainage basin. B and C: The two palaeotopographies are computed by drawing a surface between the Pyrenean, Iberian and Catalan summits to the centre of the Ebro basin that corresponds to a trough, the maximum elevation of which is 860 m (Arenas 1993). Elevation of the basin edges reaches 1000 m. From the southern limit of the Axial Zone to the limit of the South-Pyrenean zone, the palaeosurface elevation decreases from 2000 m to 1000 m. The palaeotopographies B and C are calculated with maximum slope values of the Pyrenean piedmont of 1.5° and 1°, respectively (Contour lines equidistance is 500 m).

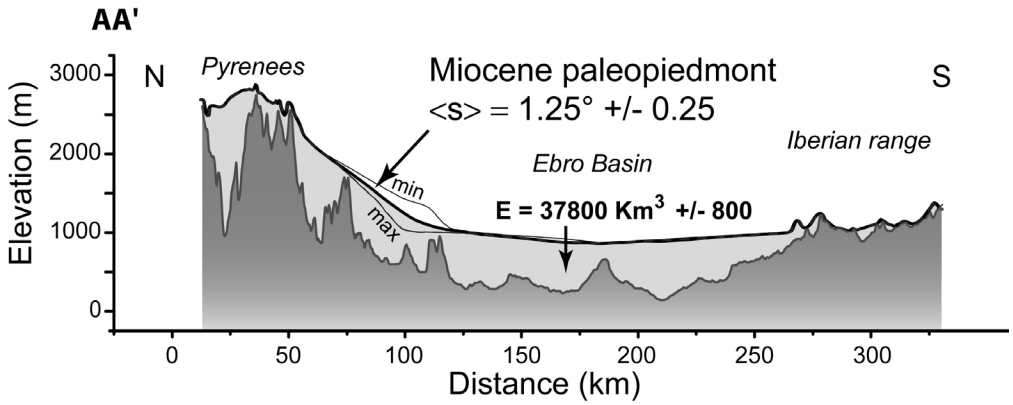

Figure 4: Estimate of the eroded volume in the Ebro catchment since the Miocene.
Dark grey: NS topographic profile across the Ebro drainage basin. Light grey: Eroded material (*E*). Mean slope value of the Miocene Pyrenean paleopiedmont <s> is 1.25° ± 0.25. The two eroded volumes are computed from the difference between two surfaces: the paleotopographies (B and C) and the current topography. The minimum (37000 km^3) and maximum (38600 km^3) estimates of eroded volume are obtained for slope values of 1.5° and 1° respectively. The eroded volume (37 800 ± 800 km^3) is comparable to that of post-Messinian deposits in the Valencia trough and Valencia fan.

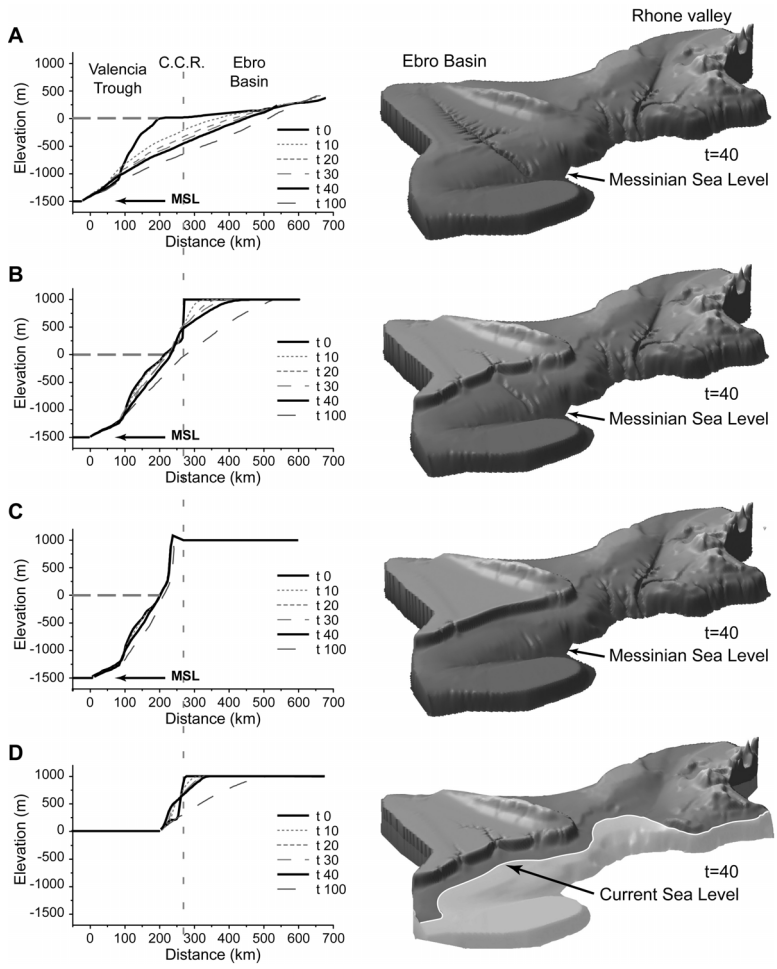

Figure 5: Numerical modelling of the western Mediterranean drainage system after a 1500 m sea-level drop (vertical dilatation x 32).

CCR-Catalan Coast Ranges; MSL-Messinian Sea-Level; t=40: numerical time that corresponds to the duration of the MSC (Loget et al.).

Three configurations (A, B, C) of the eastern edge of the Ebro basin at the onset of the MSC have been tested:

A. The Ebro river was already connected to the Mediterranean Sea (experiment 1);

B. The eastern edge of the Ebro basin corresponded to a high elevated, flat topography, resulting from the overfilling of the endorheic basin up to 1000 m a.s.l. (experiment 2);

C. The Ebro basin is separated from the Mediterranean Sea by a topographic barrier that would correspond to the CCR (experiment 3);

D. In this experiment the configuration is similar to that in B, but no sea-level drop occurred, that is, the base level is considered to be similar to the present one. This experiment has been designed to test the real influence of the MSC sea-level drop on the incision propagation (experiment 4).

3.3. Annexes à la partie 3

3.3.1. La topographie du détroit de Gibraltar.

3.3.2. L'origine des détroits est-elle commune ? Analogie du détroit de Gibraltar avec celui du Bosphore.

3.3.1. La topographie du détroit de Gibraltar

L'origine du détroit de Gibraltar est une question qui n'a pas fait débat au sein de la communauté des géologues. Au début du siècle, les interrogations scientifiques portaient sur la continuité des terrains et des structures de part et d'autre du détroit de Gibraltar afin de comprendre si la chaîne bétique et la chaîne rifaine formaient une même entité (e.g. Suess, 1921). Puis, les travaux consécutifs à la découverte de la tectonique des plaques avaient positionné le détroit de Gibraltar comme étant une limite de plaques entre la plaque Afrique et la plaque Europe (McKenzie, 1970). Or, aujourd'hui nous savons que cette limite est diffuse et s'étend sur une grande partie de l'arc de Gibraltar.

Comment alors expliquer cette structure topographique ? Des travaux réalisés à la fin des années 1950 ont permis de cartographier avec précision la morphologie sous-marine du détroit de Gibraltar (Gierman, 1961) (Figure a1 et a2). L'interprétation proposée est qu'un bloc se soit effondré en une ou deux grandes failles dans le détroit de Gibraltar sans effet sur l'arrière pays, ni du côté espagnol, ni du côté marocain (Figure a3). Néanmoins, sans remettre en cause la qualité des données issues de ces travaux et tout en sachant qu'ils pré-datent la découverte de la Crise de Salinité Messinienne, il semble aujourd'hui que la seule hypothèse d'un fossé d'effondrement reposant sur l'unique interprétation de données morpho-bathymétriques soit caduque. De plus, le schéma structural proposé par Gierman (1961), qui sera repris par la suite par Olivet et al., 1973 ou Platt et al., 1989 dans un cadre plus général, est peu compatible avec les contraintes tectoniques déduites sur le pourtour de l'arc de Gibraltar depuis la fin du Miocène. Cet exemple ne constitue pas un cas isolé dans l'amalgame qui est souvent fait entre structure topographique et structure tectonique pliocène comme cela a par exemple été le cas sur l'interprétation du bassin du Roussillon (Birot, 1937 ; Calvet, 1985 ; Clauzon, 1987).

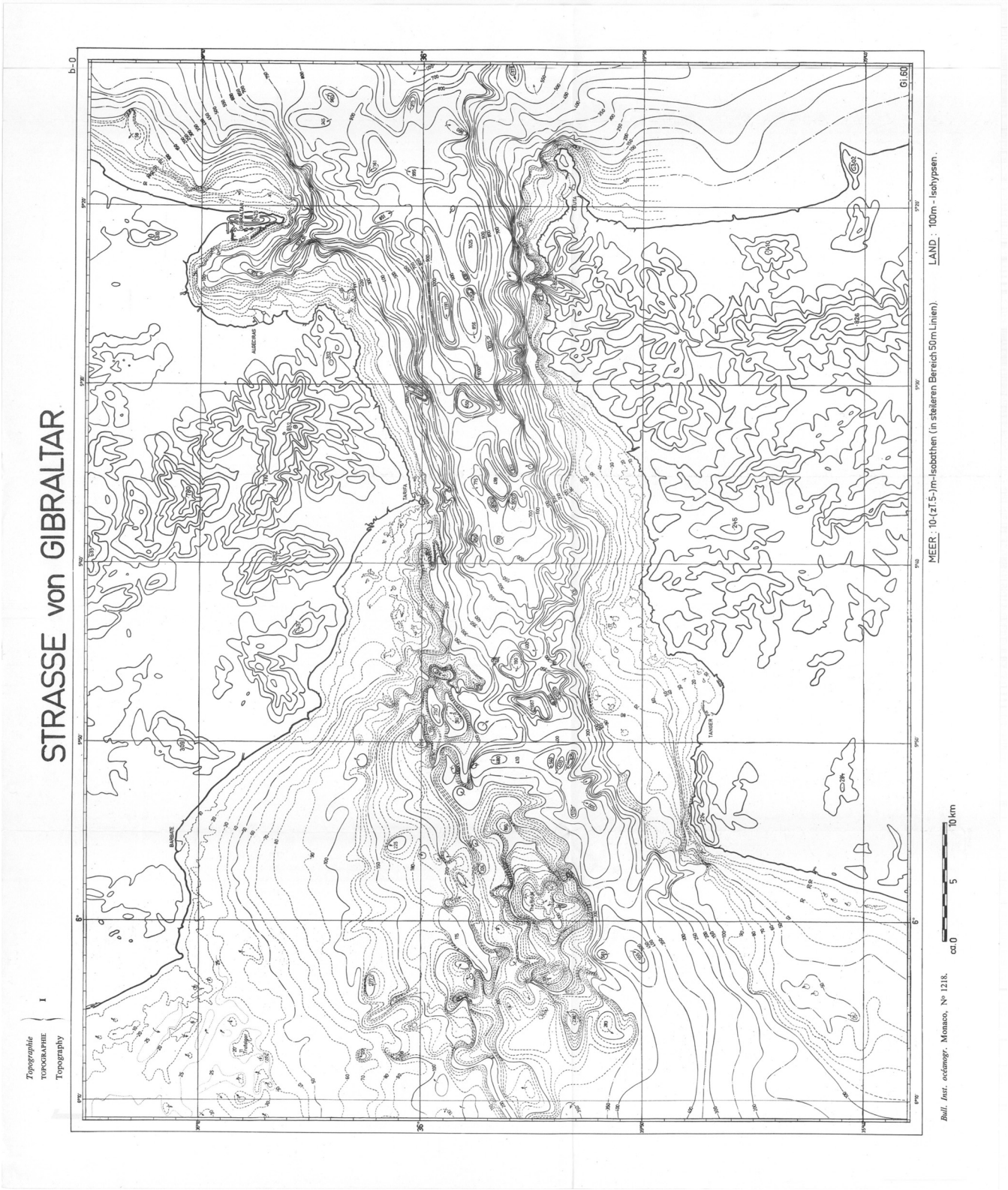

Figure a1 *: Carte bathymétrique du détroit de Gibraltar (d'après Giermann, 1961).*

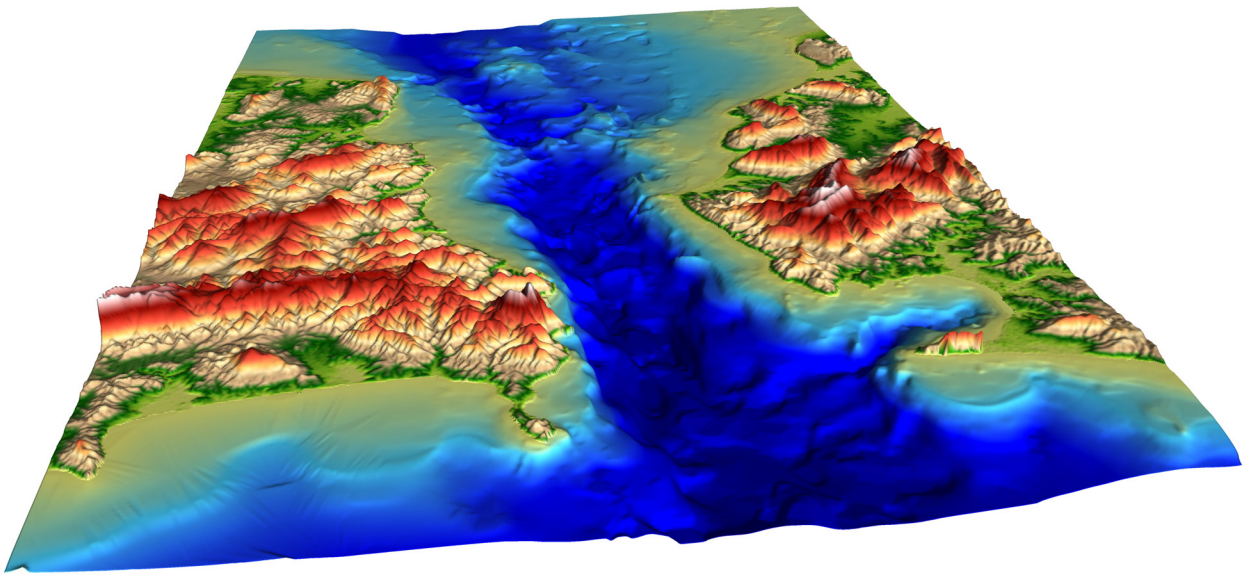

Figure a2 *: Modèle Numérique de Terrain du détroit de Gibraltar et des côtes avoisinantes (Maroc à gauche et Espagne à droite). Source: SRTM90, Giermann, 1961.*

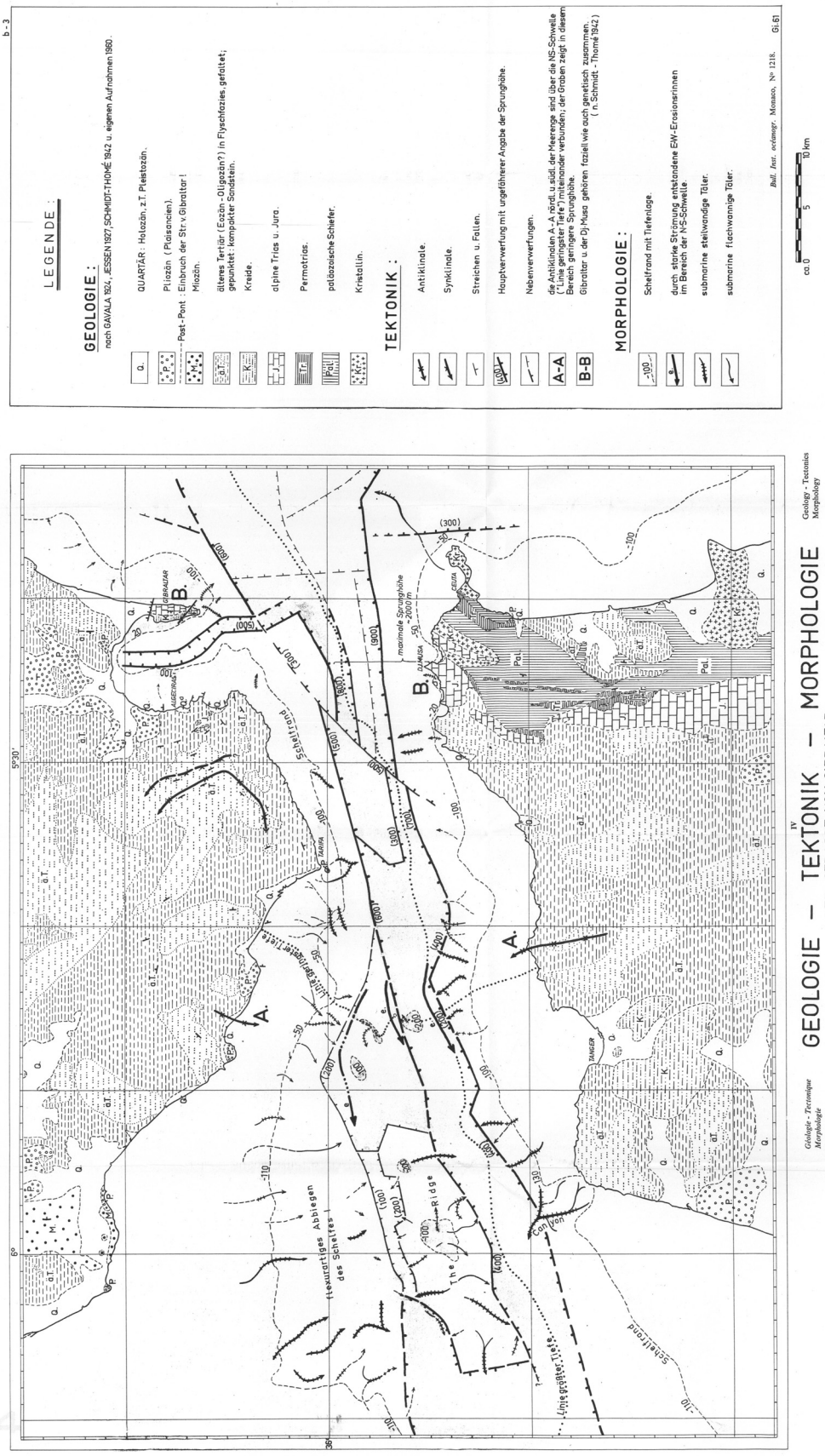

Figure a3 *: Carte structurale du détroit de Gibraltar (d'après Giermann, 1961).*

3.3.2. L'origine des détroits est-elle commune ? Analogie du détroit de Gibraltar avec celui du Bosphore.

L'origine du détroit du Bosphore a suscité les mêmes interrogations que celui de Gibraltar. Séparant la mer noire et la mer de Marmara, au Nord et au sud respectivement, le détroit du Bosphore est situé au nord de la faille Nord-Anatolienne (Figure a4), laquelle représente une faille décrochante et forme le bassin en pull-apart de Marmara (Armijo et al., 1999 ; Parke et al., 1999). La figure a5 montre une photo satellite du détroit du Bosphore où la forme du détroit rappelle étrangement celle d'une rivière. Cette observation a conduit de nombreux auteurs à imputer l'origine du détroit du Bosphore à une paléo-rivière qui a connecté à terme la Mer Noire et la mer de Marmara (e.g. Hsü, 1978 ; Gokasan et al., 1997). Une analyse détaillée du détroit du Bosphore, grâce à un maillage sismique dense, a permis d'identifier la présence de nombreuses failles dans la partie sud (Figure a6). Cette partie du détroit est imputable à la formation de grabens ou de pull-apart en relation avec la tectonique sévissant actuellement en mer de Marmara (Gokasan et al., 1997: Oktay et al., 2002). En revanche, la partie nord ne présente pas de faille majeure, mais des traces d'incisions fluviatiles. Selon Gokasan (1997), la ligne de partage des eaux séparant la mer Noire de la mer de Marmara s'est effondrée sous l'impulsion de failles reconnectant ainsi les deux mers. Cependant, les données sismiques de ce dernier montrent que les failles précédemment citées ne décalent que très légèrement les horizons sismiques. Par contre, il indique qu'une vallée fluviatile incise profondément le substratum en abandonnant des niveaux de terrasses. Cette incision aurait pu être induite par la chute du niveau de la mer en Mer Noire (~100m) durant les derniers 100 000 ans (e.g. Ryan et al., 1997; Aksu et al., 1999). Cette incision, en évoluant par érosion régressive, aurait pu entraîner à terme l'ouverture du détroit et la capture des eaux de la mer de Marmara. Ce scénario s'est peut-être déroulé plusieurs fois pendant les derniers 100 000 ans s'il on en juge par les nombreuses variations du niveau marin en Mer Noire. La dernière connexion en date remonte a 7500 ans (Ryan et al., 1997), ce qui a contribué au mythe du déluge en Mer Noire (Ryan and Pitman, 1999).

Bien que ces conclusions soient très hypothétiques, cette analogie montre que le débat sur l'origine du détroit du Bosphore est loin d'être achevé. Situé au cœur d'une zone tectoniquement active, les données géologiques ne permettent pas cependant de déterminer la part respective de l'érosion régressive et de la tectonique dans l'ouverture du détroit du Bosphore, ceci pour une chute du niveau de base de l'ordre de 100 m.

Cela laisse présager de la puissance de l'érosion régressive pour une valeur de 1500 m qui a sévi dans la région de Gibraltar durant la Crise de Salinité Messinienne.

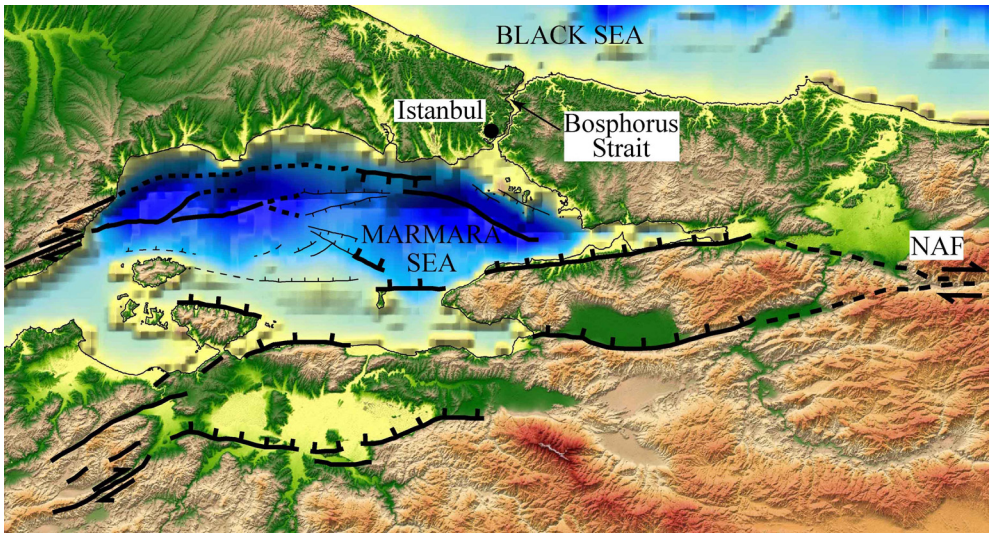

Figure a4 : *Contexte morpho-structural du détroit du Bosphore. NAF : Faille Nord Anatolienne*

Figure a5 : *Photographie satellite du détroit du Bosphore (source NASA). Notez la forte similitude de la morphologie du détroit avec celle d'une rivière.*

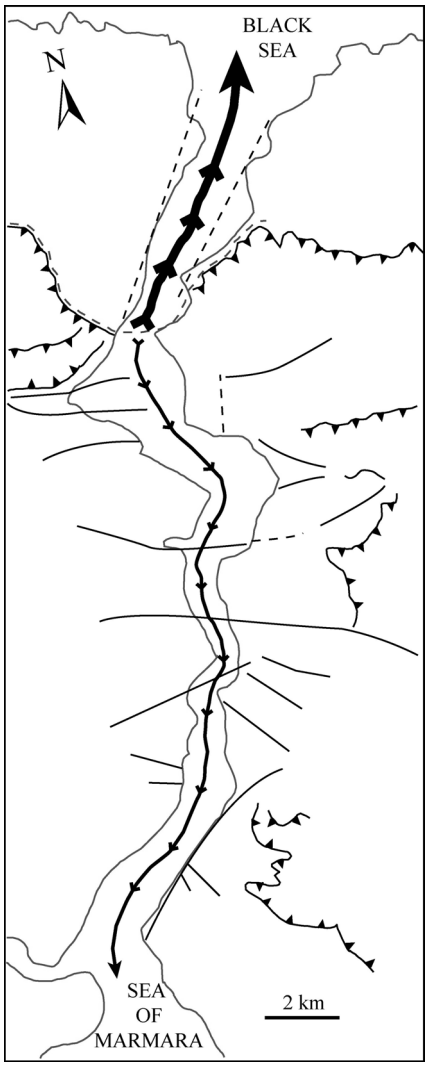

Figure a6 : *Schéma structural du détroit du Bosphore (d'après Gokasan et al., 1997). Notez la présence de deux paléo-rivières de part et d'autres de la paléo ligne de partage des eaux (en tireté gris). La puissance érosive des rivières est indiquée par l'épaisseur du trait. L'auteur interprète la connexion de la mer Noire et de la mer de Marmara par l'affaissement du bloc situé dans la partie Nord.*

4. CONCLUSION

Dans ce travail, nous avons tenté d'analyser les paramètres qui contrôlent la croissance, l'équilibre et la pérennité d'un réseau hydrographique à l'échelle des temps géologiques à travers l'exemple de la chute du niveau de base de la Méditerranée pendant la Crise de Salinité Messinienne (5,96-5,32 Ma).

Le premier constat est que la croissance d'une incision fluviatile peut s'avérer extrêmement rapide. Les exemples comme le Nil ou le Rhône messiniens, mais aussi celui entre autre du Mississippi au Quaternaire, montre *qu'une chute du niveau de base, quelle que soit son amplitude, peut entraîner la migration d'une incision sur plusieurs centaines de kilomètres en un ou quelques centaines de milliers d'années*. De telles vitesses de réaction n'avaient jusque là jamais été suspectées car les knickpoints ont tendance à se diluer dans le système amont. Cependant, une telle dynamique se développe lorsqu'un bassin versant amont préexiste, autrement dit lorsque les pentes régionales sont préalablement établies.

En s'appuyant sur un modèle numérique simulant les processus d'érosion et de dépôt ainsi que sur une analyse morphologique des incisions messiniennes à l'échelle de la Méditerranée, nous montrons que *le paramètre dominant dans le développement d'une incision est l'aire drainée amont pour des bassins versants dont les dimensions varient de 10^3 à 10^6 km²*. La pente n'apparaît pas comme un facteur discriminant, probablement du fait d'une certaine homogénéité dans les parties avales. La compilation de données pris dans la littérature semble confirmer le rôle prédominant de l'aire drainée amont sur la propagation d'une incision *quelle que soit la dimension du bassin versant préexistant*.
En outre, l'exemple messinien montre qu'à *une certaine échelle de temps (10^5 ans) et d'espace (>10^3 km²), les effets liés aux variations lithologiques, à la végétation ou à des seuils d'érosion peuvent être négligés ou considérés comme uniformes*.

Le temps nécessaire à un réseau ou à un système géomorphologique pour atteindre un état d'équilibre est très long (> 10^6 My). Dans le cas du Messinien, si les réseaux fluviatiles se

mettent très rapidement en place, ils sont cependant très loin d'avoir atteint leur état d'équilibre à la fin de la crise. Quelles ques soient les dimensions des bassins versants préexistants, les incisions messiniennes présentent des caractéristiques similaires : elles correspondent à des canyons profonds dont les versants abrupts montrent qu'ils n'ont pas eu le temps de s'adapter au creusement des rivières. Cette caractéristique morphologique est corroborée par l'étude des profils longitudinaux tels que le Rhône ou le Nil qui présentent une forte convexité, que nous attribuons à partir de la modélisation numérique à une faible distance de transport des éléments dans la rivière. *Le cas du Messinien (10^5ans) peut alors être considéré comme un stade précoce ou encore incrémental d'une longue mise à l'équilibre d'un réseau fluviatile*, équilibre qui n'aurait vraisemblablement pas été atteint avant plusieurs millions d'années voire dizaine de millions d'années au regard des temps d'équilibre proposées dans la littérature ou de l'évolution des escarpements présents sur certaines marges continentales.

Concernant la pérennité d'un réseau hydrographique, l'exemple du Messinien montre que là où se sont établies de fortes pentes régionales (et locale) le réseau de drainage reste globalement stable. Malgré son ampleur, la chute du niveau de base de la Méditerranée n'a pas entraîné de bouleversement de la morphologie des bassins versants méditerranéens depuis le Miocène et dans de nombreux endroits, les rivières actuelles empruntent le même cours que les rivières messiniennes. Autrement dit, d'un point de vue de leur drainage, *les zones orogéniques, telles que les chaînes de montagnes, peuvent être considérées comme des zones morphologiques « stables »*.

A l'inverse, là où la pente régionale est faible voire nulle, un changement de conditions aux limites tel qu'une chute du niveau de base peut entraîner un bouleversement de la morphologie par érosion régressive. C'est le cas de la connexion du bassin de l'Ebre au Pliocène, qui entraînera l'incision de celui-ci, ou encore, plus spectaculaire, celui de l'ouverture du Détroit de Gibraltar à l'origine de l'inhibition de l'incision messinienne. Nous avons montré qu'il n'était pas nécessaire et même contestable d'invoquer une quelconque structure tectonique au début du Pliocène pour expliquer le ré-ennoyage de la Méditerranée, *l'érosion régressive se suffisant à elle-même pour créer une pente régionale au niveau de l'actuel détroit de Gibraltar*. En revanche, la chute du niveau de base messinien a eu peu d'influence sur la connexion de l'Ebre à la Méditerranée, le renversement de la pente régionale étant déjà activé par la chute du niveau de base « naturel » créé par l'aggradation du bassin de l'Ebre pendant l'Oligo-Miocène. Néanmoins, le fait de ne pas retrouver d'incision

messinienne préservée dans le bassin de l'Ebre plaide pour une connexion post-messinienne. Autrement dit les régions comportant *des zones à pente régionalement faible ou nulle sont des zones morphologiques potentiellement « instables ».*

Enfin, les zones où les contraintes tectoniques ont fortement évolué depuis la fin du Miocène comme dans l'est des Bétiques, les Apennins ou la mer Egée sont par essence des zones morphologiques instables où les pentes régionales sont susceptibles d'avoir été bouleversées. Dans ce cas les réseaux messiniens n'ont pas ou peu d'affinité avec leurs équivalents actuels. Aussi l'absence de corrélation entre réseaux messiniens et réseaux actuels peut-elle refléter la présence de déformations régionales depuis la fin du Miocène en Méditerranée. Autrement dit, du fait de leur pérennité, *les réseaux de drainage peuvent constituer des marqueurs précieux de la tectonique à l'échelle des temps géologiques*.

REFERENCES

Agustí, J., Anadón, P. and Julia, R., 1983. Nuevos datos sobre el Plioceno del Baix Ebre. Aportación a la correlación entre las escalas marina y continental. *Acta Geologica Hispanica*, **18**, 123–130.

Aharon, P., Goldstein, P., Wheeler, C.W., and Jacobson, G., 1993. Sea-level events in the South Pacific linked with the Messinian salinity crisis. *Geology*, **21**, 771–775.

Aksu, A.E., Hiscott, R.N., and Yasar, D., 1999. Oscillating Quaternary water levels of the Marmara Sea and vigorous outflow into the Aegean Sea from the Marmara Sea-Black Sea drainage corridor. *Mar. Geol.*, **153**, 275–302.

Aleria Group, 1980. Le canal de Corse et les bassins nord-tyrrhéniens au Miocène supérieur et terminal (Messinien); leur évolution plio-quaternaire. *Géologie Méditerranéenne*, **7**, 5–12.

Ambert, P., Aguilar, J.P., and Michaux, J., 1998. Evolution géodynamique messinio-pliocène en Languedoc central : le paléo-réseau hydrographique de l'Orb et de l'Hérault (sud de la France). *Geodin. Acta*, **11**, 139–146.

Arasa Tuliesa, A., 1990. El terciario del Baix Ebre: Aportaciones estratigráficas y sedimentológicas. *Acta Geologica Hispanica*, **25**, 271–287.

Arenas, C., 1993. *Sedimentología y paleogeografía del Terciario del margen pirenaico y sector central de la cuenca del Ebro (zona aragonesa occidental)*.Tesis Doctoral, Universidad de Zaragoza, Zaragoza, Spain.

Armijo, R., Meyer, B., Hubert, A., and Barka, A., 1999. Westwards propagation of the North Anatolian Fault into the Northern Aegean: Timing and kinematics. *Geology*, **27**, 267–270.

Arrowsmith, J R., and Strecker, M. R., 1999. Seismotectonic range-front segmentation and mountain-belt growth in the Pamir-Alai region, Kyrgyzstan (India-Eurasia collision zone). *Geol. Soc. Am. Bull.*, **111**, 1665–1683.

Audley-Charles, M.G., Curray, J.R., and Evans, G., 1977. Location of major deltas. *Geology*, **5**, 341–344.

Azanon, J.M., Azor, A., Perez-Pena, J.V., and Carrillo, J.M., 2005. Late Quaternary large-scale rotational slides induced by river incision: The Arroyo de Gor area (Guadix basin, SE Spain). *Geomorphology*, **69**, 152–168.

Babault, J., Van Den Driessche, J., Bonnet, S., Castelltort, C., and Crave, A., 2005. Origin of the highly elevated Pyrenean peneplain. *Tectonics*, **24**, TC2010, doi:10.1029/2004TC001697.

Balanyá, J.C., García-Dueñas, V., Azañón, J.M., and Sánchez-Gómez, M., 1997. Alternating contractional and extensional events in the Alpujarride nappes of the Alboran Domain (Betics, Gibraltar Arc). *Tectonics,* **16**, 226–238.

Ballesio, R., 1972. Etude stratigraphique du Plioène rhodanien. *Doc. Lab. Géol. Fac. Sci. Lyon,* **53**, 333 p.

Barber, P.M., 1981. Messinian subaerial erosion of the Proto-Nile delta. *Mar. geol.*, **44**, 253–272.

Barr, F.T., and Walker, B.R., 1973. Late Tertiary channel system in Northern Lybia and its implications on Mediterranean sea-level changes. In: *Initial reports of the Deep Sea Drilling Project*, **13,** pp. 1244–1250, US Govern. Print. Office, Washington, DC.

Bartrina, M. T., Cabrera, L., Jurado, M. J., Guimerà, J. and Roca, E., 1992. Evolution of the central Catalan margin of the Valencia Trough (Western Mediterranean). *Tectonophysics*, **203**, 219–247.

Baulig, 1928. Le Plateau central de la France et sa bordure méditerranéenne, Thesis, Paris, 591 pp.

Baumard, B., 2001. *Valorisation de données pour l'étude de la crise messinienne dans le Gard rhodanien et la moitié est de la France*. Thèse, Ecole des Mines de Paris, 260 pp.

Beaumont, C., Fullsack, R. and Hamilton, J., 1992. Erosional control of active compressional orogens. In: *Thrust Tectonics* (K.R. McClay, ed.), pp. 1–18. Chapman & Hall, New York.

Beaumont, C., Kooi, H., and Willett, S., 2000. Coupled tectonic-surface process models with applications to rifted margins and collisional orogens. In *Geomorphology and global tectonics*, edited by Summerfield, M.A., John Wiley, pp. 29–55.

Begin, Z., 1988. Application of a diffusion-erosion model to alluvial channels which degrade due to base-level lowering. *Earth Surf. Processes Landforms*, **13**, 487–500.

Benson, R.H., Rakic-El Bied, K., and Bonaduce, G., 1991. An important current reversal (influx) in the Rifian Corridor (Morocco) at the Tortonian-Messinian boundary: the end of the Tethys ocean. *Paleoceanography*, **6**, 164–192.

Bergerat, F., 1987. Stress fields in the european platform at the time of Africa-Eurasia collision. *Tectonics*, **6**, 99–132.

Betts, H.D., and DeRose, R.C., 1999. Digital elevation models as a tool for monitoring and measuring gully erosion. *JAG*, **1**, 91–101.

Birot, P. 1937. *Recherches sur la morphologie des Pyrénées orientales franco-espagnoles*. Thèse, Paris.

Bishop, P., and Cowell, P., 1997, Lithological and drainage network determinants of the character of drowned, embayed coastlines. *J. Geol.*, **105**, 685–699.

Bishop, P., Hoey, T.B., Jansen, J.D., and Artza I.L., 2005. Knickpoint recession rate and catchment area: the case of uplifted rivers in eastern Scotland. *Earth Surf. Process. Landforms,* **30**, 767–778

Blanc, P.L., 2002. The opening of the Plio-Quaternary Gibraltar Strait: assessing the size of a cataclysm. *Geodin. Acta*, **15**, 303–317.

Blum, M.D., 1993. Genesis and Architecture of Incised Valley Fill Sequences: A Late Quaternary Example from the Colorado River, Gulf Coastal Plain of Texas. In: Siliciclastic Sequence Stratigraphy, Recent Developments and Applications (Ed. by P. Weimer & H.W. Posamentier), *Am. Ass. Petrol. Geol. Mem.*, **58**, 259–283.

Bourgois, J., Mauffret, A., Ammar, A., and Demnati, N.A., 1992. Multichannel seismic data imaging of inversion tectonics of the Alboran Ridge (Western Mediterranean Sea). *Geomar. Lett.*, **12**, 117–122.

Braga, J.C., and Martin, J.M., 1996. Geometries of reef advance in response to relative sea-level changes in a Messinian (uppermost Miocene) fringing reef (Cariatiz reef, Sorbas Basin, SE Spain). *Sedimentary Geol.*, **107**, 61–81.

Braun, J., and Sambridge M., 1997. Modelling landscape evolution on geological time scales: A new method based on irregular spatial discretization. *Basin Res.*, **9**, 27–52.

Braun, J., and Van Der Beek P., 2004. Evolution of passive margin escarpments: What can we learn from low-temperature thermochronology? *J. Geophys. Res.*, **109**, doi:10.1029/2004JF000147.

Brocard, G.Y., Van der Beek, P.A., Bourles, D.L., Siame, L.L., and Mugnier, J.L., 2003. Long-term fluvial incision rates and postglacial river relaxation time in the French Western Alps from 10Be dating of alluvial terraces with assessment of inheritance, soil development and wind ablation effects. *Earth Planet. Sci. Lett.*, **209**, 197–214.

Brown, R.W., Summerfield M.A., and Gleadow A.J.W., 2002. Denudational history along a transect across the Drakensberg Escarpment of southern Africa derived from apatite fission track thermochronology. *J. Geophys. Res.*, **107 (B12)**, 2350, doi:10.1029/2001JB000745.

Brunsden, D., 1993. The persistence of landforms. *Z. Geomorphol. Suppl*., **93**, 13–28.

Burbank, D.W., Leland, J. Fielding, E., Anderson, R.S., Brozovic, N., Reid, M.R. and Duncan C., 1996. Bedrock incision, rock uplift and threshold hillslopes in the northwestern Himalayas. *Nature*, **379**, 505–510.

Butcher, S.W., 1990. The Nickpoint Concept and its Implications Regarding Onlap to the Stratigraphic Record. In: *Quantitative Dynamic Stratigraphy* (Ed. By T.A. Cross), pp. 375–385, Prentice Hall, Englewood Cliffs, NJ.

Butler, R.W., Lickorish, W.H., Grasso, M., Pedley, H.M., and Ramberti, L., 1995. Tectonics and sequence stratigraphy in Messinian basins, Sicily: Constraints on the initiation and termination of the Mediterranean salinity crisis. *Geol. Soc. Am. Bull.,* **170**, 425–439.

Calvert, A., Sandvol, E., Seber, D., Barazangi, M., Roecker, S., Mourabit, T., Vidal, F., Alguacil, G., and Jabour, N., 2000. Geodynamic evolution of the lithosphere and upper mantle beneath the Alboran region of the western Mediterranean: Constraints from travel time tomography. *J. Geophys. Res.,* **105**, 10,871–10,898.

Calvet, M., 1985. Néotectonique et mise en place des reliefs dans l'Est des Pyrénées; l'exemple du horst des Albères. *Rev. Géol. Dyn. Géogr. Phys*., **26**, 119–130.

Campillo, A., Maldonado, A., and Mauffret, A., 1992. Stratigraphic and tectonic evolution of the western Alboran Sea. Late Miocene to recent. *Geomar. Lett.*, **12**, 165–172.

Carminati, E., Wortel, M.J.R., Meijer, P.T., and Sabadini, R., 1998. The two-stage opening of the western-central Mediterranean basins: a forward modeling test to a new evolutionary model. *Earth Planet. Sci. Lett.*, **160**, 667–679.

Chalouan, A., Saji, R., Michard, A., and Bally, A.W., 1997. Neogene tectonic evolution of the southwestern Alboran basin as inferred from seismic data off Morocco. *AAPG Bull*., **81**, 1161–1184

Chase, C.G., 1992. Fluvial landsculpting and the fractal dimension of topography. *Geomorphology*, **5**, 39–57.

Chumakov, I.S., 1967. Pliocene and Pleistocene deposits of the Nile valley in Nubia and upper Egypt (en Russe). *Acad. Science, U.S.S.R., Geol. Institute Trans. Moscou*, **170**, 5.

Chumakov, I.S., 1973. Pliocene and Pleistocene deposits of the Nile valley in Nubia and upper Egypt. In: *Initial reports of the Deep Sea Drilling Project*, **13**, pp. 1242–1243, US Govern. Print. Office, Washington, DC.

Cita, M.B. and Ryan, W.B.F., eds., 1978. Messinian erosional surfaces in the Mediterranean. *Mar. geol.*, **27**, 366 pp.

Cita, M.B., and Corselli, C., 1990. Messinian paleogeography and erosional surfaces in Italy : an overview. *Palaeogeogr., Palaeoclim., Palaeoecol*., **77**, 67–82.

Clauzon, G. 1973., The eustatic hypothesis and the pre-Pliocene cutting of the Rhone valley. In: *Initial reports of the Deep Sea Drilling Project*, **13**, pp. 1251–1256, US Govern. Print. Office, Washington, DC.

Clauzon, G., 1978. The Messinian Var canyon (Provence, Southern France). Paleogeographic implications. *Mar. geol.*, **27**, 231–246.

Clauzon, G., 1979. Le canyon messinien de la Durance (Provence, France): une preuve paléogéographique du bassin profond de dessication. *Palaeogeogr., Palaeoclim., Palaeoecol*., **29**, 15–40.

Clauzon, G., 1982. Le canyon messinien du Rhône : une preuve désicive du "dessicated deep basin model" (Hsü, Cita et Ryan, 1973). *Bull. Soc. Géol. Fr.*, **24**, 231–246.

Clauzon, G., 1987. Le détritisme néogène du bassin du Roussillon (Pyrénées-orientales, France). *Géol. Alpine*, **Mém. HS 13**, 427–441.

Clauzon, G., Aguilar, J.P., and Michaux, J., 1987. Le bassin pliocene du Roussillon (Pyrenees-Orientales, France): exemple d' evolution geodynamique d' une ria mediterraneenne consecutive a la crise de salinite messinienne. *C. R. Acad Sci. (Paris)*, **304**, 585–590.

Clauzon, G., Rubino, J.L., and Savoye, B., 1995. Marine Pliocene Gilbert-type fan deltas along the French Mediterranean coast. A typical infill feature of preexisting subaerial Messinian canyons. In: *IAS-16th Regional Meeting of Sedimentology*, Field Trip Guide Book, **23**, pp. 145–222, ASF Ed., Paris.

Clauzon, G., Suc, J.P., Gautier, F., Berger, A., and Loutre, M.F., 1996. Alternate interpretation of the Messinian salinity crisis : Controversy resoved? *Geology*, **24**, 363–366.

Clevis, Q., De Boer, P., and Wachter, M., 2003. Numerical modelling of drainage basin evolution and three-dimensional alluvial fan stratigraphy. *Sedimentary Geol.*, **163**, 85–110.

Clevis, Q., De Boer P.L., and Nijman W., 2004. Differentiating the effect of episodic tectonism and eustatic sea-level fluctuations in foreland basins filled by alluvial fans and axial deltaic systems: insights from a three-dimensional stratigraphic forward model. *Sedimentology*, **51**, 809–835.

Comas, M.C., García-Dueñas, V., and Jurado, M.J., 1992. Neogene tectonic evolution of the Alboran Basin from MCS data. *Geomar. Lett.*, **12**, 157–164.

Comas, M.J., Platt, J.P., Soto, J.I. and Watts, A.B., 1999. The origin and tectonic history of the Alboran basin: insights from Leg 161 results. *Proc. Ocean Drill. Program, Sci. Results*, **161**, 555–582.

Coney, P.J., Munoz, J. A., McKlay, and K. R., Evenchick, C. A., 1996. Syntectonic burial and post-tectonic exhumation of the Southern Pyrenees foreland fold-thrust belt. *J. Geol. Soc., London*, **153**, 9–16.

Cox, K.G., 1989. The role of mantle plumes in the development of continental drainage patterns. *Nature*, **342**, 873–877.

Crave, A., and Davy, P., 2001. A stochastic "precipiton" model for simulating erosion/sedimentation dynamics. *Computers & Geosciences*, **27**, 815–827.

Crosby, B.T., and Whipple K.X., In press. Knickpoint Initiation and Distribution within Fluvial Networks: 236 waterfalls in the Waipaoa River, North Island, New Zealand. *Geomorphology* (The Bedrock Channels Special Issue).

Davis, W.M., 1899. The geographical cycle. *Geogr. J.*, **14**, 481–504.

Davy, P., and Crave, A., 2000. Upscaling Local-Scale Transport Processes in Large-Scale Relief Dynamics. *Physics and Chemistry of the Earth (A)*, **25**, 533–541.

Delrieu, B., Rouchy, J.M., and Foucault, A., 1993. The latest Messinian erosional surface in central Crete (Greece) and around the Mediterranean: relations with the Mediterranean salinity crisis. *C. R. Acad Sci. (Paris)*, **316 (II)**, 527–533.

Denizot, G., 1952. Le Pliocène dans la vallée du Rhône. *Rev. Géogr. Lyon*, **27**, 327–357.

Depéret, C., 1895. Aperçu sur la structure générale et l'histoire de la formation de la vallée du Rhône. *Ann. Géogr.*, **4**, 432–452.

Derricourt, R.M., 1976. Retrogression rate of the Victoria falls and the Batoka gorge. *Nature*, **264,** 23–25.

de Sitter, L. U., 1952. Pliocene uplift of Tertiary mountain chains. *American Journal of Science*, **250**, 297–307.

Dewey, J.F., Helman, M.L., Turco, E., Hutton, D.W.H., Knott, S.D., 1989. Kinematics of the western Mediterranean. In: Alpine Tectonics (M. P. Coward and D. Dietrich, eds). *Spec. Publs Geol. Soc. Lond.*, **45**, 265–283.

Didon, J., 1969. *Etude géologique du Campo de Gibraltar (Espagne méridionale)*. Thèse, Faculté des Sciences, Paris, 539 pp.

Didon, J., 1973. Accidents transverses et coulissages longitudinaux dextres dans la partie N de l'arc de Gibraltar (Cordillères bétiques occidentales–Espagne). *Bull. Soc. Géol. Fr,* **15**, 121–127.

Druckman, Y., Buchbinder, B., Martinotti, G.M., Tov, R.S., and Aharon, P., 1995. The buried Afiq Canyon (eastern Mediterranean, Israel): a case study of a Tertiary submarine canyon exposed in Late Messinian times. *Mar. geol.*, **123**, 167–185.

Duggen, S., Hoernle, K., Van Den Bogaard, P., Rupke, L., and Morgan, J.P., 2003. Deep roots of the Messinian salinity crisis. *Nature*, **422**, 602–606.

Duggen, S., Hoernle, K., van den Bogaard, P., and Harris, C., 2004. Magmatic evolution of the Alboran region: The role of subduction in forming the western Mediterranean and causing the Messinian Salinity Crisis. *Earth Planet. Sci. Lett.,* **218**, 91–108.

Ellis, M.A., Densmore, A.L. and Anderson, R.S. 1999. Development of mountainous topography in the Basin Ranges, U.S.A. *Basin Res*, **11**, 21–41.

Escutia, C., and Maldonado A., 1992. Paleogeographic implications of the Messinian surface in the Valencia trough, northwestern Mediterranean Sea. *Tectonophysics*, **203**, 263–284.

Evans, G. and Arche, A., 2002. The flux of siliciclastic sediment from the Iberian Peninsula, with particular reference to the Ebro. In*:* Sediment Flux to Basins: Causes, Controls and Consequences (S.J. Jones and L.E. Frostick, eds). *Spec. Publs Geol. Soc. Lond.,* **191**, 199–208.

Faccenna, C., Piromallo, C., Crespo-Blanc, A., Jolivet, L., and Rossetti, F., 2004. Lateral slab deformation and the origin of the western Mediterranean arcs. *Tectonics*, **23**, doi:10.1029/2002TC001488.

Fagherazzi, S., Howard, A.D., and Wiberg P.L., 2004. Modeling fluvial erosion and deposition on continental shelves during sea level cycles. *J. Geophys. Res.*, **109**, F03010, doi:10.1029/2003JF000091.

Farran, M. and Maldonado, A., 1990. The Ebro continental margin shelf: Quaternary seismic stratigraphy and growth patterns. *Mar. Geol.*, **95**, 289–312.

Field, M.E., and Gardner, J.V., 1990. Pliocene-Pleistocene growth of the Rio Ebro margin, northeast Spain: A prograding-slope model. *Geol. Soc. Am. Bull.*, **102**, 721–733.

Field, M.E., and Gardner, J.V., 1991. Valencia gorge : Possible Messinian refill channel for the western Mediterranean Sea. *Geology*, **19**, 1129–1132.

Fisk, H.N., 1944. Geological Investigation of the Alluvial Valley of the Lower Mississippi River. Mississippi River Commission, Vicksburg.

Fitzgerald, P. G., Muñoz, J. A., Coney, P. J. and Baldwin, S. L., 1999. Asymmetric exhumation across the Pyrenean orogen: implications for the tectonic evolution of a collisional orogen. *Earth Planet. Sci. Lett.*, **173**, 157–70.

Fontannes, F., 1882. Note sur l'extension et la faune de la mer pliocène dans le sud-ouest de la France. *Bull. Soc. Géol. Fr.,* **II**, 103–142.

Fortuin, A.R., Krijgsman, W., Hilgen, F.J., Sierro, F.J., 2000. Late Miocene Mediterranean desiccation: topography and significance of the 'Salinity Crisis' erosion surface on-land in southeast Spain: a comment. *Sedimentary Geol.*, **133**, 167–174.

Frey-Martinez, J. M., Cartwright, J. A., Burgess, P. M. and Vicente Bravo, J., 2004. 3D seismic interpretation of the Messinian Unconformity in the Valencia Basin, Spain. In*: 3D Seismic Technology: Application to the Exploration of Sedimentary Basins* (R.J. Davies, J. Cartwright, S.A. Stewart, M. Lappin, and J.R. Underhill, eds). *Geol. Soc. London Mem.*, **29**, 91-100.

Frizon de Lamotte, D., Crespo-Blanc, A., Saint-Bézar, B., Comas, M.C., Fernàndez, M., Zeyen, H., Ayarza, P., Robert-Charrue, C., Chalouan, A., Zizi, M., Teixell, A., Arboleya, M. L., Alvarez-Lobato, F., Julivert, M., and Michard, A., 2004. Transect I: Iberia-Meseta -Guadalquivir Basin - Betic Cordillera - Alboran Sea - Rif - Moroccan Meseta - High Atlas - Sahara Domain. In *The TRANSMED Atlas - The Mediterranean region from crust to Mantle*, edited by W. Cavazza, F.M. Roure, W. Spakman, G.M. Stampfli and P.A.Z. (eds), Springer, Berlin, Heidelberg.

Garcia-Castellanos, D., Vergés, J., Gaspar-Escribano, J. and Cloetingh S., 2003. Interplay between tectonics, climate, and fluvial transport during the Cenozoic evolution of the Ebro Basin (NE Iberia). *J. Geophys. Res.*, **108(B7)**, 2347, doi:10.1029/2002JB002073.

García-Dueñas, V., Balanyá, J.C., and Martínez-Martínez, J.M., 1992. Miocene extensional detachments in the outcropping basement of the northern Alboran basin (Betics) and their tectonic implications. *Geomar. Lett.*, **12**, 88–95.

Gardner, T.W., 1983. Experimental study of knickpoint and longitudinal profile evolution in cohesive, homogeneous material. *Geol. Soc. Am. Bull.*, **94**, 664–672.

Gautier, F., Clauzon, G., Suc, J.P., Cravatte, J., and Violanti, D., 1994. Age et duree de la crise de salinite messinienne. *C. R. Acad Sci. (Paris)*, **318**, 1103–1109.

Gentil, L., 1909. Sur la formation du détroit de Gibraltar. *C. R. Acad Sci. (Paris)*, **CXLVIII**, 1227–1230.

Giermann, G., 1961, Erläuterungen zur bathymetrischen Karte der Strasse von Gibraltar. *Bull. Inst. Océanogr. Monaco*, **58 (1218 A)**, 28 pp.

Gilbert, G.K., 1885. The topographic features of the shorelines. *US Geol. Surv. Rep.*, **5**, Washington DC, pp. 75–123.

Gilchrist, A.R., Kooi, H. and Beaumont C., 1994. The post-Gondwana geomorphic evolution of southwestern Africa: Implications for the controls on landscape development from observations and numerical experiments. *J. Geophys. Res.*, **99**, 12,211–12,228.

Glock, W.S., 1931. The development of drainage systems: a synpotic view. *Geogr. Rev.*, **21**, 475–482.

Gökasan, E., Demirbag, E., Oktay, F.Y., Ecevitoglu, B., Simsek, M., Yüce, H., 1997. On the origin of the Bosphorus. *Mar. Geol.*, **175**, 67–102.

Gorini, C., 1993. *Géodynamique d'une marge passive: Le Golfe du Lion (Méditerranée occicentale)*. Thèse, Université Paul Sabatier de Toulouse III, 264 pp.

Gorini, C., Lofi, J., Duvail, C., Dos Reis, A. T., Guennoc, P., Lestrat, P. and Mauffret, A., 2005. The Late Messinian salinity crisis and Late Miocene tectonism: Interaction and consequences on the physiography and post-rift evolution of the Gulf of Lions margin. *Mar. Petrol. Geol.*, **22**, 695–712.

Griffin, D.L., 2002. Aridity and humidity: two aspects of the late Miocene climate of North Africa and the Mediterranean. *Palaeogeogr., Palaeoclim., Palaeoecol*., **182**, 65–91.

Groupe de recherche néotectonique de l'Arc de Gibraltar, 1977. L'histoire néotectonique récente (Tortonien à Quaternaire) de l'Arc de Gibraltar et des bordures de la mer d'Alboran. *Bull. Soc. Géol. Fr*, **19**, 575–614.

Guennoc, P., Gorini, C., and Mauffret, A., 2000. Histoire geologique du golfe du Lion et cartographie du rift oligo-aquitanien et de la surface messinienne. *Geol. France*, **3**, 67–97.

Gutscher, M.A., Malod, J., Rehault, J.P., Contrucci, I., Klingelhoefer, F., Mendes-Victor, L., and Spakman, W., 2002. Evidence for active subduction beneath Gibraltar. Geology, **30**, 1071–1074.

Hack, J. T., 1957. Studies of longitudinal stream profiles in Virginia and Maryland. *U.S. Geol. Surv. Prof. Pap.*, **294-B**, 97 pp.

Hack, 1960. Interpretation of erosional topography in humid temperature regions. *Am. J. Sci.*, **258-A**, 80–97.

Haq, B.U., Hardenbol, J., and Vail, P., 1987. Chronology of fluctuating sea-levels since Triassic (250 million years ago to present). *Science*, **235**, 1156–1167.

Hallet, B., and Molnar, P., 2001. Distorted drainage basins as markers of crustal strain east of the Himalaya. *J. Geophys. Res.*, **106**(B7), 13,697–13,710.

Hasbargen, L.E. and Paola, C., 2000. Landscape instability in an experimental drainage basin. *Geology*, **28**, 1067–1070.

Hassan, M.A., and Klein, M.U., 2002. Fluvial adjustment of the Lower Jordan River to a drop in the Dead Sea level. *Geomorphology*, **45**, 21–33.

Hayakawa, Y., and Matsukura, Y., 2003, Recession rates of waterfalls in Boso peninsula, Japan, and a predictive equation. *Earth Surf. Process. Landforms*, **28**, 675–684.

Herraiz, M., De Vicente, G., Lindo-Naupari, R., Giner, J., Simón, J. L., González-Casado, J. M., Vadillo, O., Rodríguez-Pascua, M. A., Cicuéndez, J. I., Casas, A., Cabañas, L., Rincón, P., Cortés, A. L., Ramírez, M. and Lucini, M., 2000. The recent (upper Miocene to Quaternary) and present tectonic stress distributions in the Iberian Peninsula. *Tectonics*, **19**, 762–786.

Hodell, D.A., Benson, R.H., Kent, D., Boersma, A., and Rakic-El Bied, K., 1994. Magnetostratigraphic, biostratigraphic, and stable isotope stratigraphy of an upper Miocene drill core from the Salé Briqueterie (northwest Morocco): A high resolution chronology for the Messinian stage. *Paleoceanography*, **9**, 835–855.

Hodell, D.A., Curtis, J.H., Sierro, F.J., and Raymo, M.E., 2001. Correlation of late Miocene to early Pliocene sequences between the Mediterranean and North Atlantic. *Paleoceanography*, **16**, 164–178.

Horton, R.E., 1945. Erosional development of streams and their drainage basins: hydrophysical approach to quantitative morphology. *Geol. Soc. Am. Bull.*, **56**, 275–370.

Howard, A.D., 1971. Optimal angles of stream junction: geometric, stability to capture, and minimum power criteria. *Water Resour. Res*., **7**, 863–873.

Howard, A.D., and Kerby G., 1983. Channel changes in badlands. *Geol. Soc. Am. Bull.*, **94**, 739–752.

Howard, A.D., Dietrich, W.E., and Seidl, M.A., 1994. Modeling fluvial erosion on regional to continental scales. *J. Geophys. Res.*, **99**, 13,971–13,986.

Hsü, K.J., Ryan, W.B.F., and Cita, M.B., 1973. Late Miocene dessication of the Mediterranean. *Nature*, **242**, 240–244.

Hsü, K.J., Cita, M.B., and Ryan, W.B.F., 1973. The origin of the Mediterranean evaporites. In *Initial reports of the deep sea drilling project*, **13**, pp 1203–1231, US Govern. Print. Office, Washington, DC.

Hsü, K.J., 1978. When the Black Sea was drained. *Sci. Am.*, **238**, 52–63.

Hsü, K.J., 1983. *The Mediterranean was a Desert. A Voyage of the Glomar Challenger*. Princeton University Press, Princeton, NJ, 183 pp.

Instituto Geologico y Minero de Espana (IGME), 1994. Mapa Geologico de la Peninsula Iberica, y Canarias, scale 1:1.000.000.

Irr, F., 1984. *Paléoenvironnements et evolution géodynamique néogènes et quaternaries de la bordure nord du bassin méditerranéen occidental, un système de pente de la paléo-marge liguro-provençale*. Thèse, 464 pp.

Jimenez-Munt, I., and Negredo, A.M., 2003. Neotectonic modelling of the western part of the Africa-Eurasia plate boundary: from the Mid-Atlantic ridge to Algeria. *Earth Planet. Sci. Lett.,* **205**, 257–271

Kastens, K.A., 1992, Did glacio-eustatic sea level drop trigger the messinian salinity crisis? New evidence from ocean drilling program site 654 in the Tyrrhenian Sea. *Paleoceanography*, **7**, 333–356.

Kooi, H., and Beaumont C., 1994. Escarpment evolution on high-evelvation rifted margins: Insights derived from a surface processes model that combines diffusion, advection, and reaction. *J. Geophys. Res.*, **99**, 12,191–12,209.

Koss, J.E., Ethridge, F.G. and Schumm S.A., 1994. An experimental study of the effecs of base-level change on fluvial, coastal plain and shelfs systems. *Jour. Sed. Res.*, **B64**, 90–98.

Krijgsman, W., Hiigeni, F.J., Raffi, I., Sierro, F.J., and Wilson, D.S., 1999a. Chronology, causes and progression of the Messinian salinity crisis. *Nature*, **400**, 652–655.

Krijgsman, W., Langereis, C.G., Zachariasse, W.J., Boccaletti, M., Moratti, G., Gelati, R., Iaccarino, S., Papani, G., and Villa, G., 1999b. Late Neogene evolution of the Taza-Guercif Basin (Rifian Corridor, Morocco) and implications for the Messinian salinity crisis. *Mar. Geol.*, **153**, 147–160.

Lague, D., Crave, A., and Davy, P., 2003, Laboratory experiments simulating the geomorphic response to tectonic uplift: *J. Geophys. Res.*, **108(B1)**, doi:10.1029/2002JB001785.

Lague, D., and Davy P., 2003. Constraints on the long-term colluvial erosion law by analyzing slope-area relationships at various tectonic uplift rates in the Siwaliks Hills (Nepal). *J. Geophys. Res*., **108 (B2)**, 2129, doi:10.1029/2002JB001893.

Leblanc, D., and Olivier, P., 1984. Role of strike-slip faults in the Betic-Rifian orogeny. *Tectonophysics*, **101**, 345–355.

Loget, N., Davy, P. and Van Den Driessche, J., 2003. Large scale erosion processes and parameters derived from a modelling of the Messinian Salinity Crisis. *Geo. Res. Abstracts*, **5**, p. 10718.

Loget, N., Van Den Driessche J. and Davy P., 2005. How did the Messinian Salinity Crisis end ? *Terra Nova*, **17**, 414–419.

Lonergan, L., and White, N., 1997. Origin of the Betic-Rif mountain belt. *Tectonics*, **16**, 504–522.

Maestro, A., Barnolas, A., Somoza, L., Lowrie, A. and Lawton, T., 2002. Geometry and structure associated to gas-charged sediments and recent growth faults in the Ebro Delta (Spain). *Mar. Geol.*, **186**, 351–368.

Maillard, A., 1993. *Structure et riftogénèse du Golfe de Valence (Méditerranée Nord-Occidentale)*.Thèse de Doctorat, Université Pierre et Marie Curie, Paris 6, Paris.

Maldonado, A., and Nelson, C.H., 1999. Interaction of tectonic and depositional processes that control the evolution of the Iberian Gulf of Cadiz margin. *Mar. geol*., **155**, 217–242.

Maldonado, A., Campillo, A.C., Mauffret, A., Alonso, B., Woodside, J., and Campos, J., 1992. Alboran Sea late Cenozoic tectonic and stratigraphic evolution. *Geomar. Lett.*, **12**, 179–186.

Maldonado, A., Somoza, L., and Pallares, L., 1999. The Betic orogen and the Iberian-African boundary in the Gulf of Cadiz: geological evolution (central North Atlantic). *Mar. geol*., **155**, 9–43.

Mandier, P., 1988. Le relief de la moyenne vallée du Rhône au Tertiaire et au Quaternaire. Essai de synthèse paléogéographique. *Doc. BRGM*, **151**.

Martìn, J.M. and Braga, J.C., 1994. Messinian events in the Sorbas Basin in southeastern Spain and their implications in the recent history of the Mediterranean. *Sedimentary Geol.*, **90**, 257–268.

Martìn, J.M., Braga, J.C., and Betzler, C., 2001. The Messinian Guadalhorce corridor : the last northern, Atlantic-Mediterranean gateway. *Terra Nova*, **13**, 418–424.

Martinell, J. 1988. An overview of the marine Pliocene of N.E. Spain. *Géol. Méditerr.*, **15**, 227–233.

Martínez-Martínez, J.M., and Azañón, J.M., 1997. Mode of extensional tectonics in the southeastern Betics (SE Spain): Implications for the tectonic evolution of the peri-Alborán orogenic system. *Tectonics*, **16**, 205–225.

Mauffret, A., Maldonado, A., and Campillo, A.C., 1992. Tectonic framework of the Eastern Alboran and Western Algerian Basins, Western Mediterranean. *Geomar. Lett.*, **12**, 104–110.

McKenzie, D.P., 1970. Plate tectonics of the Mediterranean region. *Nature*, **226**, 239–243.

Michard, A., Chalouan, A., Feinberg, H., Goffé, B., and Montigny, R., 2002. How does the Alpine belt end between Spain and Morocco? *Bull. Soc. Géol. Fr.*, **173**, 3–15.

Molnar, P., and England, P., 1990. Late Cenozoic uplift of mountain ranges and global climatic change: Chicken or egg? *Nature*, **346**, 29–34.

Montenat, C., Ott d'Estevou, P. and La Chapelle, G., 1990. Le bassin de Nijar–Carboneras et le couloir du Bas-Andarax. In: Les Bassins Néogenes Du Domaine Bétique Oriental (Espagne) (Ed. C. Montenat). *Doc. Trav. IGAL*, **12–13**, pp. 129–164.

Montgomery, D.R., and Dietrich, W.E., 1992. Channel initiation and the problem of landscape scale. *Science*, **255**, 826–830.

Morel, J.L., 1987. *Evolution récente de l'orogène rifain et de son avant-pays depuis la fin de la mise en place des nappes (Rif, Maroc)*. PhD Thesis, Univ. Paris-Sud, 583 pp.

Morel, J.L., and Meghraoui, M., 1996. Goringe-Alboran-Tell tectonic zone: A transpression system along the Africa-Eurasia plate boundary. *Geology*, **24**, 755–758.

Mulder, C.J., and Parry, G.R., 1977. Late Tertiary evolution of the Alboran Sea at the eastern entrance of the Straits of Gibraltar. In: *International Symposium on the Structural History of the Mediterranean Basins* (Ed. By B. Biju-Duval and L. Montadert), Editions Technip, Paris, pp. 401–410

Murray, A.B., and Paola, C., 1997. Properties of a cellular braided-stream model. *Earth Surf. Process. Landforms*, **22**, 1001–1025.

Nelson, C. H. 1990. Estimated post-Messinian supply and sedimentation rates on the Ebro continental margin, Spain. *Mar. Geol.*, **95**, 395–418.

Nelson, C. H. and Maldonado, A. 1990. Factors controlling late Cenozoic continental margin growth from the Ebro Delta to the western Mediterranean deep sea. *Mar. Geol.*, **95**, 419–440.

Norman, S.E., and Chase, C.G., 1986. Uplift of the shores of the western Mediterranean due to Messinian dessication and flexural isostasy. *Nature*, **322**, 450–451.

Oktay, F.Y., Gokasan, E., Sakinc, M., Yaltirak, C., Imren, C., and Demirbag, E., 2002. The effects of the North Anatolian Fault Zone on the latest connection between Black Sea and Sea of Marmara. *Mar. Geol.*, **190**, 367–382.

Olivet, J.L., Auzende, J.M., and Bonnin, J., 1973. Alboran Sea structural framework. In: *Initial reports of the Deep Sea Drilling Project*, **13**, pp. 1417– 1430, US Govern. Print. Office, Washington, DC.

Ollier, C.D., 1985. Morphotectonics of continental margins with great escarpments. In *Tectonic Geomorphology, Binghamton Symp. Geomorphol. Int. Ser.*, **15**, edited by M. Morisawa and J.T. Hack, pp. 3–25, Allen and Unwin, Boston, Mass.

Orszag-Sperber, F., Rouchy, J.M., Blanc-Valleron, M.M., 2000. La transition Messinien – Pliocène en Méditerranée orientale (Chypre): la période du Lago-Mare et sa signification. *C. R. Acad Sci. (Paris)*, **2 (331)**, 490–493.

Parke, J.R., Minshull, T.A., Anderson, G., White, R.S., McKenzie, D., Kuscu, I., Bull, J.M., Gorur, N., and Sengor, C., 1999. Active faults in the Sea of Marmara, western Turkey, imaged by seismic reflection profiles. *Terra Nova*, **11**, 223–227.

Parker, R.S., 1977. Experimental study of basin evolution and its hydrologic implications. *unpublished PhD dissertation*, Colorado State University, Fort Collins, 331 pp.

Pazzaglia, F.P., Gardner, T.W. and Merritts, D.J., 1998. Bedrock Fluvial incision and longitidinal profile development over geologic time scales determined by fluvial terraces. In *Rivers Over Rock: Fluvial Processes in Bedrock Channels*, *Geophys. Monogr. Ser.*, **107**, edited by K. J. Tinkler and E. E. Wohl, pp. 207–235, AGU, Washington, D. C.

Peizhen, Z., Molnar, P., and Downs, W.R., 2001. Increased sedimentation rates and grain sizes 2-4 Myr ago due to the influence of climate change on erosion rates. *Nature*, **410**, 891–897.

Pelletier, J.D., 2003. Drainage basin evolution in the Rainfall Erosion Facility: dependence on initial conditions. *Geomorphology*, **53**, 183–196.

Penck, W., 1924. Die Morphologische Analyse: Ein Kapital der Physikalischen Geologie. Engelhorn, Stuttgart, Germany, 283 pp.

Philip, H., 1987. Plio-Quaternary evolution of the stress field in Mediterranean zones of subduction and collision. *Annu.Geophys.*, **5B**, 301–320.

Pik, R., Marty, B., Carignan, J., and Lavé, J., 2003. Stability of the Upper Nile drainage network (Ethiopia) deduced from (U–Th)/He thermochronometry: implications for uplift and erosion of the Afar plume dome. *Earth Planet. Sci. Lett.*, **215**, 73–88.

Pinet, P., and Souriau, M., 1988. Continental erosion and large-scale relief. *Tectonics*, **7**, 563–582.

Platt, J.P., and Vissers, R.L.M., 1989. Extensional collapse of thickened continental lithosphere: A working hypothesis for the Alboran Sea and Gibraltar arc. *Geology*, **17**, 540–543.

Platt, J.P., Whitehouse, M.J., Kelley, S.P., Carter, A. and Hollick, L., 2003. The ultimate arc: differential displacement, oroclinal bending, and vertical axis rotation in the External Betic-Rif arc. *Tectonics*, **22**, 1017, doi: 10.1029/2001TC001321.

Poisson, A., Wernli, R., Kemal Saular, E., and Temz, H., 2003. New data concerning the age of the Aksu Thrust in the south of the Aksu valley, Isparta Angle (SW Turkey): consequences for the Antalya Basin and the Eastern Mediterranean. *Geol. Jour*., **38**, 311–327.

Potter, P.E. 1978. Significance and origin of big rivers. *J. Geol*, **86**, 13-33.

Potter, P.E., 1997. The Mesozoic and Cenozoic paleodrainage of South America: a natural history. *J. South Am. Earth Sci*., **10**, 331–344.

Powell, J.W. 1875., Exploration of the Colorado River of the West, US Government Printing Office, Washington, DC, 400 pp.

Rampnoux, J.P., Angelier, J., Colleta, B., Fudral, S., Guillemin, M., and Pierre, G., 1979. Sur l'évolution néotectonique du Maroc septentrional. *Géol. Méditerr.*, **6 (4)**, 439–464.

Reille, J. L., 1971. *Les relations entre tectorogénèse et sédimentation sur le versant sud des Pyrénées centrales d'après l'étude des formations tertiaires essentiellement continentales*. Doct. Etat Sci., USTL, Montpellier.

Riba, O., Reguant, S. and Villena, J., 1983. Ensayo de síntesis estratigráfica y evolutiva de la cuenca terciaria del Ebro. In*:* Comba, J. (eds) *Libro Jubilar J. M. Ríos, Geología de España*, **2**. Instituto Geológico y Minero de España, Madrid (Spain), 131–159.

Riding, R., Braga, J.C., and Martìn, J.M., 1999. Late Miocene Mediterranean desiccation: topography and significance of the 'Salinity Crisis' erosion surface on-land in southeast Spain. *Sedimentary Geol.*, **123**, 1–7.

Roca, E. 2001. The Northwest Mediterranean Basin (Valencia Trough, Gulf of Lions and Liguro-Provençal basins); structure and geodynamics evolution. In*: Peri-Tethys memoir 6; Peri-Tethyan rift/wrench basins and passive basins* (P.A. Ziegler, W. Cavazza, A.H.F. Robertson and S.S. Crasquin, eds). *Mém. Mus. Nat. Hist. Nat.*, **186**, 671–706.

Rosenbloom, N.A., and Anderson, R.S., 1994. Hillslope and channel evolution in a marine terraced landscape, Santa Cruz, California. *J. Geophys. Res.*, **99**, 14,013–14,029.

Rouchy, J.M., and Saint Martin, J.P., 1992. Late Miocene events in the Mediterranean as recorded by carbonate-evaporite relations. *Geology*, **20**, 629–632.

Rouchy, J.M., Pierre, C., Et-Touhami, M., Kerzazi, K., Caruso, A., and Blanc-Valleron, M.M., 2003. Late Messinian to Early Pliocene paleoenvironmental changes in the Melilla Basin (NE Morocco) and their relation to Mediterranean evolution. *Sedimentary Geol.*, **163**, 1–27.

Ryan, W.B.F., 1976. Quantitative evaluation of the depth of the western Mediterranean before, during and after the late Miocene salinity crisis. *Sedimentology*, **23**, 791–813.

Ryan, W.B.F., and Pitman I., W.C., 1999. *Noah's Flood: the New Scientific Discoveries about Events that Changed History*. Touchstone Book, Simion and Schuster, New York, 319 pp.

Ryan, W.B.F., Hsü, K.J. et al., 1973. *Initial reports of the Deep Sea Drilling Project*, **13**, US Govern. Print. Office, Washington, DC., 1447 pp.

Ryan, W.B.F., Pitman, I., Walter C., Major, C.O., Shimkus, K., Moskalenko, V., Jones, G.A., Dimitrov, P., Gorur, N., Sakinc, M., and Yuce, H., 1997. An abrupt drowning of the Black Sea shelf. *Mar. Geol.*, **138**, 119–126.

Sanz, J.L., Acosta, J., Herranz, P. Palomo, C., San Gil, C., 1991. *Mapa Batimétrico del Estrecho de Gibraltar*, scale 1:100 000. Instituto Español de Oceanografía, Publ. Espec. Inst. Esp. Oceangr., Madrid.

Saucier, R.T., 1996. A contemporary appraisal of some key Fiskian concepts with emphasis on Holocene meanderbelt formation and morphology. *Engineering Geol.*, **45**, 67–86.

Savoye, B., and Piper, D.J.W., 1991. The Messinian event on the margin of the Mediterranean Sea in the Nice area, southern France. *Mar. geol.*, **97**, 279–304.

Schlupp, A., Clauzon, G. and Avouac, J.P., 2001. Mouvement post-messinien sur la faille de Nîmes: implications pour la sismotectonique de la Provence. *Bull. Soc. Géol. Fr.*, **172**, 697–711.

Schoorl, J.M., and Veldkamp, A.U., 2003. Late Cenozoic landscape development and its tectonic implications for the Guadalhorce valley near Alora (Southern Spain): *Geomorphology*, **50**, 43–57.

Schumm, S.A., 1956. Evolution of drainage systems and slopes in badlands at Perth Amboy, New Jersey. *Geol. Soc. Am. Bull.*, **67**, 597–646.

Schumm, S.A., 1993. River response to baselevel change: Implications for sequence stratigraphy. *J. Geology*, **101**, 279–294.

Schumm, S.A., Mosley, M.P., and Weaver, W.E., 1987. *Experimental fluvial geomorpholgy*. New York, Wiley, 413 pp.

Seber, D., Barazangi, M., Ibenbrahim, A., and Demnati, A., 1996. Geophysical evidence for lithospheric delamination beneath the Alboran Sea and Rif- Betic Mountains. *Nature*, **379**, 785–791.

Seginer, I., 1966. Gully development and sediment yield. *Journal of Hydrology*, **4**, 236–253.

Seibold, E. and Berger, W.H., 1982. *The Sea floor. An introduction to marine geology*. Springer-Verlag, 288 pp.

Seidl, M.A., Dietrich, W.E., and Kirchner J.W., 1994. Longitudinal profile development into bedrock: An analysis of Hawaiian channels. *J. Geol.*, **102**, 457–474.

Séranne, M., Benedicto, A., and Labaum, P., 1995. Structural style and evolution of the Gulf of Lion Oligo-Miocene rifting : role of the Pyrenean orogeny. *Mar. Petrol. Geol*., **12**, 809–820.

Séranne, M., Camus, H., Lucazeau, F., Barbarand, J., and Quinif, Y., 2002, Surrection et érosion polyphasées de la bordure cévenole. Un exemple de morphogenèse lente. *Bull. Soc. Géol. Fr.*, **173**, 97–112.

Serrat, D. 1992. La xarxa fluvial dels Països Catalans. In: *História Natural dels Països Catalans* (edited by Catalana, E.), **Geologia II**, Barcelona, 375–389.

Shackleton, N.J., Hall, M.A., and Pate, D., 1995. Pliocene stable isotope stratigraphy of site 846. *Proc. Ocean drill. Prog., Sci. Res.*, **138**, 337–355.

Sissingh, W., 2001, Tectonostratigraphy of the West Alpine foreland: correlation of Tertiary sedimentary sequences, changes in eustatic sea-level and stress regimes. *Tectonophysics*, **333**, 361–400.

Snyder, N.P., Whipple, K.X., Tucker, G.E., and Merritts D. J., 2000. Landscape response to tectonic forcing: DEM analysis of stream profiles in the Mendocino triple junction region, northern California, *Geol. Soc. Am. Bull.*, **112 (8)**, 1250–1263.

Stampfli, G.M., and Höcker, C.F.W., 1989. Messinian palaeorelief from a 3-D seismic survey in the Tarraco concession area (Spanish Mediterranean Sea). *Geol. Mijnbouw*, **68**, 201–210.

Steckler, M.S., and Watts A. B., 1980. The gulf of Lion: subsidence of a young continental margin. *Nature*, **287**, 425–429.

Stock, J.D., and Montgomery, D.R., 1999. Geologic constraints on bedrock river incision using the strem power law. *J. Geophys. Res.*, **104**, 4983–4993.

Suc, J.P., and Bessais, E., 1990. Pérennité d'un climat thermo-xérique en Sicile avant, pendant, après la crise de salinité messinienne. *C. R. Acad Sci. (Paris),* **310**, 1701–1707.

Suess, Ed. 1921-24. *La face de la terre I-III.* (*Das Anlitz der Erde*). 7 vol., Colin, Paris, 3500 pp.

Summerfield, M.A., and Hulton, N.J., 1994. Natural controls of fluvial denudation rates in major world drainage basins. *J. Geophys. Res.*, **99**, 13,871–13,883.

Suter, G., 1980a. Carte géologique de la chaine rifaine au 1/500 000. Notes et mémoires Service géologique du Maroc 245a.

Suter, G., 1980b. Carte structurale de la chaine rifaine au 1/500 000. Notes et mémoires Service géologique du Maroc 245b.

Tapponnier, P., 1977. Evolution tectonique du système alpin en Méditerranée : poinçonnement et écrasement rigide-plastique. *Bull. Soc. Géol. Fr.,* **19**, 437–460.

Tucker, G., and Slingerland R., 1996. Predicting sediment flux from fold and thrust belts. *Basin Res*., **8**, 329–349.

Tucker, G.E., and Whipple K.X., 2002. Topographic outcomes predicted by stream erosion models: Sensitivity analysis and intermodel comparison. *J. Geophys. Res.*, **107**, 2179, doi:10.1029/2001JB000162.

van der Beek, P., Summerfield, M.A., Braun, J., Brown, R.W., and Fleming A., 2002. Modeling postbreakup landscape development and denudational history across the southeast African (Drakensberg Escarpment) margin. *J. Geophys. Res.*, **107 (B12)**, 2351, doi:10.1029/2001JB000744.

van der Beek, P., and Bishop P., 2003. Cenozoic river profile development in the Upper Lachlan catchment (SE Australia) as a test of quantitative fluvial incision models. *J. Geophys. Res.*, **108 (B6)**, 2309, doi:10.1029/2002JB002125.

Van Heijst, M.W.I.M., and Postma G., 2001. Fluvial response to sea-level changes: a quantitative analogue, experimental approach. *Basin Res.*, **13**, 269–292.

Vissers, R.L.M., Platt, J.P. and van der Wal, D., 1995. Late orogenic extension of the Betic Cordillera and the Alboran Domain: a lithospheric view. *Tectonics*, **14**, 786–803.

Watts, A.B., Platt, J.P., and Buhl, P., 1993. Tectonic evolution of the Alboran Sea basin. *Basin Res.*, **5**, 153–177.

Weijermars, R., 1988, Neogene tectonics in the Western Mediterranean may have caused the Messinian Salinity Crisis and an associated glacial event. *Tectonophysics*, **148**, 211–219.

Weissel, J.K., and Seidl M.A., 1998. Inland propagation of erosional escarpments and river profile evolution across the southeast Australian passive continental margin. In *Rivers Over Rock: Fluvial Processes in Bedrock Channels*, *Geophys. Monogr. Ser.*, **107**, edited by K. J. Tinkler and E. E. Wohl, pp. 189–206, AGU, Washington, D. C.

Whipple, K.X., 2001. Fluvial landscape response time: How plausible is steady-state denudation? *Am. J. Sci.*, **301**, 313–325.

Whipple, K.X., and Tucker, G.E., 1999. Dynamics of the stream-power river incision model: Implications for height limits of mountain ranges, landscape response timescales, and research needs. *J. Geophys. Res.*, **104**, 17,661–17,674.

Whipple, K.X., and Tucker, G.E., 2002. Implications of sediment-flux-dependent river incision models for landscape evolution. *J. Geophys. Res.*, **107 (B2)**, 10.1029/2000JB00004.

Wildi, W., 1983. La chaine tello-rifaine (Algérie, Maroc, Tunisie): Structure, stratigraphie et évolution du Trias au Miocène. Revue de Géologie Dynamique et de Géographie Physique, **24**, 201–297.

Wildi, W., and Wernli, R., 1977, Stratigraphie et micropaléontologie des sédiments pliocènes de l'Oued Laou (côte méditerranéenne marocaine). *Arch. Sc., Genève*, **30**, 213–228.

Willgoose, G.R., Bras, R. L., and Rodriguez-Iturbe I., 1991. Results from a new model of river basin evolution. *Earth Surf. Processes Landforms*, **16**, 237–254.

Wohl, E.E., 1998. Bedrock channel morphology in relation to erosional processes. In *Rivers Over Rock: Fluvial Processes in Bedrock Channels*, *Geophys. Monogr. Ser.*, **107**, edited by K. J. Tinkler and E. E. Wohl, pp. 133–151, AGU, Washington, D. C..

Woodside, J.M., and Maldonado, A., 1992. Styles of compressional neotectonics in the Estearn Alboran Sea. *Geomar. Lett.*, **12**, 111–116.

Young, R.W., and McDougall, I., 1993. Long-term landscape evolution: Early Miocene and modern rivers in southern New South Wales, Australia. *J. Geol.*, **101**, 35–49.

Zeck, H.P., 1997. Mantle peridotites outlining the Gibraltar Arc: Centrifugal extensional allochthons derived from the earlier Alpine, westward subducted nappe pile. *Tectonophysics*, **281**, 195–207.